5-1-2024

THE EFFECT OF ALTITUDE ON DECOMPOSITION: TOWARD AN UNDERSTANDING OF THE POSTMORTEM INTERVAL IN THE ROCKY MOUNTAIN REGION OF COLORADO.

Christiane Irene Baigent
Southern Illinois University Carbondale, cbaigent@gmail.com

THE EFFECT OF ALTITUDE ON DECOMPOSITION: TOWARD AN UNDERSTANDING OF THE POSTMORTEM INTERVAL IN THE ROCKY MOUNTAIN REGION OF COLORADO

by

Christiane Baigent

B.A. Metropolitan State University of Denver, 2012
M.Sc. University College of London, 2014

A Dissertation
Submitted in Partial Fulfillment of the Requirements for the
Doctor of Philosophy Degree

School of Anthropology, Political Science, and Sociology
in the Graduate School
Southern Illinois University Carbondale
May 2024

DISSERTATION APPROVAL

THE EFFECT OF ALTITUDE ON DECOMPOSITION: TOWARD AN UNDERSTANDING OF THE POSTMORTEM INTERVAL IN THE ROCKY MOUNTAIN REGION OF COLORADO

by

Christiane Baigent

A Dissertation Submitted in Partial

Fulfillment of the Requirements

for the Degree of

Doctor of Philosophy

in the field of Anthropology

Approved by:

Gretchen R. Dabbs, Chair

Tamira K. Brennan

Melissa A. Connor

David E. Sutton

Paul D. Welch

Graduate School
Southern Illinois University Carbondale
February 27, 2024

AN ABSTRACT OF THE DISSERTATION OF

Christiane Baigent, for the Doctor of Philosophy degree in Anthropology, presented on February 27, 2024, at Southern Illinois University Carbondale.

TITLE: THE EFFECT OF ALTITUDE ON DECOMPOSITION: TOWARD AN UNDERSTANDING OF POSTMORTEM INTERVAL IN THE ROCKY MOUNTAIN REGION OF COLORADO

MAJOR PROFESSOR: Dr. Gretchen R. Dabbs

The estimation of postmortem interval (PMI) is a critical component of medicolegal death investigation. An accurate PMI estimate has the potential to influence the allocation of investigative resources, establish the probative value of associated biological and material evidence, shape the analytical framework applied to skeletal analysis, and inform cause and manner of death. Forensic anthropologists are often tasked with PMI estimation throughout all stages of decomposition and typically rely on categorical phases of soft tissue and skeletal change purported to correspond to broad estimates of elapsed time. In an attempt to improve precision, Megyesi *et al.* (2005) developed the Total Body Score model (TBS). This quantitative method relies on qualitative assessment of value-assigned categories of tissue change within three anatomical regions to estimate accumulated degree days (ADD), and subsequently, PMI. However, the TBS model has failed to prove reliable in a diversity of region-specific validation studies, emphasizing the need for environment-specific research in taphonomy study.

Toward that end, the rate, pattern, and trajectory of decomposition was assessed among a cohort of 12 human donors in the high-altitude Rocky Mountain region of Colorado. This research was performed at Colorado Mesa University's Forensic Investigation Research Station high-altitude satellite facility, FIRS-TB40. The site lies at an elevation of 3000 meters/9840 feet above mean sea level (AMSL), in the Dfc (snow, fully humid, cool summer) climate region. With both significantly higher elevation and an unrepresented climate classification, FIRS-TB40 introduces a novel environment for the controlled study of human decomposition. This quadripartite study sought to (1) test the qualitative and quantitative aspects of the TBS model in a high-altitude environment to assess suitability of application

in the estimation of local PMI; (2) test seven atmospheric variables to assess the utility of integrating atmospheric data beyond ADD into PMI estimation; (3) establish the rate and pattern of human decomposition, isolate and describe phasic patterns of soft tissue change throughout the trajectory of decomposition, and (4) develop a region specific bioecological profile with an emphasis on the integration of human behavior.

Results: (1) Neither the qualitative or quantitative aspects of the TBS model tested well at high-altitude and are therefore not recommended for application within the study environment. The qualitative changes presented in the TBS model were not observed among the high-altitude cohort. While Megyesi *et al.* report that time and temperature - as measured by ADD - accounts for 84% of the variance observed throughout decomposition, ADD accounted for only 42% of the variance observed in decomposition within the high-altitude cohort.

(2) Seven atmospheric variables were assessed using locally estimated scatterplot smoothing (LOESS) and multivariate regression. Two of these variables - accumulated solar radiation days ($r^2 = 0.67$) and accumulated windspeed days ($r^2 = 0.65$) – explained more variance in decomposition than ADD ($r^2 = 64$).

(3) Five categories of phasic, macroscopic soft tissue change, *the suite of which* is inferred unique to high-altitude, were identified. These include adipocere formation, trajectory of soft tissue color change, fluid bloat, tissue island formation, and skin sloughing. Patterns of slope roll and slope wash were also described to inform the local taphonomic profile.

(4) A forensic bioecological profile was developed using empirically derived patterns of scavenger behavior, census and land use data, extant ethnographic data, and forensic case study. Analysis demonstrated that the data sources were cyclically informative and sufficient to develop an early phase foundational model that will benefit from future interdisciplinary research.

Summarily, the high-altitude region of Colorado is culturally and environmentally distinct. The observed disparity in rate and pattern of human decomposition between the high-altitude cohort and

the TBS model, and the inadequacy of ADD alone to predict PMI are demonstrative of the need for environment-specific model building in human taphonomy research.

ACKNOWLEDGMENTS

I would like to extend my deepest gratitude to my advisor, Dr. Gretchen R. Dabbs, for her enduring moral and academic support, and her dedication to providing thoughtful and in-depth feedback. Without your invaluable guidance, Brucey's Big Book Report would not have been possible. I would also like to thank my committee members, Drs. Tamira K. Brennan, Melissa A. Connor, David E. Sutton, and Paul D. Welch. Your individual expertise were invaluable in tackling this multifaceted project. From vintage science fiction to slipping a bit of dark humor into an otherwise formal email, each of you offered both academic and nuanced moral support that did not go unnoticed.

I am further grateful to Dr. Melissa A. Connor, Alex Smith, Sara Pickles Garcia, Colorado Mesa University's Forensic Investigation Research Station, David Kintz, Don Comstock, all of the deputies at the Park County Coroner's Office, and the Park County Commissioners for supporting the vision of high-altitude research and offering the advice, support, and resources necessary to complete this project.

I would like to acknowledge the National Institute of Justice Graduate Research Fellowship Program. I am indebted to the fellowship committee members and staff who saw the value of this project, provided financial support, and afforded academic freedom in the performance of this research.

My wonderful family - Dad, Steph, Renee, and Lukas – thank you for your unending love and support.

My wife, Emily Baigent. I simply could not do it without you, I am thankful for you every day.
I would be remiss if I did not also acknowledge our large family of fuzzos, Atlas, Rooster, Charlie, Sir Clopton Havers, and Whisky Bear. Thank you for the laughter and constant reminders to take a break.
Dr. Cassie V. Comeau, I would not have made it this far without you.
Gary Scott for the years of ceaseless support that you have provided - thank you.

Finally, my deepest and most sincere gratitude to the donors and their families. Without your generous donation and support of the forensic sciences, this research would not have been possible.

DEDICATION

To my little Frankie G.

We didn’t make it to the end together as planned, but we had a heck of a ride.

PREFACE

This volume includes references to published research papers and abstracts authored or co-authored by me. The content of these works include data related to early research in human decomposition at high-altitude, phasic observations made throughout the course of this research, research pertaining to the use of pigs as human proxies, and a comparative study of autopsied versus non-autopsied human remains. These studies were referenced to provide empirical foundation for this study, scientifically validate the use of human donors versus an analogue, and validate the inclusion of autopsied donors in this project. Additionally, human decomposition research performed in the adjacent high-elevation plains of western Colorado is referenced as a source of both corroborative and comparative data. Finally, reference is made to the Summit County Coroner's Office 2022 Annual Report to demonstrate continuity in death statistics between adjacent Summit and Park Counties. This content is included with permission from the publisher.

Baigent CI, Gaither CM, Campbell C. (2014). The effect of altitude on decomposition: a validation study of the Megyesi method. Proceedings of the American Academy of Forensic Sciences 20:485-486.
Cited in chapters 1, 2 & 7

Baigent CI, Connor MA, Dabbs GR (2019). Introducing FIRS-TB40: Scavenger Succession and Progression at a High-Altitude site in Colorado. Proceedings of the American Academy of Forensic Sciences 25:127.
Cited in chapter 2

Baigent CI, Agan C, Connor M, Hansen ES. (2020). Autopsy as a form of evisceration: Implications for decomposition rate, pattern, and estimation of postmortem interval. Forensic Sci. Int. 306(1):1-8.
Cited in chapters 3 & 5

Baigent CI (2023). Summit County Coroner's Office 2022 Annual Report. Summit County Government Office of the Coroner. https://www.summitcountyco.gov/132/Annual-Reports. Accessed 1/10/2024.
Cited in chapter 2

Connor MA, Baigent C, Hansen ES. (2018) Testing the use of pigs as human proxies in decomposition studies. Journal 249-280of Forensic Sciences, 63(5), 1350-1355.
Cited in chapter 2

Connor MA, Baigent C, Hansen ES. (2019). Measuring Desiccation Using Qualitative Changes: A Step Toward Determining Regional Decomposition Sequences. Journal of Forensic Sciences, 64(4), 1004-1011.
Cited in chapters 1, 2, & 7

TABLE OF CONTENTS

LIST OF TABLES

LIST OF FIGURES

FIGURE PAGE

CHAPTER 1

BACKGROUND AND INTRODUCTION

1.0 Predictive models in forensic anthropology

The estimation of postmortem interval (PMI) is a critical component of medicolegal death investigation. An accurate PMI estimate has the potential to influence the allocation of investigative resources, establish the probative value of associated biological and material evidence, shape the analytical framework applied in skeletal analysis, and inform cause and manner of death. Decomposition is a dynamic, but ultimately reductive process. The rate and manner of reduction are dictated by extant biotic and abiotic variables within both the postdeposition environment and the individual remains. Medicolegal professionals concerned with PMI estimation are limited by the foundational accuracy of the methods applied, with concomitant decrease in precision and accuracy over time. Forensic anthropologists are frequently consulted when tissue dissolution and/or skeletonization preclude the application of physiochemical methods for PMI estimation. Late-stage PMI estimation - characterized by skeletonization variably accompanied by desiccated tissue - is further complicated by the interaction between human remains and the post-depositional environment, which may alter or obscure features necessary for accurate analysis of PMI, trauma, pathology, and/or the biological profile. These intercalated, but unpredictable variables necessitate a high-resolution understanding of decomposition within a microenvironment to reduce the loss of precision attendant to late-stage PMI estimation and to maximize analytical robusticity.

Late-stage PMI estimation has traditionally been limited to macroscopic analysis of gross tissue change, anecdotal evidence, and observer experience (DiMaio & DiMaio 2001; Love & Marks 2003). Detailed descriptions of the environment-specific chronology of gross tissue change are relatively rare, with comprehensive examples limited to arid environments (Galloway *et al.* 1989; Galloway 1997; Rhine and Dawson 1998; Connor *et al.* 2019), the woodlands of eastern Tennessee (Bass 1997), and a low-

altitude cold environment (Komar 1998). Further, Sorg (2013) provides a macroscopic model for establishing regional patterns of microenvironmental taphonomic variation. However, these models were developed within a specific environmental context and are largely derived from retrospective, cross-sectional data, yielding analytical gaps that have high potential to impact practical and methodological outcome (Galloway *et al.* 1989; Komar 1998; Rhine & Dawson 1998). While cold weather environments have been considered in previous study (Micozzi 1986; Komar 1998; Tersigni 2007; Spencer 2013; Roberts & Dabbs 2015; Pilloud *et al.* 2016; Turpin 2017), there is currently a complete lack of longitudinal data pertaining to human decomposition within a high-altitude (> 2400 meters AMSL), cold weather environment.

Historically, the development of 'universal' predictive models was undertaken in an attempt to mitigate the analytical problems associated with regional variation and cross-sectional data sets. An important step toward understanding the relationship between the environment and the estimation of PMI was the application of accumulated degree days (ADD) to the continuum of decomposition (Vass *et al.* 1992). Accumulated degree days represent the sum of daily mean temperatures within a prescribed period of time, descriptive of the accumulation of thermal energy units necessary for chemical and biological reactions to occur, and therefore represents the product of temperature and chronological time (*ibid*). Using ADD as indices for temperature and time, research has progressively trended toward the intercalation of ADD and phasic descriptive models (Megyesi *et al.* 2005). Early attempts at qualitative measurement of decomposition were derived from gross assessment of value-assigned categories of tissue change within three anatomical regions (head/neck, thorax, limbs). The sum of these scores yields a total body score (TBS) (Megyesi *et al.* 2005). Application of TBS to the study's analytically derived regression equation provides a case-specific estimate of ADD. When applied to local retrospective temperature data, the ADD estimate in turn yields an estimate of PMI. The authors close with the recommendation for further study in different ecoregions to independently validate the model

and test the environment specific efficacy and specificity of the model (Megyesi *et al.* 2005). Vass *et al.* (2011) introduced phasic predictive models for the estimation of PMI for buried and surface depositions correlated to ADD. The authors concede that their method is heavily dependent upon user experience, thus demonstrating that attempts to quantify human decomposition remain largely dependent upon qualitative observation. Citing errors associated with rounding, temperature scale, and the data set inappropriate application of a linear regression model, Moffat *et al.* (2016) proposed an improved equation for the estimation of ADD within the TBS model. The authors modified the data set observed in the Megyesi *et al.* (2005) study based on criteria unique to their study and applied an ordinary least squares linear regression model to the data. The output was a new regression equation, which the authors assert is a superior fit to the data (Moffat *et al.* (2016) equation $r^2 = 0.91$ / TBS Model (2005) $r^2 = 0.84$). However, it is of note that while the data were derived from the 'same' sample set, Moffat *et al.* (2016) reduced the sample from 68 to 15 cases. Further, Moffat *et al.* cite ambiguity and disparities in the temperature scale applied in the TBS model, asserting that the authors present temperature data in both Celsius and Fahrenheit, and in numerous tables, wholly fail to specify which scale was used. When considering the suite of individual daily temperature means associated with individual cases presented within Megyesi *et al.*'s data set, the post hoc conversion of Fahrenheit to Celsius produces a more seasonally appropriate temperature series than those reported in the original study. Summarily the disparities identified within the original TBS study involving variables as fundamental as temperature scale are disconcerting at the least and highlight the necessity for ongoing validation study.

The dependence on observer experience in observation of phasic decomposition change is due in large part to the polyvalent nature of decomposition – the rate and pattern of gross tissue change are not catalyzed by temperature alone, as the TBS/ADD models suggest. Variables such as pH, UV exposure, ground temperature, precipitation, solar radiation, partial pressure of atmospheric gasses, slope angle, and insect, microbial, and faunal succession all have the potential to impact the local rate

and pattern of decomposition (Nawrocki 2009). The catalytic potential for each variable depends on their concentration, affinity for coexisting variables within the microenvironment, and the constituent molecular byproducts of human decomposition. Therefore, "universal" temperature-centric models for late-stage estimation are overly reductive. Several subsequent validation studies of the TBS model have failed to produce the intended results and homogenously find that predictive disparity is greatest in late-stage estimation. Regions reporting disparities include the Rocky Mountain region of Colorado (Baigent *et al.* 2014), the arid region of western Colorado (Connor *et al.* 2019), the arid region of southern Texas (Suckling 2011), southeastern Australia (Marhoff *et al.* 2016), and South Africa (Myburgh *et al.* 2013). Additionally, empirical research has demonstrated that temperature models are sensitive to local fluctuations, suggesting that the location of the temperature measurement source within a region may constitute an additional source of error (Dabbs 2010; 2015). Thus, reductive model building is not sufficient for application to complex biological processes, nor is homogeneous application appropriate within a geographic area as large, climactically, and ecologically diverse as the United States.

Analytical complexity in PMI estimation is intensified by the entanglement of intrinsic/extrinsic and biotic/abiotic variables. Decomposing human remains constitute the focus (and often foci) of an emerging ecological community defined by a myriad of climactic, pedological, floral, and faunal activity. Extant flora and fauna are spatially relative, making an understanding of local climate, geology, and ecology (biogeoclimatic variables) critical to PMI estimation. Due to the polyvalent complexity of regional decomposition patterns, Haglund and Sorg (2001) and Sorg (2013) assert that higher resolution data pertaining to the ecological context be collected to more fully understand the complex of variables that impact taphonomic processes. This has microscopic (local) implications (such as more accurate intraregional PMI estimation models and taphonomic profiles), as well as macroscopic implications (such as a more accurate understanding of the interregional variables paramount to the continuum of human decomposition).

1.1 The removal of anthropology from forensic anthropology: The Daubert Standard and its lasting impact.

Critical to the task of constructing regional decomposition profiles - but largely overlooked - is an understanding of regional patterns of living human interaction with the environment. Congram (2013) argues that passage of the Daubert standard in 1993 initiated the fracture of forensic anthropology from traditional anthropological theory and method. The Daubert standard yielded a set of criteria used to determine the admissibility of expert witness testimony in federal court and assigned the task of expert qualification to the presiding judge (509 U.S. 579 1993). Because a judge cannot be presumed to be versed in the intricacies of expert qualification across the spectrum of disciplines from which an expert may be drawn, the standard established guidelines for determining the validity of expert methodology. Within these standards, validity is based on: (1) whether the theory or technique in question can and has been tested; (2) whether it has been subjected to peer review and publication; (3) known or potential error rate; (4) the existence and maintenance of standards controlling its operation; and (5) whether it has attracted widespread acceptance within the relevant scientific community (Christensen & Crowder 2009).

The intention of the Daubert standard was to ensure the adherence of professionals to best practice in the analytical and methodological approaches that would have bearing on the course of judicial proceedings. The Daubert standard emphasized the need for practitioners within the anthropological community to critically reevaluate the techniques and methods used in skeletal examination, as well as assess the validity of the underlying scientific theories. Because osteological analysis relies on a composite of scientific theory and methodology, as well as less empirical lines of observation, case study evaluation, and practitioner experience, reaction within the discipline was dramatic (Christensen 2004; Christensen & Crowder 2009). The passing of the Daubert standard sent a ripple of urgency through the anthropological community, yielding both necessary change, as well as the

spread of misinformation and overzealous reaction (Grivas & Komar 2008). Haglund *et al.* (2001) warned that interpretation and processes of human behavior are outside of the purview of forensic anthropologists and suggested that anthropologists limit their documentation to fact and the construction of expert witness documentation. While this sentiment is critical to analytical and methodological approaches to osteological analysis, the message was extended to encompass all aspects of forensic anthropological inquiry, including field search and recovery, where the burden of methodological defense is mitigated by the practicality of the pursuit (i.e. whether or not a decedent has been recovered is unlikely to be a contested fact of a case, as successful recovery of the decedent will serve to validate the applied methodology). However, the application of patterns of human behavior to forensic anthropological practice came under fire along several analytical lines, based on the assumption that these lines of inquiry were overly qualitative in nature and therefore unable to meet the criteria set forth by the Daubert Standard.

Clandestine body disposal relies on knowledge of the landscape, type of terrain, and local patterns of technology access, proficiency, and use. Ethnography is uniquely suited to the task of establishing local patterns of human/environment interaction but has largely been avoided in forensic anthropological context. As practitioners trained in a holistic approach to human biology and behavior, forensic anthropologists are uniquely suited to assess patterns of human behavior within a local cultural complex. However, this pursuit has been restrained by the subdiscipline's (mis)interpretation of the Daubert standard. In many regards, early reaction to the Daubert standard effectively removed the 'anthropology' from forensic anthropology, leading critics within the four-field disciplines to minimize the subdiscipline as a series of practitioners applying a skill set, rather than as a fully realized subdiscipline guided by both scientific and anthropological endeavor (Armelagos 2011). In an era where the fracture of the four-field approach has become an issue of increasing concern (Calcagno 2003;

Armelagos 2011) holistic, integrative research performs the dual task of reinforcing the holistic approach and reasserting forensic anthropology into the four-field discipline.

1.2 Structural rejection of the four-field approach

The American Academy of Forensic Sciences (AAFS) was established in 1948 as a multidisciplinary, professional, collaborative society concerned with precision, professionalism, and accuracy in the application of science to law. Under the pioneering efforts of Ellis Kerley and Clyde Snow, anthropologists collectivized to form the Physical Anthropology Section in 1972. Between 1972 and 2015, the section remained largely committed to the exclusion of archaeologists, bioarchaeologists not specifically trained as forensic anthropologists, and cultural and linguistic anthropologists. This was made apparent through the engagement of arguments on the floor of the section's business meetings, and the section's refusal to formally vote on broadening their criteria for section membership. The exclusion of archaeologists involved in forensic taphonomy study and practice, and forensic search and recovery efforts was seen by many as especially egregious (Ubelaker 2018). As a result of their exclusion from the Physical Anthropology Section, archaeologists collectivized in 1984 and formally established themselves as a group under the umbrella of the AAFS General Section. In 2015, after almost 45-years of debate, the Physical Anthropology Section voted to rename the section "Anthropology." However, the history of exclusion has had a lasting impact on the section among both advocates and opponents of the change. While speaking at a 2023 AAFS symposium entitled, *Beyond the Science: The Value of Anthropological Forensics*, respected anthropologist Bruce Andersen stated, "…our discipline has been exclusionary. For years we excluded bioarchaeologists, many of whom know a hell of a lot more about the human skeleton than some forensic anthropologists do." While many forensic anthropologists were inarguably trained in bioarchaeology, those not trained by, and practicing as, a forensic anthropologist were unable to join the section. While the section continues to recognize its exclusionary 'past' toward the four-field approach, the lack of diversity among students and practitioners has more recently been

identified as a critical issue facing both the section, and the discipline as a whole today (Tallman & Bird 2022).

In 2017 the Anthropology Section Chair responded to the popular appeal to contend with this lack of diversity by creating a temporary *ad hoc* Diversity & Inclusion (D&I) Committee. In 2018 the Diversity and Outreach Committee (DOC) was established and introduced, and formally approved by voting members of the Anthropology Section in 2019 (Tallman 2020). However, debate arose when the Anthropology Section's DOC was quickly and suddenly dissolved by the governing Academy, who cited the need for an Academy wide DOC (Ropero-Miller *et al.* 2020). Initially there was support within the Anthropology Section for Academy wide expansion of the committee, but protest quickly arose when the Academy's version of the DOC was perceived as a largely inactive red herring, uninvested in the vision of the original DOC, and largely ineffective in forwarding and achieving its goals (Tallman 2020). Internally, members of the Anthropology Section were divided in opinion. Proponents of the Anthropology Section specific DOC cited the critical need to address both the section's lack of diversity, and the need for forensic anthropologists (acting as anthropologists first) to actively engage in protest against the escalating violence, racism, and structural inequalities plaguing BIPOC, LGBTQA+, and other underrepresented communities. Opponents within the section cited the need to remain impartial in sociopolitical issues to avoid alienating the law enforcement agencies for whom forensic anthropologists' consult, and to avoid potentially undermining the perception of an anthropologist's objectivity while engaging in matters of jurisprudence (Tallman 2020). The results of survey-based research presented by Winburn *et al.* (2022) identified a strong correlation between categorically defined generations and intra-section division of opinion on engagement and impartiality. Younger generations advocated for engagement, while older generations advocated for impartiality. Regardless of individual stance, it is critical to understand the historicity of division within the Anthropology Section as a means of understanding associated macroscopic values, politics, ritual, and symbolism. These

macroscopic patterns and values cyclically impact perception of group access, group mobility, individual modes of engagement within, and potential for group assimilation, which further influence the structure of membership, modes of participation, perception of opportunity, and availability of resources.

1.3 Forensic Taphonomy

In its modern form, forensic taphonomy has largely been a collaborative effort between archaeologists, bioarcheologists, and forensic anthropologists, and unique in its refusal to impose the same social and analytical restrictions on theory, research, and practice. Despite early exclusion from prominent professional organizations such as AAFS, archaeologists and bioarchaeologists have continued to make critical contributions to the field of forensic anthropology.

Broadly defined, taphonomy is the study of the sum of phenomena that affect the remains of a biological organism peri- and post-mortem – famously defined by Efremov (1940) as the transition from biosphere to lithosphere. Established at the cross section of geology, archaeology, paleontology, and biological anthropology, the 1980s and 1990s saw forensic taphonomy crystalize as a distinct subdiscipline governed by its own theory and method (Haglund & Sorg 2007b). Three primary goals of forensic taphonomy are (1) to estimate postmortem interval; (2) distinguish between human activity and natural processes; and (3) to recreate the circumstances surrounding the time of death (Haglund & Sorg 1997).

These goals are expanded upon by Nawrocki (2009) with the assertion that forensic taphonomy is concerned with multilinear interactions between environmental factors (geotaphonomy), human remains and their individual factors (biotaphonomy), and the assailant/victim interaction and subsequent decedent deposition (behavioral factors). In the forensic anthropologist's role as osteologist, the primary concern is the construction of the biological profile. Likewise, the role of the taphonomist is to produce a taphonomic profile, collected, organized, and presented within the framework of environmental, individual, and cultural factors. While "cultural factors," are largely limited to

consideration of the interaction between perpetrator and decedent, the emphasis placed on human behavior within the analytical network demonstrates that forensic taphonomists are not reticent to incorporate modes of human behavior into theory and practice. As a result, the subdiscipline is uniquely positioned to broaden the scope of environment-specific human behavior profiles, as they pertain to forensic investigation. This study is therefore concerned in part with broadening the scope of human behavior in anthropological context within the theoretical and analytical framework of forensic taphonomy.

1.4 Research Objectives

This research proposes to establish a holistic taphonomic profile of the high-altitude Colorado Rocky Mountain Region (CoRM). This profile will also be referred to as the regional forensic ecological profile. 'Forensic ecology' is used to denote the suite of competing and cooperating environmental variables that are relevant to forensic investigation. These variables include spatially and temporally distinct configurations of biogeoclimatic variables that impact the deposition, decomposition, and disarticulation of human remains in an outdoor environment, and may therefore impact the course of a forensic investigation. Development of a meaningful regional taphonomic profile necessitates: (a) local, longitudinal, multivariate, empirical assessment of the rate and pattern of human decomposition; (b) documentation of the local biogeoclimatic zone (i.e. holistic consideration of the physical environment); and (c) forensic ecological context that includes invertebrate and vertebrate behavior, with an emphasis placed in this study on integrating local patterns of human behavior into an understanding of the greater local environment (Sorg 2013; Connor *et al.* 2019). Toward that end, this study seeks to establish a multivariate taphonomic profile of the high-altitude Rocky Mountain region of Colorado. The four analytical lines of inquiry emphasized in this study are as follows:

1. Test the TBS model along two analytical lines: (1) the efficacy of the TBS model for qualitatively describing the pattern of gross decomposition change at high-altitude; and (2) test the application of the quantitative TBS regression equation for efficacy and accuracy in predicting PMI in a high-altitude environment.
2. Describe the longitudinal macroscopic rate, pattern, and trajectory of human decomposition within a sample placed in an outdoor setting at high-altitude both qualitatively, and quantitatively to assess the relationship between TBS and site-specific environmental variables not considered in the TBS model.
3. Isolate and describe gross tissue change postulated to be unique to the local rate and pattern of decomposition in a high-altitude outdoor setting, to be applied in future study to establish a score matrix and a predictive model(s) for the estimation of postmortem interval in a high-altitude environment.
4. Develop a region specific forensic ecological profile that includes local atmospheric variables, invertebrate and vertebrate behavior, and local human behavior.

1.5 Research Models

1.5.1 Qualitative Aspects

This study will score all human remains following the TBS model (Megyesi *et al.* 2005). While preliminary research suggests that the model is not appropriate for quantitative application in this high-altitude environment, the qualitative model provides a universally understood method for numerically describing the continuum of decomposition. Qualitative assessment will follow two phases:

1. Isolate the major categorical changes defined by the TBS model, including mode and trajectory of skin slippage, purge, soft tissue color change, marbling, bloat, moist decomposition in order to document the incidence and prevalence of presentation among the high-altitude cohort.

2. Establish these categorical changes as a qualitative metric against which to identify and describe divergent modes of gross tissue change.

1.5.2 Quantitative Aspects

Analyses of the quantitative aspects of this study are foundationally based on Fischer's (1956; 1971) statistical approach to scientific inference. Fischer advocates for the articulation of a null hypothesis (or null hypotheses) which asserts that no predicted relationship or analytical difference exists between two measurable variables. The null hypothesis serves as a fulcrum upon which the weight of the data (i.e., the p-value) may be accepted ($p<0.05$) or rejected ($p>0.05$). The null hypothesis affords this study numerous advantages: (1) it prevents overstatement of the statistical relationship between the variables under investigation; (2) the underlying assumption that a statistical relationship between ADD and TBS exists, as supported by previous study (Megyesi *et al.* 2005; Moffat *et al.* 2016) is tested; and (3) the underlying assumption that a statistical relationship exists between TBS and atmospheric variables not considered in the TBS model but proposed in this study is tested. Linear regression analysis was applied by Megyesi *et al.* (2005) in the development of the TBS model to derive an equation for application in the prediction of PMI. The fundamental basis for testing the power of a new data dataset within an existing model is to compare the outcome derived from the same model. Therefore, linear regression was applied in this study to compare the relationship between Total Body Score (dependent or response variable) and Accumulated Degree Days and Postmortem Interval (independent or explanatory variables). A statistical threshold of $p \leq 0.05$ was pre-established to evaluate the significance of the relationship between variables.

1.6 Research Hypotheses

Null hypotheses to be tested: Postmortem Interval

H01: Within the high-altitude sample, Accumulated Degree Days (a numeric synthesis of temperature and time) will not affect decomposition as represented by the Total Body Score model.

H02: Within the high-altitude sample, site-specific environmental variables (individually used as the numeric synthesis of variable and time) will not affect decomposition as represented by the Total Body Score model.

Null hypotheses to be tested: Reliability

H03: There will be no difference in TBS within a random subset of the sample re-scored by the author.

H04: There will be no difference in TBS within a random subset of the sample scored by a second observer.

1.6 Conclusion

The estimation of postmortem interval (PMI) is a critical component of medicolegal death investigation. However medicolegal professionals concerned with PMI estimation are limited by the foundational accuracy of the methods applied, associated error rates, and decrease in precision over time. Late-stage PMI estimation - characterized by skeletonization variably accompanied by desiccated tissue - is further complicated by the interaction between human remains and the post-depositional environment. Early attempts at homogenizing language and methodology in PMI estimation resulted in a bifurcate approach. This bifurcation was defined by one branch concerned with region-specific model building, and a second branch concerned with universal model building, undertaken in an attempt to mitigate the analytical problems associated with regional variation and cross-sectional data sets. Absent from both lines of inquiry is study of the unique variables associated with the high-altitude environment.

While 'universal' PMI estimate models are limited in scope by their temperature-centric framework, so too are the forensic ecological profiles associated with region specific model building. This trend is due in large part to both the passage of the Daubert Standard, and a history of four-field exclusion by the Physical Anthropology Section of the American Academy of Forensic Sciences. The sum of these two variables has fostered the self-imposed segregation of forensic anthropologists from the four-field anthropology community, despite the ability of the four-field approach to provide valuable insight into regional modes of human behavior that may carry forensic significance.

Forensic taphonomy provides a practical and analytical framework within which to synthesize the contributions of all four fields to the forensic sciences. A collaborative effort between

archaeologists, bioarcheologists, and forensic anthropologists, forensic taphonomy is unique in its refusal to impose the same analytical and methodological restrictions on theory, research, and practice. This study is therefore concerned with testing the efficacy of the discipline's primary 'universal model,' (the TBS model) for application in a high-altitude environment, establishing the rate and pattern of human decomposition at high-altitude, and establishing a region-specific forensic ecological profile to include vertebrate and invertebrate scavenger behavior, human behavior, atmospheric variables beyond temperature, and forensic case study.

CHAPTER 2

LITERATURE REVIEW

2.0 Human Decomposition Research Facilities in North America: A Case for High-altitude Study

Human taphonomy research facilities study human decomposition in natural, outdoor contexts. While research protocols, policy, and procedure are unique to each facility, goals trend toward the development of a local ordinal scale to describe the trajectory of human decomposition, from fresh tissue to advanced decay. Human decomposition research facilities in the United States increased from one in 1981 to eight in 2019. With the exception of the Forensic Investigation Research Station (FIRS) at Colorado Mesa University, and the Forensic Research Outdoor Station (FROST) at Northern Michigan University, these facilities are climatically and topographically collectivized within 'the southeast region,' of the United States (Figure 2-1). While this collectivization does not accurately represent distinct local patterns of environment specific variation observed throughout the southeast (encapsulated by ecoregional variation; see Figure 2-6), it does demonstrate the need for empirical data derived from regions outside of the broad temperate-humid climate classification zone within which each of these facilities is established.

In 2012, Colorado Mesa University commenced construction of the Forensic Investigation Research Station (CMU-FIRS). CMU-FIRS is located on Colorado's Western Slope, a geographic region named and defined by its position west of the Continental Divide. The facility is distinct from similar taphonomy research facilities in both elevation (1350 meters/4430 feet), and climate (semi-arid – steppe). The FIRS is currently the highest elevated facility in the United States, followed by Western Carolina University, oriented at 645 meters/2116 feet AMSL. Under the Directorship of Melissa Connor, the first human donor was placed in 2013 and represented the initiation of controlled study of human remains both within Colorado, and west of the 100th meridian. Decomposition at the FIRS is characterized by rapid desiccation, resulting in a prolonged period of dermal and visceral retention, a

trajectory demonstrated to be unique to the region (Connor *et al.* 2019). Located east of the FIRS, the Colorado Rockies rise abruptly from the eastern plains and the western high-elevation plateaus, bisecting the two regions with imposing average elevations of 3300 meters/10800 feet - 4400 meters/14400 feet (Madole *et al.* 1987). While adjacent to the Colorado Rockies, CMU-FIRS is oriented at a significantly lower elevation. Extant decomposition research performed in the Colorado Rockies is limited to small scale studies using human analogues. However, while limited in depth and breadth, these studies, concerned with forensic entomology (DeJong & Chadwick 1999; Allaire 2002) and the TBS model (Baigent *et al.* 2014) consistently suggest that decomposition at high-altitude varies significantly from published patterns established at lower elevations. To date, no empirical human decomposition research has been performed within Colorado's high-altitude Rocky Mountain region among a cohort of human donors.

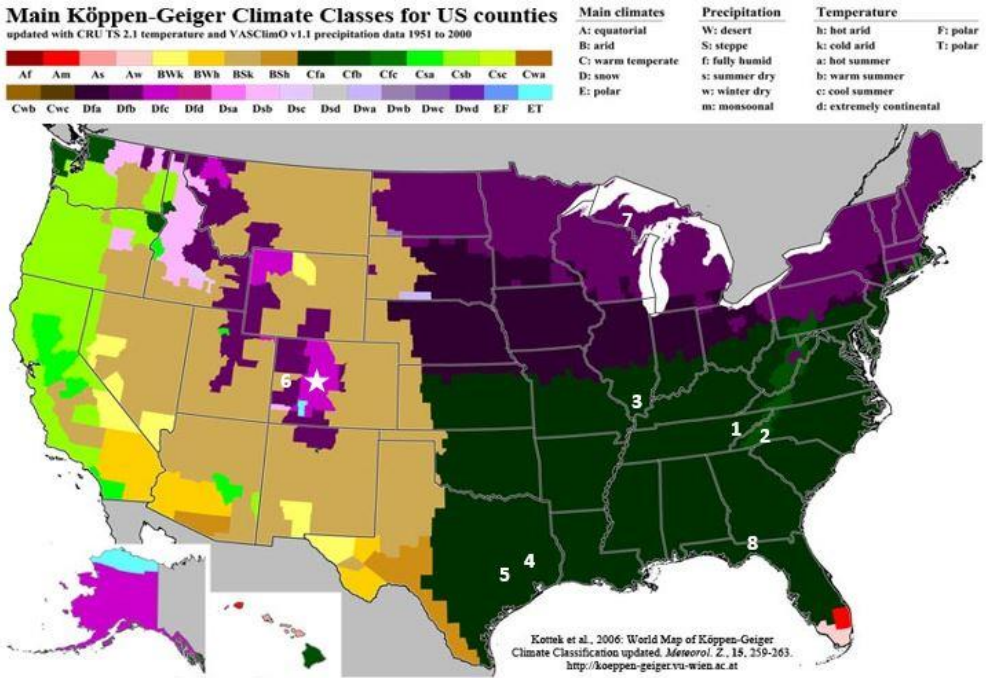

Figure 2-1: Distribution of Decomposition Facilities within the United States and their respective Köppen-Geiger Climate Classes. Star indicates project location, FIRS TB-40 (Kottek *et al.* 2006; numeric data added).

In an effort to address this analytical gap, the Commissioners of Park County Colorado deeded 40-acres of land to Colorado Mesa University for the purpose of human taphonomy research. In 2018, the site was formally inaugurated as a CMU-FIRS satellite facility (FIRS-TB40; indicated by star on map, Figure 2-1). FIRS-TB40 is located in the town of Como, in Park County Colorado. The site lies at an elevation of 3000 meters/9840 feet AMSL, in the Dfc (snow, fully humid, cool summer) climate region. With both significantly higher elevation and an unrepresented climate classification, FIRS-TB40 introduces a novel environment for the controlled study of human decomposition.

The importance of empirical research related to practical forensic casework within the Rocky Mountain region cannot be overstated. The heavily populated Denver Metro area, east of the Rocky Mountains, has experienced exponential annual population growth since the 2012 legalization of recreational marijuana (World Population Review 2024). With the exception of a slight decrease in 2019, between 2018 and 2022 (most recent year of reporting) the National Uniform Crime Reporting Program (UCR), Colorado Bureau of Investigations (CBI) reports a steady increase in violent crime throughout Colorado (Colorado Bureau of Investigations 2024). Within a two-hour drive of the Denver Metro area, Park County represents 2211 square miles of rural space primarily populated by farms, ranches, homesteads, and licensed and illegal marijuana grow operations. Statistics reported by the Park County Coroner's Office demonstrate that 22% of deaths reported in 2022 were out-of-county residents (D. Kintz, Personal Communication), while the adjacent Summit County Coroner's Office reports that out-of-county residents represented 47% of deaths in 2022 (Baigent 2023). These statistics are highly indicative of the region's large visiting, and attendant, transient populations.

While Summit County is more densely populated, Park County and surrounding rural counties are ideal for clandestine body disposal, although clandestine body disposal is not the only source of body deposition in the region. High-altitude is identified as a major risk factor in suicide. While studies support a significant correlation between altitude and suicide, current hypotheses variably attribute the

phenomenon to hypoxia, individual characteristics, firearms ownership and access, and differences in population density. Despite the range, the causal mechanism has not been isolated. (Reno *et al.* 2017; Betz *et al.* 2011). The region is also popular for recreation and supports a robust industry of local and out-of-state visitors that travel to the region to participate in outdoor recreation. Not all visitors are adequately prepared for the vast, mountainous, rugged terrain, which has high potential to result in injury or death. Additionally, altitude has the potential to exacerbate pre-existing chronic conditions as well as initiate acute pathogenesis. For example, acute mountain sickness may initially present as benign, but rapidly progress to potentially fatal forms of high-altitude cerebral edema (HACE) and high-altitude pulmonary edema (HAPE) (Netzer *et al.* 2013). While suicide and accidental death are unlikely to result in litigation, they do necessitate the allocation of investigative resources in order to safely perform search and recovery operations, and accurately identify, estimate postmortem interval, and designate cause and manner of death to known and unknown human remains.

2.1 Empirical Research - Decomposition in the Colorado Rocky Mountains

Empirical research has demonstrated that decomposition at high-altitude is unique in rate and pattern. Allaire (2002) investigated the composition of arthropod succession, and the rate of decomposition using three pig carrion within three biogeoclimatic zones ranging in elevations from 2040 meters/6700 feet to 3353 meters/11100 feet. Results suggest that the rate of decomposition slows as elevation increases, which the author attributes to prolongation of the bloat stage. Further, natural mummification - defined as drying of the epidermis and loss of body hair - was observed at the two highest elevation sites (2900 meters/9600 feet and 3353 meters/11100 feet, respectively).

DeJong and Chadwick (1999) assessed arthropod succession in north central Colorado using rabbits as a human analogue. The study cohort was situated at five sites ranging from 2713 and 4191 meters AMSL. Macroscopic patterns of decomposition were described in relation to generations of insect development. The authors observed a correlation between increase in elevation, and: (a)

reduction in arthropod species diversity; (b) delay in carrion biomass reduction; (c) prolongation of the bloat stage; and (d) reduction in successful development of larval cohorts. Scavenging was a notable catalyst for the acceleration of decomposition rate at higher elevation sites, while slower rates were concomitantly observed among members on the un-scavenged cohort. The authors attribute the arrest in decomposition rate to colder temperatures and freezing associated with overwintering at higher elevation sites.

Baigent *et al.* (2014) conducted a small sample (n = 4) study using porcine carrion sharing similar size and body composition. Carrion were concurrently placed at high-elevation (2800 meters AMSL) and lower-elevation (1,200 meters AMSL) sites within Colorado. The TBS model was applied following Megyesi *et al.* (2005) to visually assess decomposition, and accumulated degree days (ADD) were used as indices for time and temperature to compare the rate and pattern of soft tissue change within and between the two sites. Results demonstrated that rate, pattern, and trajectory of decomposition varied significantly between the two sites. While the TBS model suggests that the relationship between decomposition and temperature is paramount, resulting in a (mostly) linear relationship, observation at high-altitude suggests greater complexity in the relationship between decomposition and temperature. A quantitative comparison of TBS and site specific ADD shows a dramatic disparity between the curve of the two categories. Specifically, as predicted by the TBS model, ADD increases linearly across time. However, in contrast to this linear path, the TBS scores derived from observation at the high-altitude site present dramatic undulations (Figure 2-2). While Megyesi *et al.* (2005) report that temperature accounted for 80% of observed variance in decomposition in their study, a comparison of actual TBS to concomitant local precipitation at high-altitude demonstrates that precipitation has a substantial impact on the rate and pattern of TBS presentation across time in the high-altitude Colorado Rockies (Figure 2-3). While the sample was too small to derive any statistical power, a simple graph of the data is compelling.

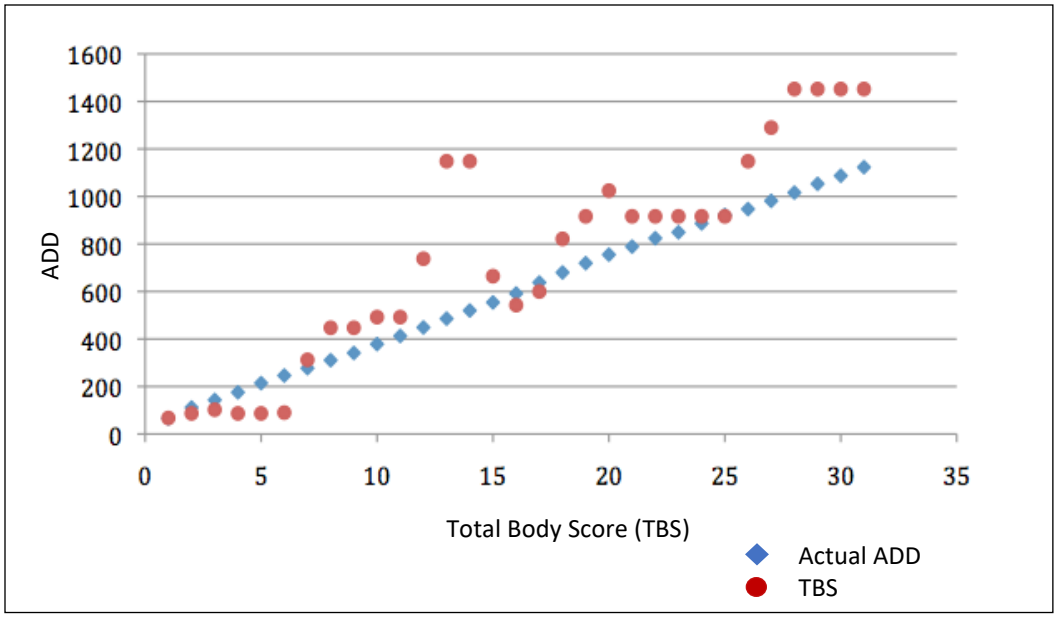

Figure 2-2: Actual ADD (blue) versus actual TBS (red) at high-altitude site: note the incidence of score undulation, contrasting the assumption of the TBS model that TBS and ADD will share a linear relationship across time (Baigent *et al.* 2014).

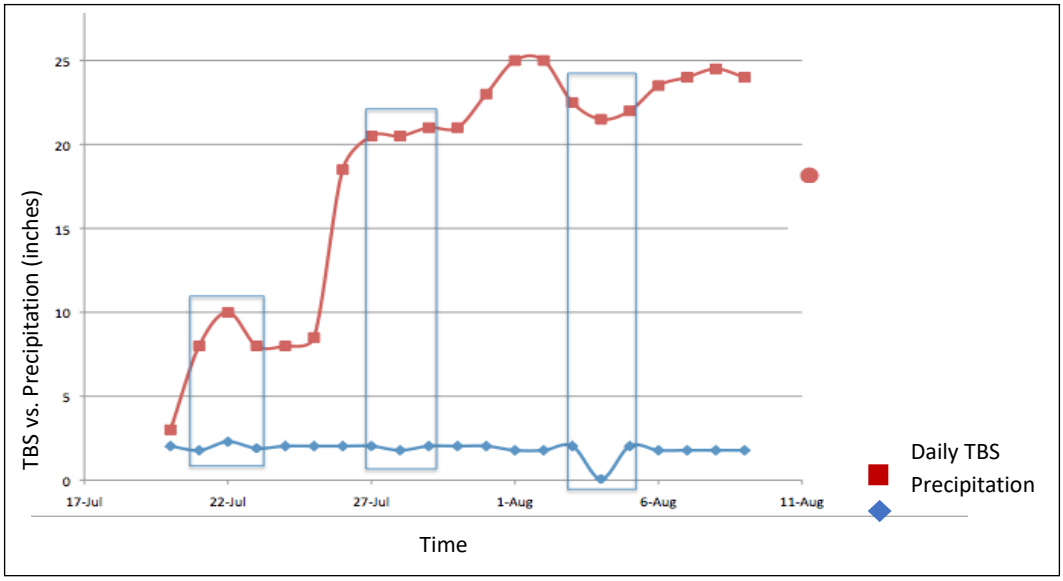

Figure 2-3: Daily total body scores (red) at high-altitude versus actual precipitation (blue). Note correspondence between rapid score reduction and precipitation (Baigent *et al.* 2014).

Further, the qualitative TBS model was not sufficient for describing gross decomposition change at either site. At the lower altitude site, porcine remains desiccated, resulting in stasis of gross decomposition at TBS=24. These results are consistent with longitudinal observations subsequently made at the FIRS within a large human cohort (Connor *et al.* 2019). At high-altitude, decomposition was

characterized by transcutaneous eruption of the viscera, proliferative maggot colonization, and interdigitated saponification of dermal layers which slowed the rate of late-stage decomposition (Baigent *et al.* 2014).

The results of these studies aid in establishing Colorado's high-altitude region as analytically and investigatively distinct. However, the sample sizes are small and subsequent research has established numerous problems associated with the use of pigs as human proxies (Connor *et al.* 2018; Dautartas *et al.* 2018). Research advocating for the continued use of pigs as human proxies do so while suggesting reform. These studies argue that the use of pigs in TBS study minimally necessitates the application of a modified scoring model sufficient to encapsulate the anatomical and physiological differences that exist between pigs and humans (Keogh *et al.* 2017). On a larger scale, quantitative studies comparing the rate and pattern of porcine versus human decomposition suggest that the use of pigs as human analogues in decomposition studies is specious, and recommend that care be taken when a porcine study cohort is applied to (in)validation of studies performed among human cohorts (Connor *et al.* 2018; Dautartas *et al.* 2018).

2.2 Empirical research – Cold environment decomposition

Human derived data pertaining to taphonomic change in cold and high-altitude environments are restricted to the observation of archaeological bone, and animal bone used as a human analogue to describe patterns of cold and ice-induced osseous change. In a series of controlled exposure experiments, Turpin (2017) subjected 52 lamb bone segments (2-4 cm in length) to cold, freeze-thaw cycles, freeze-drying, and water immersion to assess the impact of cold on the microstructure of bone. After treatment, bone segments were thin-sectioned and examined under a stereomicroscope. Cold exposure resulted in microscopic cracking across all treatment groups, with morphological differences presenting between treatment groups. While transverse cracks occurred across all treatment groups,

osteonal microfracture was limited to sections exposed to rapid freezing. Macroscopic cracking was limited to one bone segment in the freeze-dry treatment group.

While presented as foundational research, several aspects of this study are problematic. In cross-section, the microstructure of human (haversian) bone is composed of a series of cylindrical canals surrounded by a network of canaliculi and lacunae housing osteocytes, these cylindrical structures repeat in layers of concentric lamellae to form the osteon. In gross simplification, haversian bone is a series of osteons that facilitate dynamic processes of osseous deposition and resorption throughout the life cycle (Hillier 2007). Conversely, animal (plexiform) bone is the result of mineral buds that develop first transversely, then longitudinally in relation to the outer bone surface, producing a brick like infrastructure (*ibid*). Due to fundamental differences in structure, patterns in microfracture in human bone cannot reasonably be extrapolated from microfractures observed in animal bone. Likewise, thin sections of bone subjected to cold temperature variables are not reasonably representative of whole bones, as sections are subject to direct interface between freezing elements and internal structures. Additionally, differences in surface area to volume ratio, closed cortices, and overall morphology present several significant variables that cannot be overcome in a thin section study. These inferences are supported by a study of microstructural differences of human bone resulting from samples subjected to prolonged freezing, and samples never frozen. While scanning electron microscopy revealed the presence of microfractures, fractures lacked pattern or systematic distribution (Tersigni 2007). The disparity between the two studies reinforces the need for data derived from human samples.

Although limited to case study, studies of whole human bone in a cold environment have been performed. Pilloud *et al.* (2016) present a case study of historic bones recovered 60 years postmortem from an aircraft crash site on the Alaskan Colony Glacier. Observations made within the case study yielded a taphonomic signature characterized by (1) movement of the remains (estimated to be approximately 300 meters per year and attributed to glacial movement); (2) dispersal of remains (the

displacement of both fragmentary and whole skeletal elements from anatomical orientation due to glacial movement); (3) altered bone margins (exposure of trabecular bone and the 'fraying' or crushing of overlying cortices as a result of glacial load and ice); (4) splitting of skeletal elements (longitudinal cracking of flat bones attributed to the freeze-thaw cycle and moisture loss; and (5) soft tissue preservation and adipocere formation (the retention of the 'fresh' qualities of bone, preservation of connective tissue, preservation of soft tissue through sublimation, and adipocere formation). This study is limited to one historic individual that decomposed at a maximum elevation of 320 meters. However, the taphonomic profile derived from longitudinal decomposition in a cold environment has the potential to provide a basis (either divergent or convergent) for taphonomic cold weather changes at high-altitude.

More broadly, research suggests that bodies subjected to variables similar to those experienced in the Rocky Mountain Region yield distinct rate and pattern of decomposition. Komar (1997) performed a retrospective analysis of cases of advanced human decomposition submitted to the Medical Examiner's Office in Edmonton, Alberta, Canada, a region that experiences an annual average of five months of consecutive freezing. Accumulated degree days (ADD) were applied to known postmortem interval to estimate seasonal rate of decomposition. Skeletonization typically occurred in less than six weeks in the summer, and within four months in winter, despite freezing temperatures. The author concludes that while overwintering significantly slows the rate of decomposition, it does not arrest the process, as has been previously suggested in the literature (Megyesi *et al.* 2005; Vass 1992).

Micozzi (1986) assessed the effect of freezing and thawing on the trajectory of decomposition among a cohort of Wister rats. The control group presented predictable patterns of decomposition catalyzed internally by microbiota, resulting in putrefaction of the viscera. Conversely, the frozen-thawed group presented decompositional change that initiated externally, resulting in degradation of superficial dermal and connective tissue structures, which in turn facilitated infiltration by external

microbiota and arthropods. Summarily, the rate of decomposition was comparatively accelerated in the frozen-thawed group and the pattern of decomposition was distinct. Similarly, Roberts and Dabbs (2015) report significant differences in rate and pattern of decomposition between frozen and never frozen porcine subjects. However, in this study, frozen subjects decomposed significantly slower than the unfrozen control group. While divergent in their conclusions, the results of these studies suggest that freeze and freeze-thaw patterns observed in the cold-weather environment have a high potential for impact on the presentation and trajectory of human soft tissue and skeletal decomposition.

The sum of the data suggests that universal models for predicting rate and pattern of decomposition are insufficiently equipped to contend with regional biogeoclimatic diversity. While some of the variables associated with decomposition in cold environments have been studied in isolation, there is a need for a comprehensive, longitudinal, empirically based study of decomposition at high-altitude to establish a meaningful model for the estimation of postmortem interval.

2.3 The Use of Categorical Models to describe Gross Decomposition

Initial steps taken toward describing the trajectory of human decomposition were done through establishment of phasic or categorical stages of soft tissue and skeletal change. Early comprehensive examples are limited to arid environments (Galloway *et al.* 1989; Galloway 1997; Rhine & Dawson 1998), the woodlands of eastern Tennessee (Bass 1997), and a low-altitude cold environment (Komar 1998). The earliest of these human decomposition studies were performed in eastern Tennessee. While documenting insect succession and progression within a sample of four human donors, Rodriguez (1982), following Reed (1958), categorized human decomposition into four qualitative stages (fresh, bloat, decay, and dry). Bass (1997) expanded upon this model to define five stages of human decomposition (fresh, fresh to bloat, bloated to decay, dry, and bone breakdown). Galloway *et al.* (1989) and Galloway (1997) defined five categories of change retrospectively observed within a forensic case series derived from Arizona's Sonoran Desert (fresh, early, advanced decomposition, skeletonization,

and extreme decomposition). Galloway's model diverged from contemporaries and predecessors with the addition of sequential, phase specific, descriptive subcategories of change that yielded a higher resolution model of decomposition within the region.

Because categorical models were necessarily broad and largely lacked intracategorical description relevant to all microenvironments, the pursuit of establishing a 'universal model,' for PMI estimation became paramount. An early attempt made by Vass *et al.* (1992) relied on biochemical change to demonstrate that the sequential degradation of volatile fatty acids collected from cadaver soil and ADD shared a positive relationship. Vass *et al*. define ADD as the sum of daily mean temperatures within a prescribed period of time, descriptive of the accumulation of thermal energy units necessary for chemical and biological reactions to occur, and therefore representative of the product of chronological time and temperature combined. While this model has garnered little attention in practice, it: (a) more broadly introduced anthropologists to Van't Hoff's Rule, which states that as temperatures increase by 10 ˚C, chemical reactions catalyze 2-3 times faster; and (b) provided a renewed interest in the application of ADD as an index for temperature and time in human decomposition studies.

With the introduction of the TBS model, Megyesi *et al.* (2005) provided the first synthesis of categorical (qualitative) and mathematical (quantitative) model building into one comprehensive predictive model. The TBS model is predicated upon the relationship between decomposition and ADD - purported to be (mostly) linear – to provide an estimation of PMI. Following Galloway *et al.* (1989) the TBS model divides decomposition into four stages (fresh, early, partial, skeletonization); each stage contains intra-categorical descriptions assigned a point value. Resolution is further increased through division of the body into three anatomical sections (head/neck, trunk, limbs), each governed by a unique score matrix. The sum of scores derived from each body section on a single observation day yields the total body score (TBS), which when applied to the study's regression equation, yields an estimate of ADD. Estimate ADD represents a mathematical approximation, while actual ADD represents the sum of

daily mean temperatures within a prescribed period of time. The ADD timeline is defined by the date of discovery, and retrospective, site-proximal temperature data are used to count actual ADD backward from this point in time. When actual ADD (correlated to a specific calendar day) and estimate ADD approximate the same sum, an estimate of PMI is produced. A summary of the TBS model's analytical flow in PMI estimation is presented in Figure 2-4.

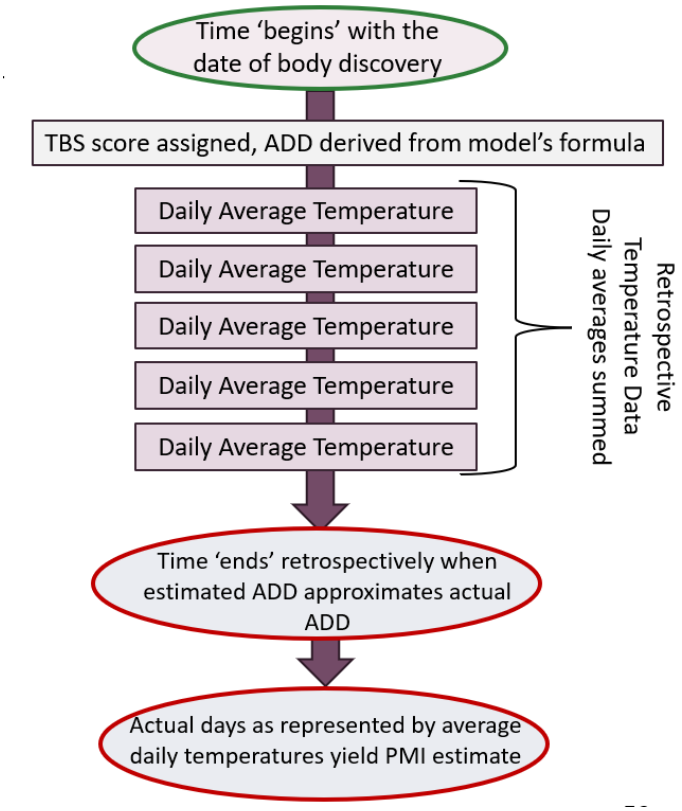

Figure 2-4: Summary of steps performed in PMI estimation as outlined by the TBS model (created following Megyesi *et al.* 2005).

Within its intracategorical descriptions, the TBS model uses 'classic,' descriptions of decomposition change (skin slippage, purge, soft tissue color change, marbling, bloat, moist decomposition). These categories were once considered to be both universal and sequential, (demonstrated by the mode and pattern of their use in the TBS model) but have increasingly been proven to diverge in sequence and instance of presentation, and in weight as a catalyst for

decomposition (Connor *et al.* 2019). Because these categories will serve as a source of qualitative inference in this study, a brief description of each category is provided.

A. *Skin slippage:* An early postmortem change catalyzed by the release of hydrolytic enzymes by cells lining the dermal-epidermal junction. As the dermal interface barrier is compromised, the epidermis begins to separate from the deeper, denser, keratinized dermis. The upset of structural integrity results in superficial tissue layers that may form fluid filled pockets (bulla), provide shelter for feeding larvae, or otherwise be easily removed or displaced (Clark *et al.* 2006).

B. *Marbling:* Postmortem staining of the intima of large blood vessels by hemolysis (autolysis of red blood cells) and gravitational settling of blood. This process is visible on external surfaces of the body and morphologically maps the large blood vessels of the circulatory system (*ibid*).

C. *Bloat: In vivo* homeostatic processes dictate volume and type of bacterial growth. The postmortem breakdown of carbohydrates, proteins, and lipids catalyze unbridled bacterial growth. A byproduct of bacterial metabolization is the release of gases which aggregate and expand when trapped within the lumen of the stomach, resulting in distention of the abdomen, proximal limbs, and the neck (*ibid*).

D. *Purge:* Concomitant to the confinement of gasses is the release of a major constituent element, hydrogen sulfide (H_2S). H_2S is a major progenitor in the decomposition of internal organs. Because the source of H_2S is the gas entrapped in the lumen of the stomach, the gastrointestinal tract is especially sensitive to its effects. As liquefaction occurs in the gastrointestinal tract, the trapped gasses provide the pressure necessary to expel these fluids through peripheral openings, including the anus, eyes, ears, nose, and mouth (*ibid*).

E. *Soft Tissue Color Change:* Color change is a dynamic process that occurs throughout decomposition. The progenitors of color change are not well understood but are the byproduct of at least two decomposition phenomena. These include: (1) the decomposition of hemoglobin and conversion of the heme constituent into a series of bile pigments; and (2) formation of precipitates of H_2S within vessels and tissues. The macroscopic phenomenon of color change is the result of these byproducts interacting with tissues composed of different cellular volume and type, affected extrinsically by environmental variables (Gill-King 2006).

F. *Moist decomposition:* The presentation of the collective process of endogenous decomposition (putrefaction) as bacterial metabolization pushes gasses to organ and peripheral tissue structures. As the structural integrity of superficial tissue structures begin to degrade, the macroscopic purging of fluids is visible across affected body surfaces (*ibid*).

2.4 The Colorado Rocky Mountains: A Unique Environment

Of equal importance to the endogenous factors of decomposition are the exogenous variables within the local environment, which may serve to accelerate or impede the trajectory of decomposition. The Rocky Mountain Region of Colorado extends more than 3000 miles from northern British Columbia, Canada to the state of New Mexico in the Southwestern United States. While the region presents general trends in geological, altitudinal, and ecological continuity, the Colorado Rocky Mountains (CoRM) present several spatially distinct characteristics. Traits that distinguish the CoRM from the contiguous Rocky Mountain chain include unique: (a) geology; (b) climate; (c) altitude; and (d) ecology. FIRS-TB40 is located in the South Park (Park County) Region of the Colorado Rockies. South Park is a grassland flat oriented within the basin of the Mosquito and Park Mountain Ranges in Central Colorado (Figure 2-5). This position is important because it constitutes an interface between the Eastern and Western slopes, which are biogeoclimatically distinct, largely due to their spatially unique interaction with trade winds and attendant climate patterns as they cross the continental divide (Cannings 2005). As

such, the position of the South Park Basin between the two slopes yields an amalgam of biogeoclimatic variables otherwise independently observed, providing an analytically neutral research domain reflective of both the East and the West slopes.

2.4.1 Geology

Homogenous geologic features of the contiguous Rocky Mountain chain include Precambrian metamorphic rock, and sedimentary argillite superimposed by Paleozoic limestone and dolomite. Regionally distinct patterns of geologic formation began during the Pennsylvanian, when Precambrian metamorphic rock was thrust upward through layers of limestone and dolomite, forming the Ancestral Rocky Mountains. Erosion throughout the Paleozoic and Mesozoic eras resulted in exposure of extensive sedimentary beds. Geologic division characterized the northern and southern Rockies throughout the remainder of their formation. While uplift of the Canadian Rockies was the result of tectonic collision, the CoRM were formed by subduction of the Farallon plate beneath the North American plate. The result of this subduction was the dramatic uplift of crust, resulting in the angular thrust of superimposed sedimentary layers, hypothesized to have exceeded 6100 meters/20,000 feet in height. Erosion spanning 60 million years has yielded the current landscape of the CoRM, characterized by the highest peaks in the Rocky Mountain chain (4400 meters/14,440 feet) and transient landscapes defined by dramatic slopes, rapid erosion, and dynamic, high mineral content soils (Cannings 2005).

The South Park region is primarily undercut by Paleozoic and Mesozoic sedimentary and volcaniclastic rocks that host a stratabound uranium deposit superimposed by a layer of glacial moraine. The moraine promotes high drainage capacity while the underlying granitoid rock yields mineralization that make local soils dynamic and rapidly mutable as minerals and sediment filter through the environment (Scarbrough 2001). Locally, FIRS-TB40 is bisected north to south by a steep, rocky moraine-like ridge, making it representative of regional geologic patterns. When these dynamic, well-drained soils are contextually collated with the dramatic slopes that characterize the CoRM, the product is a

capricious landscape where the confluence of gravity, slope, and geology constitutes a powerful taphonomic agent. In sum, yielding a spatially relative and characteristically unique environment that serves to promote the movement of human remains and the drainage of decomposition fluids.

2.4.2 Climate of the Colorado Rocky Mountains

The climate of the Rocky Mountain region is recognized as among the most extreme on the continent, a phenomenon largely attributed to complexity yielded by the interaction between high-altitude and competing trade winds (Cannings 2005). The competing physical effects of gravity and temperature result in the net reduction of atmospheric pressure at high-altitude. As pressure drops, the adiabatic lapse rate results in a concomitant temperature decrease of approximately 1 °C for every 100 meters (300 feet) of elevation gain. Climatic patterns in the region are unpredictable and characterized by rapid change. Summers are mild, and winters are defined by heavy snowfall (215 cm annual average) with persistent snow overburden and high precipitation (35 cm annual average). Annual temperatures reach average lows of -12.78 °C; winters are characterized by snowfall and high winds that produce white-outs and promote a perpetual state of atmospheric motion, despite the presence of an 'inert' layer of snow overburden. Annual average high temperatures reach 20.55 °C; summers are characterized by rapid and dramatic changes in air pressure and summer storms that yield wet summers in a phenomenon referred to as the North American Monsoon. In the spring and summer, a high-pressure system develops over the middle of the Great Plains and transports warm, moist air from the Gulf of Mexico north to the Rockies. The humid air is lifted by the afternoon sun, a phenomenon promoted by updrafts associated with the crossing of high mountain peaks. This cycle results in rapid cooling and the release of moisture in dramatic thunderstorms. When local temperature and humidity are sufficient, moisture release may constitute 5-10 percent of a site's annual rainfall within the span of one hour (Cannings 2006). Moisture run-off is promoted by steep mountain slopes and dynamic soils. Dramatic influxes of moisture are punctuated by hailstorms, flash floods, and forest fires that may be

swept into the apex of competing winds, creating firenadoes – a column of air and fire that sweeps the landscape and promotes the spread of natural wildfires. While the Canadian Rockies are steeper and more jagged in appearance, and the Alaskan mountain ranges more treacherous in wildlife, the respective environments are largely characterized by slow glacial movement, rendering them less dynamic and chaotically complex than the Colorado Rockies. Summarily, the region is defined by complex climatic patterns that are unparalleled in the continental United States (Cannings 2006), and therefore the cross-section of these competing and cooperating weather systems is anticipated to have a dramatic impact on the local rate and pattern of decomposition.

2.4.3 Ecology of the Colorado Rocky Mountains

The contiguous Rocky Mountain chain is bisected by the Wyoming Basin's arid plain of short-grass prairie, which interrupts the distribution of floral and faunal species, rendering the CoRM biologically distinct from the northern Rockies (Figure 2-6). Because the local microenvironment has a direct impact on the rate and pattern of decomposition, the entanglement of climate and geography with local flora and fauna necessitates the intercalation of these variables into local ecoregion classifications. The distribution of ecoregions across the United States is presented in Figure 2-7 and further demonstrates the distinctiveness of the CoRM from both the contiguous Rocky Mountain Chain, and the broader United States. These classifications generalize regions but also serve to provide higher resolution models for local natural diversity. The United States Department of Agriculture (USDA) defines ecoregions along four hierarchical levels: (1) domains represent groups of related climates based on temperature and precipitation; (2) divisions represent a higher resolution climactic model based on precipitation pattern and level and temperature within a domain; (3) provinces constitute the subdivision of divisions based on vegetation and other natural land covers; and (4) sections represent the highest resolution local model based on the subdivision of provinces by terrain and feature.

In mountainous regions, sections may be assessed in increasing levels of complexity in areas that exhibit different ecological zones based on elevation. The Rocky Mountain Region of Colorado is designated M331 Temperate steppe regime mountains: domain – dry; division - Southern Rocky Mountains steppe – open woodland – coniferous forest; province - alpine meadow. The region is designated several divisions to represent altitudinal zonation, named from the spectrum of zones from lower to upper (subnival). Altitudinal zonation is associated with changes in climate, and local floral and faunal populations, adding an additional layer of biological complexity to the region.

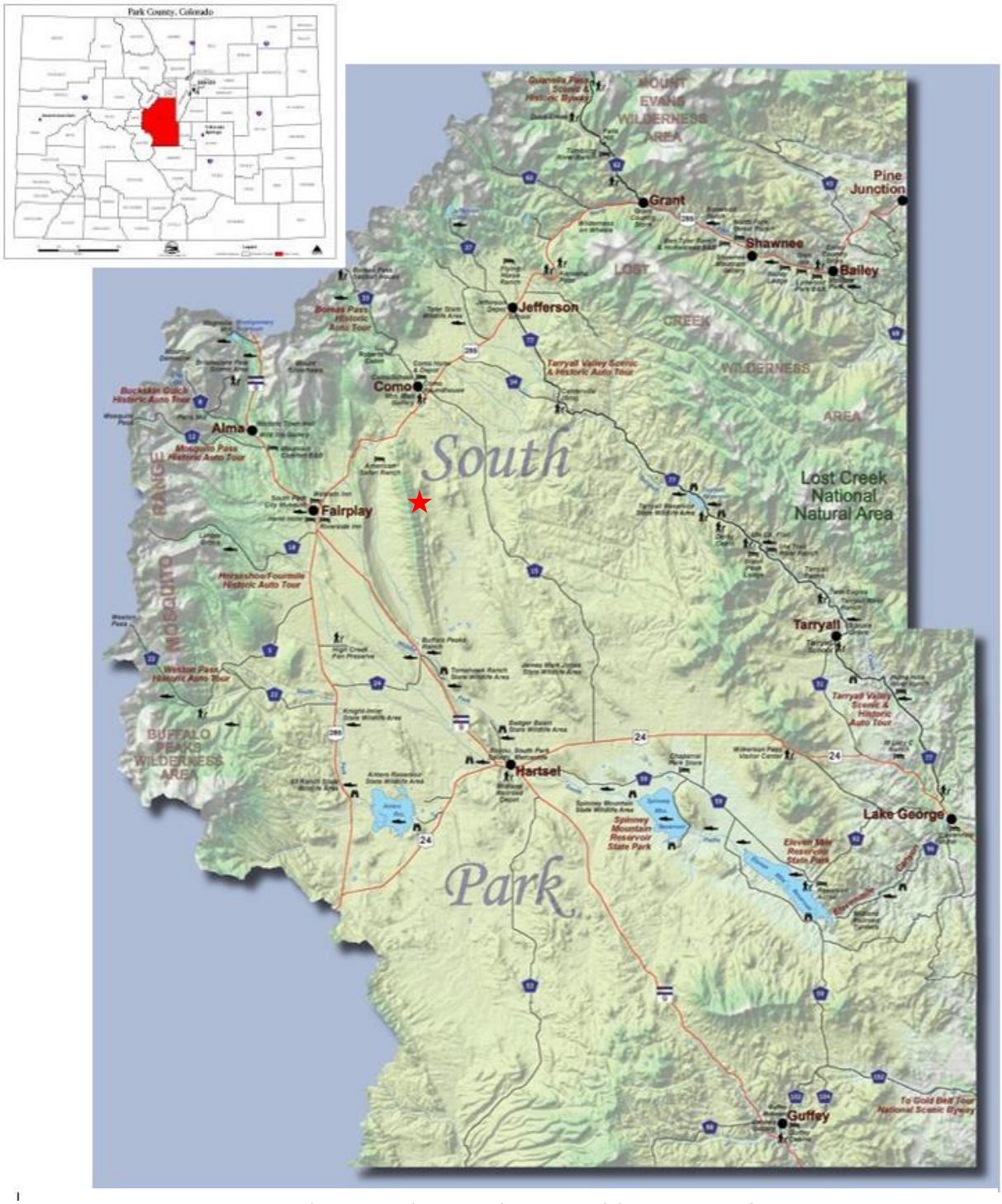

Figure 2-5: Park County (South Park) region of Colorado: (a) orientation of Park County within the counties of Colorado (upper left); and (b) topographic map of Park County, approximate location of study site indicated by red star (https://exploreparkcounty.com/maps-brochures/).

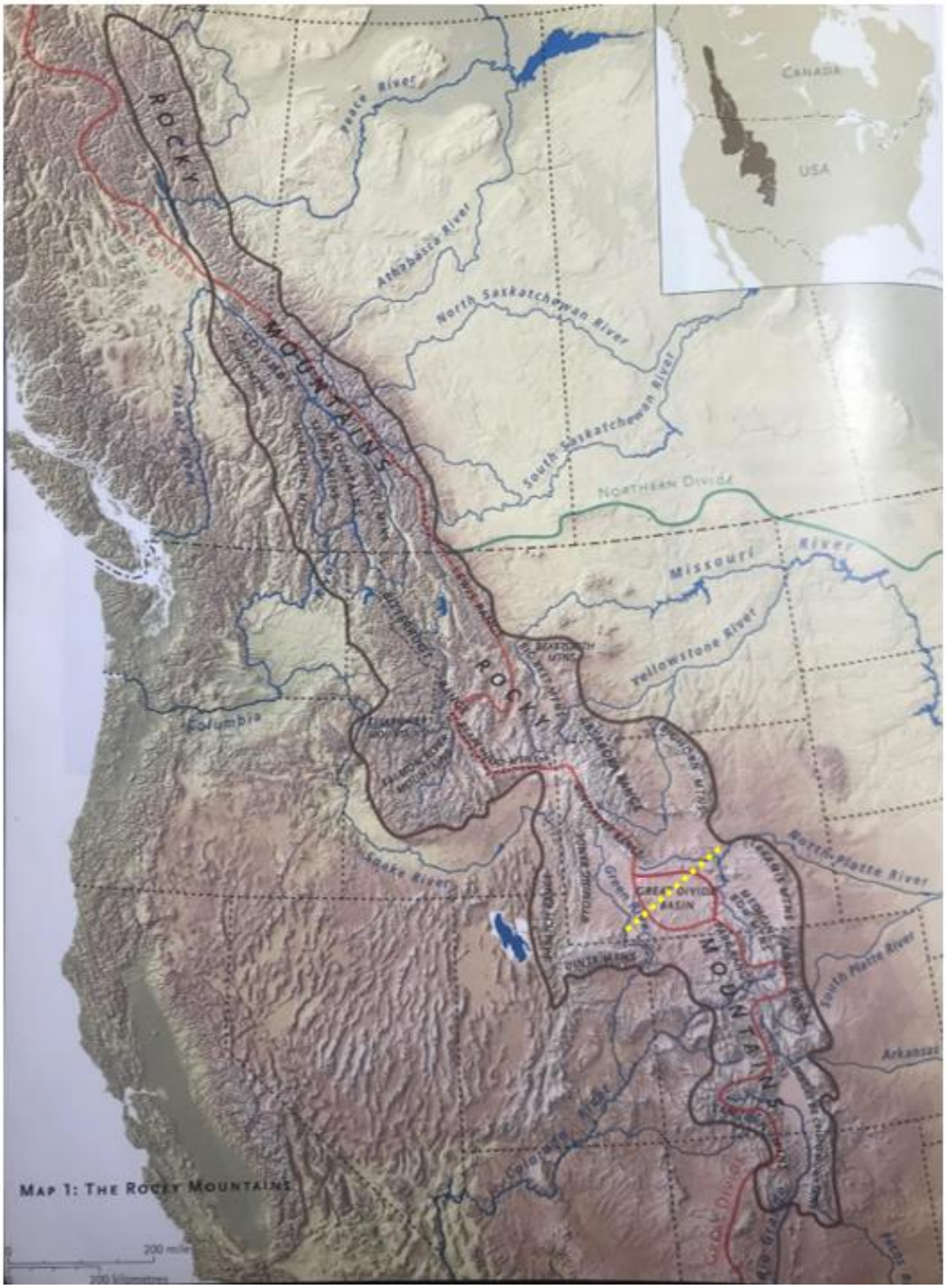

Figure 2-6: Geographically classified Rocky Mountain Region with the north/south slope divided (red line) and an approximation of the great divide indicated in yellow (Cannings 2005).

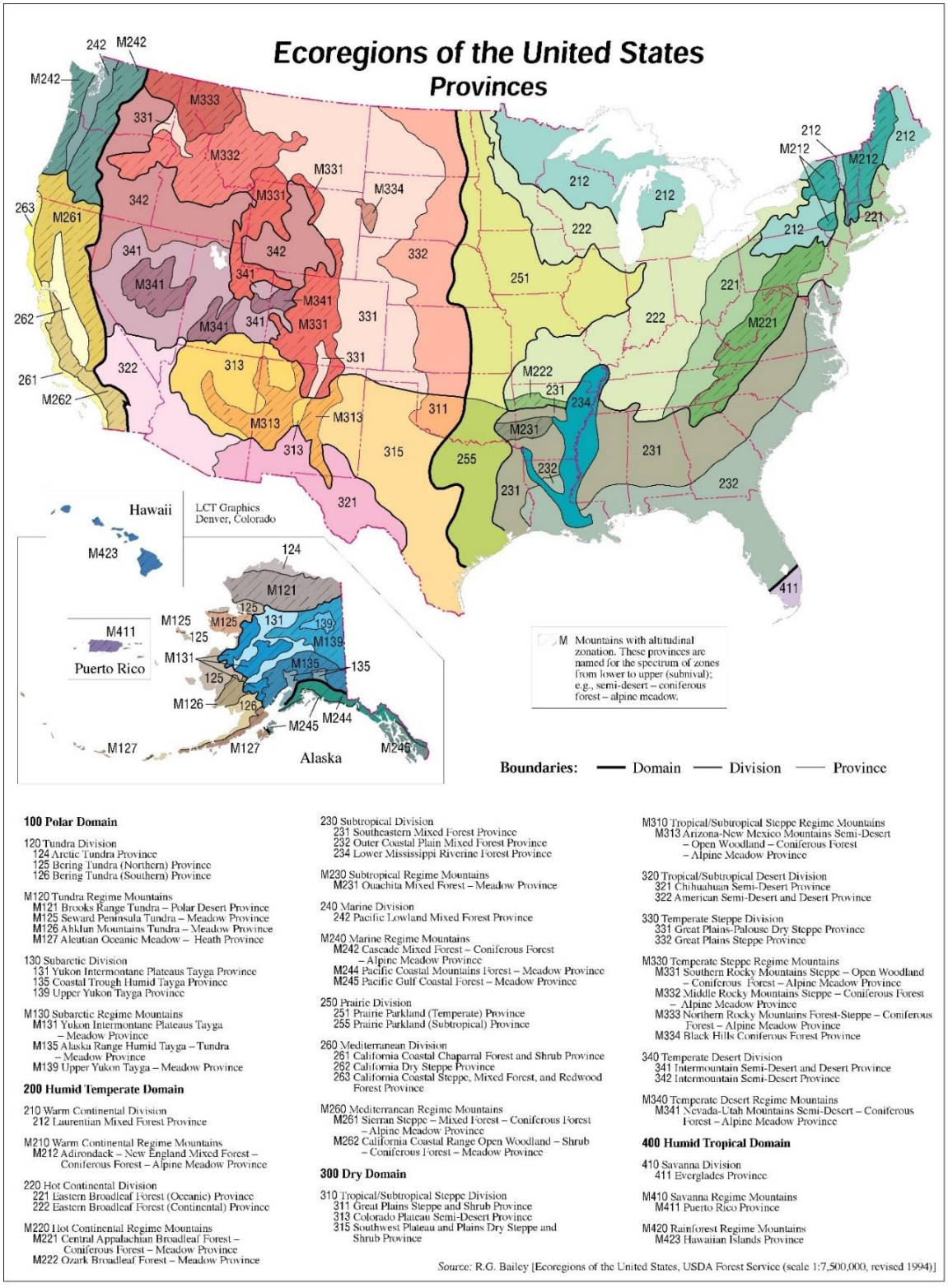

Figure 2-7: Ecoregions of the United States. The Colorado Rocky Mountains are designated M331 domain – dry; division - Southern Rocky Mountains steppe – open woodland – coniferous forest; province - alpine meadow (Bailey 1995).

2.4.4 Site flora

High-altitude and the associated atmospheric variables yield a distinct local landscape at FIRS-TB40. Primary site flora includes scrub grasses and stunted juniper with low canopy cover. Brush, weeds, and grasses grow to variable heights within the understory and include wormwood, sagebrush, fireweed, blue grass, cord grass, and sedges. While tree populations are sparse, the shedding of pine needles across time has resulted in a substantial layer of tree duff on the eastern slope. The site is further characterized by tree fall in various stages of decomposition and short spiney cacti.

2.4.5 Site fauna

Park County hosts a diversity of wildlife including large-bodied ungulates such as elk and moose, medium-bodied ungulates such as white-tailed deer and ibex, and diverse taxa of rodents, avians, reptiles, and arthropods. From a forensic perspective, arthropod and vertebrate scavengers have the highest potential for interaction with decomposing human remains and are therefore of primary interest. Baigent *et al.* (2019) assessed local scavenger succession and progression at TB40 using four pig carrion. The results indicated that turkey vultures (*Cathartes aura*), ravens (*Corvus corax*), and black-billed magpies (*Pica hudsonia*), were the three primary cooperative avian species that shared an affinity for scavenging throughout early and advanced decomposition. Coyotes (*Canis latrans*) were less numerous but facilitated greater gross tissue loss. American black bears (*Ursus americanus*) constituted the final wave of scavenger succession. While documented onsite, black bears did not exploit carrion, an observation consistent with those reported by Baigent *et al.* (2014) at a second high-altitude site in Colorado Rockies. Figure 2-8 presents an overview of scavenger succession and progression observed within the first 30 days of this study.

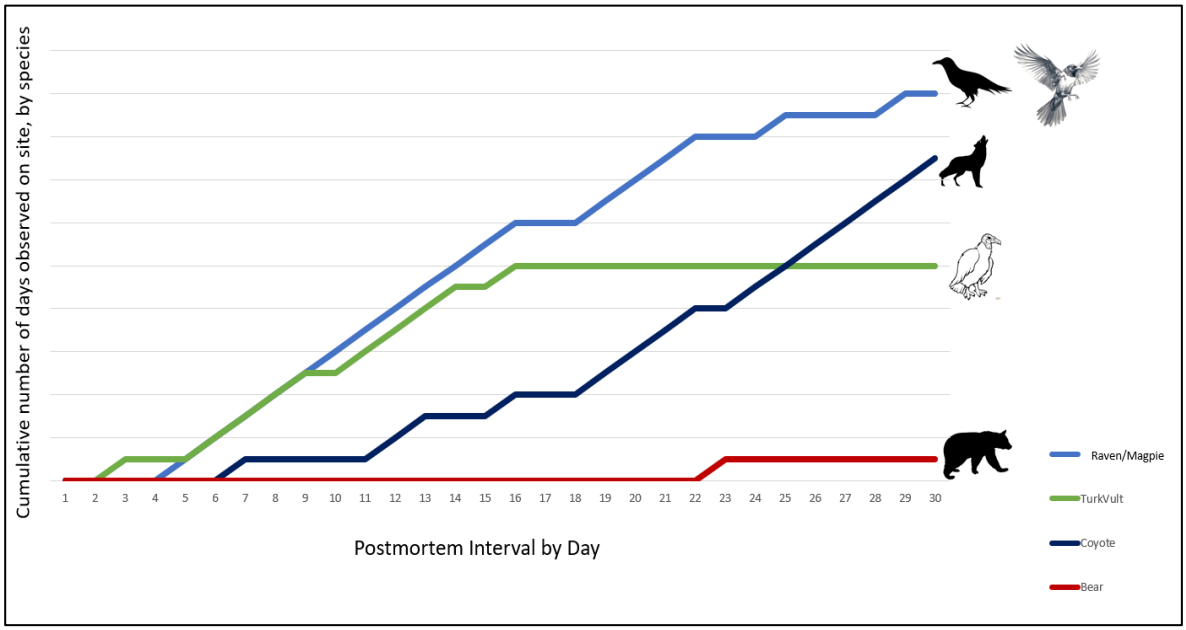

Figure 2-8: Overview of daily scavenger succession and progression by species, observed in the first 30 days of study among a cohort of pigs at the study site Baigent *et al.* (2019).

2.4.6 Human Physiology – High-altitude Environments

In addition to environmental distinctiveness, high-altitude regions are associated with behavioral and physiological distinctiveness. 'High-altitude' is clinically defined by three subcategories that reflect elevation and the amount of oxygen available in the atmosphere, these categories include: (a) high altitude (1500 – 3500 m); (b) very high altitude (3500 – 5500 m); and (c) extreme altitude (5500+ m). Environmental and physiological effects become appreciable above 2400 meters (Imraya *et al.* 2010). Physiological adaptations associated with high-altitude structurally and functionally impact the oxygen transport chain, and among many variables, include increased (1) efficiency in oxygen transport (Scheinfeldt & Tishkof 2010); (2) hemoglobin production and concentration (Rupert & Hochachka 2001); (3) nitric oxide synthesis to promote blood flow regulation; and (4) increased rate of respiration (Beall & Goldstein 1987). In high-altitude regions, these physiological changes are spatially and temporally distinct, suggesting that they have been selected for repeatedly, but with variable, population specific outcomes (Windsor & Rodway 2007). In addition to these longitudinal adaptive changes, multiple

pathways for temporary physiological change associated with acclimatization to hypoxia have been identified.

Modes of acclimatization have been more generally and heterogeneously adapted among and between human populations. In the early phase of hypoxia, cardiopulmonary metabolic demands are favored, a byproduct of which is the suppression of short-term non-essential metabolic function such as digestive efficiency. Hyperpnea and an increase in cardiac beats per minute with a concurrent decrease in stroke rate define early acclimatization. Blood pH is elevated (pH > 7.45) as a byproduct of increased respiration (respiratory alkalosis), with concomitant reduction in arterial levels of carbon dioxide. Full acclimatization is achieved across days and weeks, during which respiratory alkalosis is mitigated by renal excretion of bicarbonate. Carbohydrate catabolism is slowed, resulting in a decrease in lactate and pyruvate production which summarily upsets the rate of adenosine triphosphate (ATP) synthesis. Decreased plasma volume due to increased red blood cell mass results in increased hematocrit, signaling anastomosis formation resulting in higher concentration of capillaries in skeletal muscle tissue containing increased levels of the iron- and oxygen-binding protein myoglobin, mitochondria, aerobic enzyme concentration, 2,3 Diphosphoglyceric Acid (2,3-BPG), a three carbon isomer that decreases the affinity of hemoglobin for oxygen, hypoxic pulmonary vasoconstriction, and right ventricular hypertrophy. Peripheral to the heart, pulmonary artery pressure is increased in an attempt to increase blood oxygenation. Long term physiological response to the high-altitude environment include environment specific cascades of circulatory, respiratory, and hematological adaptations, highlighting the range of phenotypic diversity in altitude-response phenotypes (Bigham & Lee 2014).

2.4.7 Cultural patterns of the Colorado Rocky Mountains

Like physiological adaptation, cultural adaptation to high-altitude is temporally and spatially relative. Broadly, these changes include locally distinct subsistence patterns, especially among mode and pattern of plant and animal domestication, novel fuel sources, clothing technology, ritual modeled to

promote respiratory efficiency, and marriage and kinship configurations (Barton 2016). Locally, the CoRM serves as a gateway to North America's 'Wild West' and as a result has been imbued with cultural narrative, rendering the mimesis iconic in American popular culture. The dramatic landscape of the CoRM is spatially and visually distinct, resulting in its idealization and mythologization, yielding complex and heterogeneous cultural geographies that are historically, temporally, and spatially distinct (Holtkamp *et al.* 2018).

Heterogeneity in 'mountain culture' may be related to early settlement patterns within the American West. Early settlement was heavily influenced by the physical environment, resulting in communities isolated by distance and inhospitable terrain (Gastil 1976). Longitudinally, this pattern of discrete settlement resulted in a nodal pattern of cultural development. Historicity in the Rocky Mountain region is most deeply influenced by indigenous populations, followed temporally by French fur trappers whose passage into the region was delayed by isolation and rugged terrain, making it one of the last regions of colonial settlement in the Continental United States (Gastil 1976). Colonization of the vast and harsh landscape necessitated deployment of extensive industrial resources, industry centered on resource extraction, and extensive manipulation of the inhospitable landscape. As a result, successful settlement was characterized by individuals physically and psychologically suited to contend with the unique demands of the harsh environment (Woodward 2011; Holtkamp *et al*. 2018). Across time, increased ease of inter- and intra-region travel, and high amenity values have resulted in greater cultural admixture and fluidity within the contemporary Rocky Mountain west. However, distinct cultural differences between longtime residents and in-migrating residents remain palpable (Mountain Migration Report 2021).

2.5 Introducing Cultural and Environmental Perception Theory to Forensic Anthropology

Because local culture is distinct in all areas of practice, it has the potential to play an integral role in forensic investigation. Statistics provided by both the Park and Summit County Coroner's Offices

demonstrated that out-of-county deaths constitute a substantial percentage (22-47%) of each county's annual deaths. While outdoor deaths in the region may be the result of an acute medical event, accident, or suicide, these statistics further imply that while the mountainous terrain is difficult to traverse, the rural, wooded landscape does not dissuade clandestine body deposition. However, while present in practice, behavioral complexity associated with 'entering' remote landscapes suggests that back country death and body deposition is sensitive to modes of individual habitude.

Despite the vast landscape and the percentage of state and federal lands that facilitate access to the outdoors, 'entering' the Rockies is not a simple task, as the rugged terrain makes access to off-highway rural landscapes complex. Practical consideration is rendered more complex by formal and informal sanctions associated with property ownership. Rural homesteads and ranches are typically characterized by extensive fence and firearm protection, while legal and illegal drug production has resulted in the synthesis of locally controlled 'territories' that are recognized by local residents - but unlikely by outsiders - as dangerous or no-access zones. When discussing outdoor recreation in the CoRM, a common question posed by people unfamiliar with the region is, "but how do you know where to go?" This simple question makes a critical point. Despite the existence of volumes of publications pertaining to outdoor recreation in the Rocky Mountain region, and thousands of mapped trails, an individual unfamiliar with the region may feel limited by a lack of personal knowledge of the landscape (Dyson-Hudson & Smith 1978).

Formal and informal sanctions and individual proficiency act as barriers to individuals attempting to access a landscape. Environmental perception theory offers a framework within which to understand the complexity with which the human-environment relationship is imbued. In theorizing modes of environmental perception, Gibson (1979) argued against the dichotomized mind and body and instead asserted that a network of sensory pathways facilitates the perceiver's immersion into his or her environment. In this model, the environment is a dynamic, multilinear process of sensory input and

processing that promotes construction of the environment and self-perception. Drawing on Gibson, Ingold (2000) argues against the dualistic approach to the biophysical and sociocultural human that pervades along four-field intradisciplinary lines. While forensic anthropologists recognize and purport to observe the biocultural approach, many remain guilty of prioritizing human morphology and *post hoc* consideration of behavioral patterns derived from spatial analyses in forensic investigation. Ingold suggests that human perception of the environment is an ongoing project brokered by skills incorporated into the human organism through practice and training in the environment. Since practice implies change in proficiency, the implication is that perception of the environment is an ongoing, dynamic project with historic, spatial, and temporal relevance. The 'person' is not an organism walking around on the environment, but an organism immersed in the environment. Nor is the person a mosaic entity composed of discrete but complementary parts such as mind/body/culture, but a "singular locus of creative growth within a continually unfolding field of relationships" (Ingold 2000:4-5).

Ingold (*ibid*) considers environment perception theory along three primary analytical lines: (1) cultural differences are foundationally rooted in differences in skill; (2) skill does not reflect a generalized set of capacities, nor is it innate; and (3) skill can only be understood in the context of the environment. Ingold does not regard 'skill' as a simple series of technical tasks performed by the body, but reflective of the totality of the whole organic-being, manifest in their capabilities of action and perception within an environment. As properties of the indivisible human composed of mind/body/environment, skills are both biological and cultural. Skill is reflective of the sum of the biocultural experience and therefore the term is not used to refer to a general set of technical capacities that are transferable or innate. Culture facilitates the sharing of knowledge - culture does not ensure proficiency in skill. As a result, skills are regrown and reincorporated across generational lines in an ongoing series of human development modulated by training and experience through performance. Subsequently, skill can only be understood in the context of active engagement with the constituents of

the (social, physical, biological) environment. Humans are one form of organism in a world composed of manifold types of human and non-human forms. Therefore, relations among humans – while often regarded as unique social beings – are merely a subset of ecological relations. The thrust of Ingold's theory is the ongoing project of skill acquisition which serves to reorient an individual within an environment across time and space. Urban dwellers express a discomfort with entering rural Rocky Mountain landscapes because they have not acquired the skill to gain a sense of confidence and proficiency within the environment.

Environmental perception theory thus provides a framework for understanding why individual perception of local environments may differ, and the impact this may have on how the environment is accessed, utilized, and experienced. While a full ethnographic study is outside of the purview of this project, it is proposed that 'rapid ethnography' may provide the framework for which future, holistic ethnographic study may be achieved. For the purpose of this study, the integration of local human behavior will be preliminarily achieved (1) macroscopically through a review of human behavior unique to the local environment, in anthropological perspective; and (2) microscopically through presentation of local land use and its potential to inform local patterns of human behavior, case data, and a discussion of human behavior in the local environment.

2.5.1 Human Behavior in Forensic Anthropological Context: Current State

The grounds for the lack of theory-driven ethnography performed to integrate human behavior into a local forensic ecological profile are many. From a practical perspective, biological anthropologists are variably trained in cultural anthropology and ethnographic field methods throughout the course of their education. Once immersed in one's own subdiscipline, the performance of ethnographic field work in addition to discipline-specific academic and case consult demands is not practical or viable. However, resistance to the integration of cultural anthropology into forensic anthropology has deeper roots that must be considered.

The cross-section of behavioral, physiological, and cultural modification catalyzed by high-altitude environments demonstrates active human engagement on multiple levels. This study therefore proposes to integrate human behavior into the forensic ecological profile. Aspects of the four-field approach are currently present in forensic anthropology theory, method, and practice. Field search and recovery operations are heavily informed by archaeological theory and method (Dupras *et al.* 2012; Manheim *et al.* 2006; Listi *et al.* 2007). Similar calls have been made for the consideration of material culture/biocultural complexes in ancestry attribution (Birkby *et al.* 2008) and the integration of material culture analysis into forensic case work (Skinner *et al.* 2009). Congram (2013) argues that humans catalyze the most destructive aspects of forensic taphonomy, especially as it pertains to clandestine body disposal. However, forensic anthropologists have largely remained silent on the consideration of *Homo sapiens* as a taphonomic agent. It may be superficially argued that human behavior, psychology, and motivation are too variable and complex to derive meaningful analysis. However, this would negate the utility of centuries of work performed by cultural anthropologists, who have steadily demonstrated that meaningful patterns of behavior can be derived from local cultural complexes. Additionally, the forensic taphonomy literature is replete with case studies, cross-sectional studies, and (more recently) empirical observation of vertebrate and invertebrate scavenger behavior (Haynes 1983; Haglund *et al.* 1988; Haglund *et al.* 1989; Willey & Snyder 1989; Komar & Beattie 1998; Reeves 2009; Spradley *et al.* 2012; Dabbs & Martin 2013; Saladie 2013; Olson *et al.* 2016; Sincerbox & DiGangi 2018), which have historically been argued to be equally complex (Moleón *et al.* 2014). Further, the distinction made between 'human behavior' and 'scavenger behavior' is demonstrative of the analytical propensity for extracting human behavior from the environmental complex.

Regional ecological profiles tend to be limited to consideration of the ambient environment, local scavenger guilds, and behavioral interactions between perpetrator and decedent. By failing to consider localized patterns of human culture and behavior in the construction of the ecological profile,

forensic anthropologists are guilty of distinguishing between human behavior and the environment, as opposed to incorporating human behavior into the local environment. Both directly and indirectly, *Homo sapiens* constitute a formidable taphonomic agent. However, human behavior in forensic context is typically limited to a superficial cluster of macroscopic patterns used to generally inform the structure of an outdoor search, or are narrowly focused on the behavioral interaction between perpetrator, decedent, and (post)deposition environment (Nawrocki 2009). Examples of these macroscopic patterns include the spatial relationship between remains and the nearest road or major point of ingress (Manheim *et al.* 2006; Listi *et al.* 2007; Sorg 2013) and rate of movement across a landscape based on topography (Cox *et al.* 2008). However, these patterns are limited by data sets composed of bodies that have been found and cannot be considered representative of the continuum of regional patterns of body deposition.

This paper argues in part that when considered relative to a sociopolitical niche, local patterns of human ecological behavior can be meaningfully integrated into the regional forensic ecological profile using an ethnographic approach. Sorg (2013) advocates interdisciplinary collaboration in the construction of regional taphonomic profiles and presents a panel of interlocuters that includes local outdoor guides and wildlife experts from which passive ethnography may be derived. To date, a theory driven ethnography performed with the goal of integrating human behavior into a local forensic ecological profile has not been performed.

2.6 Conclusion

Early models for describing local patterns of human decomposition were largely descriptive in nature and relied on phasic or categorical stages of soft tissue and skeletal change based largely on point presentation culled from retrospective case data. Because categorical models were necessarily broad and largely lacked intracategorical descriptions relevant to all microenvironments, the pursuit of establishing a 'universal model,' for PMI estimation became paramount. The Total Body Score model

(Megyesi *et al.* 2005) provided the first synthesis of categorical (qualitative) and mathematical (quantitative) model building into one comprehensive predictive model. However, the TBS model has performed poorly in subsequent validation studies.

Rather than rely on point observation of retrospective case data, human taphonomic research facilities promote longitudinal observation of rate and pattern of human decomposition in an environment specific setting. The number of human taphonomy research facilities within the United States has increased from one in 1981 to eight in 2019. Located in Grand Junction, Colorado, the Forensic Investigation Research Station (FIRS) at Colorado Mesa University is the most westerly oriented facility, and until 2018, the highest elevated facility in the United States. In 2018, FIRS-TB40 was formally inaugurated as a CMU-FIRS satellite facility. Situated in the Colorado Rockies at an elevation of 3000 meters/9840 feet AMSL, FIRS-TB40 is the first facility in the United States to undertake high-altitude study of human decomposition, and served as the site for this study. Variables that distinguish FIRS-TB40 from similar research facilities include altitude, climate, geology, local flora and fauna, human physiology, and local cultural patterns.

While intraregional study of decomposition and broader patterns of cold weather decomposition exist, a fusion is lacking. Environmental perception theory provides a theoretical framework within which to synthesize these environmental, physiological, and behavioral variables. Intraregional study has been undertaken through the use of human analogues. Summarily, the results of these studies aid in establishing Colorado's high-altitude region as analytically and investigatively distinct. Macroscopically, interregional cold weather study of human decomposition has: (a) offered competing results and conclusions; (b) been limited to non-human study analogues; and (c) been limited to case study of archaeological bone. While divergent in study sample, research design, and conclusions, the results of these studies suggest that the cold-weather environment has a high potential for impact on the presentation and trajectory of human decomposition. The sum of these data further suggest that

universal models for predicting rate and pattern of decomposition are insufficiently equipped to contend with regional biogeoclimatic diversity, necessitating the advancement of environment specific research design and study.

CHAPTER 3

MIXED RESEARCH: MATERIALS AND METHODS

3.0 Materials and Methods

To achieve the outlined goals, two primary research models were used: (1) mixed research (the collection of qualitative and quantitative data through direct observation in a semi-controlled outdoor environment); and (2) explanatory research (the use of literature, culled population and land use data, and case studies to elucidate cultural relationships).

3.1 Study Site and Infrastructure - FIRS-TB40

FIRS-TB40 is located in the Colorado Rockies Dfc (snow, fully humid, cool summer) climate region at an elevation 3000 meters/9840 feet AMSL. With both significantly higher elevation and an unrepresented climate classification, FIRS-TB40 represents a novel environment for the controlled study of human decomposition. Following its inauguration as a CMU-FIRS satellite facility, pilot research began in 2018 using a porcine cohort, followed by the placement of the first human donor in March 2020.

FIRS-TB40 is a 40-acre site enclosed by a 1.25-meter-high barbed wire fence. Within the perimeter fence, donors are protected from large-bodied scavengers within three-meter by three-meter five-panel galvanized steel cages anchored by 60 centimeters of subterraneous digdefense ™ scavenger deterrent panels (Figure 3-1). These cages were successfully field tested for proficiency using large-bodied roadkill as a scavenger attractant prior to the onset of this study. A centrally placed Onset HOBO weather station was deployed to record hourly atmospheric data, including temperature, wind (direction, speed, gust speed), precipitation, soil water content, rain, relative humidity, solar radiation, and atmospheric pressure.

Figure 3-1: 3m x 3m five-panel galvanized steel cage anchored by scavenger deterrent panels.

3.2 Study Sample

Human donors were obtained under the auspices of the FIRS human donation program. A cohort of 12 human donors was placed between March 2020 and December 2021. Seven donors were placed in 2020, five were placed in 2021. Because methods for postmortem interval estimation must be robust enough to encompass the suite of variables that may present in a forensic investigation, age, sex, stature, ancestry, body mass, trauma, pathology, and autopsy were not exclusionary in sample selection. During intake, each donor was unclothed and photographed on the anterior plane, posterior plane, and by body section (head/neck, thorax, limbs). Height was measured on a flat plane prior to placement using a standard metric measuring tape and level perpendicular edge. Weight at death was sourced from coroner records. Observed biological sex, ancestry, presence of medical devices, healed and active trauma and pathology, physiological anomalies, body modification, and initial decomposition changes were described and recorded in field notes. The FIRS standardized donation intake paperwork includes living biodemographic data (e.g. physical characteristics, occupation, medical history, and social

behavior), reported *in vivo* by living donors, or postmortem by next of kin. These data were recorded and logged in the research database.

The acceptance of donors, and the timing of their placement in the outdoor facility was necessarily opportunistic. In an effort to minimize PMI prior to placement, donors were placed with immediacy (within 24-48 hours following death); when administrative or investigative variables precluded immediate placement, donors were placed in cold storage (2-4 ˚C) in the interim. Postmortem interval prior to placement within the facility ranged from 2-24 days. Each donor's placement date was adjusted to reflect the actual date of death and the average of the morgue cooler temperature (2+4 ˚C /2) was used to reflect the daily average temperature. This model allowed for the integration of time and temperature into a donor's overall accumulated degree days. The placement TBS score for all donors ranged from 3-7 (fresh - very early decomposition). Because the cooling process aids in the arrest of decomposition, the TBS score presented at the time of placement was regarded as consistent throughout the cooling interval. While a biodemographically balanced and seasonally representative research cohort was the ideal, the reality of human donor programs – which tend to be skewed in age (older), sex (male), and ancestry (white) – precluded symmetry within the cohort structure. Seasonality could not be controlled for due to the unpredictable nature of the donor program (i.e. an individual's date of death cannot be forecast). Priority was instead placed on cohort size (an available donor was not passed over in the hope of a more temporally appropriate donor becoming available).

Data collection was further complicated by variables associated with winter in the High Rockies. Heavy snowfall precluded regular site access and visual assessment of the study cohort across the winter months. Donors were typically covered in c. one meter of snow between December and April. Weekly site visits were made via snowshoe throughout periods of heavy snow overburden, and environmental data (snow texture/morphology, depth, berm formation, and animal tracks) were recorded. While seasonal access was a limiting factor of this study, it is representative of real-life

regional scenarios in which issues of environmental obscurement, access, and safety prevent search and recovery efforts until spring. Meticulous documentation on both seasonal ends facilitated a more robust image of the changes that occurred during periods of inaccessibility.

Donor biodemographics are presented in Table 3-1. The study cohort was composed of 12 individuals. Four donors were autopsied. Baigent *et al*. (2020) suggest that autopsy incisions approximate sharp force trauma such as might be seen in a forensic case. In a study comparing rate and pattern of decomposition between autopsied and non-autopsied cohorts, no significant difference in rate or pattern of decomposition was observed between the two groups. Therefore, autopsy was not considered an exclusionary variable. Bodies were placed unclothed, in supine position at surface level. Two donors were placed in each of the described scavenger cages approximately one meter apart. Because placement was opportunistic, six donors were concurrently placed; six were asynchronously placed, resulting in presentation of divergent stages of decomposition between two donors sharing a cage. Cages were placed on an approximately 45˚slope created by the natural terrain to encapsulate gravity and slope wash as variables that may contribute to the rate and/or pattern of decomposition. All donors were placed parallel to the slope; ten donors were placed head upslope/feet downslope, two donors were placed feet upslope/head downslope. Small variation in the placement model was performed to assess whether head/foot orientation appreciably affected macroscopic patterns of decomposition. Two motion activated game cameras (one trained on each donor) were mounted to the interior of each cage to document the presence, species, and temporal activity of scavengers, and their individual mode of scavenging. Game camera captures were downloaded daily to correlate the species present with changes in the environment, and soft tissue and osseous artifact of species-specific scavenging behavior.

Table 3-1: Biometric data, placement and maximum TBS, placement and recovery dates, and maximum ADD by Donor (* indicates a donor is still located in the outdoor facility, TBS Max reflects terminus of study period).

Donor ID	Age	Sex	Ancestry	Height (cm)	Weight (kg)	Autopsied	Pre-Placement PMI (Days)	Placement Date	Placement TBS	Collection Date	Final TBS	Final ADD ˚C
20-101	69	Male	White	178	115.7		8	03/31/2020	3	11/5/2022*	26	6107
20-102	64	Male	White	175	68.9	Yes	12	03/31/2020	5	11/5/2022*	26	6122
20-103	51	Male	Black	180	84.4		23	05/28/2020	7	11/5/2022*	29	5767
20-104	75	Male	White	188	74.8		3	06/10/2020	4	11/5/2022*	28	5523
20-105	89	Female	White	150	40.8		6	07/23/2020	7	8/22/2022	33	4201
20-106	64	Male	White	173	74.8	Yes	11	07/25/2020	3	11/5/2022*	25	4832
20-107	53	Female	White	160	72.6	Yes	9	08/28/2020	3	11/5/2022*	27	4237
21-101	55	Male	White	175	70.3	Yes	17	01/07/2021	3	11/5/2022*	25	3929
21-102	65	Male	White	185	83.5		14	01/07/2021	7	11/5/2022*	27	3916
21-104	73	Female	White	178	111.1		2	08/22/2021	5	7/3/2022	31	1129
21-105	73	Male	White	178	81.6		18	10/15/2021	3	7/3/2022	31	533
21-106	72	Male	White	178	115.7		24	10/25/2021	3	11/5/2022*	31	401

3.3 Measuring Decomposition

Decomposition changes were recorded daily when site access allowed. The TBS descriptive model following Megyesi *et al.* (2005) was employed to document daily changes in gross tissue composition. While a pilot study performed within the region suggested that the TBS regression equation was not a reliable predictor of PMI at high-altitude, it has yet to be tested among a larger sample human cohort (Baigent *et al.* 2014). Additionally, the TBS model lends both a qualitative and quantitative framework to this study. The quantitative framework is derived from the value assigned categories of change defined by the model, facilitating mathematical description of the trajectory of decomposition. The qualitative framework is derived from the model's categorical description of gross tissue change. Within its intracategorical descriptions, the TBS model uses six 'classic,' descriptions of decompositional change (skin slippage, purge, specific patterns of soft tissue color change, marbling, bloat, and moist decomposition). These macroscopic categories were used as the basis for recording convergence and divergence between the changes observed within the study cohort, and those described in the TBS model.

Due to the qualitative and quantitative benefits afforded by the framework of the TBS model, data collection was performed throughout the study period following Megyesi *et al.* (2005). Observation and scoring were conducted within three anatomical regions: head/neck; trunk; and limbs (Figure 3-2). The standard TBS scoring matrices (presented in Table 3-2a-c) were applied to each body section. Each body was photographed from three angles in the anterior aspect (superior-inferior, inferior-superior, right or left lateral - dictated by donor's position in the cage) and each body section was photographed and scored independently during field observation. Additionally, both the presence and persistence of categorical macroscopic tissue change (as defined by the model) were photographed and recorded in field notes throughout the study period. These categorical descriptions were also used to aid in the identification of gross tissue change hypothesized to be unique to the high-altitude study cohort. In year

one, priority was given to scoring donors using the TBS model, and identifying, photographing, describing, and documenting environment specific gross tissue change. At the end of the first study year, unique categorical changes present within 80% of the cohort were isolated. The 80% threshold was assigned based on the associated certainty of identifying a statistically significant outcome with the alpha value set at 0.05, should the hypothesis be true for the population (Andrade 2020). In year two, a revised data sheet was created to: (1) field document the incidence, timing, and presentation of these categorical changes within donors placed throughout the second year; and (2) retrospectively document the presence of these traits using field photographs taken in the first year of data collection.

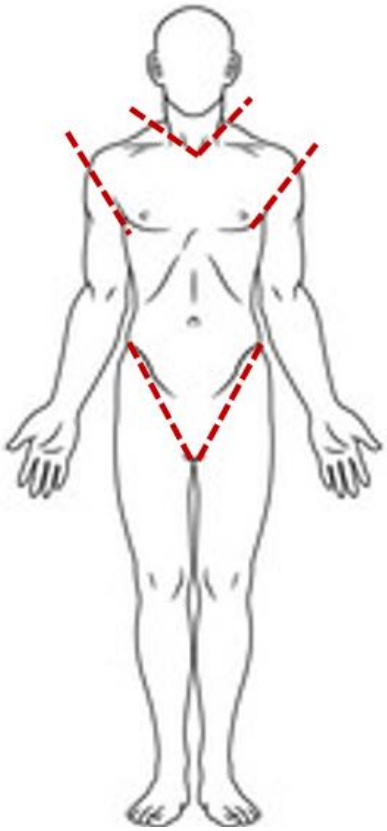

Figure 3-2: Division of the body into analytical regions defined by the TBS Model as the head/neck, trunk, and limbs (following Megyesi *et al*. 2005)

Table 3-2a-c: Categorical change associated with the: (a) head/neck; (b) trunk; and (c) limbs as defined by Megyesi *et al*. (2005).

Table 3-2a: Head/Neck: Categorical changes as defined by Megyesi *et al*. (2005).

A. Fresh	
(1 pt)	1. Fresh, no discoloration.
B. Early decomposition	
(2 pts)	1. Pink-white appearance with skin slippage and some hair loss.
(3 pts)	2. Gray to green discoloration: some flesh still relatively fresh.
(4 pts)	3. Discoloration and/or brownish shades particularly at edges, drying of nose, ears and lips.
(5 pts)	4. Purging of decompositional fluids out of eyes, ears, nose, mouth, some bloating of neck and face may be present.
(6 pts)	5. Brown to black discoloration of flesh.
C. Advanced decomposition	
(7 pts)	1. Caving in of the flesh and tissues of eyes and throat.
(8 pts)	2. Moist decomposition with bone exposure less than one half that of the area being scored.
(9 pts)	3. Mummification with bone exposure less than half that of the area being scored.
D. Skeletonization	
(10 pts)	1. Bone exposure of more than half of the area being scored with greasy substances and decomposed tissue.
(11 pts)	2. Bones exposure of more than half the area being scored with desiccated or mummified tissue.
(12 pts)	3. Bones largely dry, but retaining some grease.
(13 pts)	4. Dry bone.

Table taken from Megyesi and colleagues (2005), Table 2

Table 3-2b: Trunk: Categorical changes as defined by Megyesi *et al.* (2005).

A. Fresh	
(1 pt)	1. Fresh, no discoloration.
B. Early decomposition	
(2 pts)	1. Pink-white appearance with skin slippage and marbling present.
(3 pts)	2. Gray to green discoloration: some flesh still relatively fresh.
(4 pts)	3. Bloating with green discoloration and purging of decompositional fluids.
(5 pts)	4. Postbloating following release of the abdominal gases, with discoloration changing from green to black.
C. Advanced decomposition	
(6 pts)	1. Decomposition of tissue producing sagging of flesh; caving in of the abdominal cavity.
(7 pts)	2. Moist decomposition with bone exposure less than one half that of the area being scored.
(8 pts)	3. Mummification with bone exposure less than half that of the area being scored.
D. Skeletonization	
(9 pts)	1. Bones with decomposed tissue, sometimes with body fluids and grease still present.
(10 pts)	2. Bones with desiccated or mummified tissue covering less than one half of the area being scored.
(11 pts)	3. Bones largely dry, but retaining some grease.
(12 pts)	4. Dry bone.

Taken from Megyesi and colleagues (2005), Table 3

Table 3-2c: Limbs: Categorical changes as defined by Megyesi et al. (2005).

A. Fresh	
(1 pt)	1. Fresh, no discoloration.
B. Early decomposition	
(2 pts)	1. Pink-white appearance with skin slippage of hands and/or feet.
(3 pts)	2. Gray to green discoloration; marbling; some flesh still relatively fresh.
(4 pts)	3. Discoloration and/or brownish shades particularly at edges, drying of fingers, toes, and other projecting extremities.
(5 pts)	4. Brown to black discoloration, skin having a leathery appearance.
C. Advanced decomposition	
(6 pts)	1. Moist decomposition with bone exposure less than one half that of the area being scored.
(7 pts)	2. Mummification with bone exposure less than half that of the area being scored.
D. Skeletonization	
(8 pts)	1. Bone exposure over one half the area being scored, some decomposed tissue and body fluids remaining.
(9 pts)	2. Bones largely dry, but retaining some grease.
(10 pts)	3. Dry bone.

Taken from Megyesi and colleagues (2005), Table 4

All data were stored in an Excel spreadsheet, recorded by donor and data collection date. Individual body segment scores were input, and a total body score was auto-summed. Categorical changes were indicated as present (1) / absent (0). To maintain the resolution of data specific to each categorical change, field notes were entered in separate, category specific cells that corresponded to the change they were describing. This facilitated flagging of individual data days with a color-coded system to indicate a significant change (red), an unusual change (orange), or the persistence of a unique phenomenon (green). This also simplified donor-specific longitudinal review of each categorical change in post data collection analysis.

In instances of decomposition equivocating between two categorical stages, the point value assigned was the average of the two scores, as defined by Megyesi *et al.* (2005). In cases where the observed tissue change was not accurately described by the TBS model (e.g. a specific definition of color change), the score most closely reflective of the field observation was used and flagged with a description of the divergence during data entry.

3.4 Calculating the Suite of Atmospheric Variables

Accumulated degree days (ADD) represent the sum of daily mean temperatures within a prescribed period of time. The sum is descriptive of the accumulation of thermal energy units necessary for chemical and biological reactions to occur, and therefore represent the product of chronological time and temperature. The same principle was applied to site specific atmospheric data to calculate accumulated *x* days, with *x* representing a specific atmospheric variable. Data derived from the onsite HOBO weather station provided hourly data points for the following atmospheric variables (as defined by meteorology; Ahrens & Hensen 2018):

a. *Temperature (measured in F, converted to C; used to calculate ADD):* The temperature of the air near the surface of the earth. All temperature data were collected in Fahrenheit to the hundredth degree. These data were converted to Celsius in Excel using the formula C = 5/9(F-32).
b. *Atmospheric pressure (measured in hectopascals (hPa); used to calculate aAPD):* The force (total height of the air column of the atmosphere above it) acting on an area around a defined point. Atmospheric pressure drops as altitude increases.
c. *Precipitation (measured in mm; used to calculate aPreD):* Any product of the condensation of atmospheric water vapor, the fall of which is mediated by gravity. Primary forms of precipitation include rain, sleet, snow, ice pellets, graupel, and hail.
d. *Rain (measured in mm; used to calculate aRD):* Water droplets formed by condensation of atmospheric water vapor, the fall of which is mediated by gravity.
e. *Relative humidity (measured as a percentage of actual humidity vs. total possible humidity; used to calculate aRHD):* A ratio of the amount of water vapor present in a specified area of air, versus the amount of water vapor needed for saturation within the same specified area, at the same temperature.

f. Solar radiation (measured as kilowatt-hours per square meter (kWh/m2); used to calculate aSRD): Electromagnetic radiation (X-rays, ultraviolet and infrared radiation, radio emissions, and visible light) emanating from the Sun.

g. Wind speed (measured as meters per second (m/s); used to calculate aWSD): The temperature mediated movement of air from high to low pressure.

Hourly data were collapsed into a daily average for each data category by calculating the sum of hourly data points and dividing the total by 24. This yielded the daily units used to calculate Accumulated Degree Days (ADD), Accumulated Atmospheric Pressure Days (aAPD), Accumulated Precipitation Days (aPreD), Accumulated Rain Days (aRD), Accumulated Relative Humidity Days (aRHD), Accumulated Solar Radiation Days (aSRD), and Accumulated Wind Speed Days (aWSD). All weather data were uploaded from the onsite weather station, transferred to an Excel spreadsheet, and categorically collapsed into daily averages using the Excel add-in Kutolls™ advanced function for merging and splitting rows.

The source of temperature data and the calculation of ADD used in this study moderately diverge from the TBS model. The TBS model uses data culled from the National Weather Service (NWS) to calculate the daily average of maximum and minimum air temperatures. Because this is a pilot study primarily concerned with establishing the rate and pattern of decomposition at high-altitude, the low-resolution TBS temperature model used by Megyesi *et al.* was substituted with a higher resolution, site specific temperature and atmospheric variable model.

3.5 Quantitative analysis: Tests by Inquiry

3.5.1 Reliability

To test reliability, a random generator function (Microsoft Excel RAND) was used to create a sample subset to test intra- and inter-observer reliability.

1a. To test intraobserver reliability, a subset series of 50 packets representing one day of decomposition was scored by the author using field photographs. Results were analyzed using Spearman rank-order correlation coefficient.

1b. To test interobserver reliability, 15 second observers were solicited to apply the TBS model to donor decomposition using 15 field photograph packets, each containing an average of seven multi-focal photographs representing one day of decomposition. In addition to sample scoring, participants were asked to self-report their experience level using the TBS model (beginner, intermediate, advanced), education level (Undergraduate, Masters, Ph.D., Professional [Ph.D. or Masters]), and invited to comment on any aspect of their experience applying the TBS model to the high-altitude cohort (SIUC IRB Approved Protocol #22214). The test for interobserver reliability was selected following Gwet's (2014; Figure 1.7.1) decision chart for selecting an agreement coefficient. Krippendorff's alpha was selected because it adjusts to small sample sizes, and is applicable to: (a) any number of raters; (b) any number of values available for coding a variable; and (c) binary, nominal, ordinal, interval, ratio, polar, and circular metrics (Gwet 2014). While Krippendorff's alpha is similar to Fleiss' kappa (a variant of Cohen's kappa designed to assess three or more raters), the models diverge in their definition of expected agreement. Fleiss' kappa defines the sample size as infinite, while Krippendorff's alpha uses the actual sample size, rendering Krippendorff's alpha more precise for data higher than nominal order (Zapf *et al.* 2016). Krippendorff's alpha was run using the krippen.alpha.raw( ) function in R-Studio (irrCAC package version 1.0, Gwet 2019) to determine the relationship between TBS scores generated by the group of independent observers.

3.5.2 Test of the TBS Model

Study goal one: Test the TBS model along two analytical lines: (a) the efficacy of the TBS model for qualitatively describing the pattern of gross decomposition change at high-altitude; and (b) test the

application of the quantitative TBS regression equation for efficacy and accuracy in predicting PMI in a high-altitude environment.

3.5.2a. Qualitative Assessment

The efficacy of the TBS model for describing qualitative patterns of gross decomposition change was assessed by isolating the categorical changes defined within the model (skin slippage, purge, specific descriptions of soft tissue color change, marbling, bloat, and moist decomposition) and scoring them as present (1) / absent (0) throughout the trajectory of decomposition. Category specific present/absent scores were summed at the terminus of data collection to establish the percentage of the cohort within which each categorical change presented. When a donor presented the defined change, presentation and duration of presentation were described in terms of ADD to comparatively test for homogeneity in the timing of presentation between donors. *Post-hoc* power analysis was performed for each trait. The 80% threshold for trait presentation within the cohort was applied. When a categorical change failed to meet the 80% threshold, it was eliminated as a variable of interest in future model building.

3.5.2b. Quantitative Assessment

To perform an impartial and accurate comparison, the quantitative efficacy of the Total Body Score Model was tested among the high-altitude cohort following the Megyesi *et al.* (2005) study design. Specifically:

- *Data set:* The data set used to establish the TBS model limited PMI to less than one year. Data analysis among the high-altitude cohort was limited to an individual donor's first year of decomposition.

- *Temperature:* The TBS model argues that cessation of decomposition occurs at 0 ˚C. In accordance with the model, site specific temperatures below 0 ˚C were converted to zero in the calculation of ADD.
- *Distribution:* The distribution of ADD and PMI were plotted against TBS. Because TBS is used to predict ADD and subsequently PMI, TBS was plotted on the x-axis, and ADD and PMI were plotted on the y-axis.
- *Transformation:* ADD and PMI were Log_{10} transformed to normalize the data; TBS was squared to approximate modeling a non-linear relationship and address heteroscedasticity.
- *Analysis:* Linear regression was performed, and a regression line fit to the transformed data.

3.5.3 Quantitative Analysis: Rate and Pattern of Decomposition at High-altitude

Study goal two: Quantitatively describe the longitudinal macroscopic rate and trajectory of human decomposition within a sample placed in an outdoor setting at high-altitude to assess the relationship between TBS and site-specific atmospheric variables not considered in the TBS model.

3.5.3a. Temperature Scales

Although Megyesi *et. al* apply a temperature correction based on the assumption of decompositional arrest at 0 ˚C , the authors concede that "…it is not known at what temperature decomposition processes actually cease" (2005; 5). Therefore, the trajectory of intracohort TBS was first compared to three ADD temperature scales: ADD Celsius (ADD C), ADD Celsius greater than zero (ADD C>0), and ADD Kelvin (ADD K) to assess general trends within, and variation between, each scale.

3.5.3b. Data Distribution: LOESS

Data distribution was next assessed by individual donor and individual atmospheric variable using distribution plots fitted with a locally estimated scatterplot smoothing (LOESS) curve. While one of many non-parametric models, LOESS is arguably one of the most flexible

(Jacoby 2000). Flexibility is derived from the relaxation of conventional regression methods. Rather than estimate parameters within the confines of y = mx+b, nonparametric regression is concerned with the fitted curve. In this model, the fitted points and their standard errors are estimated with respect to the whole curve - as opposed to one estimate - and overall uncertainty measured by how well the estimated curve fits the population curve (Cleveland 1979, Cleveland & Devlin 1988). Equally, if not more advantageous, is the lack of function specificity. LOESS requires that the analyst provide a smoothing parameter value (window span) and polynomial degree, but does not require that the analyst specify a function to fit a model to all of the data in a sample. The LOESS smoothing function favors reflexivity by making minimal assumptions about the relationships among variables. LOESS uses a series of sliding 'windows' that encapsulate a defined number of points subjected to sum of least squares analysis. Each 'window' informs a section of the curve and the structure of the next window, collectively these windows determine the shape of the curve. The result of LOESS application is a line through the moving central tendency of the stressor-response relationship, facilitating visual assessment of the relationship between two variables (Cleveland 1979). This serves to propagate reflexivity, making LOESS ideal for modeling complex processes lacking a central or agreed upon theoretical model (NIST/ SEMATECH 2023).

The loess( ) function was used in R; the function's default settings (fit a parabola and a defined window span of $\alpha = 0.75$) were applied. Future model building will be established on a better understanding of the predictive power of each atmospheric variable. Data distribution was structurally considered toward that end; TBS is plotted on the x-axis and accumulated atmospheric variables are plotted on the y-axis; all data are presented on the LOG scale.

3.5.3c. Multivariate Regression

Following gross analysis of data distribution, a multivariate regression model simultaneously incorporating all atmospheric categories as the response variables, and TBS as the single explanatory variable was performed. The R-squared value associated with each variable were compared to determine the percentage of variation in decomposition explained by each atmospheric category. Polynomial order was tested using the first, second, and third degrees using the default window span of $\alpha = 0.75$.

3.5.4 Qualitative Description of Phasic Tissue Change

Study goal three: Isolate and describe gross tissue change postulated to be unique to the local rate and pattern of decomposition in a high-altitude outdoor setting, to be applied in future study to establish a score matrix, and a predictive model for the estimation of postmortem interval in a high-altitude environment.

Throughout the study period, the incidence and prevalence of the 'classic' categories of decomposition change incorporated into the TBS model (skin slippage, purge, specific descriptions of soft tissue color change, marbling, bloat, and moist decomposition) were documented. Similarly, the 'classic' categorical descriptions were used as indices from which to identify and derive categorical divergence (i.e. gross macroscopic changes observed within the high-altitude cohort not described in the TBS model). All changes were assessed and recorded as present (1) / absent (0) on each data day. Specific descriptions of 'classic' changes were described from the onset of the study, allowing immediate assessment and documentation of presence/absence. Conversely, high-altitude specific categorical change had to be identified and described. As a result, novel changes were primarily observed, described, and variably scored as present (1) /absent (0) in the first year, then documented and scored more precisely in the second year. A standard data collection sheet was created and a retrospective

study of the first-year donor cohort was performed using field photographs to more accurately assess the presence of novel traits within the collective study cohort.

Foundationally, all categories were individually coded in the study's master database as present (1) / absent (0). Each data category was sorted to extract the 'present' code, yielding frequency of trait presentation within the cohort. Presence/absence was scored on every data day, facilitating a correlation between the presentation of a trait and ADD. When a categorical change was present, it was associated with a donor specific ADD point, and an ADD range (the continuum of ADD within the cohort based on individual ADD points). Inter-donor ADD ranges were collated to assess the breadth of ADD range. *Post-hoc* power analysis was performed for each trait. The 80% trait presentation threshold was applied. When a categorical change failed to meet the 80% threshold within the cohort, it was eliminated. When a categorical change met the 80% threshold, it was retained and described in terms of a collective (cohort-wide) ADD range in order to assess temporal specificity and by extension, potential power as a temporal marker in descriptive model building.

3.5.5 Forensic Ecological Profile

Study goal four: Develop a region specific forensic ecological profile that includes local atmospheric variables, invertebrate and vertebrate behavior, and local human behavior.

3.5.1 Local atmospheric variables

In addition to their potential impact on the trajectory of human decomposition, local atmospheric variables (described in detail in section 3.4) were considered in the forensic ecological profile. Temperature, atmospheric pressure, precipitation, rain, relative humidity, solar radiation, and wind speed data derived from the onsite HOBO weather station were considered individually and in sum. Daily data points, accumulated x days (where x = a specific atmospheric variable), and seasonal aggregates (e.g. snow overburden) were considered with

regard to their ability to influence vertebrate and invertebrate scavenging behavior, human behavior, and human decomposition.

3.5.2 Scavenger behavior

Vertebrate and invertebrate scavenger behavior, succession, and progression were documented daily through use of game cameras programmed to collect both time lapse and motion activated photographs. These images recorded environmental changes, midden and nest construction, soft tissue and osseous scavenging artifacts, scat, tracks, and feather fall. While scavenger cages barred large-bodied scavenger access to human remains, their exclusion allowed smaller-bodied scavengers to radiate, providing rare insight into their segregated behavior.

3.5.2a Vertebrate scavenging

Scats and tracks were identified using a Colorado Rocky Mountain Region standard field guide (Halfpenny & Tellander 2015). Middens, nests, scat, tracks, feather fall, and environmental change were all considered presumptive evidence of species-specific scavenging. Identification of the scavenger group present and attribution of scavenging defects to a specific species was achieved by: (a) observation of a new soft tissue defect between consecutive data days; (b) game camera capture of a specific species engaged in scavenging behavior within the timeseries; and (c) the absence of a cooperative or competitive scavenger species within the same timeseries. On data days where two or more species were present, tissue defects were not attributed to any group unless direct evidence was recorded on game camera images. Osseous and soft tissue defects were photographed and described in field notes, assigned to a specific species when field evidence was sufficient, and logged in the study database.

Scavenging species were individually coded in the study's master database as present (1) / absent (0) as they were field-identified. Each species category was sorted to extract the 'present' code, yielding frequency of presence within the cohort; a detailed description of associated defects was documented with each data point. At the end of the first data year, species and defect descriptions were extracted from the database and a data collection form was created to standardize documentation in the second year. A retrospective study of the first year donor cohort was performed using field photographs to more accurately assess the presence of tissue defects within the collective study cohort. In addition to standardized documentation, first year field methods were observed throughout the second year study period.

3.5.2b Invertebrate scavenging

Adult invertebrate scavengers were captured using sweep net (Pterygota) or collected manually as opportunity presented (Apterygota). In both models, insects were transferred to a kill jar containing plaster of Paris and ethyl acetate. Specimens were pinned following standard protocol (Sanford *et al.* 2020). Species identification was limited to family and achieved using standard dichotomous keys (Jones *et al.* 2019; Weidner & Powell 2021). Larvae were collected and preserved following standard protocol (Sanford *et al.* 2020) and identified using a standard key for immature morphological traits (Thyssen 2010).

3.5.3 Explanatory research: Materials and methods

The application of an explanatory research model (the use of literature, population and land use data, and case studies) was adopted in an attempt to identify and describe broad cultural patterns and relationships with Colorado's Rocky Mountain Region (Blatter & Haverland 2012). This approach is beneficial to the integration of local cultural configurations into the forensic ecological profile for three

reasons: (1) it provides a limited, but more holistic composite of human behavior within a defined region; (2) in scope and magnitude, it constitutes a more surmountable task for the forensic anthropologist immersed in their primary discipline; and (c) it facilitates the isolation of intraregional cultural groups and modes of behavior that may be extended to cultural and linguistic anthropology students as subject of advanced study. This performs the dual task of expanding the sphere of knowledge pertaining to local cultural groups, and actively serves to integrate cultural and linguistic anthropologists into forensic anthropological research.

3.5.3a Cultural trends culled from desk research

An endeavor as broad as 'establishing a cultural framework within which literature review constitutes one component,' necessitates a concise analytical framework to ensure that the study is both goal oriented and replicable. The provision of tangible methodological steps serves to address both demands. The literature review in this study was performed following Bladder & Haverland (2012), who propose that analyzing text involves four governing tasks: (1) Identifying themes and subthemes; (2) paring themes down to a manageable suite of those most relevant to the project; (3) hierarchically ordering themes; and (4) linking themes into theoretical models.

Toward that end, an overview of environmental perception theory was provided to establish a macroscopic view of the relationship between humans and their proficiency within the environment (Dyson-Hudson & Smith 1978; Gibson 1979; Ingold 2000). Literature considered foundational to theme identification included first, peer reviewed publication concerned with modern culture in the Rocky Mountain Region, and second, analytically (but not necessarily regionally) adjacent literature. Publications were culled from the Morris library online database at Southern Illinois University, Carbondale. Preference was given to the university database because it reflects the literature resource most readily available to researchers across all levels of academia. Search keys were intentionally broad in an effort to encapsulate a broad range of topics that may be

relevant to establishing a diverse cultural profile. Additionally, locally produced literature including county profiles, county reports, regional data, reports generated by government agencies, and local newspaper articles were used to inform microscopic, temporally specific cultural trends.

3.5.3b Population and land use data

The U.S. Census Bureau (2023) was referenced to establish local population density, population demographics (age, sex, and ancestry distribution), education, health, income, and poverty. Land use databases were referenced to establish local zoning laws and patterns of land use (MRLC Consortium 2022; Park County Colorado GIS 2022).

3.5.3c Case study

While limited in scope, case studies facilitate multifaceted exploration of complex issues and have long been utilized as an analytical and educational tool in forensic anthropology (Steadman 2008). There are three methodological approaches to case study: (1) critical (challenging one's own assumptions); (2) interpretive (understanding meaning, context, and processes as perceived from different perspectives to understand individual and shared social meanings); and (3) positivist (establishing variables for study in advance to assess the degree to which they fit in with the findings) (Crowe *et al.* 2011). The interpretive approach was used in this study to assess the degree to which a local cultural profile is reflected in forensically significant context.

Case studies were culled from case data maintained by the Park County Coroner's Office (PCCO). The search parameters were intentionally broad and established to reflect the parameters of the overall study design. The parameters applied to the case data search were: (1) cases involving an outdoor death scene; (2) cases in a non-residential or non-traditional residential location; and (3) cases that have been resolved through investigation and - when relevant - litigation. The records search encompassed 12 years of case data (2010 – 2022) and yielded 72 cases matching the search criteria. A random generator function (Microsoft Excel RAND) was used to create a sample subset to

prevent bias in case selection. Sampling was performed without replacement allowing application of the 10% condition to ensure that (a) the sampling process did not significantly impact the probability of population distribution; and (b) individual samples were considered independent (Lindstrom 2010). Sampling resulted in seven cases. Outdoor scenes were selected because they match the parameters of the broader study design (i.e. the decomposition of human donors in an outdoor environment). When available, recorded data included case circumstance, decedent biodemographic data, circumstance leading to discovery, tool use in deposition and/or recovery, and prominent cultural artifacts noted on scene. Because a case must be legally resolved prior to dissemination as a case study, cases pending litigation were removed from the sample (Steadman 2008). Case study data are reported within the context of literature derived cultural trends and population and land use data to qualitatively assess the degree of symmetry between the three data lines.

3.6 Conclusion

This study is concerned with four primary research goals, necessitating reflexivity in research design. Two primary research models were used: (1) mixed research (the collection of qualitative and quantitative data through direct observation in a semi-controlled outdoor environment); and (2) explanatory research (the use of literature, culled population and land use data, and case studies to explain cultural relationships). Data collection was performed at FIRS-TB40, a high-altitude satellite facility nested under Colorado Mesa University's Forensic Investigation Research Station. The FIRS-TB40 is located in the Colorado Rockies Dfc (snow, fully humid, cool summer) climate region at an elevation 3000 meters/9840 feet AMSL, rendering it a novel research environment. Site infrastructure includes a barbed wire perimeter fence, 3m x 3m steel welded scavenger cages, a centrally placed onsite HOBO weather station, and motion activated game cameras.

Twelve human donors were placed across a two-year study period. Data were collected daily following a standard study protocol. An 80% threshold was established to sort qualitative traits. Statistical analyses include Spearman rank-order correlation coefficient (intraobserver error), Krippendorff's alpha (interobserver error), linear regression (test of the TBS model), and Locally Estimated Scatterplot Smoothing (LOESS) and multivariate regression (to assess site specific atmospheric variables). Finally, a pentagonal approach to establishing a forensic ecological profile was introduced.

CHAPTER 4

RESULTS: QUANTITATIVE ANALYSIS

4.0 Tests for reliability

4.0.1 Intraobserver error

A random number generator was used to create a subset study sample to test intraobserver error. Spearman correlation was run using the cor.test function in R-Studio to determine the relationship between field scored TBS and the subset of rescored data days. There was a strong positive correlation between original TBS and rescored TBS ($r_s(8) = 0.85$, $p = 0.004$).

4.0.2 Interobserver error

A random number generator was used to create a second subset from the study sample to test interobserver reliability. Fifteen observers scored 15 donor data packets, resulting in 225 data points. Observers ranged in education level (Undergraduate n = 4, Masters n = 3, Professional [Masters or PhD working fulltime in the field] n = 3, and PhD n= 4), and in self-reported experience level using the TBS model (Beginner n = 4, Intermediate n = 4, Advanced n = 7). Krippendorff's alpha was run using the krippen.alpha.raw( ) function in R-Studio (irrCAC package version 1.0, Gwet 2019) to determine the relationship between TBS scores generated by the group of independent observers. The results ($\alpha = 0.26$, $p= 0.0001$) indicate that agreement among observers was minimal.

4.1 Quantitative Test of the TBS Model

A test of the TBS Model was performed following the original study design. TBS within the truncated data set (PMI ≥ one year) ranged from 3-31. The distribution of PMI (Figure 4-1) and ADD (Figure 4-2) were plotted against TBS. Because TBS is used to predict ADD and subsequently PMI, TBS was plotted along the x-axis, and ADD and PMI were plotted along the y-axis.

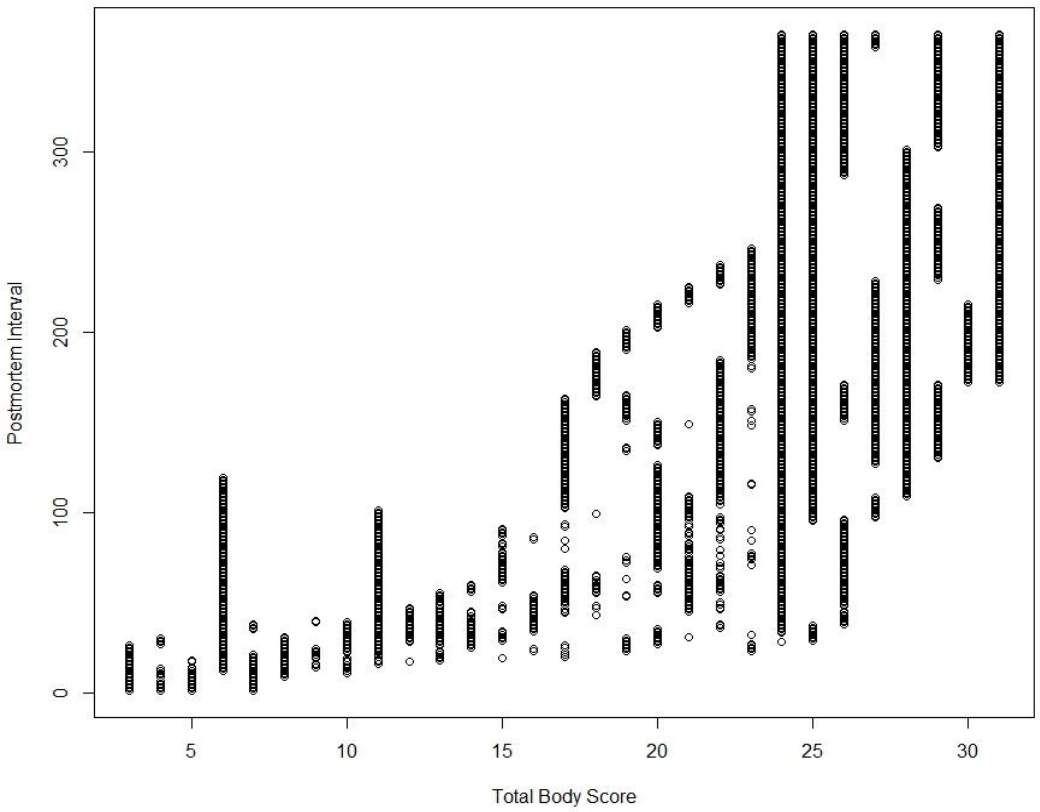

Figure 4-1: Scatterplot of untransformed postmortem interval (in days; y-axis) vs. total body score (x-axis) among all donors in the high-altitude cohort.

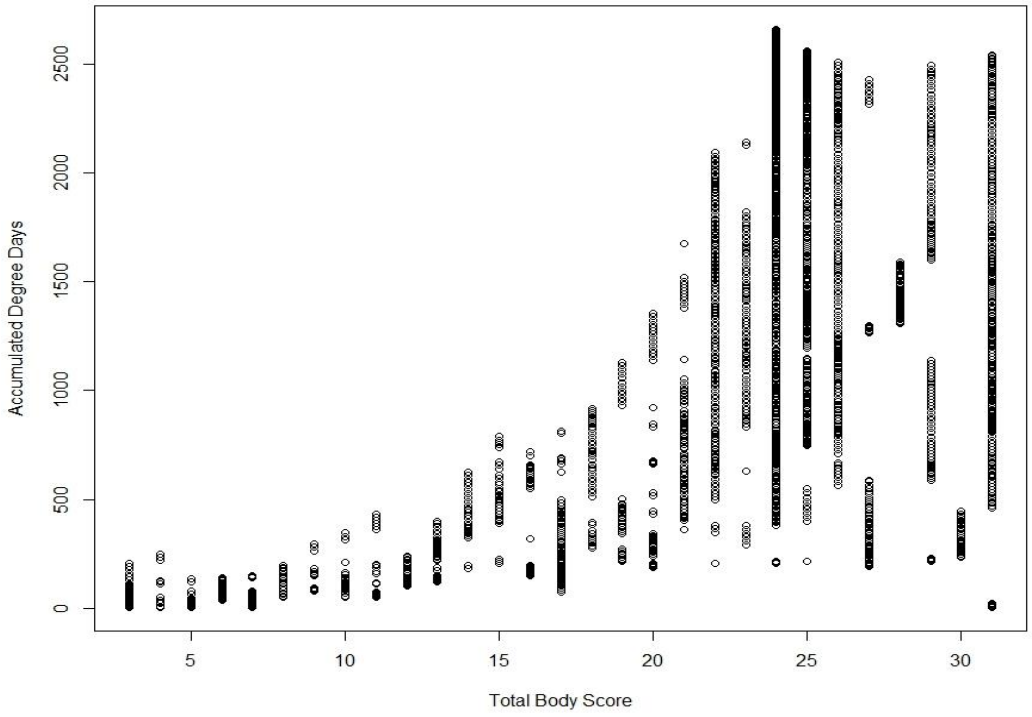

Figure 4-2: Scatterplot of untransformed accumulated degree days (y-axis) vs. total body score (x-axis) among all donors in the high-altitude cohort.

Scatterplots demonstrate that as ADD and PMI increase, TBS increases and begins to plateau with the passage of time (PMI). Neither relationship is linear, so PMI and ADD were Log_{10} transformed, and TBS squared following the original model design. The relationship between both ADD vs. TBS and PMI vs. TBS was tested using linear regression; plots of each test with regression line fitted are presented in Figures 4-3 and 4-4.

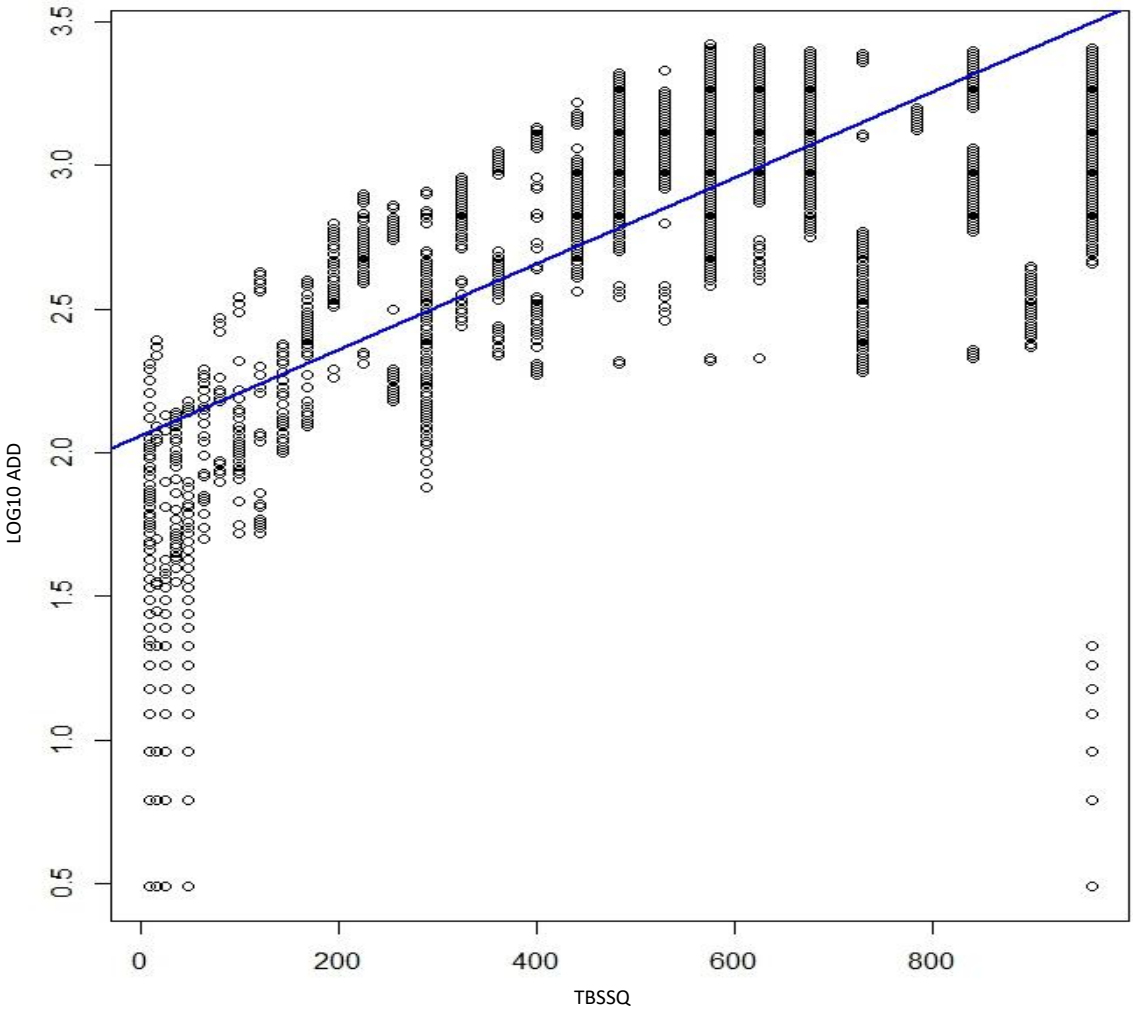

Figure 4-3: Log_{10} transformed ADD vs. TBS squared with fitted regression line, high-altitude data.

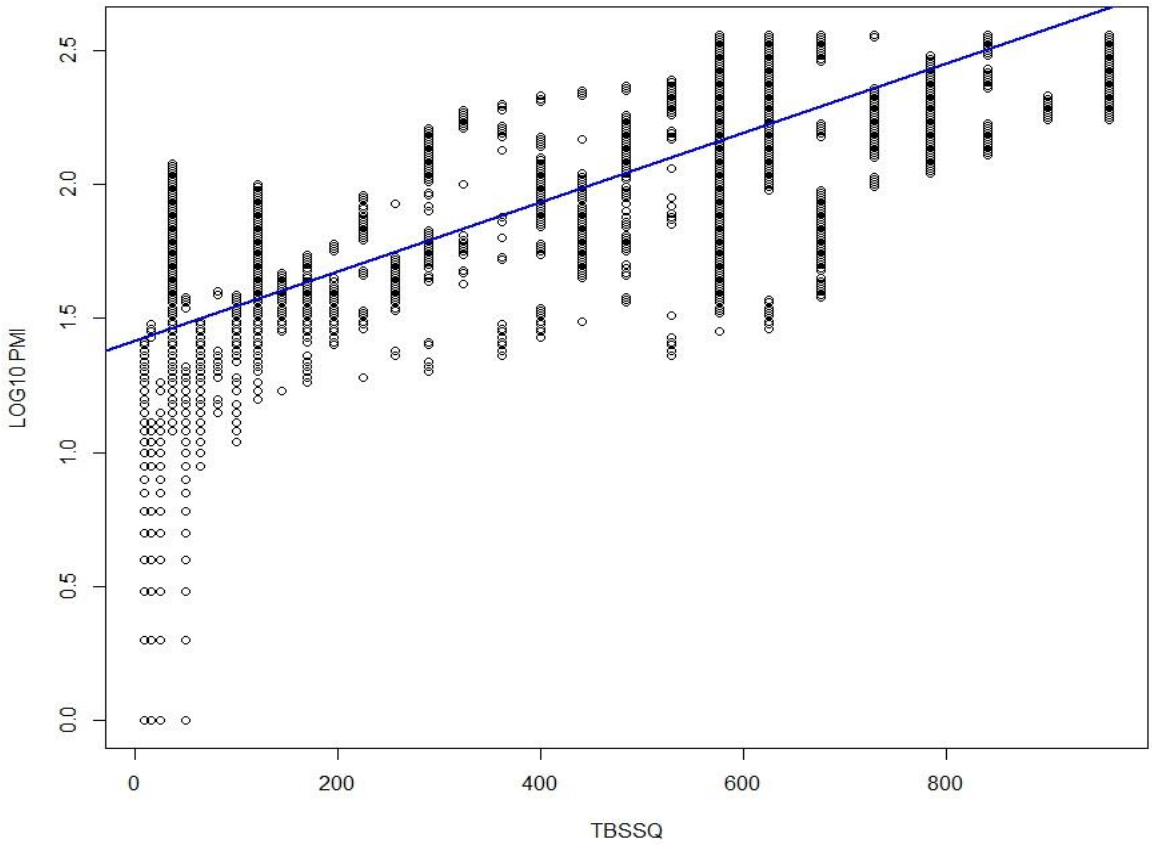

Figure 4-4: Log_{10} Transformed PMI vs. TBS squared with fitted regression line, high-altitude data.

Transformation marginally served to normalize the data but the regression lines suggest that the TBS model is not a correct fit. Adjusted R-squared values support the model's poor performance when applied to the high-altitude cohort; Log10ADD vs. TBSSQ (0.42) and Log10PMI vs. TBSSQ (0.54). Megyesi *et al.* (*ibid*) report substantially higher R-squared values for Log10ADD vs. TBSSQ (0.84) and for Log10PMI vs. TBSSQ (0.70). Log10ADD performed better than Log10PMI within the Megyesi cohort, leading the authors to conclude that time and temperature served as better indices for predicting PMI than time alone. The inverse was true within the high-altitude cohort where Log10PMI vs. TBSSQ performed better than Log10ADD vs. TBSSQ. Because PMI directly reflects time, this suggests that a variable or variables encapsulated by time may serve as a better predictor or predictors than ADD alone at high-altitude.

4.2 Quantitative Analysis of Atmospheric Variables

Because the high-altitude data suggests that a variable or variables encapsulated by time may serve as better predictors than ADD alone, the distribution of atmospheric variables was investigated. This investigation is the first step - and the foundation for - the future development of a PMI predictive model specific to the high-altitude environment. The ADD temperature scale built into the TBS model converted negative temperature values to 0 ˚C based on the argument that decomposition ceases at 0 ˚C. There is a paucity of data to support this supposition, so intracohort TBS distribution was first considered along three temperature scales: ADD Celsius greater than zero (ADD C > 0), ADD Celsius (ADD C), and ADD Kelvin (ADD K). Plots of each temperature scale and cohort wide TBS distribution are presented in Figures 4-5 - 4-7.

Plotting TBS against ADD C > 0 demonstrates a basic trend in early, rapid increase in TBS scores among all donors (between approximately 0 ADD – 1000 ADD) followed by a generally persistent plateau in TBS scores following 2000 ADD.

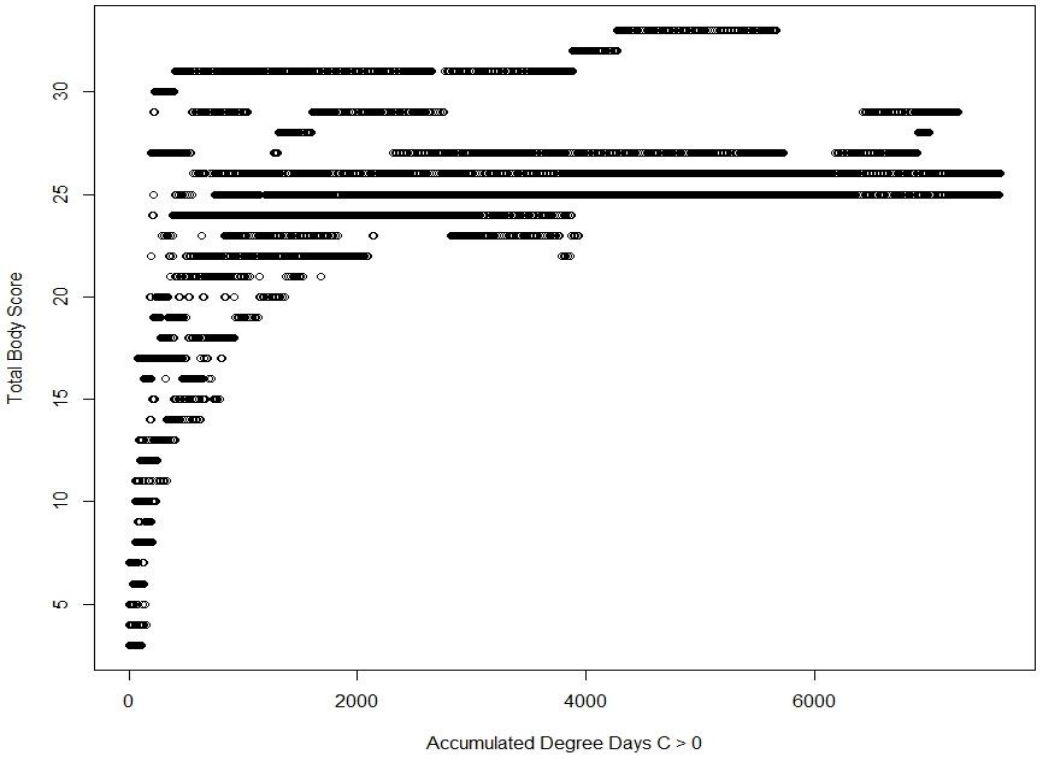

Figure 4-5: Scatterplot of TBS vs ADD Celsius > 0, negative values converted to zero following Megyesi *et al.* (2005), among the high-altitude study cohort.

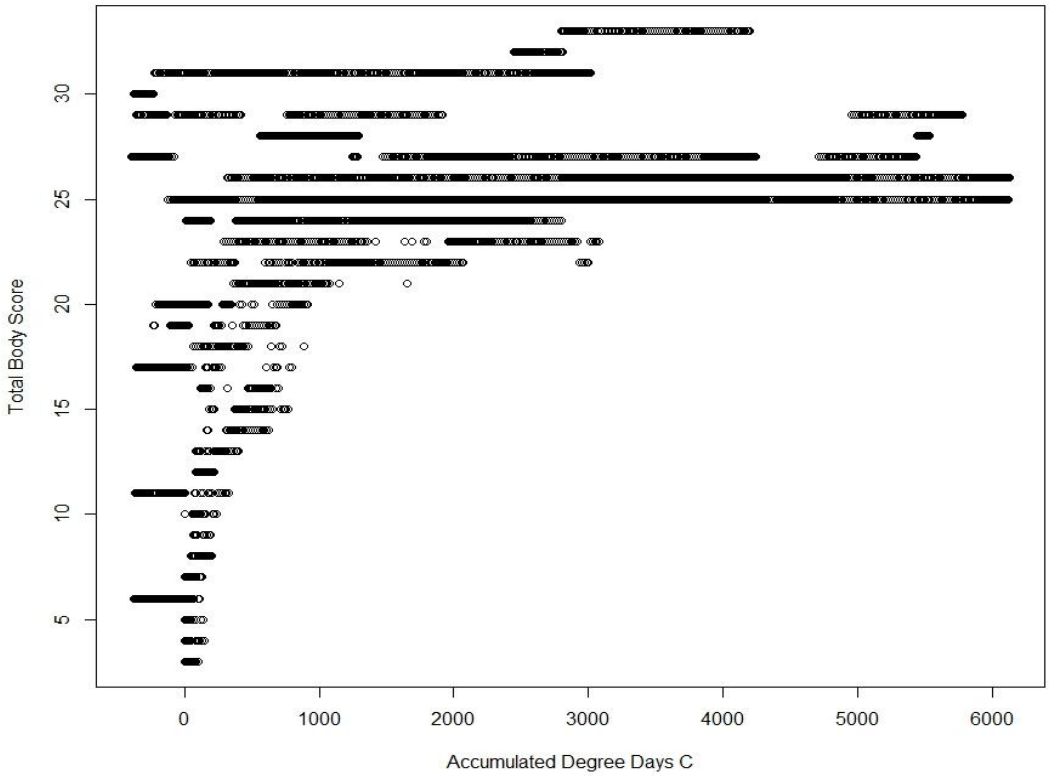

Figure 4-6: Scatterplot of TBS vs ADD Celsius among the high-altitude study cohort.

Plotting TBS against actual ADD C demonstrates the same overall trend in early, rapid increase in TBS scores among all donors between approximately 0 ADD – 1000 ADD, followed by a generally persistent plateau in TBS scores. While the overall trend in data distribution between ADD C > 0 and ADD C bear resemblance, simple distribution plots are only suggestive of trends, particularly when considering a large data set. Considering the data in relationship to actual ADD C demonstrates its true complexity, as TBS and ADD undulate between seasonally associated positive and negative temperature values. This has an overall impact on the structure of the curve and demonstrates the potential for decomposition trends to be obscured within the confines of a reductive temperature model.

Plotting TBS against ADD Kelvin demonstrates the same rapid climb/plateau trend observed in the Celsius temperature scales, however the data are more widely distributed within the TBS 15-25 range, and within the 25-33 range, where the sharp angle presented by both Celsius scales is smoothed and data are more broadly distributed to the right. Because negative temperatures are not possible on the Kelvin scale ($K = C^{o}+273.15$), the distribution of TBS and ADD Kelvin has the potential to reconcile the disparities observed between the ADD C and ADD C>0 temperature scales.

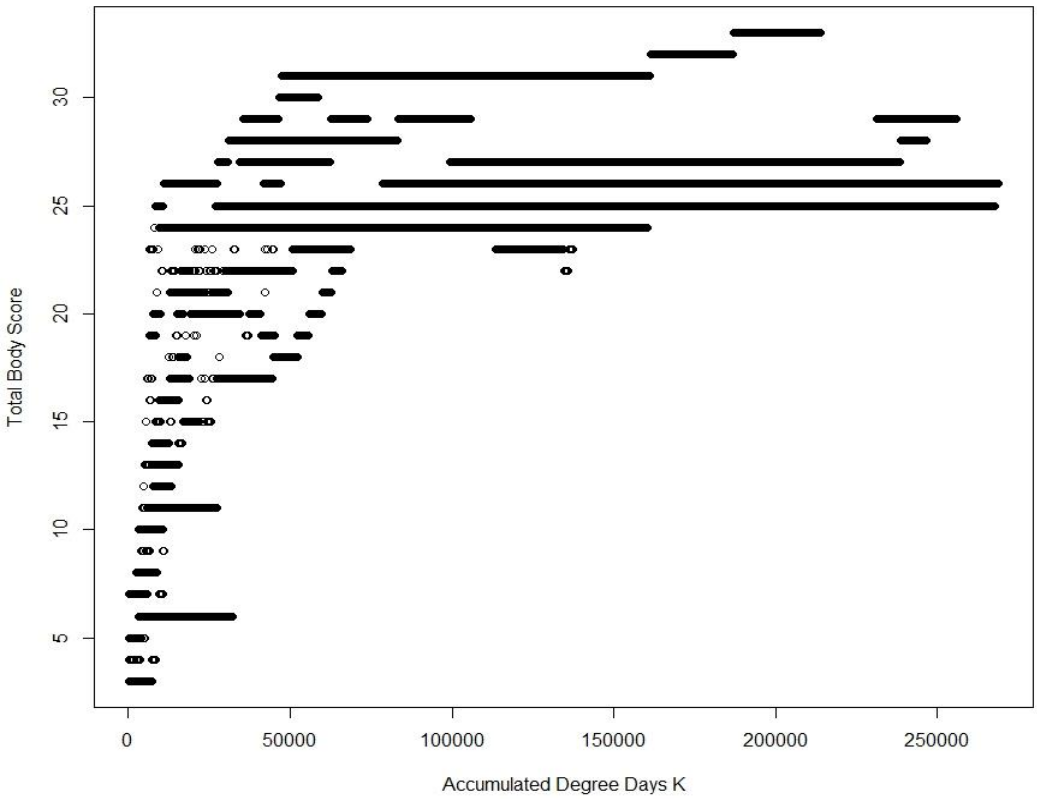

Figure 4-7: Scatterplot of TBS vs ADD Kelvin among the high-altitude study cohort.

To better understand individual donor trajectories obscured by the volume of cohort-wide data distribution, the trajectory of individual donor TBS was assessed along each ADD temperature scale using LOESS: ADD C (Figure 4-8), ADD > 0 (Figure 4-9), and Kelvin (Figure 4-10). While small in scale, Figure 4-11 presents individual donor distributions along each of the temperature scales to facilitate macroscopic comparison. Donor position and color are consistent throughout all plots.

4.2.1 Results: Scatterplots of the three temperature scales (ADD C, ADD C>0 and ADD K), by donor

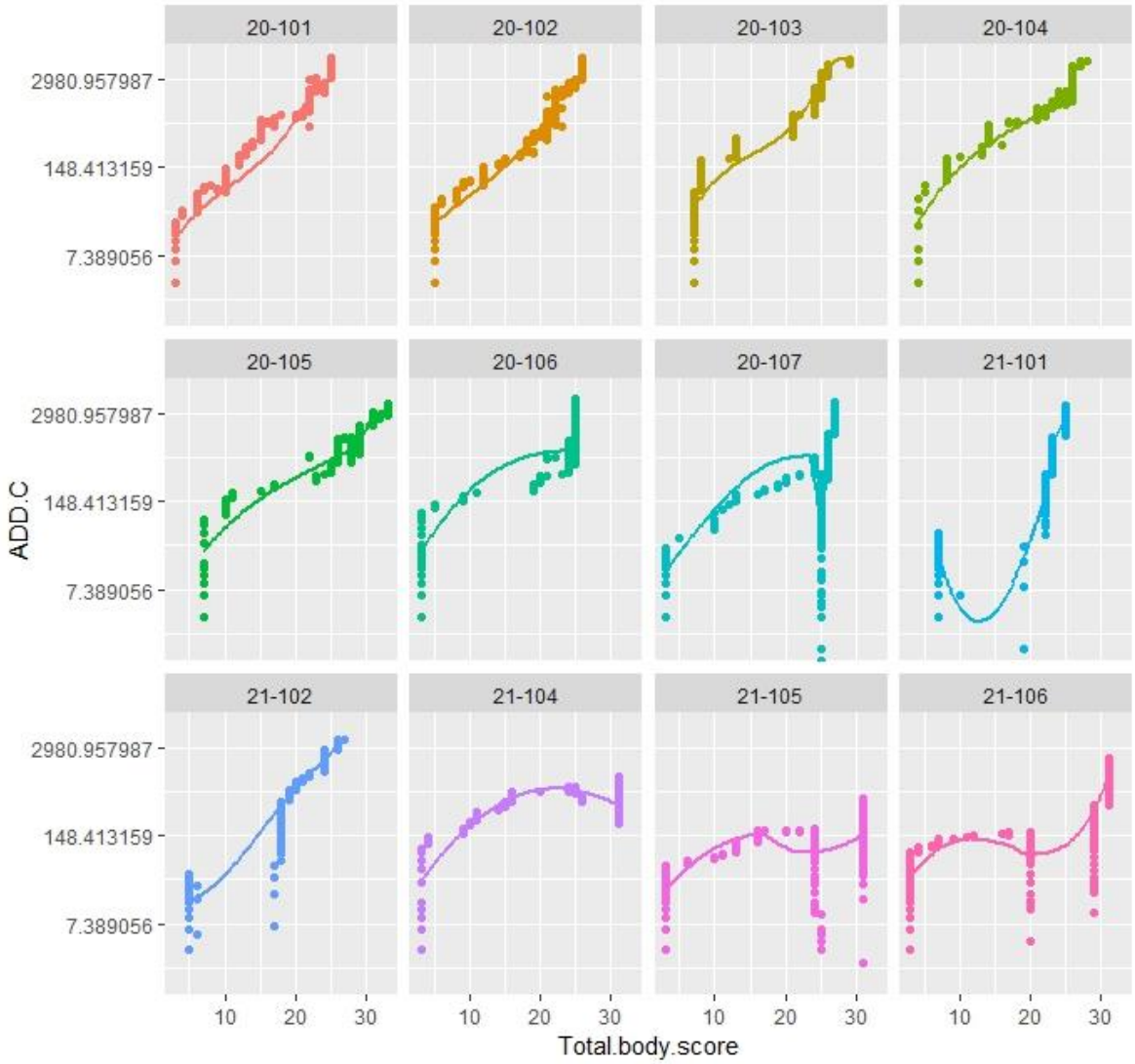

Figure 4-8: LOESS distribution plots of TBS vs ADD C on the LOG scale, by individual donor within the high-altitude cohort.

When considering the the ADD C scale by individual, the complexity associated with negative temperature values becomes more apparent. Further, that complexity is more dramatic within in a subset of donors. Specifically donors 20-107, 21-101, 21-102, 21-105, and 21-106 present pronounced negative plateaus when compared to the sum of the cohort. With the exception of 20-107 (placed in late August), all remaining individuals were placed in the winter. While the sum of the cohort presented a general trend in early, rapid increase in TBS followed by a broad plateau, individual donors generally

present a series of TBS score plateaus associated with increasing PMI, demonstrating that a plateau should not be regarded as a period of stasis. Donors 20-101 and 20-102 were placed on the same day, as were donors 21-101 and 21-102. Donors 21-105 and 21-106 were placed ten days apart. Each pair presents a similar, but not identical distribution, demonstrating that the individual trajectory of decomposition is sensitive to both macroscopic variables (resulting in visual similarities in data distribution) and individual microscopic variables (resulting in variation despite temporal continuity in placement).

Eliminating negative temperature values and applying a LOG transformation yields a marked difference in data distribution. The most apparent (and most expected) change is the loss of the dramatic negative plateaus associated with overwintering, and the normalization of the overall distribution curves. While the overall trend in early rapid increase in TBS, followed by a score plateau remains the general theme, both the rapid increase and the late-stage plateau are dramatized by the elimination of negative values. This creates an overall inaccurate picture of both trends, and understates the analytical complexity associated with building a predictive model able to contend with the rapid climb/plateau disparity in data distribution. On the ADD C scale, donors 20-107, 21-101, 21-102, 21-105, 21-106 presented distinct distribution curves. On the ADD >C scale, donors 20-101 – 21-102 present overall simialrity in distribution curves. Donors 21-104 - 21-106 share the same similarity, but are marginally distnct from the larger group. What remains apparent between both temperature scales is that the data are not linear, and score undulations and reversals are prevalent. Of further note, with the exception of 20-107, the LOESS curves associated with the donors presenting the most dramatic winter undulations on the ADD C scale (21-101, 21-102, 21-105, and 21-106), bear similarity to those on the ADD C>0 scale. This demonstrates the reflexivity of the LOESS model in deriving overall trends from complex, data dense distribution plots.

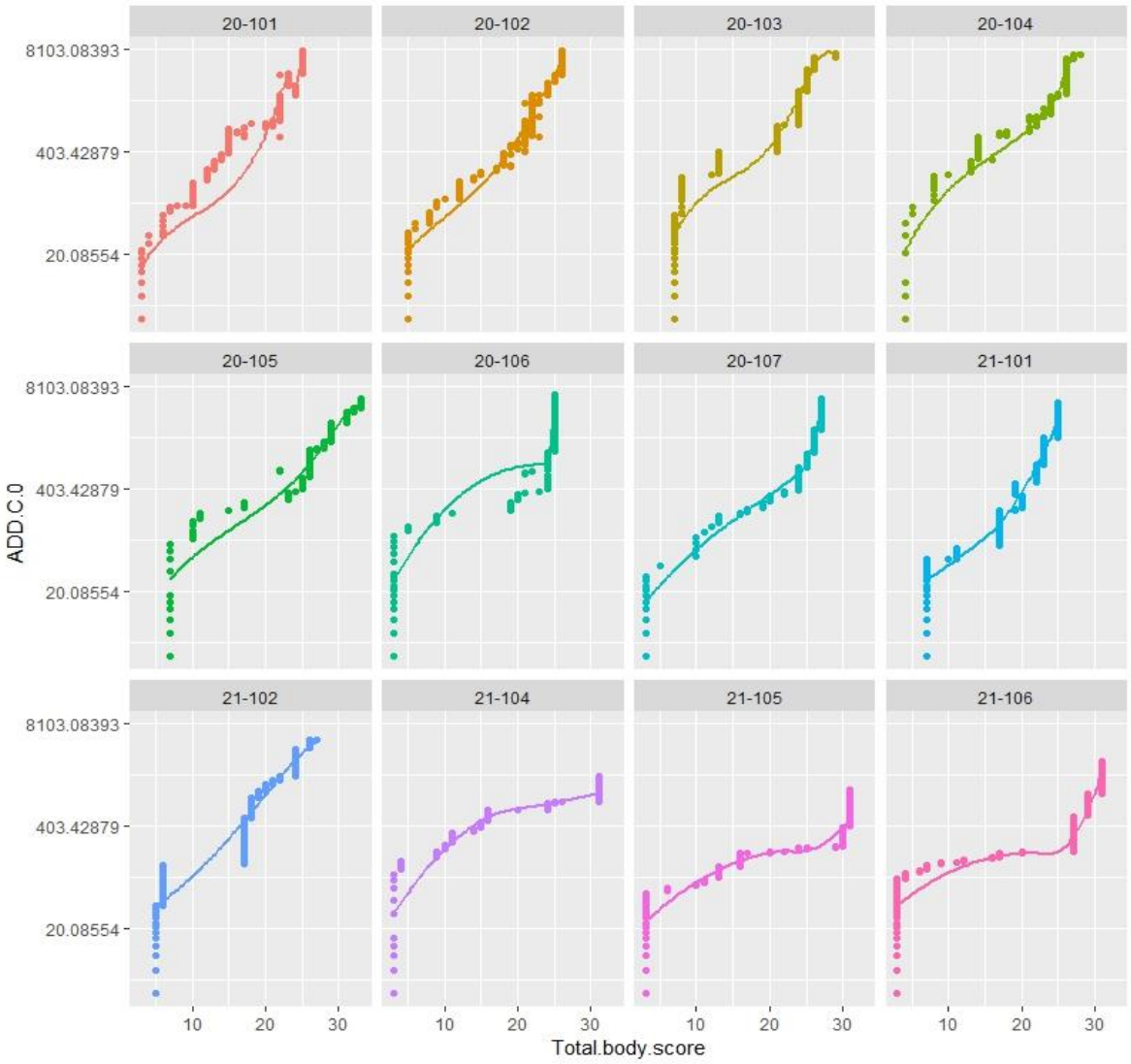

Figure 4-9: LOESS distribution plots of TBS vs ADD C>0 on the LOG scale, by individual donor within the high-altitude cohort.

The application of the ADD K temperature scale produces marginal differences in distribution when compared to ADD C>0. This is an expected outcome, as neither scale contains values less than 0. Overall, ADDK produces changes in score plateaus, which are truncated on the ADD C>0 scale and marginally elongated on the ADD K scale. These elongations are likely due to the incorporation of the negative values observed on the ADD C scale, as opposed to the elimination of negative values observed on the ADD C>0 scale. This yields a more comprehensive quantification of available thermal energy. Due to the scale of ADD K and the incorporation of negative values, overall distribution shifts to the right,

increasing normalization of the curve and yielding higher resolution in both late-stage plateaus, and in score undulation throughout decomposition.

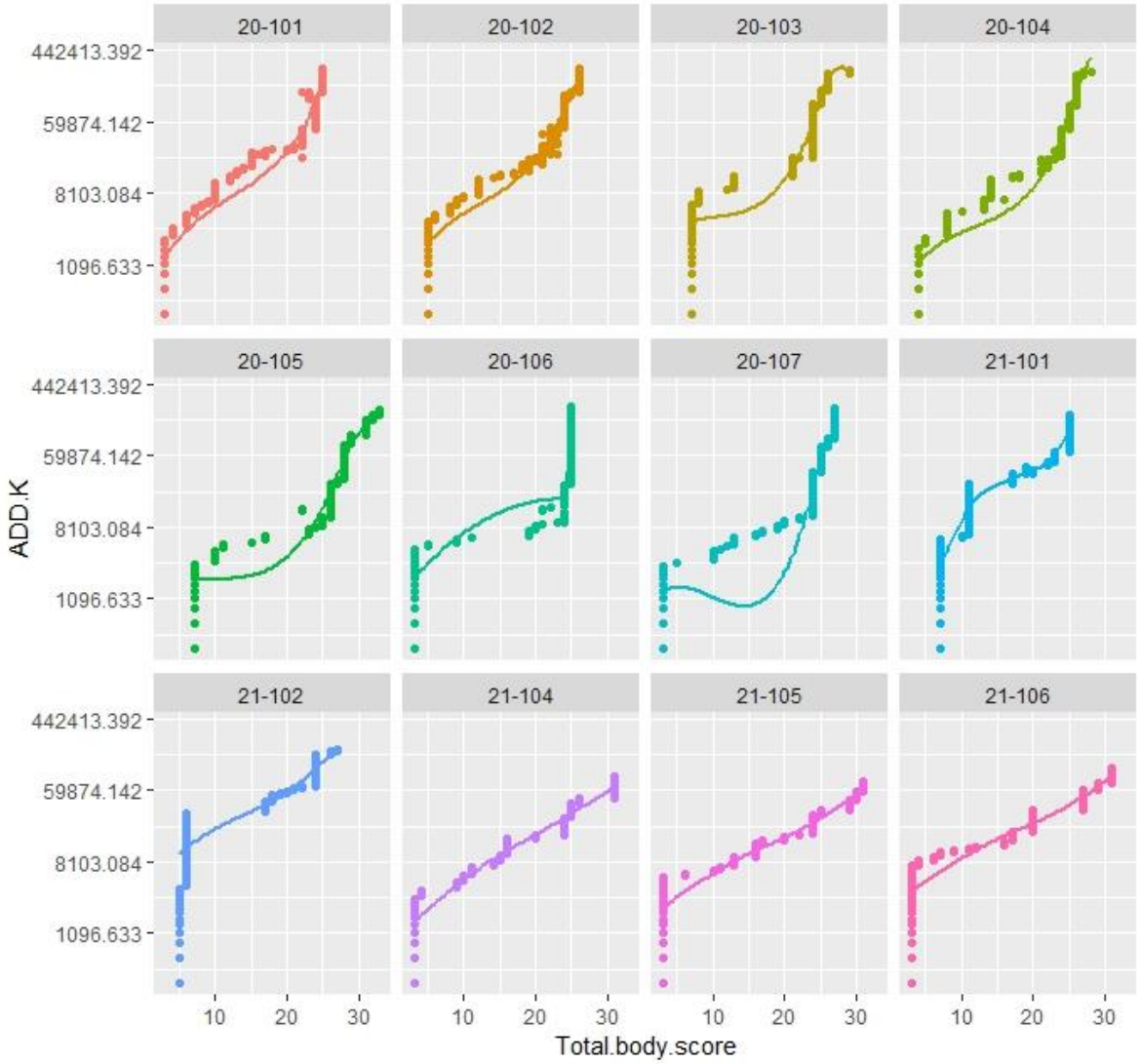

Figure 4-10: LOESS distribution plots of TBS vs ADD K on the LOG scale, by individual donor within the high-altitude cohort.

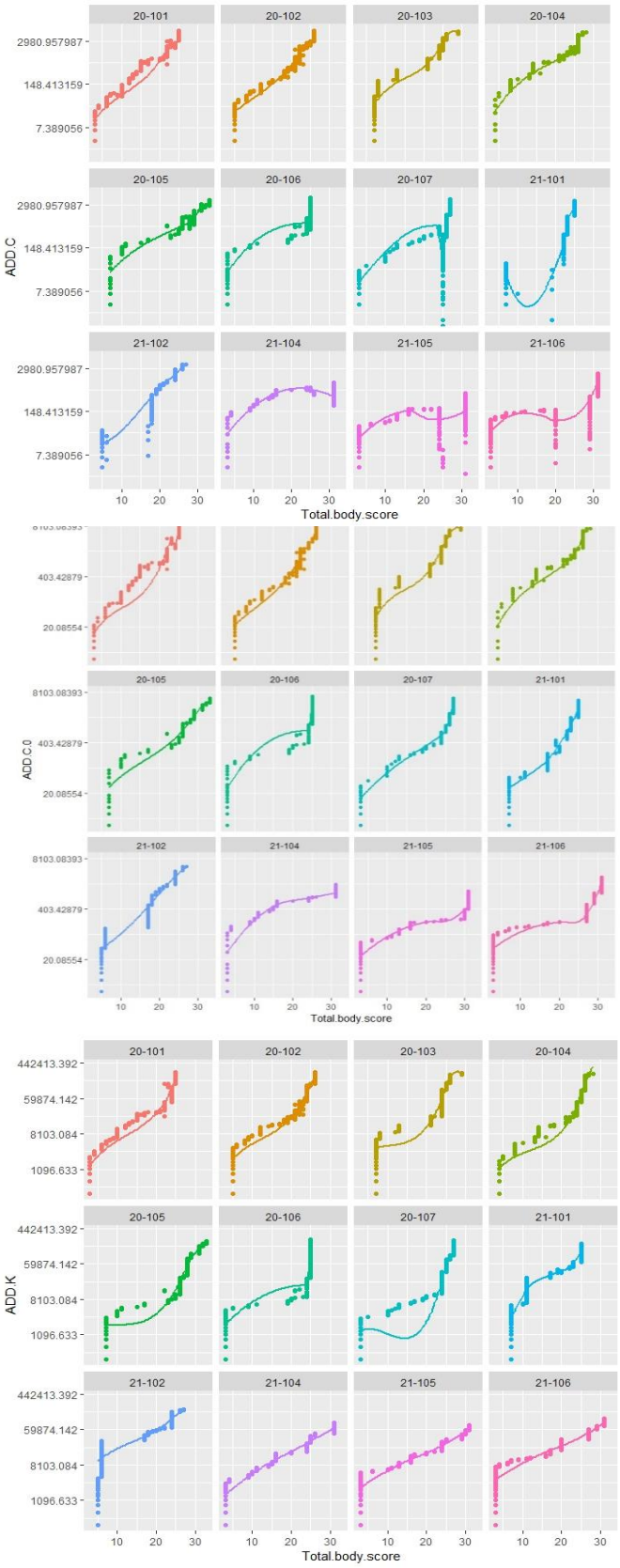

Figure 4-11: LOESS distribution of individual donor TBS on the three temperature scales, ADD C (top), ADD C>0 (middle), and ADD K (bottom), among the high-altitude cohort. Donor position and color are consistent across variables.

4.2.2 Results: Individual atmospheric variables by donor

In addition to the three temperature scales, TBS was individually plotted against the accumulated sum of six atmospheric variables: accumulated pressure days (APD; Figure 4-12 & 4-13), accumulated rain days (ARD; Figure 4-14 & 4-15), accumulated precipitation days (APreD; Figure 4-16 & 4-17), accumulated relative humidity days (ARHD; Figure 4-18 & 4-19), accumulated solar radiation days (ASRD; Figure 4-20 & 4-21), and accumulated wind speed days (AWSD; Figure 4-22 & 4-23). Distribution plots fitted to a LOESS curve are presented by donor; comparison plots between individual weather variables and ADD K follow. Because sufficient evidence to support the cessation of decomposition at 0 ˚C is lacking, negative values on the ADD C scale create visual complexity, and ADD K integrates negative temperature values into a positive scale, atmospheric data are compared to the ADD K scale.

4.2.2a *Accumulated pressure days (APD)*

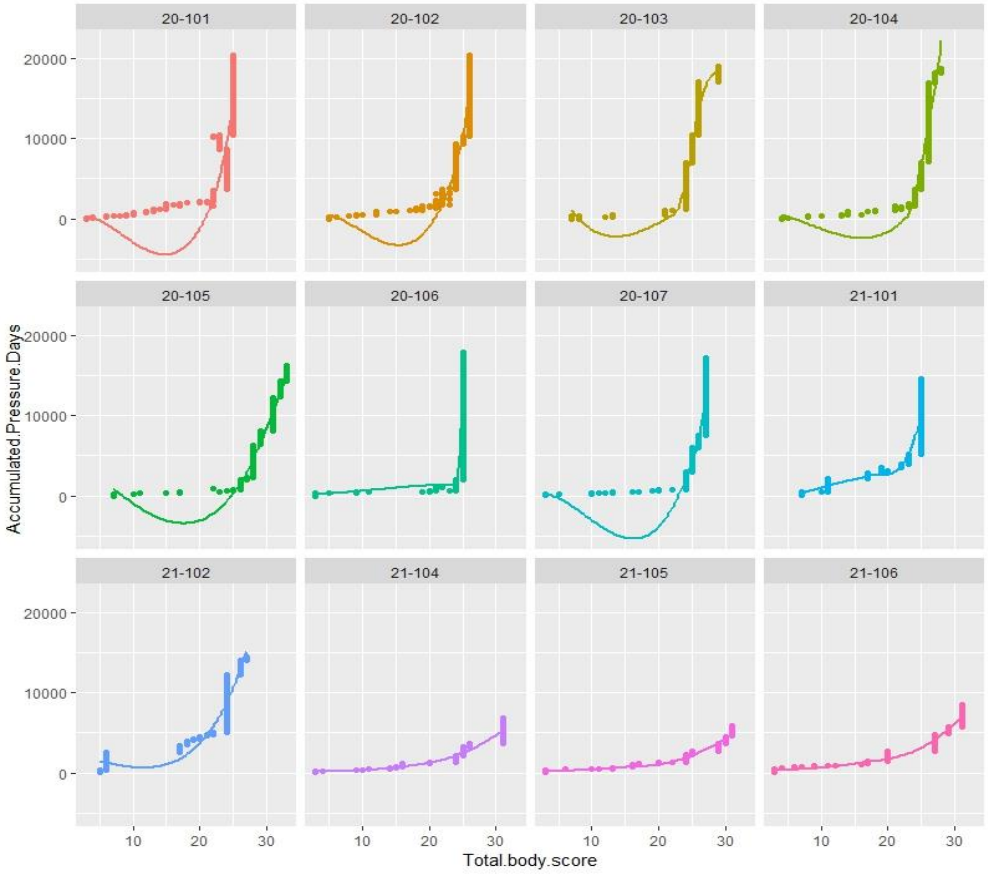

Figure 4-12: LOESS distribution of individual donor TBS vs APD among the high-altitude cohort.

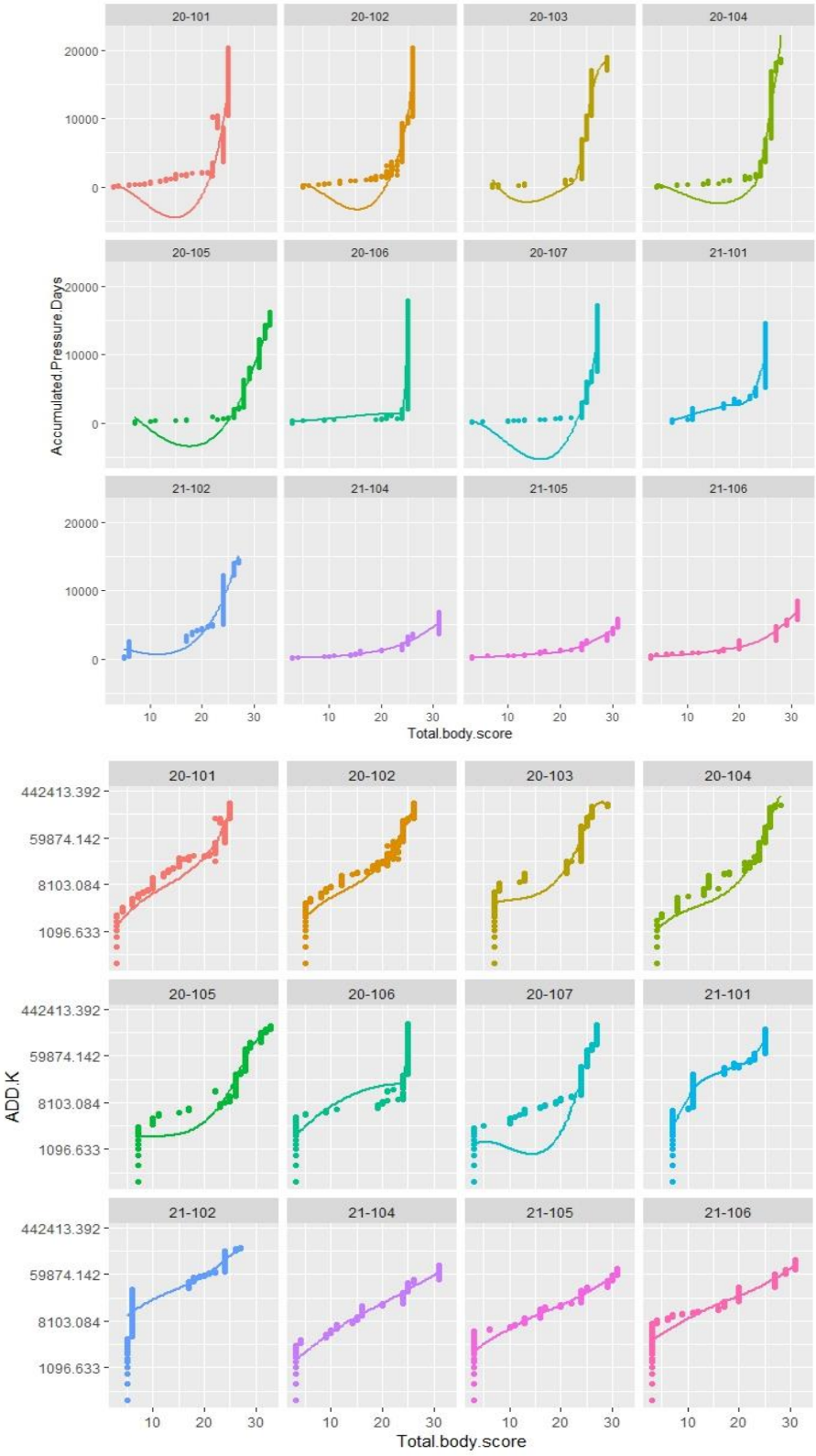

Figure 4-13: LOESS comparison of APD and ADD K distribution. Note the generally shared trend in rapid increase of TBS with PMI. Donor position and color are consistent across variables.

Accumulated pressure days (APD) share a compelling relationship with ADD K. Both of the scales demonstrate a rapid increase in TBS followed by a plateau. The distribution of APD presents a steeper, more linear climb than ADD K, indicative of a more rapid increase in TBS in early PMI than is associated with temperature. However, APD and ADD K share the same general trend, suggesting the potential utility of APD in PMI estimation.

4.2.2b *Accumulated rain days (ARD)*

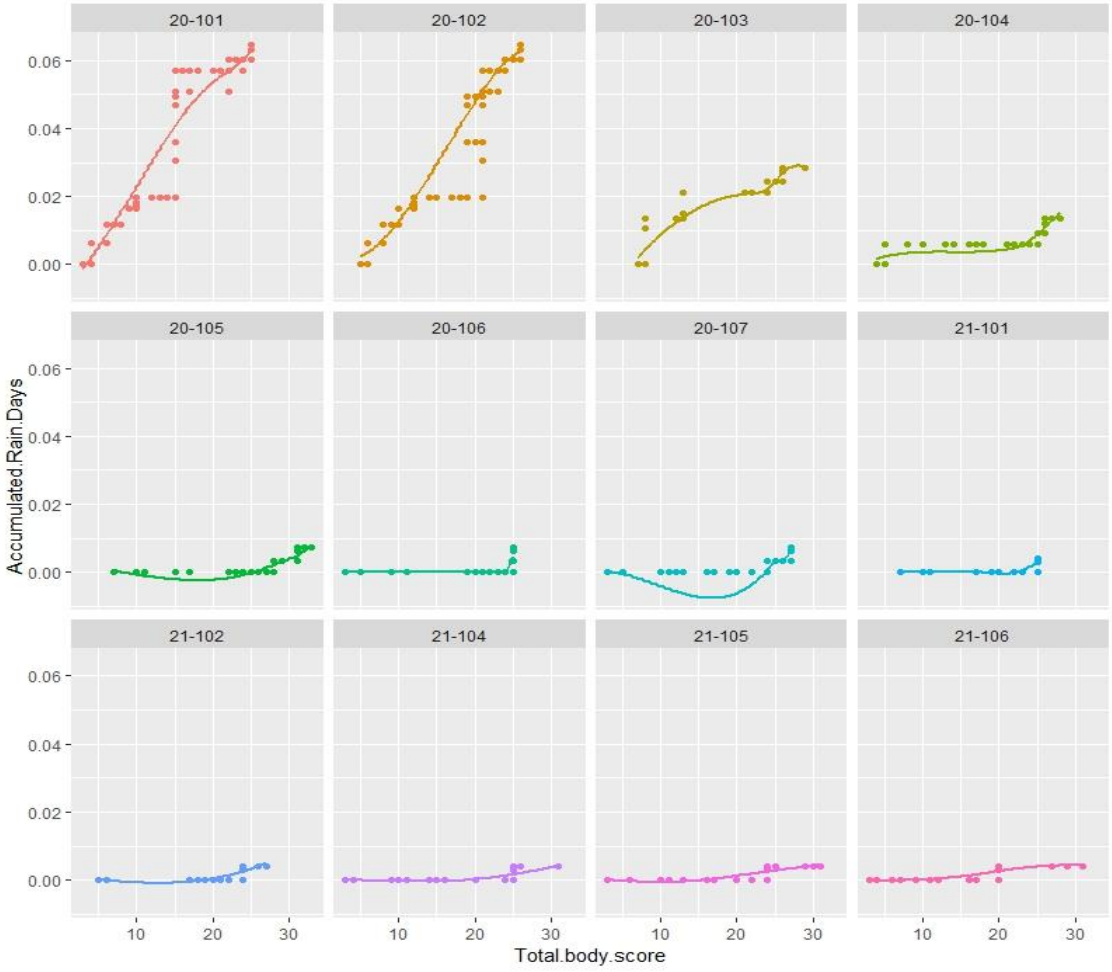

Figure 4-14: LOESS distribution of individual donor TBS vs ARD among the high-altitude cohort.

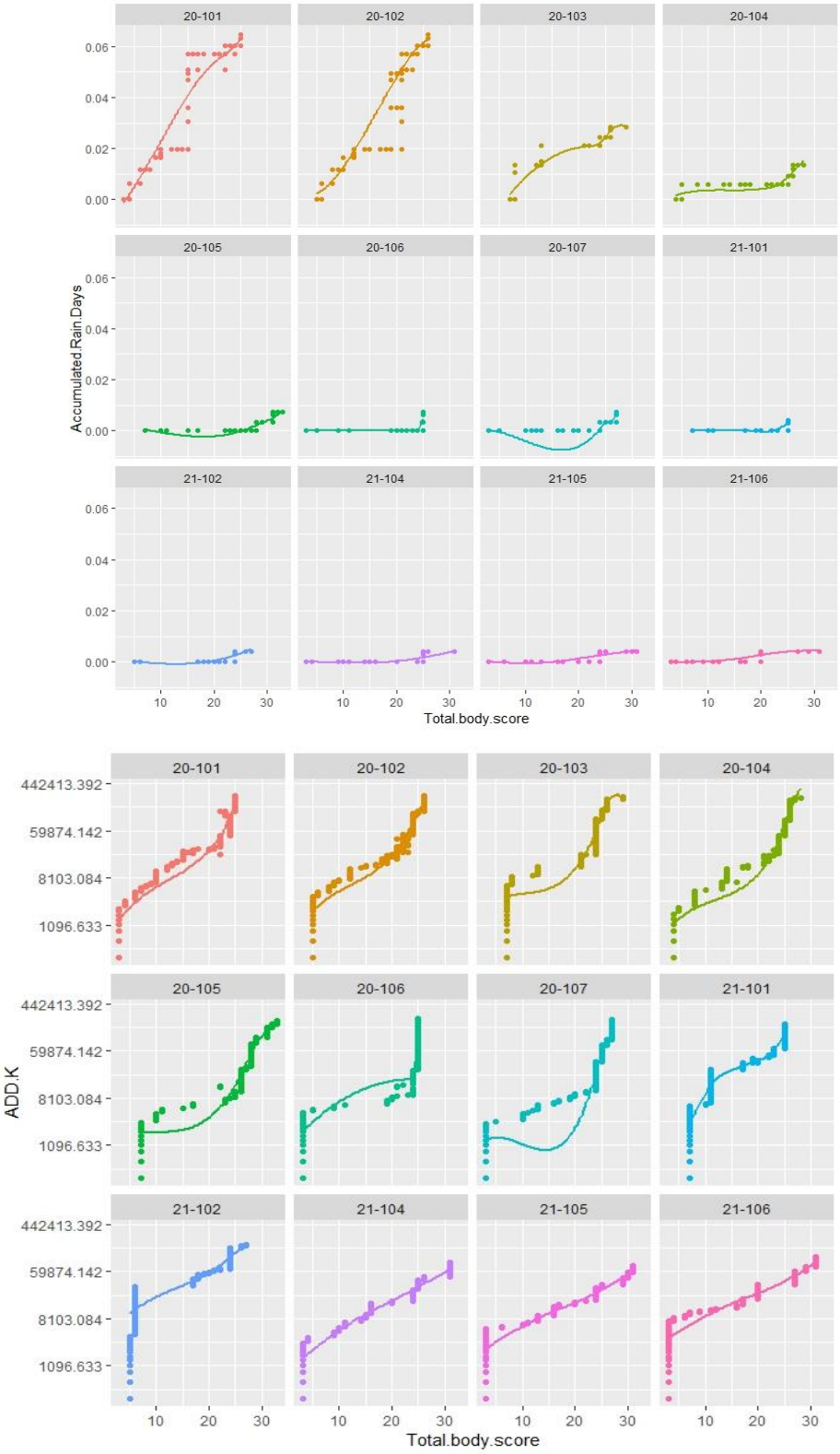

Figure 4-15: LOESS comparison of ARD and ADD K distribution plots. Note the overall lack of shared distribution as ARD values remain relatively constant across PMI. Donor position and color are consistent

With the exception of donors 20-101 – 20-103 - who share moderate similarity in accumulated rain days (ARD) distribution with ADD K – ARD are largely horizontal linear throughout PMI and tend to fluctuate at or around zero. This is likely an artifact of the temporal structure of rainstorms in the High Rockies, characterized by punctuated instances of heavy, but relatively brief downpours throughout the summer months. While the punctuated structure of summer storms has an impact on the trajectory of decomposition (e.g. eradicating maggot masses and rehydrating tissue) the overall distribution suggests that ARD will serve as a poor index for PMI estimation.

4.2.2c *Accumulated pressure days (APreD)*

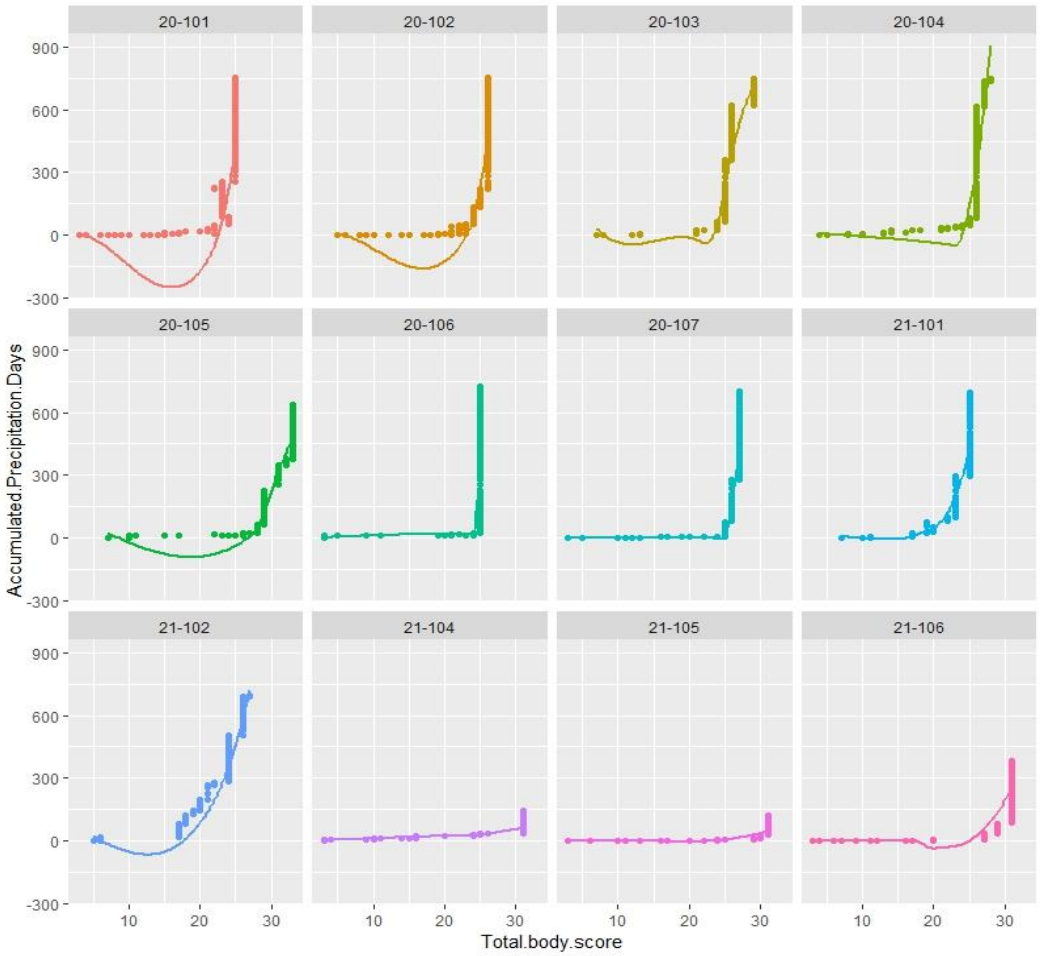

Figure 4-16: LOESS distribution of individual donor TBS vs APreD among the high-altitude cohort.

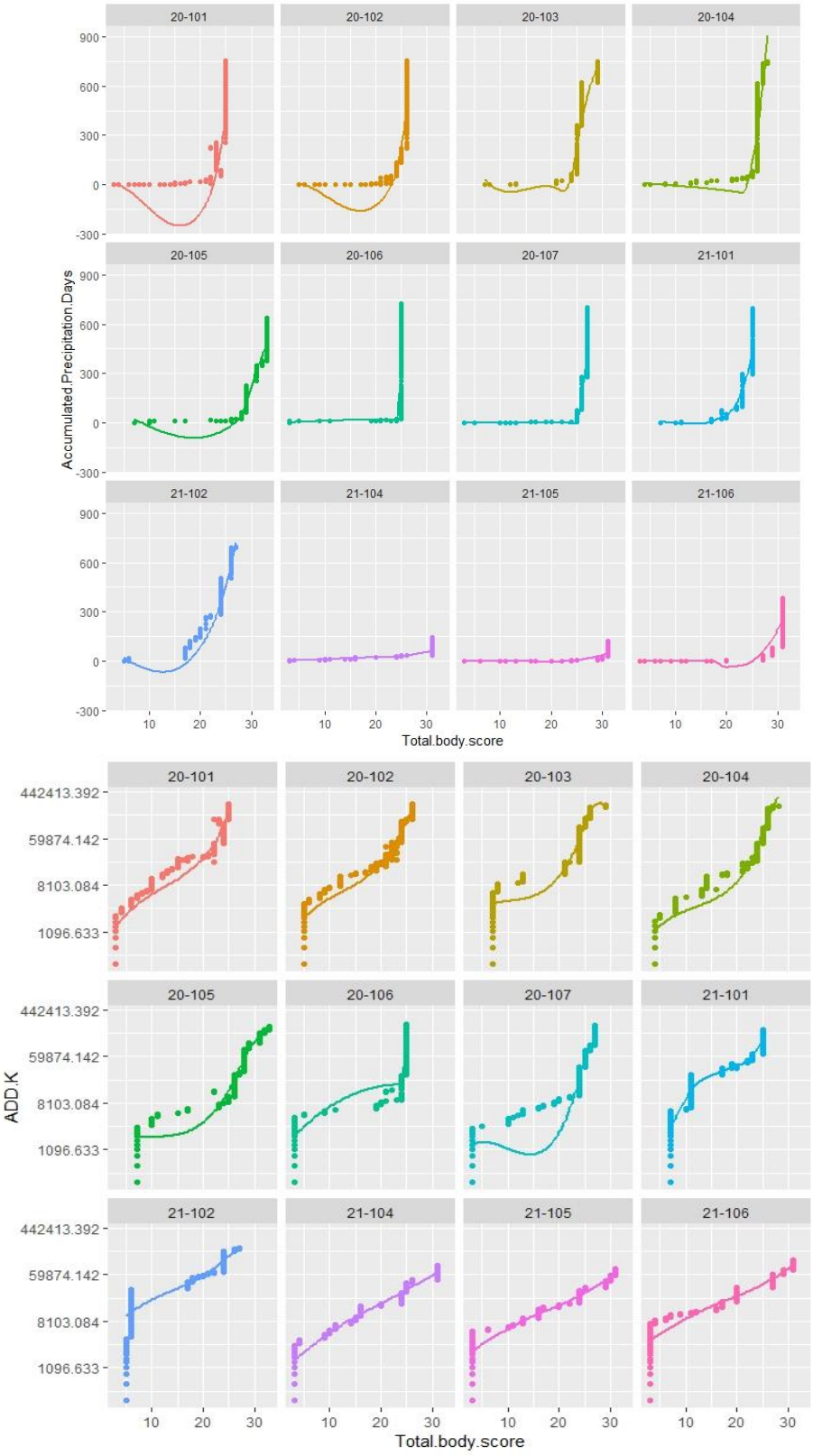

Figure 4-17: LOESS comparison of APreD and ADD K distribution plots. Note the generally shared trend in rapid increase of TBS with greater PMI. Donor position and color are consistent across variables.

The distribution of accumulated precipitation days (APreD) is similar in structure to accumulated pressure days. Unlike rainfall, defined as the amount of rain that falls on one day, APreD encapsulates any product of atmospheric water vapor (such as rain, sleet, snow) that falls from clouds due to gravitational pull. Both ADD K and APreD demonstrate a rapid increase in TBS followed by a score plateau. The distribution of APreD presents a steeper curve, indicative of a more rapid increase in TBS throughout early PMI than is associated with temperature. However, APreD shares the same overall distribution structure as ADD K, suggestive of the potential utility of APreD in PMI estimation.

4.2.2d *Accumulated relative humidity days (ARHD)*

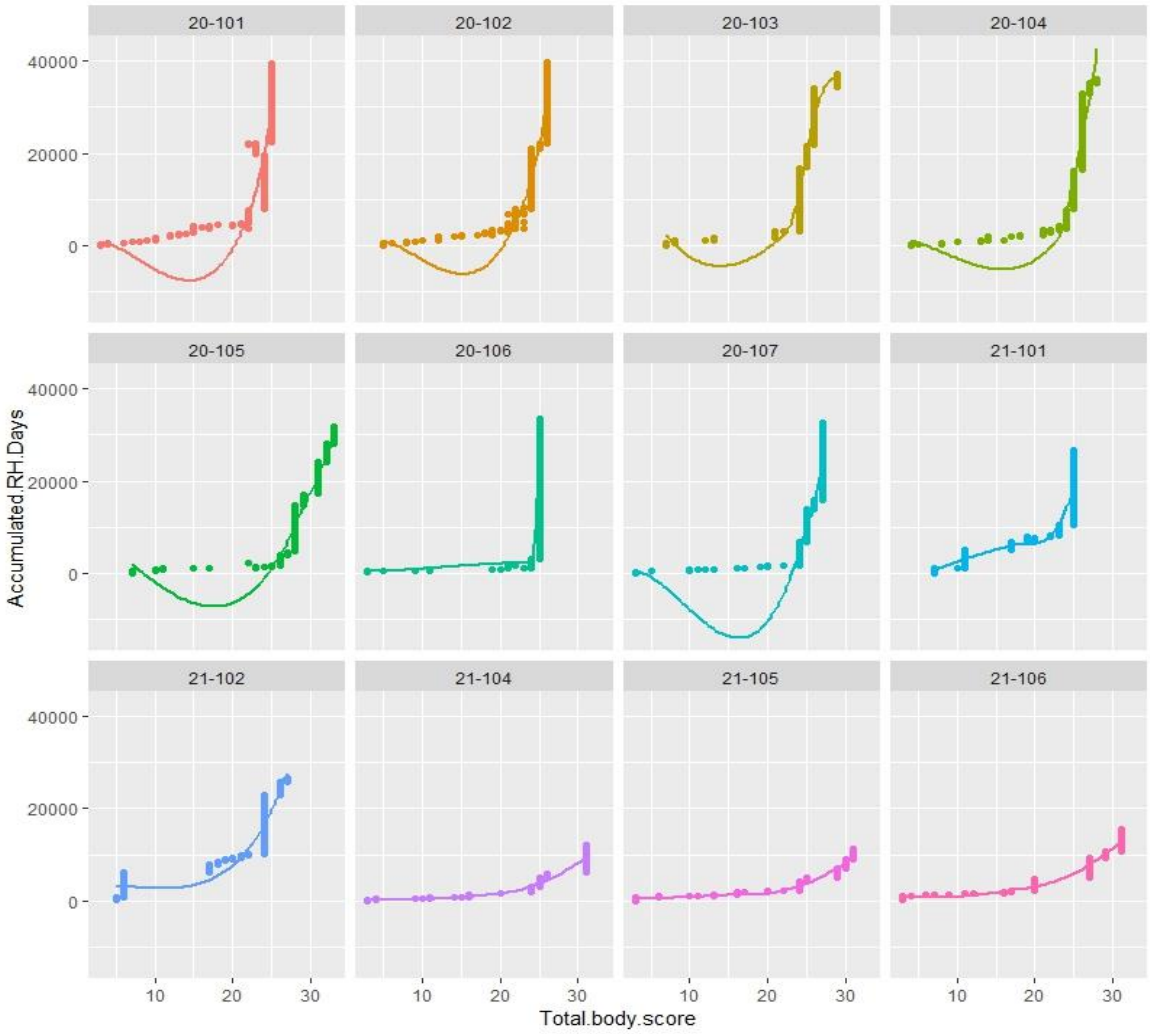

Figure 4-18: Distribution of individual donor TBS vs ARHD among the high-altitude cohort.

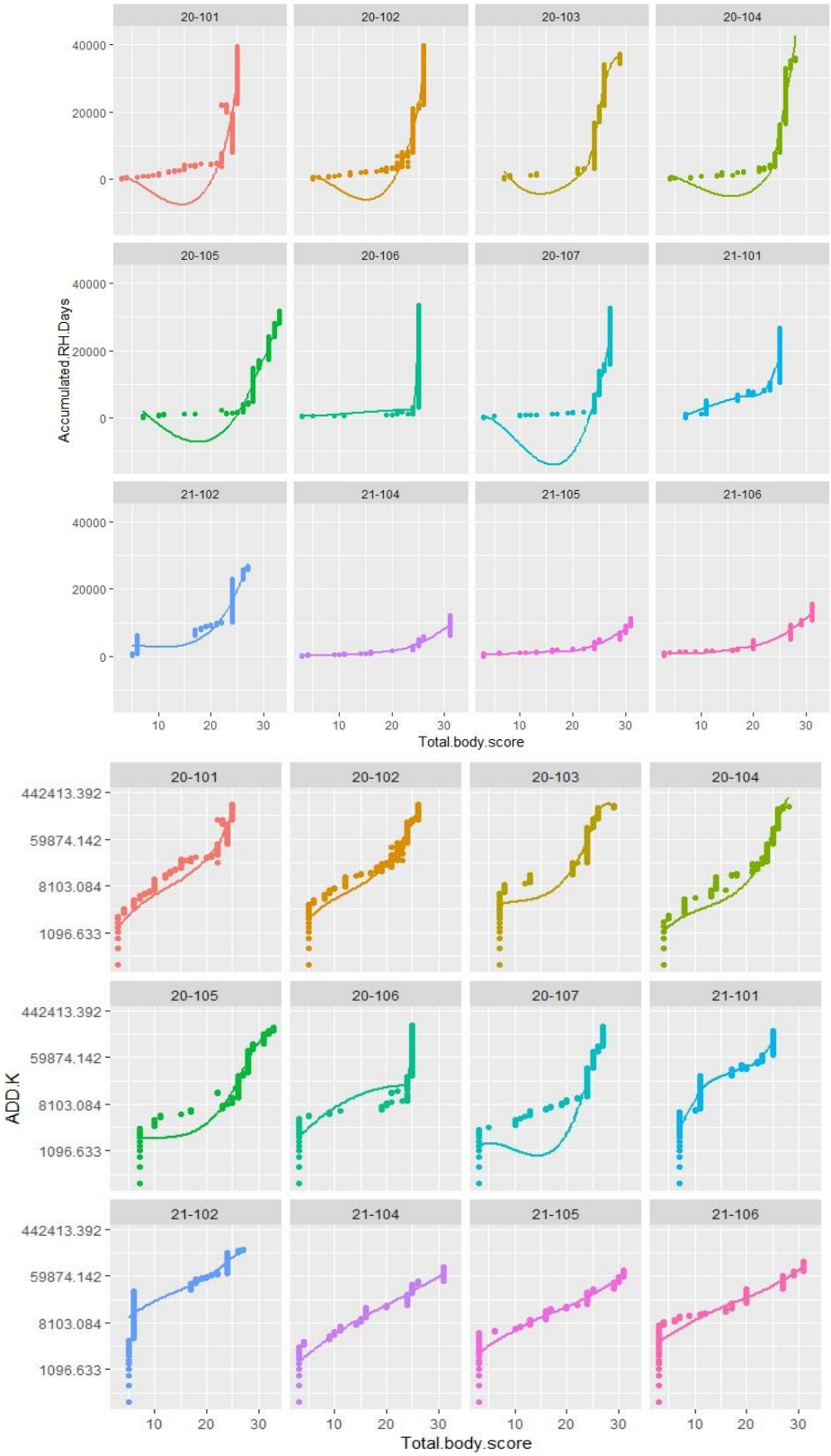

Figure 4-19: Comparison of ARHD and ADD K LOESS distribution plots. Note the generally shared trend in rapid increase of TBS with increase in PMI. Donor position and color are consistent across plots.

The distribution of accumulated relative humidity days (ARHD) is similar in structure to APD, and APreD. Both ADD K and ARHD demonstrate a rapid increase in TBS that plateaus with an increase in PMI. While the distribution of ARHD presents a similar structure, the 'plateau' phase is characterized by a continued slow climb among the majority of donors. However, ARHD shares the same overall distribution structure as ADD K, which suggests the potential utility of ARHD in the estimation of PMI.

4.2.2e *Accumulated solar radiation days (ASRD)*

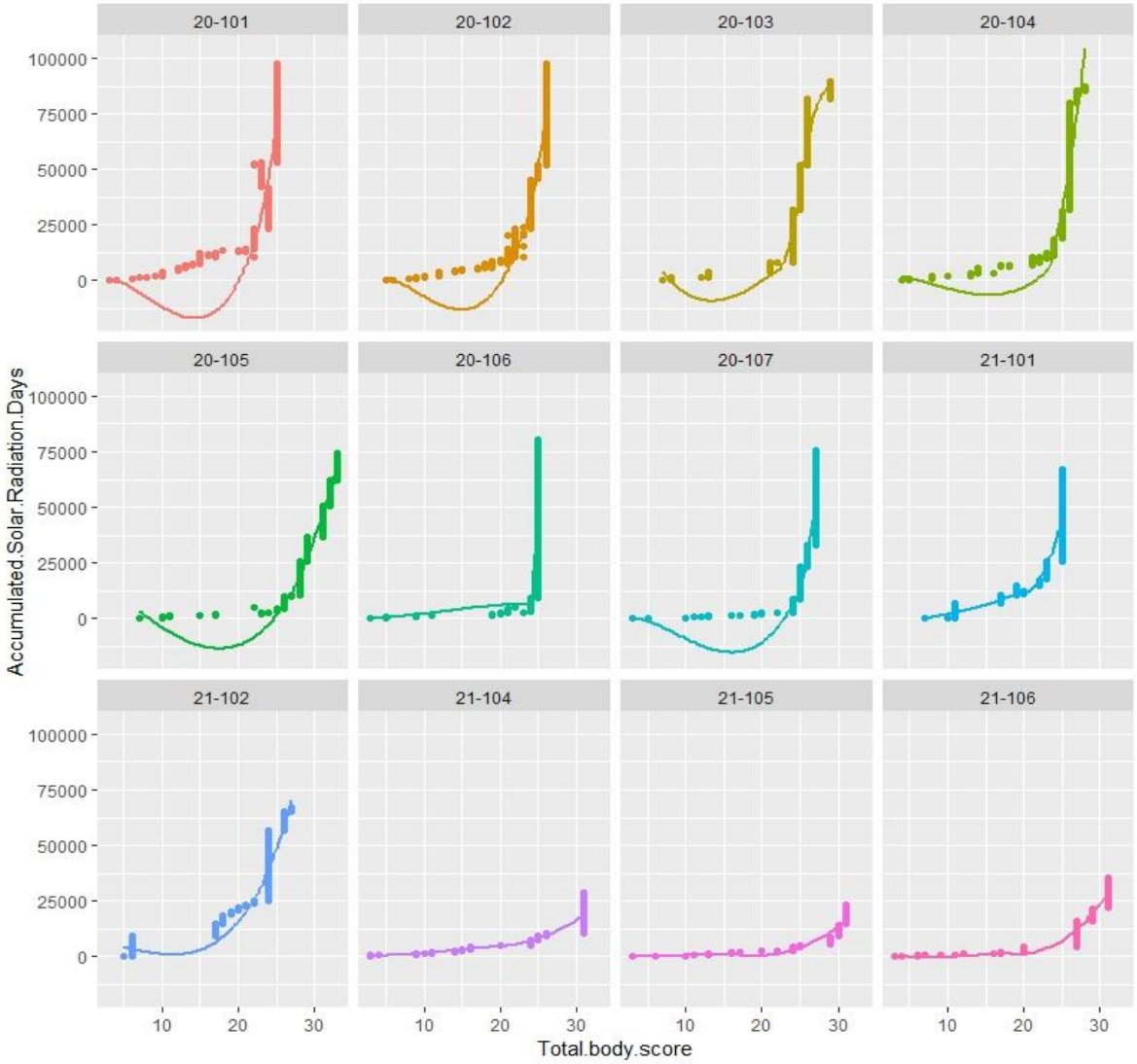

Figure 4-20: Distribution of individual donor TBS vs ASRD among the high-altitude cohort.

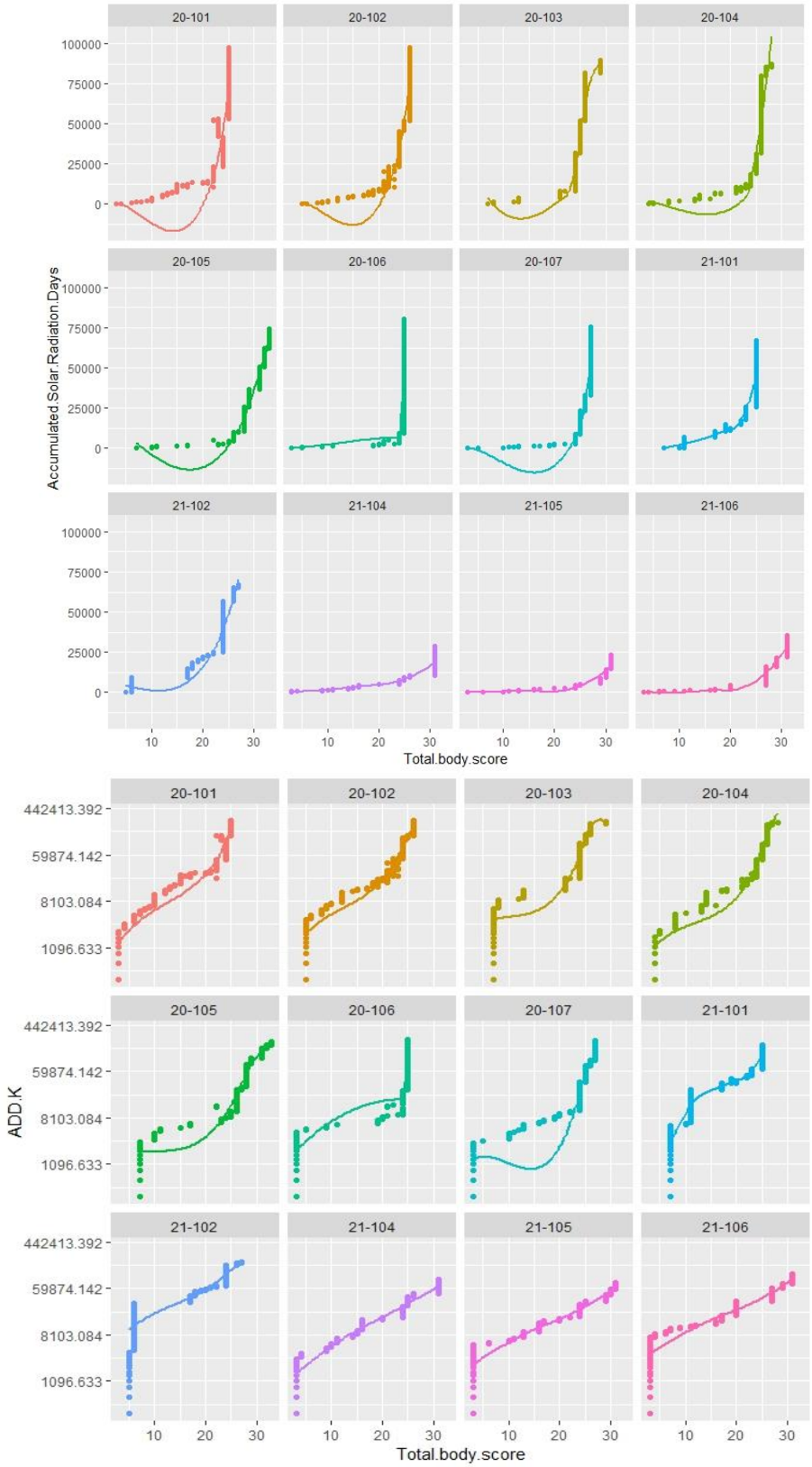

Figure 4-21: LOESS comparison of accumulated SRD and ADD K distribution plots. Note the generally shared trend in rapid increase with PMI. Donor position and color are consistent across plots.

Both ADD K and ASRD demonstrate an increase in TBS with an increase in PMI, followed by a plateau. However, the 'plateau' observed in ASRD is composed of several linear plateaus that increase with greater PMI. The (paradoxically named) 'dynamic plateau,' associated with ASRD suggests its potential to serve as a powerful predicter in the estimation of late-stage PMI.

4.2.2f *Accumulated wind speed days (AWSD)*

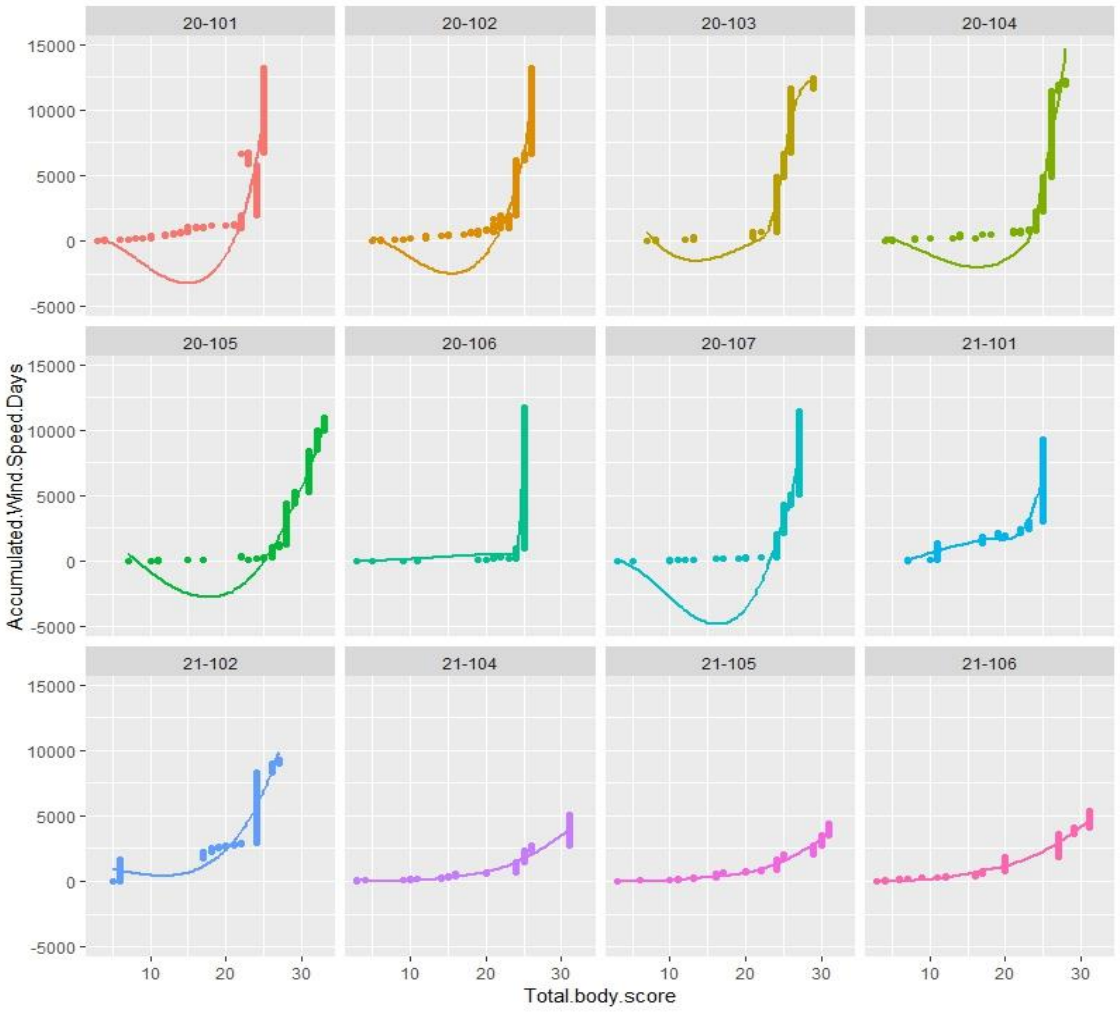

Figure 4-22: Distribution of individual Donor TBS vs AWSD among the high-altitude cohort.

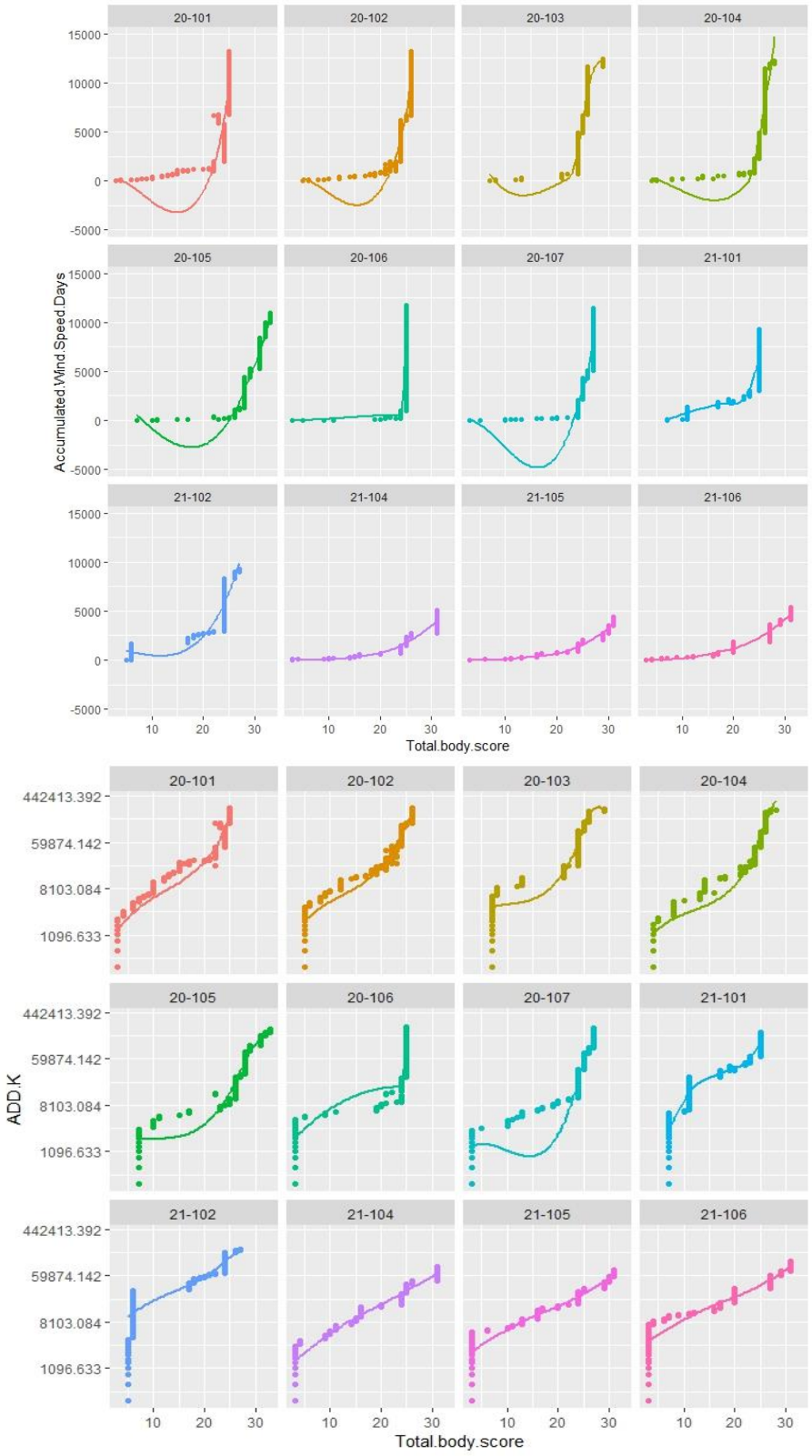

Figure 4-23: LOESS comparison of AWSD and ADD K distribution plots. Note the generally shared trend in rapid increase of TBS with increase in PMI. Donor position and color are consistent across plots.

Both ADD K and AWSD demonstrate a rapid increase in TBS associated with early PMI, although AWSD presents an early horizontal trend in climb that is not present on the ADD K scale. While less dynamic than the plateau series associated with ASRD, late stage ASWD presents a similar trend. While differences are distinct in early PMI, AWSD shares an overall similar distribution with ADD K, with the added benefit of the dynamic late-stage plateau series, suggesting the utility of AWSD in PMI estimation.

4.2.3 Results: Multivariate regression

The application of a LOESS curve to each of the atmospheric variables invariably demonstrates that the data are not linear. A multivariate regression model simultaneously incorporating each of the atmospheric variables as the response variable, and TBS as the single explanatory variable was performed. A comparison of R-squared values to assess the explanatory power of variation in decomposition associated with each variable was performed. Polynomials were tested in the first, second, and third orders using the default window span of $\alpha = 0.75$. R-squared values for each degree are presented in Table 4-1. While ADD K was used to eliminate negative temperature values in visual assessment of LOESS plots, there is a paucity of data supporting the scale's use in taphonomic study. As a result, all subsequent data are considered along the ADD ˚C scale.

Table 4-1: Comparison of R-squared values among atmospheric variables tested using the first, second, and third orders.

Weather Variable	First order R^2	Second order R^2	Third order R^2
Accumulated Degree Days ˚C	0.5464	0.6092	0.6435
Accumulated Pressure Days	0.5481	0.5692	0.5904
Accumulated Rain Days	0.0056	0.0803	0.0965
Accumulated Relative Humidity Days	0.5274	0.5523	0.5716
Accumulated Solar Radiation Days	0.5555	0.6646	0.6663
Accumulated Precipitation Days	0.4507	0.4602	0.4962
Accumulated Wind Speed Days	0.5906	0.6540	0.6539

With the exception of ARD, all atmospheric variables perform almost as well as ADD, and some better than ADD based on order. This general pattern was observationally predicted within the data fitted with a LOESS curve. R-squared values associated with the first (linear) order explained the least amount of variation in decomposition, an expected outcome of analysis of non-linear data. However, the R-squared values associated with APD, ASRD, and AWSD exceeded ADD. Both the second and third orders are parabolic, and both categories present higher R-squared values when compared to those of the linear model. R-squared values associated with ASRD and AWSD explained more variation in decomposition than ADD in the second order. While the R-squared value associated with APD increased, it failed to rise above that of ADD. The third order yielded the highest R-squared values across all atmospheric variables, an unsurprising result based on the complexity of the data structure demonstrated by LOESS. In the third order, the R-squared values associated with ASRD and AWSD exceeded that of ADD, followed by APD, ARHD, APreD, and ARD, respectively.

Consideration must be given to the selection of window span and the degree of the polynomial order, as each constitutes a tradeoff between bias and variance. A small window span limits the data proximal to x which may result in insufficient data and an inaccurate fit, resulting in large variance. A large window span results in over-smoothing, with subsequent loss of information, resulting in large bias. The polynomial selected carries equal weight. While a high-degree polynomial provides a better approximation of the population mean (less bias), the model incorporates more factors (greater variance). Because this is an exploratory analysis designed to generally assess the potential predictive power of atmospheric variables in future model building, analytical priority was given to the R-squared value.

Because multivariate regression models yield slope and intercept, a series of predictive equations may be derived from the data. However, due to the poor qualitative and quantitative performance of the TBS model at high-altitude, these equations are not considered applicable to the

data in this study, and therefore have not been presented. However, they do demonstrate the analytical power associated parabolic modeling and with early exploratory analysis.

4.3 C*onclusion*

Quantitative analysis of the high-altitude data within the TBS model indicates that it is not a good fit for these data, rendering application of the model in a high-altitude environment inappropriate. Distribution plots demonstrate that the high-altitude data are not linear. Because there is a paucity of evidence to support the cessation of decomposition at 0 ˚C, the high-altitude TBS data were considered along three temperature scales, ADD C, ADD C>0, and ADD K and plotted using LOESS. The distribution of ADD K and ADD C>0 presented similarities attributable to the removal of negative values from the data set. Conversely, the distribution of ADD C was characterized by complexity resulting from undulations associated with negative values. Overall, ADD K detected changes in late-stage score plateaus that were obscured by the ADD C>0 scale. This is likely due to the incorporation of small increments of thermal energy into the ADD K scale, as opposed to their removal from the ADD C>0 scale. Further research devoted to the use of temperature scales in predictive model building is needed, however ADD K is a promising scale for integration of negative values and for application in environments associated with negative temperature values, as predicted by Dabbs (in press).

The distribution of six atmospheric variables were assessed using LOESS. With the exception of accumulated rain days, each distribution shared varying degrees of similarity in structure with ADD K. Multivariate regression performed in the first, second, and third orders confirmed these observations. The lowest R-squared values were observed in the first (linear) order, a predictable outcome based on the non-linear data set. The R-squared values associated with accumulated solar radiation days and accumulated wind speed days exceeded those of ADD in the second and third orders, indicating both explain more of the variation in decomposition at high-altitude than temperature. Future study devoted to the integration of two or more ADD atmospheric variables into model building is warranted.

CHAPTER 5

RESULTS QUALITATIVE ANALYSIS

5.0 Qualitative analysis: Classic categories of tissue change

Within its intracategorical descriptions, the TBS model uses six 'classic,' descriptions of decomposition change: skin slippage, purge, specific patterns of soft tissue color change, marbling, bloat, and moist decomposition. Each category was scored as present (1) / absent (0) on each data day, facilitating correlation between the categorical change and ADD. Each variable, and the interdonor range in ADD point presentation are presented in Figure 5-1. Because the goal of category identification is to create a descriptive matrix unique to high-altitude, the range is presented as opposed to each ADD point to: (1) establish earliest presentation; and (2) establish the range of ADD within which a categorical trait first presents. Categorical traits possessing a wide range of presentation (i.e. presenting across a broad range of ADD), are less likely to serve as strong temporal markers and are therefore less likely to benefit future development of a predictive model. This study established an 80% threshold for intracohort trait presentation. Traits failing to meet the 80% threshold were rejected from future model building. The temperature scale used is ADD ˚C, however because temperature models were previously discussed in terms of ADD C, ADD C>0, and ADD K, ADD^{C} is substituted for clarity.

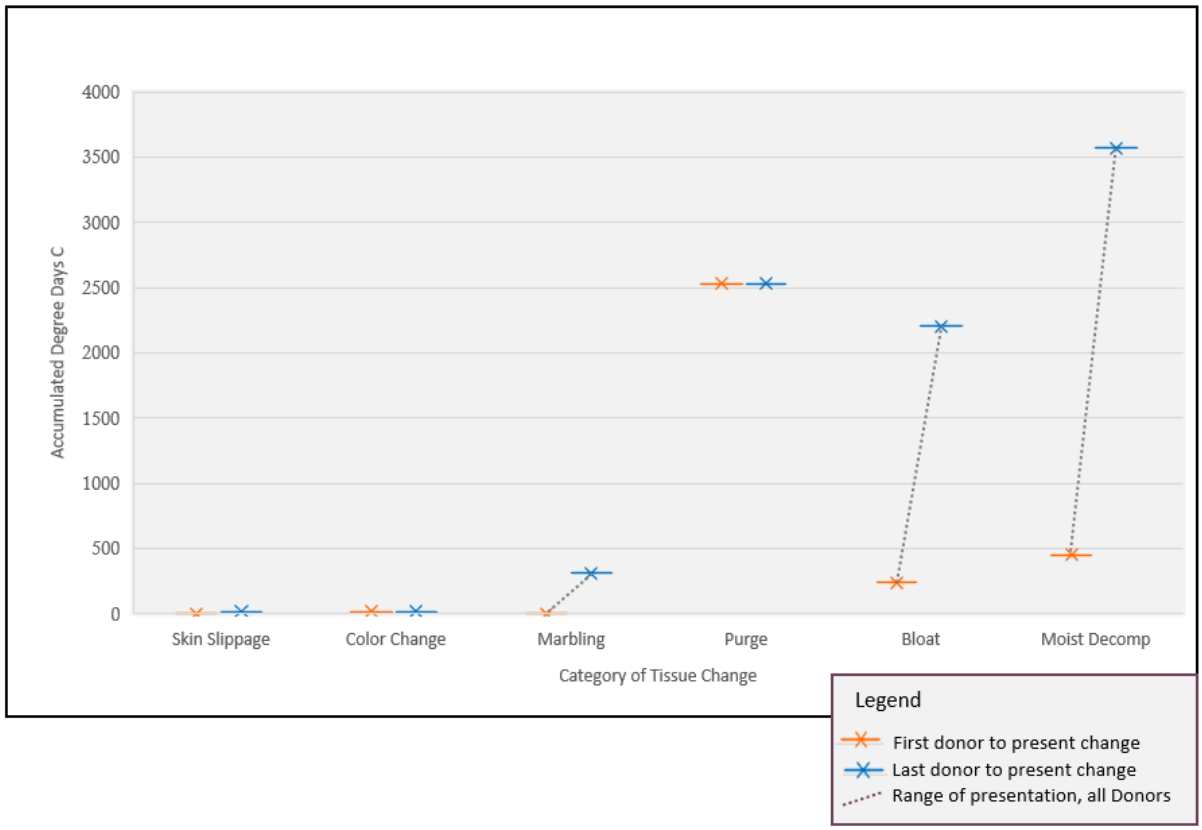

Figure 5-1: Cohort range in ADD^{c} point presentation, by classic decomposition variable. Orange represents the earliest point presentation of a named trait; blue represents the latest point presentation of a named trait. The space between represents the range of trait presentation across all donors.

5.1 Presentation of classic categories within the high-altitude cohort

5.1.1 Skin Slippage: Skin slippage was observed in three donors (25% of sample); the range of first point of presentation was 0 - 18 ADD^{c}. This variable failed to meet the established 80% intracohort threshold, and is rejected from future model building.

5.1.2 Purge: Purge was observed in one donor (8% of the sample); the point of first presentation was 2533 ADD^{c}. This variable failed to meet the established 80% intracohort threshold, and is rejected from future model building.

5.1.3 TBS Model Specific Pattern of Color Change: While all donors presented distinct patterns of color change, the initial step was to assess the degree to which the observations made at high-altitude were encapsulated by the TBS model. The TBS model presents four categories of

color change: (1) fresh, no discoloration; (2) pink to white; (3) gray to green; and (4) brown to black. Fresh, no discoloration is considered foundational to all decomposition trajectories, and therefore was not subject to analysis.

5.1.3a *Pink to white discoloration*: The pink to white category is problematic because 11 of the 12 donors are White and therefore naturally present as pink to white in early decomposition. Additionally, the pink to white category presupposes that the subject of a PMI estimate is White. This category is rejected because it fails to encapsulate the broad spectrum of *in vivo* skin color that may present for forensic analysis.

5.1.3b *Gray to green discoloration*: This category was observed in one donor (8% of the sample); the point of first presentation was 18 ADD^{c}. This variable fails to meet the established 80% intracohort threshold, and is rejected from future model building.

5.1.3c *Black to brown discoloration:* This category variably presented in circumscribed areas of color change throughout decomposition. However, neither presented as the dominant mode of color change, or with phasic consistency to the TBS model. Brown (specifically, umber) did present as a dominant color change within the high-altitude cohort, however this was associated with late advanced decomposition, as opposed to a phasic characteristic of early decomposition as presented by the TBS model. Likewise, the TBS model identifies black discoloration as a dominant phase within early decomposition. While high-altitude donors presented black discoloration, it was typically circumscribed as opposed to dominant and observed in mid to late decomposition. Because the presentation of black to brown tissue discoloration fails to correspond with the phasic pattern of color change presented within the TBS model, both are rejected from future model building.

5.1.4 Marbling: Eight donors presented marbling (67% of sample). The range of first point presentation was 1 - 309 ADD^c. This variable fails to meet the 80% intracohort threshold and is rejected from future model building.

5.1.5 Bloat: Bloat was presented by eight donors (67% of sample). The range of first point presentation was 239 - 2206 ADD^c. While presentation of bloat approaches the 80% intracohort threshold, the range of ADD presentation is broad, suggesting that it does not possess the resolution necessary to act as a temporal predictor in this high-altitude environment. This variable failed to meet the 80% intracohort threshold, and is rejected from future model building.

5.1.6 Moist decomposition: Moist decomposition was presented by 10 donors (83% of sample). The range of first point presentation was 450 - 3572 ADD^c. This variable meets the established 80% intracohort threshold, and is accepted for future model building.

5.2 Categorical change identified at high-altitude

From the onset of the study, the 'classic,' categories of decomposition served as indices against which to identify a suite of decompositional change within the high-altitude cohort. Because high-altitude specific categorical change had to be identified and described, emphasis was placed on isolating and describing environment specific categories of change and the frequency with which they presented within the cohort. This was performed within the first-year cohort (2020; Donors 20-101 – 20-107) and constituted an eight-month study period (3/31/2020 – 1/7/2021). Once isolated, these categorical changes were documented and scored as present (1) / absent (0) more precisely in the second year. Field documentation of the isolated variables began with the first placement of the year 2021 cohort, on January 7, 2021. A retrospective study of the first donor cohort was performed using field photographs to holistically assess the presence of high-altitude changes within the collective study cohort.

The result was the identification of seven categorical changes. While several of these categories are well-documented in research and in case study, the suite of changes is hypothesized to be unique to the high-altitude environment. These categories include: (1) environment specific pattern and trajectory of soft tissue color change; (2) adipocere formation; (3) fluid bloat; (4) tissue island formation (localized differential decomposition); (5) skin sloughing; (6) pseudoburial; and (7) slope roll. Each variable, and the interdonor range of ADD point presentation are presented in Figure 5-2. The ultimate goal of category identification is the creation of a descriptive matrix unique to high-altitude. As such, the range of trait presentation is emphasized as opposed to each donor's ADD point presentation. This was done to: (1) establish earliest point presentation; and (2) establish the range of ADD point presentation within which a categorical trait presents. A categorical trait possessing a wide range of point presentation (i.e. presenting across a broad range of ADD), is less likely to serve as a strong temporal marker and therefore less likely to be of benefit in future model building. The 80% threshold for intracohort trait presentation established to test the 'classic' categories was also applied to high-altitude categorical change. Traits failing to meet the 80% threshold were rejected from future model building.

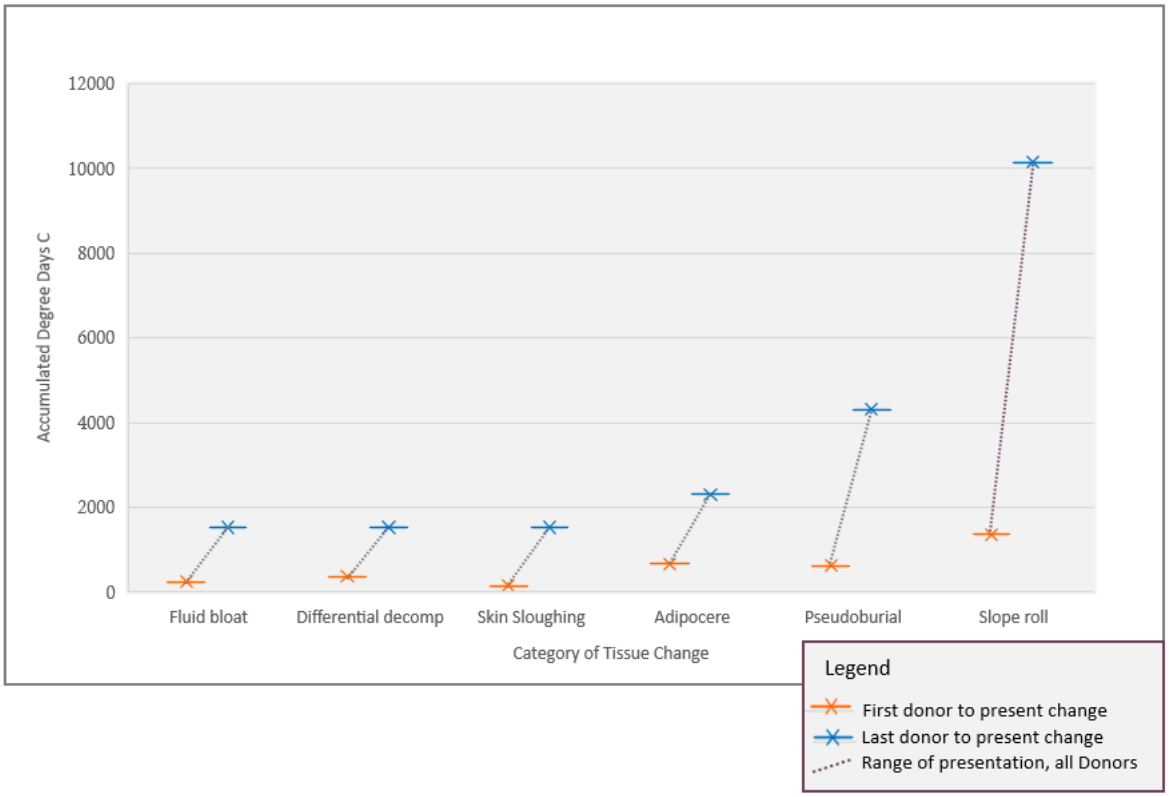

Figure 5-2: Cohort range in ADD^{c} point presentation, by decomposition variable. Blue represents the earliest point presentation of a named trait; orange represents the latest presentation of a named trait. The space between represents the range of trait presentation across all donors.

5.2.1 Adipocere formation: Adipocere formation occurs in environments where water content (endogenously and/or exogenously sourced) is high and oxygenation is low. The result is hydrolysis (the cleaving of chemical bonds by a molecule of water) and hydrogenation (the process through which a molecule - in this case lipid molecules - are reconfigured through their affinity for dihydrogen molecules). The result is a structural reconfiguration of the lipid base, resulting in a solid or semi-solid fat. As lipids are converted to fatty acid, pH drops, inhibiting bacterial growth and promoting soft tissue preservation (Clark *et al.* 2006).

Adipocere formation presented in 12 donors (100% of sample); the point presentation range was 668 – 2313 ADD^{c}. This variable meets the established 80% intracohort threshold and is accepted for future model building. Three modes of adipocere formation were observed: (1) superficial aggregates; (2) defect bound aggregates; and (3) interstitial and intracellular adipocere formation.

5.2.1a Superficial Adipocere Formation: Superficial aggregates ranged from lipid dense focal aggregates (Figure 5-3) to structurally prominent and widely dispersed films (Figure 5-4). Superficial lipid dense adipocere formation begins in moisture folds and builds upon itself in both aggregate height and breadth. At the apogee of formation, aggregates lose their pliable quality and density resembles candlewax in appearance and palpation. As time progresses, density is lost, and morphology is characterized by bulk shedding of aggregates into the surrounding environment. Low-lying, widely dispersed films are retained further into the postmortem interval; morphology is characterized by sequential desiccation, cracking, and sloughing. A time series progression of superficial adipocere formation is presented in Figure 5-4.

Figure 5-3: Left - Lipid dense focal adipocere aggregate L 35.50cm x W 13cm x H 10cm at the furthest projection points; **Right** - Broad distribution of superficial lipid dense aggregates (indicated by arrows).

Figure 5-4: Time series formation of superficial lipid dense adipocere formation. Formation begins in moisture folds and builds upon itself in both aggregate height and breadth of dispersal, until eventual desiccation and sloughing. Pictured: PMI 240-336 days; TBS 29-31; ADD^{c} 36 - 1636

5.2.1b Defect Bound Adipocere Formation: Gross observation of focal adipocere formation was observed in tissue defects introduced by scavenging packrats (*Neotoma cinerea*; the bushy tailed woodrat) and boring magpies (*Pica hudsonia*). Adipocere formation was both focal and circumscribed due to the barrier created by the walls of tissue defect. A less frequent variant of this phenomenon was adipocere formation in pronounced anatomical depressions (e.g. the abdomen following tissue collapse).

Focal, circumscribed adipocere formation was characterized by tissue defect formation, most typically introduced by a small-bodied scavenger. Defect bound aggregate formation followed a predictable course: (1) defect introduction; (2) infiltration of defect by endogenous fluid; (3) active bubbling of fluids (effervescence) within the defect as gasses are released; (4) introduction and increase of fluid opacity as lipid infiltration progresses; and (5) transition from lipid dense fluid to soft ceraceous paste. The lipid dense adipocere served as a valuable food source for nesting packrats, who returned to the defect to scavenge newly formed adipocere. The cycle of defect introduction, adipocere formation, and scavenging, repeated until moisture and lipid content were no longer sufficient to propagate the series (Figure 5-5). Magpies also demonstrated a propensity for boring into tissue containing superficial adipocere aggregates (Figure 5-6).

Figure 5-5: Defect bound adipocere formation. **Top**: Fluid infiltration of scavenger induced defect with active bubbling as gasses and lipids are released. **Middle**: Adipocere fermentation followed by scavenging of lipid dense wax and second-generation infiltration of defect by endogenous fluids. **Bottom**: Second-generation of lipid sparse adipocere formation, followed by scavenging of adipocere and third-generation fluid infiltration.

5.2.1c Interstitial and intracellular adipocere formation: Interstitial and intracellular adipocere formation are hypothesized to be catalyzed by endogenous H_2O and subdermal hydrolysis and hydrogenation of lipid dense cellular membranes, cellular compartments, interstitial fluid, and adipocytes. Interstitial and intracellular adipocere formation followed two modes of presentation. In individuals with a lower body mass index (BMI<30), formation presented as a waxy epidermal sheen (Figure 5-6), a diffuse morphological structure (Figure 5-7), or as subcutaneous aggregates resembling large, deep, wax filled bullae. Wax filled bullae were often scavenged late into the postmortem interval, revealing fresh adipocere filled pockets within ceraceous desiccated tissue (Figure 5-8). When the tissue was palpated, the consistency of deep dermal layers was waxy and pliable. Superficial interstitial adipocere formation was characterized by a bright tissue surface sheen. When manipulated, the tissue had the consistency of thin sheets of beeswax. In advanced decomposition, as desiccated tissue expanded and contracted, waxy longitudinal cracks presented. Due to the presence of interstitial adipocere, tissue adopted an elastic character and environmentally mediated mechanical stress and strain were insufficient to result in tissue failure. Instead, tissue responded elastically, evident in the macroscopic presentation of stress and strain lines (elastic deformation) and gross morphological change (plastic deformation). Neither phenomenon was associated with failure (Figure 5-9). In addition to the above outlined tissue change, individuals with a higher BMI (BMI>30) presented macroscopically visible intracellular adipocere formation. Intracellular adipocere formation is hypothesized to be the result of appreciable expansion of superficial adipocytes following endogenous adipocere formation. Intracellular adipocere formation is evident in longitudinal retention of cellular expansion across the postmortem interval. Retention of cellular expansion is followed by cellular retraction during intermediate to

advanced decomposition, a pattern consistent with macroscopic patterns of adipocere formation, desiccation, and retraction across time (Figure 5-10).

Figure 5-6: Top: Thorax presenting interstitial adipocere formation, characterized by a waxy sheen to the tissue and a beeswax like quality when palpated; note superficial widely dispersed adipocere aggregate (right shoulder; yellow arrows) and subcutaneous abdominal aggregate (white arrows). **Bottom left**: Adipocere containing entrapped maggots, formed in depression following abdominal collapse. **Bottom right:** Magpie boring in tissue containing a superficial desiccated adipocere aggregate (right thigh, midline).

Figure 5-7: Interstitial adipocere formation as a diffuse morphological structure. All yellow surfaces are dense layers of adipocere beneath superficial dermal layer.

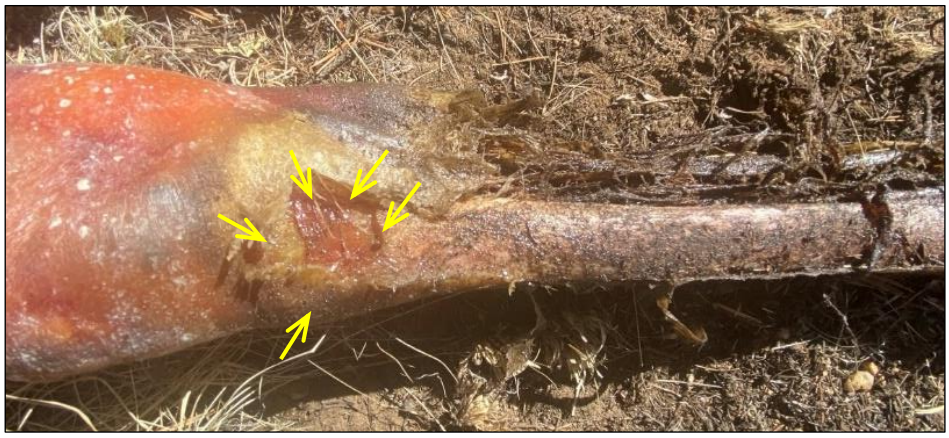

Figure 5-8: Scavenging of an adipocere filled pocket in late-stage decomposition (indicated by arrows). Note the retention of 'fresh' waxy moisture, contrasting the surrounding waxy desiccated tissue and skeletonization.

Figure 5-9: Interstitial adipocere in advanced decomposition. Elasticity afforded by interstitial adipocere prevents tissue failure during mechanical stress and strain.

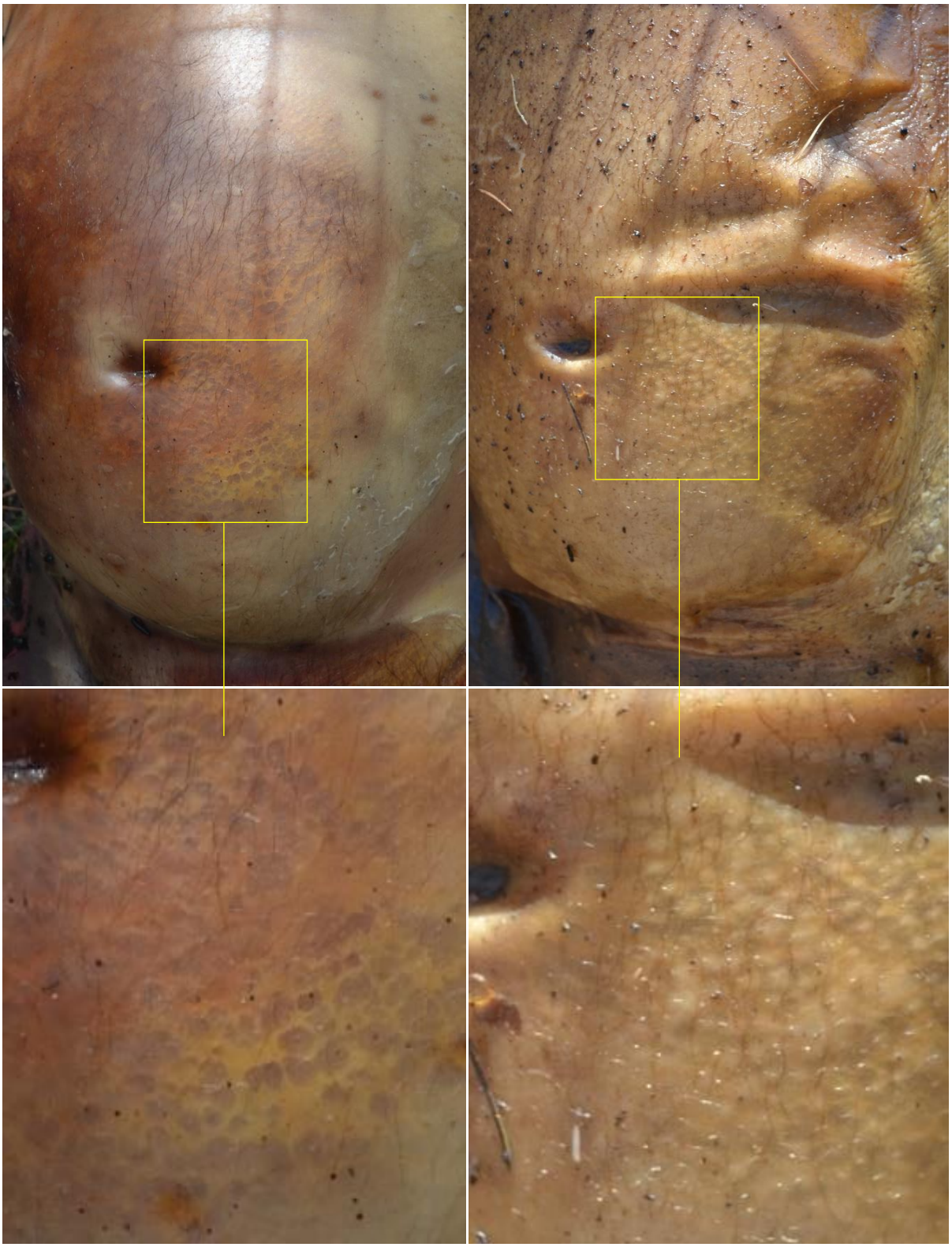

Figure 5-10: Intracellular adipocere formation, macroscopic (top) and detail view (bottom). **Left**, early subdermal intracellular adipocere formation (PMI 70 days, TBS 15, ADD^{c} 465). **Right**, changes in subdermal intercellular adipocere formation in advanced decomposition. Cellular structure has retracted but adipocere structure retains general morphology (PMI 130 days, TBS 22, ADD^{c} 1395).

5.2.2 Fluid Bloat: Fluid bloat was presented by 10 donors (83% of sample); the range of first point presentation was 239 - 1530 ADD^c. This variable meets the 80% intracohort threshold and it is accepted for future model building.

Fluid bloat resembles gaseous bloat in that it results in expansion of an affected anatomical region. Gaseous bloat is observed in anatomical regions most closely associated with lumina of the digestive tract (abdomen, neck, proximal limbs). Conversely, fluid bloat most typically presents in downslope oriented, peripheral aspects of the body (distal limbs/hands and feet). Two donors (20-103 & 20-104) were placed head downslope, feet upslope. Both presented fluid bloat in the shoulders, neck, and lateral cranium. The remaining donors were placed head upslope, feet downslope. In this orientation, fluid bloat presented in the enclosed capsule of the hands and feet. This suggests that the catalyst for fluid bloat is the displacement of fluid across tissue gradients due to gravity.

Fluid bloat occurs when migrating fluids reach a dermal barrier and aggregate, causing expansion of the surrounding tissue. The application of pressure to the affected area causes fluids to displace and the overlying tissue to blanch. An important byproduct of fluid bloat in the hands and feet is the passive displacement of skeletal elements to a more superficial position. Time series observation of fluid bloat formation revealed a macroscopic pattern of: (1) endogenous fluid infiltration of the affected region with dermal entrapment; (2) expansion of the affected body region as dermal collagen and elastin stretch to accommodate increases in fluid volume while the dense keratinization of the dorsal and palmar surfaces of the hands/feet prevent tissue failure; (3) muscle dense keratinized palmar/dorsal surfaces create a modified anatomical simple machine where entrapped, pressurized fluid creates a dynamic fulcrum, the diaphysis of manual/pedal long bone acts as a beam, the cortico-trabeculae dense epiphyses act as the load, and the relatively static keratinized palmar/plantar surfaces approximate effort (a fixed counter weight). The result is the superficial displacement of associated skeletal elements as fluid volume increases; (4) tissue expansion associated with phasic increases in fluid

volume perpetuates superficial displacement of skeletal elements; (5) cessation of tissue expansion occurs when the volume of infiltrating fluid exceeds the spatial capacity of the affected anatomical region; (6) the attainment of maximum volume is followed by a decrease in fluid volume with concomitant drying of the overlying dermis. This process does not present in a manner similar to moist decomposition, suggesting forced redistribution of fluids back into surrounding (and now dehydrated) tissue, slow evaporation, or a combination of both; and (7) the trend in fluid loss and tissue drying advances. Skeletal elements are further displaced and their superficial displacement emphasized as retracting tissue tightly shrink wraps the related skeletal element. The resulting, intimately associated tissue-bone complex is sufficient to emphasize skeletal elements as diminutive as sesamoid bones. Summarily, the process of fluid bloat, superficial reorientation of skeletal elements, fluid loss, and intimate tissue-bone complex result in rapid skeletal exposure with concomitant vulnerability to scavengers and gravity motivated patterns of disarticulation and environmental transport. A time series progression of fluid bloat is presented in Figure 5-11.

Figure 5-11: Time Series progression of fluid bloat in the hand. **Top**: fluid aggregation and superficial displacement of distal metacarpals. **Middle**: Increase in fluid volume with concomitant superficial displacement of the proximal phalanges, followed by fluid volume decrease and drying of overlying tissue. **Bottom**: Fluid loss and tissue drying resulting in further morphological emphasis of underlying skeletal elements.

5.2.3 Tissue Island formation/localized differential decomposition: Tissue Island formation/localized differential decomposition was presented by 10 donors (83% of sample); the range of first point presentation was 374 - 1530 ADD^c. This variable meets the 80% intracohort threshold and is accepted for future model building.

Tissue Island formation/localized differential decomposition presents as both focal and diffuse areas of tissue dehydration. Both modes advance to coalescence with surrounding tissue over time. In areas of diffuse tissue drying and retraction, large areas of waxy desiccated dermis are interrupted by circumscribed areas of fresh tissue (i.e., tissue islands). These 'tissue islands,' are distinct from bullae (postmortem blisters containing serous fluid) in structure and density. Unlike bullae, these circumscribed structures retain tissue structure and density, emphasized by the relief of surrounding tissue (Figure 5-12). Tissue island pronouncement increases with time, suggesting that islands are the byproduct of phasic periods of fluid displacement and interstitial adipocere formation. Concomitant peripheral tissue drying and retraction results in pronounced differences in the composition of islands and adjacent tissue. In their final phase of presentation, islands are incorporated into the surrounding tissue, suggesting fluid displacement, and subjectivity to the same physiological processes manipulating the surrounding tissue.

In focal presentation, the inverse is true. Focal presentation is characterized by circumscribed areas of dry tissue and interstitial adipocere formation surrounded by fresh tissue. Tension generated by the retraction of dry tissue creates peripheral tension lines in the adjacent fresh tissue. The circumscribed area of dry tissue invariably presents maroon or orange tissue discoloration that expands in anatospatial area with the increase of time (Figure 5-13).

Figure 5-12: Pictured: Right proximolateral leg. **Top** - Tissue islands retain the structure and density of fresh tissue, emphasized by the relief of surrounding tissue (PMI 29 days; TBS 8; ADD ^{c} 139). **Middle** – Island pronouncement increases with time suggesting phasic tissue retraction (PMI 42 days; TBS 13; ADD^{c} 340). **Bottom** - Eventual incorporation of islands into surrounding tissue (PMI 52 days; TBS 21; ADD^{c} 482).

Figure 5-13: Differential decomposition characterized by tissue dehydration/interstitial adipocere formation. **Left** - Wide dispersal of focal differential decomposition (45cm x15.25cm) presenting orange discoloration and central tissue islands. **Right** - Small circumscribed area of differential decomposition (3.80cm x 3.54cm) presenting maroon/rose tissue discoloration. Note tension generated by the retraction of dry tissue resulting in peripheral tension lines in fresh tissue.

5.2.4 Tissue Sloughing: Tissue sloughing was presented by 12 donors (100% of sample); the range of first point presentation was 148 - 1530 ADD^c. This variable meets the 80% intracohort threshold and is accepted for future model building.

Tissue sloughing is distinct from skin slippage in both timing and mechanism. Skin slippage is catalyzed by the release of hydrolytic enzymes by cells lining the dermal-epidermal junction – as a cellular-mediated process, it necessarily occurs in early decomposition before cell death is complete. Tissue sloughing is defined as a later-stage multivariate process of tissue loss due to extrinsic mechanical processes acting upon intrinsic tissue structure. As decomposition degrades the structural integrity of organ and tissue structures, and interstitial adipocere formation advances, the dermis mechanically retracts. The result is punctuated incidences of large-scale sloughing of the most superficial layer of desiccated tissue. As is observed with tissue island formation/localized differential decomposition, tissue sloughing takes two forms: (1) dynamic; and (2) idle.

5.2.4a Dynamic tissue sloughing is most typically observed during early to intermediate decomposition and is anatomically focal (e.g. a punctuated event may be limited to the cranio-facial

region). Tissue loss is characterized by the uplift of large, delicate, desiccated tissue segments. Tissue segments may maintain structural cohesion as they coil and separate from the underlying dermis, or slough independently in large flakes. Tissue loss is invariably associated with tissue color change across each generation of sloughing. A weekly time series of dynamic cranio-facial tissue loss is presented in Figure 5-14.

5.2.4b Idle tissue sloughing is associated with advanced decomposition. Idle tissue loss is characterized by homogenous drying of tissue and minute separation of tissue layers associated with large relatively flat anatomical segments (e.g. the chest or abdomen). Early-stage minute tissue separation is almost imperceptible but lends the affected area an opaque quality. As idle separation advances, the affected tissue begins to crack while maintaining an intimate but tenuous relationship with the interfacing dermal layer. The result is an expanse of tissue that resembles a pane of cracking glass. Tissue 'shatter' is followed by the successive sloughing of delicate tissue layers. This process is phasic and repetitive throughout mid- to late- decomposition and is invariably associated with color change in the underlying tissue. A weekly time series of idle tissue loss is presented in Figure 5-15.

Figure 5-14: Weekly time series presenting dynamic tissue sloughing. Each line presents one week of change anterior aspect (left), anterolateral aspect (right). Phases 1 -3.
Phase 1 (PMI 43 days; TBS 12; ADD 180): Note maroon/orange/plum mottling with no apparent tissue uplift.
Phase 2 (PMI 50 days; TBS 17; ADD 276): Note plum/maroon color homogenization and proliferative tissue separation in the superior and lateral aspects of the face and neck.
Phase 3 (PMI 57 days; TBS 18; ADD 388): Note fading of maroon discoloration in the cheeks, tissue discoloration trending toward diffuse plum. Active tissue sloughing has resulted in reduced breadth of sloughing clusters.

Figure 5-14: Weekly time series presenting dynamic tissue sloughing. Phases 4-6.
Phase 4 (PMI 63 days; TBS 19; ADD 425): Note homogenously plum facial discoloration and prominent separation of sloughing clusters into large individual flakes.
Phase 5 (PMI 71 days; TBS 20; ADD 547): Note plum discoloration trending toward brown/umber with maintenance of plum undertones. Appreciable sloughing with reduction in size of tissue clusters has occurred.
Phase 6 (PMI 78 days; TBS 21; ADD 733): Note dramatic change in tissue discoloration from plum/brown/umber to central umber and peripheral pale brown/yellow following terminus of tissue sloughing.

Figure 5-15: Weekly time series presenting idle tissue sloughing, phases 1-6.
Phase 1 (PMI 60 days; TBS 24; ADD^{c} 645) Abdominal discoloration homogenously yellow with slight opacity.
Phase 2 (PMI 66 days; TBS 24; ADD^{c} 669) Early, intimate separation and cracking at tissue interface with yellow discoloration shifting to maroon/rose/orange/yellow mottling.
Phase 3 (PMI 74 days; TBS 24; ADD^{c} 707) Diffuse shattered glass appearance over maroon/rose/orange/yellow mottling. Circumscribed areas of tissue sloughing present homogenous color change (indicated by arrows).
Phase 4 (PMI 82 days; TBS 24; ADD^{c} 736) Sloughing resulting in additional circumscribed areas of color change (indicated by arrows).
Phase 5 (PMI 90 days; TBS 24; ADD^{c} 762) Tissue trending toward diffuse vibrant orange while retaining overlying layer of tissue separation.
Phase 6 (PMI 96 days; TBS 24; ADD 773) Expansive tissue sloughing resulting in homogenous vibrant orange tissue discoloration. Note tissue collapse, waxy adipocere sheen, and lateral yellow/brown discoloration due to adipocere formation.

5.2.5 Pseudoburial: Pseudoburial was presented by 12 donors (100% of sample); the range of first point presentation was 600 - 4300 ADD^{c}. This variable meets the 80% intracohort threshold accepted for future model building. However, the point of first presentation range is broad and the associated changes wholly dependent upon the extrinsic environment, suggesting that this trait may not possess

the resolution necessary to act as a strong temporal marker. Pseudoburial is therefore considered an important component of the local taphonomic profile, but is rejected for use in future model building.

Pseudoburial is a dynamic process observed throughout the period of bodily exposure to environmental elements. Pseudoburial is an extrinsic process within which decomposing remains are acted upon by the ambient environment. While not unique to, nor homogenous across, the high-altitude environment, documentation of the local complex of environment specific patterns of taphonomic change contributes to the holistic picture of local patterns of decedent-environment interaction. A greater understanding of local patterns of passive change – such as pseudoburial – have the potential to inform variables such as taphonomic overprinting and the design of search and recovery missions. Summarily, pseudoburial encompasses the processes by which a body becomes buried over time. Three primary modes of pseudoburial were observed (a) active; (b) passive; and (c) animal mediated.

5.2.5a Active pseudoburial is catalyzed by movement of the surrounding matrix downslope through environmental processes such as slope wash - the transportation of soil and rock downslope by gravity and water. Active pseudoburial is an additive process, as displaced matrix aggregates around the body, dries, and is built upon by subsequent generations of wash. Over time, overlying layers begin to create depth around the body, resulting in partial to complete burial of the affected area (Figure 5-16).

5.2.5b Passive pseudoburial is catalyzed by aerial transport of debris that settle on the body's surface, in depressions, and beneath tissue layers in areas of anatomical ingress (Figure 15-17). Matrix, pine needles, sticks, pinecones, pine fascicles, seed caps, and fine sediment may aggregate on body surfaces or within exposed cavities, individually or in sum. Summarily, passive pseudoburial serves to obscure the body within the landscape and has the potential to catalyze decomposition by acting as an exfoliant, or by chemical induction, such as the

introduction of environmentally metabolized volatile alcohol and oxides sourced from monoterpene rich pine needles (Figure 5-17 & 5-18). Additionally, in the case of donors presenting superficial adipocere formation, surface adipocere acts as an adhesive, binding debris, including those that act as chemical exfoliants, masking color change, and facilitating environmental camouflage (Figure 5-19).

Figure 5-16: Active pseudoburial catalyzed by the movement of matrix, rock, and surface debris downslope by gravity, water, and snow drift. Note the almost complete burial of the right arm (indicated by arrows), and the density of rock and soil infiltration of the proximal legs and groin area.

Figure 5-17: Passive pseudoburial. **Left** – Thorax obscured by falling pine fascicles, pinecones, pine needles, and sticks. **Right** – lower thorax, inguinal region, and proximal legs obscured by surface soil aggregates, cast pine seed shells, rocks, and pine needles.

Figure 5-18: Complex passive pseudoburial. Thorax obscured by infiltration of pine needles, pinecones, rocks, matrix, and sticks. The visual image is further complicated by differential staining of osseous and connective tissues, skeletal scavenging and localized scatter, differential cortical weathering, cortical sloughing, and delamination.

Figure 5-19: Passive pseudoburial**. Left** – abdominal overview. **Right** - detail view. Superficial adipocere formation acting as a surface adherent for environmental debris. Note the moist, ceraceous surface and entrapped pine needles and sediment.

5.2.5c Animal mediated pseudoburial is the byproduct of vertebrates scratching, digging, or burrowing into the matrices adjacent to a body, resulting in partial coverage of the associated anatomical region. Due to the intentional exclusion of large-bodied scavengers, scavenging was limited to insect, rodent, and avian species. Avian-promoted pseudoburial is characterized by scratching and boring in the surrounding matrix and is invariably accompanied by discernable avian tracks. Rodent-promoted pseudoburial is characterized by the unidirectional 'tossing' of matrix associated with burrowing into the body or the surrounding environment (Figure 5-20). The result is partial burial of a body surface, or surfaces associated with the site of soil disturbance.

The three subprocesses of pseudoburial may present individually, or in sum. Because it has the ability to (1) obscure the body in the environment; (2) create an inaccurate picture of body deposition (e.g. surface deposition misinterpreted as partial burial); (3) obfuscate or provide evidence for a primary versus secondary deposition site; and (4) encourage tissue loss through abrasion, exfoliation, and introduction of localized sources of destructive chemical compounds, pseudoburial is considered a critical component of the regional forensic ecological profile. However, due to the multiple modes of

pseudoburial, the unpredictability associated with the surrounding ecozone in producing a mode, and analyst inability to predict mode interaction, it is not considered a positive predictive variable.

Figure 5-20: Animal mediated pseudoburial. Burrow hole in lateral thorax indicated by arrow, note the almost complete coverage of the right proximal arm by displaced matrix.

5.2.6 Slope Roll: Slope roll was presented by eight donors (67% of sample); the point of first presentation range was 1355 - 10142 ADD^c. Because this variable presents a wide breadth of first point presentation, and did not meet the established 80% intracohort threshold it is rejected from future model building. However, like pseudoburial, slope roll represents an important component of the local taphonomic profile.

Slope roll is defined as the displacement of a whole body, or body parts, by a disturbance (typically scavenging or gravity) on a slope. Unlike pseudoburial – descriptive of environmentally mediated burial of human remains over time – slope roll describes the modes and patterns of the transport of human remains through the environment across time (Figure 5-21 & 5-22). Eight donors presented variably perceptible modes of slope roll (Table 5-1). Mode and timing of each is considered important to building an overall composite of the role the environment plays in displacing skeletal elements over time. In examples associated with autopsy incision (e.g. Donor 20-107), skeletal

fragments are regarded as a reasonable approximation of skeletal disarticulation that may result from trauma such as would be seen in partial or comminuted fracture of the cranium.

Table 5-21: Left - Calotte in approximate anatomical orientation (PMI 50-days). **Right** - calotte post-movement downslope (approximately 4.60 meters; 85 days postmortem) as a byproduct of avian scavenging and gravity.

Figure 5-22: Donors 21-103 and 21-104, commingled and displaced downslope. Note the soil erosion line (indicated by yellow line), contributing to the movement of both articulated skeletons downslope.

Table 5-1: Mode and pattern of slope roll, summary of circumstance, TBS and ADD at the inception of movement.

Donor ID	Affected Area	Catalyst	Summary	TBS	ADD
20-102	Sternal plate	Scavenging/gravity	Sternal plate passively removed by small-bodied scavengers as they consumed adjacent tissue, sternal plate migrated further downslope due to gravity.	22	1965 ℃
20-103	Limbs	Scavenging	A medium bodied canid scavenger burrowed into the cage. Passive, lateral displacement of the right and left arms occurred as the hands were actively scavenged.	29	6493 ℃
20-104	Limbs	Scavenging	A medium bodied canid scavenger burrowed into the cage and displaced the right leg, laterally and downslope.	29	6493 ℃
20-105	Cranium	Gravity	Cranium separated from the postcranium due to tissue decomposition followed by downslope roll.	31	3873 ℃
20-107	Calotte	Gravity	Calotte separated from cranium in autopsy. As tissue decomposition progressed, displacement from the cranium and movement downslope occurred.	24	720 ℃
21-101	Whole body	Gravity	Body placed mid-winter above snow line; approximately one meter of downslope movement was observed during spring melt.	17	128 ℃
21-104	Whole body	Scavenging/gravity	Disarticulation of skeleton by scavengers, subsequent movement of skeletal elements both up and downslope by scavengers and gravity.	31	821 ℃
21-106	Whole body	Scavenging/gravity	Disarticulation of skeleton by scavengers, subsequent movement of skeletal elements both up and downslope by scavengers and gravity.	31	821 ℃

5.2.7 Color change: While the patterns of soft tissue color change described in the TBS model failed to present within the high-altitude cohort, a distinct series of color changes were observed. The pattern of color change observed at high-altitude is a complex and dynamic process. Two primary color trajectories were observed: (1) orange dominant; and (2) maroon dominant. Two subcategories of color change associated with both primary trajectories, including (1) mottling – a pattern of irregular marks, spots, patches, or blotches of different shades or colors; and (2) ombre – the blending of one color hue into another, were further observed. While the precise trajectory of color change varied between donors, color change followed one primary continuum, and is therefore considered a powerful temporal predictive marker. The continuum of color change is presented in Figure 5-23 and summarized in Table 5-2. The ADD^C range represents the approximate length of time each color phase presented.

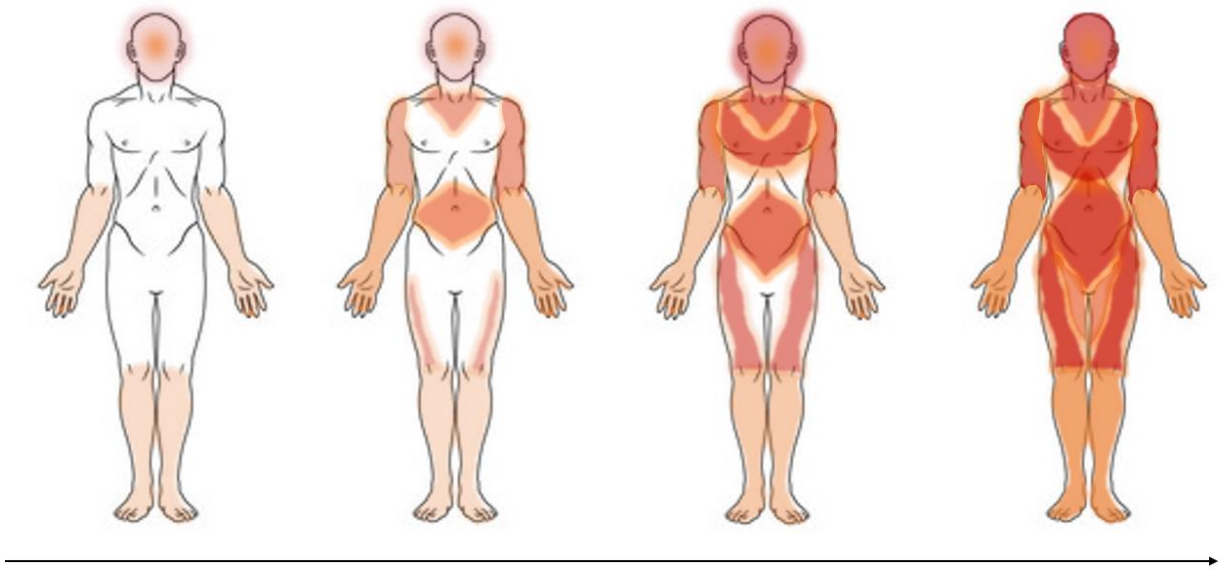

Figure 5-23: General anato-spatial trajectory of tissue color change throughout the postmortem interval.

Table 5-2: Summary of major phases of color change, categorized by ADD.

ADD ℃	Head/Neck	Thorax	Limbs
3 – 55 ℃	Deep maroon/purple or orange blush around the eyes and cheeks that advances to diffuse purple or orange flush	Deep maroon/purple or orange blush across the chest. Small, circumscribed areas of tissue drying with vibrant orange or maroon color change usually present in thorax and limbs.	Early purple or orange blush in hands and soles of feet advancing to rose/maroon or orange ombre blush in distal limbs.
56 – 179 ℃	Diffuse maroon or orange discoloration interrupted by prominent display of the inverse color (bright orange or maroon) on the bridge of the nose and on the cheeks.	Maroon or orange blush in chest deepens and extends laterally toward the shoulders. The abdomen presents a focal area of maroon or orange color change. A bridge of 'fresh' soft tissue bisects the two regions.	Hands/feet and distal limbs advance toward diffuse maroon or orange discoloration.
180 – 260 ℃	First generation tissue sloughing reveals vibrant orange or maroon discoloration with peripheral deep plum discoloration.	Lateral extension of chest discoloration coalesces with shoulder discoloration. Abdominal and chest discoloration remain distinct but begin to interrupt the tissue bridge bisecting the two regions and extend toward coalescence.	Distal arms and legs present vibrant diffuse maroon or orange discoloration. Early color changes in the proximal arms and legs, often with a 'blush' appearance that may include maroon/orange mottling.
261 – 670 ℃	Second generation of diffuse tissue sloughing reveals diffuse gray/plum* discoloration.	Coalescence of tissue discoloration in proximal arms and lateral shoulders/chest. Coalescence of abdominal and chest discolorations. Homogeneity in color between the chest, abdomen, and inguinal region.	Coalescence of discoloration in proximal and distal limbs, interrupted by 'fresh' tissue bridge at the elbow/knee. Distal limbs present diffuse discoloration, proximal limbs present variation of maroon/ rose/orange ombre.
671 – 1730 ℃	"Color creep" phase. Umber introduced to midfacial region with retention of gray/plum discoloration of the periphery.	"Color creep" phase. Chest and lateral shoulders maintain homogenous discoloration. Midline chest, abdominal region, inguinal region, and immediate proximal limbs share homogenous orange, maroon, or maroon/rose/orange ombre discoloration.	"Color creep" phase. homogenous orange, maroon, or maroon/rose/orange ombre discoloration of distal limbs coalesces with discoloration in proximal limbs.
1731 – 2540 ℃	Loss of vibrancy phase. Loss of gray/plum periphery; homogenization of diffuse umber.	Loss of vibrancy phase. Diffuse maroon fades to deep plum, oranges fade to yellow/orange ombre.	Loss of vibrancy phase. Diffuse maroon fades to deep plum, oranges fade to yellow/orange ombre.
2541 – 2636 ℃	Homogenization of diffuse umber.	Diffuse umber in chest and shoulders. Pale yellow/umber ombre in lateral chest, abdomen, inguinal region, and immediate proximal limbs.	Pale yellow/umber ombre in proximal limbs, diffuse umber in distal limbs.
Color change > 2636 ADD ℃	Diffuse umber	Diffuse presentation of umber or pale yellow, advancing to pale brown with increase in ADD ℃.	Diffuse presentation of umber or pale yellow, advancing to pale brown.

* While the TBS model describes a gray to green discoloration, it is described and observed in very early decomposition. The plum/gray observed in this study presents two to three months postmortem and is foundationally derived from the vibrant orange/maroon that precedes it.

5.2 Honorable Mentions

Honorable mentions are changes observed within the study cohort that lack a strong phasic correlation, or are hypothesized to have an impact on the gross or chemiophysical trajectory of decomposition. These traits were not quantified in preliminary trait discernment and definition. These categories include (1) limb float; (2) effervescence; (3) capillary marbling; and (4) snow metamorphism, creep, and ice accretion.

5.2.1 Limb float

Limb float is defined as the creation of negative space between a limb and the underlying matrix. Prominent limb float was observed in five donors (42% of cohort). The hands and feet were most often affected; in one case the cranium presented enduring float following placement in mid-winter and snowmelt in the spring. Based on limited observation, limb float is catalyzed by two primary modes: (1) tissue desiccation followed by faunal mining and displacement of underlying matrix (Figure 5-24a); and (2) slow but persistent repositioning of the body by snow creep, followed by rapid drying as might be catalyzed by sublimation (Figure 5-24b). Limb float informs unique, environmentally mediated modes of postmortem bodily manipulation resulting in alteration or repositioning of affected anatomical regions. Limb float has the potential to act as a temporal marker, as presentation is associated with advanced PMI and/or overwintering, or as a component of the local taphonomic profile.

5.2.2 Effervescence

Effervescence describes the formation of gas bubbles in a liquid by a chemical reaction. Effervescence is an ephemeral variable, typically present for one to three days, precluding an accurate estimate of intracohort presentation. In high-altitude environments, decreased atmospheric pressure

results in expansion of gases to a greater volume. Active bubbling of fluids was observed in tissue defects throughout early to late-intermediate decomposition (Figure 5-25). The physiochemical properties of effervescence have both the potential to impact rate and pattern of decomposition, and inform the suite of variables that have the potential to affect high-altitude decomposition individually or in sum.

5.2.3 Capillary marbling

Capillary marbling is characterized by the dissemination of hydrogen sulfide gas and resultant color change within capillaries, the delicate branching blood vessels that form a complex network between the arterioles and venules. While the presentation of 'traditional' marbling was relatively prominent within the high-altitude cohort (67% of cohort), capillary marbling was presented by 12 donors (100% of cohort). Capillary marbling presented in circumscribed areas of the body throughout the postmortem interval and was most typically characterized by vibrant orange tissue discoloration threaded by a network of delicate, complex maroon/rose marbling (Figure 5-26).

5.2.4 Snow Metamorphism, Creep, and Ice Accretion

Holistically, snow metamorphism, creep, and ice accretion constitute a complex suite of intercalated variables that have the potential to affect the rate and pattern of decomposition. Snow metamorphism broadly refers to dynamic patterns of snow structure dictated by atmospheric conditions, and temporally associated thermal clines within snow overburden. Creep refers to the gradual, gravity catalyzed movement of snow downslope and is hypothesized to affect limb float. Depending on ground conditions and atmospheric variables, signs of both snow metamorphism and snow creep may be macroscopically visible (Figure 5-27). Ice accretion refers to the complex modes of interaction between ice, gross morphology, and circumscribed tissue layers. Because the resolution of data collection in this study was not sufficient to facilitate individual, microscopic investigation, this complex suite of variables are considered in sum (Figures 5-28 & 5-29). Summarily these seasonally

circumscribed variables indicate high potential to impact both gross, and physiochemical characteristics and therefore warrant future investigation.

Figure 5-24a Top: Limb float resulting from faunal matrix mining. Note fresh upturned soil. Yellow lines indicate relationship between palmar surface, slope, and 8 cm void
Figure 5-24b Bottom: Limb float resulting from snow creep and rapid drying. Yellow lines indicate relationship between the posterior cranium, slope, and 17 cm void.

Figure 5-25: Effervescence, dynamic fluid bubbling and moisture wicking at the base of a thoracic autopsy incision, indicated by arrows.

Figure 5-26: Capillary marbling, characterized by a delicate network of capillaries (indicated by arrows) presenting a maroon/rose discoloration within orange tissue discoloration (right proximolateral leg).

Figure 5-27: Snow metamorphism and creep. Note ice dense structure of snow with wind sweep lines, pitting and overall morphology that follows tissue surface, indicative of structural change in snow overburden. Wind sweep lines oriented downslope provide a visual representation of snow creep (indicated by arrows).

Figure 5-28: Cross-section of ice aggregates affecting the craniofacial region.
Top: Ice aggregates following morphology of face and maintained during snow melt.
Bottom: Wind turbinated snow in right orbital, resulting in the formation of a compact ice sphere.

Figure 5-29: Cross-section of modes of postcranial ice aggregates.
Top: Ice aggregates retained on fresh tissue surface following primary snowmelt (arrows; note relative absence of snow in peripheral environment). The retention of longitudinal ice aggregates suggests subdermal freezing to maintain the temperature necessary to maintain superficial aggregates.
Bottom: Adherent ice aggregates entrapped in desiccated tissue folds.

5.3 Donor Specific Trajectory of Decomposition

Table 5-3 presents donor biodemographics, placement, and collection data; this table is presented in duplicate for ease of reference. Donor specific trajectory of decomposition from placement to study terminus are presented in Tables 5-4 – 5-16 . Phases are defined by TBS range and reported with associated ADD and PMI.

Table 5-3: Biometric data, placement and maximum TBS, placement and recovery dates, and maximum ADD by Donor *indicates a donor is still located in the outdoor facility, TBS Max reflects terminus of study period).

Donor ID	Age	Sex	Ancestry	Height (cm)	Weight (kg)	Autopsied	Pre-Placement PMI (Days)	Placement Date	Placement TBS	Collection Date	Final TBS	Final ADD˚C
20-101	69	Male	White	178	115.7		8	03/31/2020	3	11/5/2022*	26	6107
20-102	64	Male	White	175	68.9	Yes	12	03/31/2020	5	11/5/2022*	26	6122
20-103	51	Male	Black	180	84.4		23	05/28/2020	7	11/5/2022*	29	5767
20-104	75	Male	White	188	74.8		3	06/10/2020	4	11/5/2022*	28	5523
20-105	89	Female	White	150	40.8		6	07/23/2020	7	8/22/2022	33	4201
20-106	64	Male	White	173	74.8	Yes	11	07/25/2020	3	11/5/2022*	25	4832
20-107	53	Female	White	160	72.6	Yes	9	08/28/2020	3	11/5/2022*	27	4237
21-101	55	Male	White	175	70.3	Yes	17	01/07/2021	3	11/5/2022*	25	3929
21-102	65	Male	White	185	83.5		14	01/07/2021	7	11/5/2022*	27	3916
21-104	73	Female	White	178	111.1		2	08/22/2021	5	7/3/2022	31	1129
21-105	73	Male	White	178	81.6		18	10/15/2021	3	7/3/2022	31	533
21-106	72	Male	White	178	115.7		24	10/25/2021	3	11/5/2022*	31	401

Table 5-4: Trajectory of decomposition - Donor 20-101

Donor TB20-101: Placement Date: 03/31/2020; Placement TBS 3; Pre-placement PMI 8 Days; Pre-placement ADD 24 ˚C		
TBS	**ADD/PMI Range**	**Observed changes**
3-6	3-60 ˚C PMI 1-16 Days	TBS 5 was not observed. Early maroon blush diffuse in face, neck, and superior chest. diffuse discoloration in inguinal region. Circumscribed areas of skin slippage with vibrant orange or maroon color change in underlying tissue. Marbling commences in feet and advances to distal legs and proximomedial thighs. All areas of marbling associated with maroon/rose color change that begins to coalesce in feet with advancing PMI.
7-10	64-144 ˚C PMI 17-39 Days	Marbling in feet/distal legs presents diffuse maroon/orange discoloration and is coalescing into early stage diffuse color change. Pronounced fluid bloat observed in feet; fluid bloat expansion observed with increase in PMI. Longitudinal tissue removal observed in lateral aspect of right manual digit II (likely rodent). New marbling in right and left proximal arms. Flies observed on and around the body.
11-14	158 – 358 ˚C PMI 40-60 Days	TBS 11 was not observed. Color change becoming more pronounced in face with circumscribed areas of vibrant maroon discoloration in the nose and cheeks. Dramatic 'stained glass' tissue sloughing observed in face and left distal leg, revealing second generation vibrant maroon/red color change. Color change initiated in proximal arms, legs, and chest. Fluid bloat observed in right and left hands. Maggot colonization of orbitals, nares, and mouth. Small, focal area of moist decomposition in the face. Scavenger defect in right and left medial feet.
15-19	369 -886 ˚C PMI 61-99 Days	TBS 19 was not observed. Color change diffuse in distal arms and legs and advancing in proximal arms and legs. Lateral creep of color change in chest toward right and left shoulders, focal color change in abdomen with later stage bridging of discoloration across all body sections. Subdermal adipocere formation with visible lipid cell expansion in the abdomen, dermal plaque of adipocere formation on right and left lateral thorax and posterolateral right thigh, and focal adipocere formation in the defect of the left foot. Several areas of differential decomposition (dry tissue presenting color change adjacent to fresh tissue). Prolific oral maggot activity; small black beetles present on all body surfaces. Early-stage abdominal bloat.
20-22	593-3001 ˚C PMI 79-486 Days	Overlap in ADD between body score groups due to score reversal (environmental variables catalyzing the primary presentation of characteristics associated with earlier TBS categories). Overall trend toward homogenous color change; umber at midline, brown on periphery. Pronounced inguinal and abdominal bloat. Peripheral moisture observed in matrix around all body segments. Debris (pine needles, dirt, plant matter) adhering to all body surfaces. Adipocere aggregates on right/left

		lateral thorax and posterolateral right thigh advanced in volume and in distribution, new adipocere formation on the left posterolateral thigh. All adipocere aggregates presented drying followed by crumbling and phasic shedding as PMI progressed. Post-bloat collapse of the abdomen with superficial drying of all dermal layers with retention of waxy, interstitial adipocere quality.
23-24	2053 -3081 ˚C PMI 171-491 Days	Thorax presents umber discoloration with the introduction of pale-yellow discoloration laterally, and in proximal legs. The presence of yellow discoloration advances with ADD, first presenting as mottling in all body sections, before homogenizing and advancing toward umber. All tissue surfaces present an overall trend in drying with retention of interstitial adipocere. Pronounced slope wash; aggregate dirt and tree duff is present in all depressions. Two rodent burrow holes are present in the ground between the thorax and the left arm. Phasic packrat and avian scavenging of hands, feet, distal limbs, scrotum, cranium, and mandible is sufficient for skeletal exposure in all affected areas with eventual loss of the right distal manual phalanges.
25-26	3100 – 6107 ˚C PMI 492-962 Days	Trend of discoloration progressing from pale yellow to homogeneous burnt umber/pale brown. Tissue remains a mix of the two colors at the terminus of the study period. Adipocere presents as diffuse waxy sheen as a result of interstitial formation. The proximal thighs and lateral thorax present a thin, dry, superficial film of adipocere that begins to flake with advancing ADD. Packrat scavenging progresses in the left and right feet. Avian scavenging is more pronounced, evident in bore holes in the abdomen and proximal arms, with ribboning of desiccated tissue.
Terminus	TBS 25 PMI 957 Days ADD 6107 ˚C	Donor TB20-101 remains in the research facility; ‘terminal’ data refers to the data presented at the end of the study period.

Table 5-5: Trajectory of decomposition - Donor 20-102

Donor TB20-102: Placement Date: 03/31/2020; Placement TBS 5; Pre-placement PMI 12 Days; pre-placement ADD 37 ˚C		
TBS	**ADD/PMI Range**	**Observed changes**
3-6	3-49 ˚C PMI 1-16 Days	TBS 3-4 were not observed. 'Medical purge,' associated with all autopsy incision sites (i.e. purging of fluids related to presence in thoracic cavity and gravity as opposed to purge catalyzed by intra-lumen buildup of gasses). Inferior abdomen presents green discoloration that rapidly fades between post-placement days 2-4 (ADD 6-12 ˚C). Head, neck, chest, arms present diffuse pink blush.
7-10	47-87 ˚C PMI 17-28 Days	TBS 7 was not observed. Faint marbling, distal legs and hands. Drying of all edges (ears, lips, nose, distal fingers, and toes). Circumscribed areas of orange discoloration in distal feet and legs. Maroon blush diffuse in head, neck, chest; circumscribed areas of orange present on nose and cheeks. Discoloration of head, neck, and chest advance to deep plum. Bloat in abdomen and proximal legs catalyzes fluid purge from autopsy incision. Hands and feet present orange/maroon ombre. Scavenging of tissue along right inferior border of autopsy incision. Early fluid bloat in hands.
11-14	81-173 ˚C PMI 29-45 Days	TBS 11 & 13 were not observed. Drying of fingers and toes sufficient to define underlying skeletal elements. Hands and feet present deep maroon/orange ombre. Fluid bloat in right hand becomes more pronounced with increase in PMI. Adipocere formation in autopsy 'Y' incision. Scavenging of right/left borders of autopsy incision advance superiorly and laterally. Facial discoloration advances to plum/gray/maroon ombre; ombre advances to deep maroon of peripheral head and diffuse orange blush on cheeks. Neck and chest present deep maroon/plum ombre. Arms present diffuse maroon blush. Scavenging progresses to the peeling of the thin tissue form the dorsum of the right and left toes; color change of associated underlying tissue is vibrant orange. Fly oviposition in ears and along borders of autopsy incision. Tissue sloughing observed on peripheral face (all tissue surfaces surrounding facial features) and lateral chest.
15-19	184-481 ˚C PMI 46-65 Days	TBS 16 was not observed. Flies and environmental debris present on all body surfaces. A prominent rodent game trail (a trail created by habitual faunal use) travels to the left lower corner of cage, in the area of the feet. Bulla formation, distal right and left legs (downslope). Autopsy sutures release (unravel from tissue perforations), revealing sternal plate. Lipids associated with sternal plate and incision borders present vibrant orange color. Fluids present in the thorax display pronounced, active bubbling. Face, neck, and chest retain deep diffuse plum discoloration, drying of

		associated superficial tissue advances with PMI. Fluid bloat pronounced in hands, feet, and distal legs, advances to include distal arms. Hands present deep diffuse maroon discoloration that progresses up both arms and begins to bridge with discoloration of the chest. Feet present circumscribed areas of vibrant orange/maroon discoloration and superficial drying, bordered by fresh tissue. Distal legs present diffuse maroon/yellow ombre. Skin sloughing associated with peripheral face and chest becomes increasingly active and pronounced until it becomes prolific in face, chest, medial arms, and lateral thorax with advancing PMI. Moist decomposition limited to inguinal region and tissue presents deep vibrant orange that advances to rose/maroon. Tissue at ground-body interface presents large diffuse areas of maroon color change. General trend in differential decomposition, with areas of fresh but discolored tissue retained, with adjacent superficial drying of large tissue sections.
20-22	384-2070 ˚C PMI 66-175 Days	Overlap in ADD is due to several instances of score reversal (environmental variables catalyzing the primary presentation of characteristics associated with earlier TBS categories). Score reversal was observed throughout TBS 20-22. Overall trend toward homogenous color change in arms, chest, and shoulders; all associated tissue sections present deep maroon discoloration. This trend advances to all body sections with increase in PMI; circumscribed areas of orange/maroon/rose mottling retained. Inguinal moist decomposition persists and becomes more pronounced with advancing PMI. Beetles are present on all body surfaces; all tissue surfaces present perforations post beetle migration. Tissue presents pattern of circumscribed areas of drying with underlying fluid pocket formation. Formation of adipocere in open thorax advances with PMI. All tissue surfaces present trend toward superficial drying. ‘Waxy cracking,’ (the mechanical stretching of tissue revealing interstitial adipocere) is observed in the chest. Discoloration advances to brown/umber in peripheral tissue, and pale yellow in face and midline thorax.
23-24	608-2212 ˚C PMI 84-442 Days	Overlap in ADD is due to several instances of score reversal. Perforations associated with beetle scavenging begin to coalesce into larger tissue defects. Pronounced slope wash results in partial burial of right arm. All depressions/body surfaces contain tree duff. Facial tissue has dry, granular quality. Avian scavenging is prominent in face; extant coalesced beetle defects are bridged by soft tissue removal. Bird scat present on all body surfaces and characteristic tissue boring with concomitant tissue ribboning present in arms and legs. All tissue surfaces present umber discoloration with areas of longitudinal cracking associated with tissue desiccation.
25-26	2226-6122 ˚C PMI 443-962 Days	Chest presents advanced waxy cracking and legs present interstitial adipocere sheen. New adipocere formation in inguinal region with shedding of aggregates into soil between legs. Proliferative infill of tree

		duff in thorax. Small scale skeletonization of face in areas of coalesced beetle defects. Sternal plate separates from body and migrates downslope. Distal phalanges removed from right hand and skeletonization due to longitudinal tissue cracking advances up right arm. New scavenging with ribboning present in right lateral thorax and right dorsal aspect of foot. Avian scratching around periphery of body present and distinct.
Terminus	TBS 26 PMI 962 Days ADD 6122 ˚C	Donor TB20-102 remains in the research facility; 'terminal' data refers to the data presented at the end of the study period.

Table 5-6: Trajectory of decomposition - Donor 20-103

Donor TB20-103: Placement Date: 05/28/2020; Placement TBS 7; Pre-placement 23 PMI; Pre-placement ADD 70 ˚C		
TBS	**ADD/PMI Range**	**Observed changes**
3-6		TBS 3-6 were not observed.
7-10	3-187 ˚C PMI 1-31 Days	TBS 9-10 were not observed. Red blush and plum discoloration of facial tissue. Circumscribed areas of tissue discoloration present postcranially, resulting in vibrant orange discoloration of affected areas. Body trends toward diffuse purple blush with advancing PMI. Early oviposition was eradicated by a rainstorm. Fluid bloat presents in right and left hands.
11-14	204-397 ˚C PMI 32-46 Days	TBS 11 & 14 were not observed. Body presents diffuse maroon tissue discoloration interrupted by vivid orange blush in proximal legs. Color change advances to deep plum discoloration of the head and neck, diffuse vivid orange/maroon mottling in legs, while the arms, shoulders, chest, hands, and feet present a vivid maroon/purple discoloration. Moist decomposition is present and limited to the inguinal region. Fluid bloat is present in the right and left feet and in early stages in the shoulders and cranium (oriented downslope). Pronounced differential decomposition results in tissue island formation in the right and left legs. Early stage pseudoburial in right axial region. Second generation of oviposition orally and inguinally. Capillary marbling present in circumscribed areas of tissue loss and vibrant orange discoloration. Pronounced abdominal bloat. Skin slippage is pronounced in the feet and advances to diffuse slippage of the epidermis and proliferation of migrating maggots at tissue interface.
15-19		TBS 15-19 were not observed due to rapid progression into moist decomposition.
20-22	410-886 ˚C PMI 47-76 Days	TBS 20 was not observed due to rapid progression into moist decomposition. Proliferative maggot activity oral/otic/optic, within tissue interface, and at ground-body interface. Activity at ground-body interface is sufficient to result in peripheral enzyme frothing. Maggot migration leads to drying and sloughing of uplifted tissue, resulting in tissue color change to diffuse maroon/orange ombre. Tissue color change rapidly advances to brown/umber discoloration at midline with peripheral tissue maintaining maroon discoloration. Abdominal bloat remains prominent. Fluid bloat in hands and feet is pronounced. Hands present circumscribed areas of interstitial adipocere formation; trend advances to include all body surfaces resulting in diffuse presentation of waxy adipocere sheen. A fluid island characteristic of moist decomposition is evident in the soil

		beneath the head and shoulders and progresses to diffuse moist decomposition and tissue collapse with increasing PMI.
23-24	903-1532 ˚C PMI 77- 353 Days	TBS 23 was not observed. Overlap in ADD with TBS 21-22 is due to 'score reversal' following cyclical periods of moist decomposition, rapid drying, and re-initiation of moist decomposition. Tissue discoloration advances from midline umber/peripheral maroon to diffuse umber. Circumscribed areas of dense interstitial adipocere formation with lipid expansion observed in abdomen. Superficial adipocere aggregate in the abdominal depression contains entrapped maggots. Interstitial adipocere formation presents diffusely. Right and left lateral cranium present superficial adipocere aggregates that dry and flake with advancing PMI. Superficial drying of tissue results in 'waxy cracking,' as mechanical separation of tissue stresses and stretches interstitial adipocere. Pseudoburial advances with PMI, resulting in complete burial of right and left arms, buildup of matrix and rock in the right and left axillary regions, and matrix infill of exposed areas of the head, neck, and abdomen. Heavy coverage of the thorax and legs by excavated matrix following animal burrowing/soil scratching. This begins a persistent cycle of superficial coverage of body surfaces by excavated matrix, rain, transformation of matrix into mud, drying, introduction of new matrix, etc. resulting in slow burial of exposed body surfaces. Avian scavenging and tissue removal result in skeletal exposure of the right lateral mandible and partial exposure of the cervical vertebrae. Rodent burrow under thorax and magpie and packrat tracks evident in snow.
25-29	1534-5767 ˚C PMI 354-915 Days	TBS 28 was not observed. Avian boring in the thorax creates circumscribed defects that coalesce over time, resulting in skeletal exposure of vertebrae and iliac blades. Waxy stretching and cracking diffuse in abdomen. Diffuse umber discoloration in tissue progresses to diffuse pale yellow. Peripheral pseudoburial pronounced; cyclical pattern of moisture introduction, drying of matrices, and incorporation of loose rock results in concrete like structure. New rodent burrow under right shoulder with concomitant scavenging of the right hand resulting in skeletal exposure of the distal phalanges. Longitudinal tissue loss in the right and left legs due to avian scavenging. Unidentified canid scavenger causes appreciable disturbance, including disarticulation and displacement of right arm, displacement of left arm, right leg, and left leg, and removal of the distal foot. Disturbance of overlying tissue results in several areas of new skeletal exposure.
Terminus	TBS 29 PMI 915 Days ADD 5767 ˚C	Donor TB20-103 remains in the research facility; 'terminal' data refers to the data presented at the end of the study period.

Table 5-7: Trajectory of decomposition - Donor 20-104

Donor TB20-104: Placement Date: 06/10/2020; Placement TBS 4; Pre-placement PMI 3 Days; pre-placement ADD 9 ℃		
TBS	**ADD/PMI Range**	**Observed Changes**
3-6	3-79 ℃ PMI 1-8 Days	TBS 3 & 6 were not observed. Flies present. Face and scrotum present early maroon discoloration. Distal legs present early maroon/orange ombre.
7-10	97 – 210 ℃ PMI 9-17 Days	TBS 7 & 9 did not present. Orange blush entering face and integrating with maroon to create early orange/maroon ombre that becomes more pronounced with progression of PMI. Circumscribed areas of vibrant orange in nose and cheeks. Deep purple blush observed in (downslope) superior face with concomitant purple racooning of periorbital tissue and fluid bloat of head and shoulders. Orange blush entering hands and feet and distal arms and legs. Chest presents diffuse maroon discoloration. Oral/nasal/optic colonization by early instar maggot larvae.
11-14	224-626 ℃ PMI 18-42 Days	TBS 11-12 were not observed. Skin sloughing in face resulting in second generation purple discoloration; cheeks present vibrant orange. Orange blush extends from hands to distal arms trends toward orange/maroon ombre with advancing PMI. Circumscribed areas of vibrant orange in areas of tissue drying on abdomen. Tissue sloughing resulting in second generation vibrant orange discoloration in left thigh. Fluid bloat persists in head and neck. Tissue island formation/differential decomposition present in shoulders. Diffuse areas of skin slippage containing migrating maggots. Marbling present in neck/superior chest/shoulders, proximal arms, and proximal thighs. Pronounced abdominal bloat and inguinal moist decomposition.
15-19	316-725 ℃ PMI 24-48 Days	TBS 15 & 19 were not observed. Score reversal observed between TBS 17-18 and 14-16. Superior face diffuse plum, inferior face diffuse orange. Chest retains marbling with circumscribed areas of tissue drying and maroon discoloration. Distal legs present maroon/orange/fresh tissue ombre, while proximal left leg presents diffuse orange. Focal orange discoloration in abdomen. Arms present diffuse maroon/rose blush with vibrant orange/maroon ombre in hands. Skin slippage and bulla formation in right leg. Inguinal moist decomposition. Rapid trend toward diffuse orange discoloration in lateral chest, abdomen, inguinal region, and proximal legs with advancing PMI. Interstitial adipocere formation characterized by visible cell expansion present in abdomen and left thigh. Heavy maggot mass colonization at the ground-body interface. Skin slippage in proximal arms. Inguinal moist decomposition and abdominal bloat persist.

20-22	739-1143 ˚C PMI 49-73 Days	TBS 20 was not observed. Diffuse postcranial vibrant orange tissue discoloration, all body surfaces with circumscribed areas of rose/maroon/brown. Second generation of skin slippage and moist decomp in inguinal region. Face and neck present deep plum discoloration. Definition of interstitial lipid cell expansion in abdomen increases with advancing PMI. Lateral drying of thorax with pockets of interstitial adipocere formation. Thoracic bloat begins to collapse. Diffuse drying of superficial tissue with retention of interstitial adipocere sheen. Avian scavenging right distal arm. Black marbling remains prominent in chest and moist decomposition remains prominent in, but limited to, the inguinal region.
23-24	1107-1952 ˚C PMI 71-172 Days	Maroon/orange ombre presents in distal limbs. Trend advances to dark brown/black discoloration in peripheral limbs and maroon/orange ombre in thorax/inguinal region/proximal thighs. Skin sloughing in face reveals second generation maroon discoloration. Adipocere shedding, aggregates present in surrounding soil. Slope wash initiated in axillary region and advances in depth with increasing PMI. Scavenging of scrotum, right lateral face, and right lateral thorax characterized by peeling of superficial tissue. Marked post bloat collapse of abdomen. Drying of superficial tissue with maintenance of waxy interstitial adipocere sheen.
25-28	1944-5523 ˚C PMI 173-882 Days	Color change following snow melt presents as diffuse yellow/umber ombre that progresses to homogenous umber, then light brown with increasing PMI. Tissue characterized by waxy interstitial adipocere sheen. Sheen diminishes with increasing PMI, resulting in desiccation with circumscribed areas of interstitial adipocere retention. Slope wash increasingly prominent with heavy peripheral buildup of solidified mud and infiltration of all downslope defects by mud and soil. Surface adhesions (plant and dirt) present on all body surfaces. Scavenger tunneling under body with displacement of dirt. Facial scavenging advances to include right lateral neck. Tissue peeled from plantar surfaces of feet; removal is sufficient for skeletal exposure. Late PMI drying and longitudinal cracking of desiccated tissue.
Terminus	TBS 28 PMI 882 ADD 5523 ˚C	Donor TB20-104 remains in the research facility; ‘terminal’ data refers to the data presented at the end of the study period.

Table 5-8: Trajectory of decomposition - Donor 20-105

Donor TB20-105: Placement Date: 07/23/2020; Placement TBS 7; Pre-placement ADD 6 Days; Pre-placement ADD 18 ℃		
TBS	**ADD/PMI Range**	**Observed Changes**
3-6		TBS 3-6 were not observed.
7-10	3 -154 ℃ PMI 1-15 Days	TBS 8-9 were not observed. Green discoloration of abdomen at placement. Early skin slippage in distal arms revealing circumscribed areas of vibrant orange discoloration. Face, chest, distal arms and legs present early orange/maroon blush.
11-14	169 -200 ℃ PMI 16-18 Days	TBS 12-14 were not observed. Orange discoloration forming in cheeks; nose presents maroon/purple discoloration. Face, neck, chest, and arms advance to diffuse maroon discoloration. Breasts, chest, superior cranio-facial region, inguinal region, and adjacent proximal thighs present maroon/orange ombre. Abdomen retains fresh tissue quality; circumscribed areas of green discoloration are retained. Adipocere formation on lateral cranium and neck. Heavy avian scavenging characterized by removal of eyes, tongue pulled from mouth, tissue removal from lateral neck, and proximal arms and legs sufficient to result in partial skeletonization with advancing PMI. Tissue loss is juxtaposed by adjacent fresh tissue. Skin sloughing in face and breasts results in second generation vibrant orange color change. Tissue islands present in right arm and abdomen with adjacent circumscribed areas of drying, tissue tension, and color change.
15-19	217-271 ℃ PMI 19-22 Days	TBS 16, 18 & 19 were not observed due to scavenger activity.
20-22	681-695 ℃ PMI 46-47 Days	TBS 20-21 were not observed due to scavenger activity. Slight transient abdominal bloat. Peripheral moisture in soil, no moist decomposition observed on tissue surfaces. Tissue islands in abdomen and right arm increase in prominence and tissue retains fresh quality. New avian bore holes in abdomen, face, and legs. Several juxtaposed areas of tissue discoloration: arms deep maroon, abdomen mottled brown, lateral thorax and distal legs orange, inguinal region advances to plum, and proximal thighs present maroon/orange ombre. Tissue sloughing observed in face. Avian scat present on all body surfaces and tissue removal has advanced to chest and proximal arms.
23-24	290-380 ℃ PMI 23-28 Days	Juxtaposed areas of postcranial tissue discoloration rapidly evolve to diffuse maroon/umber. Third generation tissue sloughing on forehead/superolateral cranium resulting in color change of the frontal and temporal regions from umber to maroon/orange ombre. Avian bore holes increasing in size and magnitude across all body sections. Removal

		of tissue from the head/neck is sufficient to result in exposure of the mandible. Skeletal exposure following tissue peeling from distal legs reveals maroon/orange discoloration of right and left tibiae and fibulae.
25-28	399-752 ˚C PMI 29-301 Days	Pronounced pseudoburial of arms and shoulder following heavy rain with concomitant adhesion of environmental debris. Mud and rodent scat aggregate in the abdomen. Packrat burrowing evident in matrix to the right of the thorax with subsequent migration and construction of a nest within the right shoulder. Nest construction results in the displacement of associated ribs. Tissue loss is observed in the metatarsals and pedal phalanges. Avian scratching in the peripheral soil gives the false appearance of peripheral moisture. Temporally associated loss of vibrant maroon discoloration in periosteum of tibiae and fibulae and associated connective tissue; color transitions from maroon to ivory. Drying and cracking of exposed ribs and costal cartilage is observed with contemporaneous sloughing of the cranial periosteum and bleaching of the exposed mandible. Appreciable increase in scavenging as winter approaches.
29-33	763-4201 ˚C PMI 302-767 Days	Remaining tissue presents pale yellow/umber discoloration. With the exception of the abdominal region, all body sections present complete skeletonization. Exposed bone begins to bleach and present early signs of longitudinal cracking. At ADD 18084.26 tissue loss is sufficient for the cranium to separate from the post-cranium and roll downslope. Movement is impeded by the base of the cage. Scavenging and bioturbation results in the removal and displacement of the right arm to the left side of the body with concomitant displacement of the cervical vertebrae. Trabecular mining is pronounced in the distal femora.
Terminus	TBS 33 PMI 767 Days ADD 4201 ˚C	Due to the extent of skeletal drying and scavenging, Donor TB20-105 is removed from the facility for maceration and skeletal curation.

Table 5-9: Trajectory of decomposition - Donor 20-106

Donor TB20-106: Placement Date: 07/25/2020; Placement TBS 3; Pre-placement PMI 11 Days; Pre-placement ADD 34 ℃		
TBS	**ADD/PMI Range**	**Observed Changes**
3-6	3 – 135 ˚C PMI 1-18 Days	TBS 4 & 6 were not observed. Donor is autopsied. Medical purge at placement. Circumscribed areas of maroon, and maroon/orange ombre tissue discoloration; dura exposed by removal of calotte at autopsy presents maroon discoloration. Left eye presents periocular maroon/orange color change. Fly spatter all body surfaces.
7-10	150-181 ˚C PMI 19-21 Days	TBS 7-8 & 10 were not observed. Differential decomposition/tissue tension observed at circumscribed areas of color change. Flies present on all body surfaces.
11-14	198-198 ˚C PMI 22 Days	TBS 12-14 were not observed. Diffuse orange/maroon ombre discoloration in hands, feet, and distal arms. Face, neck, and chest present diffuse maroon/plum discoloration. Tissue island formation/differential decomposition in proximal thighs. Heavy, diffuse, first instar maggot colonization involving oral/otic/optic, axillary, and inguinal regions, within autopsy incised thorax, and at ground-body interface. Skin slippage in right/left hands, left distal arm, and inguinally. Environmentally mediated pseudoburial (pinecones, pine needles, pine seed casings, and dirt) characterized by adherence to all exposed visceral/lipid/moisture dense surfaces and infill of anatomical depressions.
15-19	216-271 ˚C PMI 23-26 Days	TBS 15-18 were not observed. Rapid termination of maggot activity following heavy thunderstorms. Inguinal bloat. Peripheral (head/neck, arms, inguinal region, distal legs) color change primarily vibrant orange. Midline face retains plum/brown color. Viscera displaced from thorax and partially consumed by avian scavengers. Tissue discoloration vibrant maroon at ground-body interface. Talon stamping in left proximal arm. Moist decomposition in neck, shoulders, and thorax.
20-22	288-676 ˚C PMI 27-50 Days	TBS 20 was not observed. Soil wet due to rain with retention of moisture in thorax and rehydration of all tissue giving the impression of moist decomposition. Tissue discoloration in legs presents vibrant orange/maroon/rose/plum mottling; arms present yellow/orange/brown mottling. Face presents peripheral orange discoloration and plum/umber mottling at midline. Subdermal adipocere aggregates of varying size and density in proximal legs and inguinal region. Interstitial adipocere formation in early stages of drying characterized by pliable waxy desiccation with collapse of underlying tissue. Several beetle species are present on tissue surfaces. Avian scavenging results in ribboning of tissue in lateral thorax and movement of the autopsy incised sternal plate down slope.

23-24	380 -1182 ˚C PMI 32-94 Days	Tissue discoloration characterized by orange at midline, periphery advancing toward plum/black ombre; general trend toward diffuse umber with advancing PMI. General trend in tissue collapse persists, especially in proximal thighs. Spiderweb cracking (shattered glass appearance) and skin sloughing observed in several body surfaces. Further movement of calotte and sternal plate downslope. Extensive thoracic infill of environmental debris and adhesion to all body surfaces. New generation of avian scavenging, characterized by introduction of new bore holes, reflection of thoracic tissue, displacement of ribs, and removal of desiccated costal cartilage. Peripheral soil burrowing and scratching gives the false appearance of peripheral moist decomposition. Heavy rainstorms result in hygroscopic rehydration of tissue, reviving moist, waxy desiccation and catalyzing score reversal. Feet present moisture bloat that advances to deep adipocere formation in the plantar surfaces.
25-28	1190 – 4831 ˚C PMI 95-845 Days	Tissue discoloration advances to diffuse umber with the introduction of circumscribed areas of pale yellow with advancing PMI. Perforation of facial tissue likely resulting from beetle scavenging. Renewal of avian scavenging of the thorax following snowmelt. Tissue removal consistent with packrat behavior, including complete tissue removal from plantar surfaces of the feet, and layered peeling of the right arm and right lateral cranium observed into the spring. Soil excavation around and under the hands (potentially resulting from scavenger excavation, slope wash, or both) result in a pedestaled appearance. Pronounced skeletal taphonomy (categorized as subaerial weathering), including bleaching of all areas of exposed bone, and delamination of os coxa, and pleural ribs, begins and advances with PMI throughout this period.
Terminus	TBS 25 PMI 845 Days ADD 4832 ˚C	Donor TB20-106 remains in the research facility; ‘terminal’ data refers to the data presented at the end of the study period.

Table 5-10: Trajectory of decomposition - Donor 20-107

Donor TB20-107: Placement Date: 08/28/2020; Placement TBS 3; Pre-placement PMI 9; Pre-placement ADD 28 ℃		
TBS	**ADD/PMI Range**	**Observed Changes**
3-6	3 – 43 ˚C PMI 1-11 Days	TBS 4 & 6 were not observed. Autopsied and tissue donor (abdomen and legs), resulting in exposure of subdural lipid dense tissue layer. Early vibrant orange blush in face. Trend in progressive orange discoloration in exposed lipid dense tissue layer introduced.
7-10	56 -98 ˚C PMI 12-15 Days	TBS 7-9 were not observed. Early color change characterized by circumscribed areas of orange in face, distal arms, and inguinally. Circumscribed areas of color change become more vibrant with advancing PMI until face and distal arms present almost diffusely orange. New circumscribed areas of orange color change in abdomen and chest. Eyes removed by avian scavengers and an attempt to scavenge desiccated lips results in anterior extension and displacement. Avian scratching of chest and shoulders, and bore holes introduced to the inguinal region. Flies present; no visible oviposition.
11-14	116 -183 ˚C PMI 16-22 Days	TBS 14 was not observed. Orange/maroon present on all body surfaces in circumscribed and coalescing areas. Deep maroon exposed following proliferative tissue sloughing in the shoulders. Face diffusely orange/maroon; all areas of orange/red/maroon beginning to coalesce. Tissue presents deep purple/maroon discoloration at ground body interface. Presentation of tissue islands persists. Discoloration in exposed lipid layer advances from orange to maroon/rose and begins to dry and crack. Early tissue island formation/differential decomposition presents in right and left arms. Faint marbling in left shoulder and inguinal bloat observed.
15-19	187-270 ˚C PMI 23-30 Days	TBS 15 & 18 were not observed. Face quickly fading from orange to yellow/orange at periphery, and maroon at midline that radiates into neck and chest. The abdomen and limbs predominantly present mottled orange discoloration. This trend progresses with PMI toward facial discoloration characterized by peripheral orange, plum/gray at midline that radiates into neck and chest. The breasts and abdomen become homogenously orange, and the limbs present gray/plum/maroon mottling. Subdermal adipocere motivated expansion of lipid cells are visible in the hands, and right and left lateral hips. Superficial tissue presents waxy, pliable characteristics of interstitial adipocere formation. Abdominal and facial tissue present early drying and collapse. Autopsy sutures released (thread unraveled from tissue perforations) following avian scavenging of left arm and

		lateral chest, compromising the organ bag, and resulting in the release of organs within. Viscera removed from autopsy bag and strewn across thorax throughout the process of consumption. Organ and tissue scavenging persists throughout this window. Moist decomposition present in abdomen, especially in areas of medically mediated dermal removal, and scavenging. Marked reduction in tissue islands with advancing PMI as tissue collapses and the superficial epidermis begins to dry.
20-22	282-376 ˚C PMI 31-38 Days	TBS 21 was not observed. Facial discoloration progresses to diffuse umber with retention of small surface area residual orange in cheeks. Tissue above breasts diffusely gray/plum that radiates into maroon/orange ombre in inferior thorax. Adherent debris on all body surfaces. Second compromise of organ bag via defects introduced by avian scavenging in the left shoulder results in removal of additional organs. Boring and muscle mining of the left proximal arm sufficient to result in early skeletal exposure. Moist decomposition in abdomen and arms with moisture visible in surrounding soil. Pronounced collapse of facial tissue. General trend in superficial drying of all tissue surfaces, characterized by interstitial waxy desiccation.
23-24	391-377 ˚C PMI 39-138 Days	TBS 23 was not observed. Facial discoloration progresses to diffuse umber. Diffuse gray/plum tissue discoloration in chest radiates into abdomen, which presents first as maroon/plum with residual orange, then gray/plum, then umber as PMI advances. Feet advance from deep orange to orange/maroon with capillary marbling. Deep purple/maroon discoloration maintained at ground body interface. Heavy dirt aggregates adhere to all tissue surfaces, obfuscating and homogenizing tissue discoloration, which appears to trend toward diffuse umber. Muddy aggregates and film are removed during a thunderstorm, revealing vibrant maroon/plum discoloration. General trend in tissue collapse and waxy desiccation; head and neck present loss of waxy character and advance toward dry desiccation. Subdermal adipocere aggregates visible in upper thigh and lower abdomen. Feet and abdomen retain tissue density with waxy interstitial adipocere characteristics. Bore holes and ribboning introduced to the right and left lateral thorax, and proximal legs. Longitudinal tissue removal in distal left arm sufficient to result in skeletal exposure that encompasses the metacarpals and progresses proximally with advancing PMI. Tissue peeling consistent with packrat scavenging sequentially presents in the pedal phalanges, the plantar surface of the left foot sufficient to result in skeletal exposure, the volar surface of the right hand, the left maxilla and mandible first, followed by the right mandible. Packrat scavenging is followed by renewed interest among avian scavengers, resulting in the

		introduction of new bore holes to the neck, arms, and inguinal region.
25-28	372-4237 ˚C PMI 139-809 Days	Post snowmelt, tissue discoloration is diffusely brown/umber. Exposed post-cranial bone presents ivory color and greasy character consistent with fresh bone. Craniofacial areas of skeletal exposure present bleaching and hairline cracking. Remaining tissue retains waxy, pliable characteristics of interstitial adipocere formation. Longitudinal sloughing of facial tissue promotes increased skeletal exposure with advancement of PMI. Persistent avian scavenging of the thorax is sufficient to result in exposure of the anterior parietal rib surfaces. The introduction of bore holes persists within the increasing paucity of structurally sound tissue. Beetle larvae present on the exposed bones of the right foot.
Terminus	TBS 27 PMI 809 Days ADD 4237 ˚C	Donor TB20-107 remains in the research facility; ‘terminal’ data refers to the data presented at the end of the study period.

Table 5-11: Trajectory of decomposition, Donor 21-101

Donor TB21-101: Placement Date: 01/07/2021; Placement TBS 3; Pre-placement ADD 17 Days; Pre-placement ADD 52 ℃		
TBS	**ADD/PMI Range**	**Observed Changes**
3-6		TBS 3-6 were not observed.
7-10	3 - ˉ1 ℃ PMI 1-23 Days	TBS 8-9 were not observed. Tattoos present of right and left proximolateral arms and left proximal leg. Donor placed on approximately 12” of snow. Face presents early maroon blush that radiates into deep pink/maroon blush in neck, superior chest, proximal arms, and lateral thorax. A circumscribed area of orange tissue discoloration interrupts color continuity in the right lateral chest.
11-14	ˉ0.78 - ˉ360 ℃ PMI 24-101 Days	TBS 12-14 were not observed. Data collection is limited by the temporal increase in snow overburden. Maroon tissue discoloration deepens and becomes more diffuse. Pink marbling is present in the lateral thorax. Rodent scavenging is evident in tissue removal from the fingertips of the right hand.
15-19	ˉ356 – 32 ℃ PMI 102-165 Days	TBS 15-16 and 18 were not observed. The face and neck present maroon tissue discoloration that radiates into the chest and shoulders. The abdomen presents appreciable avian scratching, the defects of which are associated with maroon and orange tissue discoloration. Tissue sloughing associated with advancing PMI results in subsequent second-generation maroon/orange color change in the chest and abdomen. The distal arms and legs present diffuse deep maroon discoloration that radiates into maroon/pink discoloration in the proximal arms and legs. Subsequent maroon/plum/black color change in distal limbs, and deep maroon/plum in proximal limbs is associated with progressing PMI. Moderate abdominal bloat, and moist decomposition limited to the inguinal region. Drying of the superficial dermis shares a temporal relationship with advancing PMI but overall tissue quality retains pliable waxy sheen characteristic of interstitial adipocere formation. A prominent adipocere aggregate forms on the left lateral thorax and phasically dries and flakes into the surrounding environment. Tissue island formation/differential decomposition presents in the legs and abdomen. Tissue islands evolve into subdermal adipocere aggregates as overlying superficial tissue dries and is characterized by waxy desiccation. Scavenging consistent with packrat peeling is introduced to the left lateral face and neck and is sufficient to result in skeletal exposure.

20-22	- 356 – 367 ˚C PMI 166-184 Days	TBS 21 was not observed. Third generation prolific shattered glass skin sloughing reveals diffuse deep maroon/plum tissue discoloration interrupted by maroon/rose/orange discoloration in the superior abdomen. The lateral thighs present faint marbling. Moderate bloat is maintained with superficial drying of abdominal tissue. Superficial tissue drying in the legs is interrupted by the retention of tissue with fresh quality in the knees. Subdermal adipocere aggregates persist in left lateral abdomen, proximal legs, and inguinal region. Formation of a broad, superficial adipocere plaque on the right lateral thigh is attendant to escalating inguinal moist decomposition. Avian scavenging characterized by tissue ribboning promotes skeletal exposure in the neck.
23-24	391 – 1354 ˚C PMI 185-246 Days	TBS 24 was not observed. Face and all limbs deep plum, midline thorax presents mottled orange/yellow/maroon tissue discoloration. A general trend in homogenous, whole-body plum/brown discoloration follows, and evolves into peripheral brown and centrally umber discoloration. All tissue maintains pliable, waxy quality with adherence of surface debris. Inguinal moist decomposition evolves to include the proximal limbs and thorax, characterized by heavy surface and ground moisture followed by phasic reduction and termination with advancing PMI. Bloat with drying of overlying abdominal tissue begins to collapse. Structure provided by partially desiccated abdominal tissue results in a transverse linear depression bisecting the abdomen that serves to collect water and attract fruit flies. Post moist decomposition, tissue surfaces cyclically present surface moisture introduced by seasonal rainstorms, which serve to rehydrate tissue and maintain waxy, pliable, interstitial adipocere quality. Black beetle larvae colonization follows periods of punctuated moisture introduction. Larval scavenging results in small but widely dispersed circumscribed and coalesced tissue punctures that serve to collectively undermine structural integrity over time, resulting in small scale skeletal exposure. Craniofacial tissue desiccation and sloughing result in separation of mandibular and maxillary tissue and bone, resulting in skeletal exposure and loss of attendant mustache and beard. Exposed bone retains a fresh, ivory colored, greasy quality throughout this period.
25-28	1372 – 3929 ˚C PMI 247-685 Days	Tissue surfaces are diffusely umber. Tattoos remain visible. Tissue characterized by waxy desiccation interrupted by areas of desiccation. Surface aggregates of matrix and environmental debris, and peripheral foliage overgrowth serve to camouflage the body in the environment. Scavenging characterized by tissue peeling and consistent with packrat behavior is initiated in the left plantar foot and left palmar hand. Exposed skeletal elements begin to bleach and small-scale delamination present in facial bone.

Terminus	TBS 25 PMI 685 Days ADD 3929 ℃	Donor TB21-101 remains in the research facility; ‘terminal’ data refers to the data presented at the end of the study period.

Table 5-12: Trajectory of decomposition - Donor 21-102

Donor TB21-102: Placement Date: 01/07/2021; Placement TBS 7; Pre-placement PMI 14 Days: Pre-placement ADD 43 ℃		
TBS	**ADD/PMI Range**	**Observed Changes**
3-6	3 - 317 ℃ PMI 1-119 Days	TBS 3-4 were not observed. Donor TB21-102 placed on approximately 12" of snow. Neck and chest present cardiac mottling. Chest presents orange blush down midline. Large defect (etiology unknown) on right lateral neck presents rose/maroon discoloration that advances to vibrant maroon and underlying capillary marbling with advancing PMI. Distal right and left arms and legs present pink blush. Faint marbling in lateral thighs.
7-10		TBS 7-10 were not observed due to snow overburden.
11-14		TBS 11-14 were not observed due to snow overburden.
15-19	-315 – 680 ℃ PMI 120-201 Days	TBS 15-16 were not observed due to snow overburden. The face and neck present several iterations of change throughout this phase associated with increasing PMI. Initially the face presents maroon/orange ombre, neck trends toward deep plum discoloration, ears are deep plum with circumscribed areas of vibrant maroon discoloration. The head trends toward homogeneity in discoloration, the face progresses toward brown/umber with peripheral maroon that darkens to deep plum before evolving into diffuse umber with pale green undertones. Chest presents circumscribed areas of maroon/orange mottling that begins to coalesce into homogenous orange and markedly increase in vibrancy with advancing PMI. Abdomen retains overall fresh tissue quality with circumscribed areas of maroon/orange discoloration associated with avian scratching; circumscribed discoloration coalesces over time, resulting in orange/maroon ombre. A bridge of fresh tissue separates discoloration in the chest and abdomen. Hands and feet present orange blush that evolves into diffuse vibrant maroon; distal arms and legs present vibrant maroon/rose ombre that evolves into homogenous deep maroon discoloration distally, with proximal radiations of maroon mottling. The distal arms and legs, hands and feet trend toward deep plum discoloration and prolific skin sloughing with increasing PMI. Proximal arms and legs trend toward maroon/orange discoloration but retain areas of tissue with fresh quality. Discoloration in the proximal arms bridges with the shoulders/chest. Discoloration in the proximal legs bridge with discoloration in the inguinal region and abdomen to present homogenous vibrant maroon discoloration with undertones of vibrant orange. Prolific tissue sloughing resulting in diffuse color change is associated with advanced PMI. The peripheral body sections (neck, limbs, and lateral thorax) present diffuse plum discoloration that radiates into maroon proximally. The midline (thoracic and inguinal) regions present a vibrant red orange ombre. Subdermal adipocere

		aggregates of various size and density observed in right arm and left chest. Tissue at ground-body interface is characterized by the maintenance of a fresh quality with faint yellow discoloration. A progression toward maroon blush and subdermal adipocere formation is observed at the phasic interface. Fluid bloat in right and left feet. Tissue removal characterized by small areas of peeling is observed in tip of the nose, left lateral cranium, right anterior surface of the distal manual phalanges, and left dorsal surface of the distal pedal phalanges. The superior half of the left ear is removed. Prolific avian scratching is observed on all body surfaces. Early moist decomposition is limited to the inguinal region. Flies are present and initial oviposition is observed in the inguinal region, and in areas of fluid runoff at the ground-body interface. The face presents early phase drying and granular exfoliation.
20-22	691 - 1270 ˚C PMI 202-237 Days	Facial tissue retains diffuse umber discoloration; tissue is dry and granular. Postcranial tissue discoloration retains previous phase's iteration. Peripheral body sections (neck, limbs, and lateral thorax) present diffuse plum discoloration that radiates into maroon proximally, the midline (thoracic and inguinal) regions present maroon/ vibrant orange ombre. Peripheral tissue discoloration trends toward the introduction of brown with advancing PMI. Colors remain brightest and most vibrant at skeletal prominences. Tissue collapse in all body sections but retains waxy, pliable characteristics of interstitial adipocere formation. Moist decomposition persists but remains limited to the inguinal region. Heavy colonization of large black beetle larvae creates the illusion of moist decomposition as a byproduct of enzyme induced tissue dissolution. Active larvae of various instars are present on all body surfaces; primary colonization is at the ground-body interface with a heavy aggregate on the ground directly associated with the groin area. Heavy moisture is present in the peripheral matrix which dries with advancing PMI and sudden, rapid migration of larvae. Perforations are present in all tissue surfaces following beetle migration. Avian scavenging resumes during larval colonization, resulting in longitudinal tissue removal from the left arm with characteristic ribboning. Body surfaces present more 'traditional' moist decomposition with increasing PMI, characterized by the weeping of moisture from tissue on all body surfaces.
23-24	391 – 2797 ˚C PMI 238-577 Days	TBS 23 was not observed. Tissue discoloration is diffusely brown/umber following overwintering. Adipocere aggregates present superficially following rehydration by snow. Scavenger induced tissue defects reveal subdermal adipocere in the left arm. General anterior displacement of the body is observed following snowmelt, resulting in anterior flexion of the cervical vertebrae, aerial orientation of the craniofacial region, and displacement of the posterocranium approximately 17 cm above ground level. A resurgence of avian scavenging results in tissue loss in the right and left arms, and anterolateral thorax sufficient to result in skeletal exposure of the anterior parietal rib surfaces. Tissue

		perforations introduced throughout beetle scavenging begin to coalesce, resulting in ‘peekaboo’ exposure of facial skeletal elements. All tissue presents early desiccation but remains primarily characterized by waxy desiccation.
25-28	2813 - 3929 ˚C PMI 578-681 Days	TBS 25 was not observed. Retention of superficial adipocere plaques on all body sections. Face and shoulders retain waxy moisture with active weeping of lipids; posterior cranium presents appreciable drying of tissue. Substantial infiltration of dirt and environmental debris visible in thoracic cavity and weeping of lipids results in superficial aggregates of matrix adherence. Thoracic scavenging persists, resulting in progressive exposure of the anterolateral ribs. Exposed ribs present bleaching and cracking with increasing PMI. New areas of scavenging are introduced to the left hand and foot, characterized by tissue peeling sufficient to result in almost complete skeletal exposure, with no associated skeletal loss. The underlying bone and periosteum present maroon/rose discoloration. A third wave of focused avian scavenging results in substantial loss of inguinal tissue sufficient for exposure of the ischiopubic rami, and longitudinal tissue loss and skeletal exposure in the right and left proximomedial legs, and in the left distal leg. Remaining soft tissue is desiccated, but overall, pliability is retained and continues to present areas of lipid weeping.
Terminus	TBS 27 PMI 681 Days ADD 3916 ˚C	Donor TB21-102 remains in the research facility; ‘terminal’ data refers to the data presented at the end of the study period.

Table 5-13: Trajectory of decomposition - Donor 21-104

Donor TB21-104: Placement Date: 08/22/2021; Placement TBS 5; Pre-placement PMI 2 Days; Pre-placement ADD 6 ℃		
TBS	**ADD/PMI Range**	**Observed Changes**
3-6	3 - 145 ˚C PMI 1-13 Days	TBS 5-6 were not observed. Face presents early orange blush; arms, legs, and abdomen present widely distributed circumscribed areas of yellow/orange color change. Ants heavily colonize the face and concomitantly produce circular abraded defects in the face and proximal arms.
7-10	160 - 233 ˚C PMI 14-19 Days	TBS 7-8 were not observed. Facial discoloration trends toward diffuse orange but is interrupted by umber discoloration at midline. Distal arms and legs present diffuse orange discoloration; chest and abdomen present early orange blush. Faint marbling is visible in proximomedial legs and distal arms.
11-14	248 - 375 ˚C PMI 20-28 Days	TBS 12-13 were not observed. Discoloration in face, neck, and chest coalesce into diffuse vibrant orange; maroon/rose mottling is introduced to the chest with advancing PMI. Abdomen presents mottling of fresh tissue and early orange blush. Hands present diffuse maroon discoloration, while arms initially present diffuse orange interrupted by circumscribed areas of brown discoloration. Maroon/rose discoloration in hands progressively radiates into distal arms with advancing PMI, diffuse orange discoloration is retained in proximal arms. Legs present diffuse rose blush. Periorbital tissue presents subdermal moisture pooling while ears, nose, fingers, toes, and all other membranous regions present drying of edges. Avian scat is widely and heavily distributed with subsequent removal of the eyes. Flies are present; no discernable oviposition.
15-19	388 - 644 ˚C PMI 29-54 Days	TBS 17-19 were not observed. General collapse of tissue in face and neck, accentuating underlying skeletal structures. Face and neck present an amalgam of color change characterized by purple discoloration of midline face, peripheral vibrant orange, maroon in the chin and temples, and maroon/orange/yellow mottling in the neck that trends toward diffuse umber with advancing PMI. The lateral chest and shoulders are maroon that radiates into a vibrant orange ombre at midline and bridges into an abdominal orange blush. Abdominal discoloration presents as circumscribed areas of orange discoloration that evolves into diffuse vibrant orange with advancing PMI. The arms present diffuse rose/orange mottling that evolves into diffuse distal maroon discoloration that fades to rose, then orange as it advances proximally. The legs are diffusely orange with prominent rose marbling. Expansion of lipid cells is visible in the abdomen. Ant colonization with subsequent abraded defects persists. Avian scavenging of peri- and intraocular tissue. Slight bloat advances to prominent abdominal bloat followed by early post-bloat

		abdominal collapse. Prolific, diffuse, superficial tissue sloughing results in diffuse, whole body, orange color change.
20-22	648 - 647 ˚C PMI 55-59 Days	TBS 21-22 were not observed. Post-bloat abdominal collapse complete. Orange discoloration fades to yellow following heavy rainstorms and structural, subdermal adipocere formation is present throughout the body with punctuated aggregates of varying size and density present in the breasts, lateral abdomen, and proximal legs. New avian scavenging is present in the distomedial left leg.
23-24	645 - 772 ˚C PMI 60-99 Days	TBS 23 was not observed. All tissue presents diffuse pale orange/yellow discoloration that reverts to diffuse vibrant orange with areas of rose mottling as PMI advances. Stained glass tissue cracking and sloughing around the periphery of the inguinal region exposes new areas of vibrant orange. Rose discoloration is introduced to the midline abdomen and proximal legs with advancing PMI. Several generations of shattered glass tissue sloughing results in dynamic color change. Color change trends back toward umber with increase in PMI. Facial discoloration reverts to yellow/umber, then progresses into umber/brown. Brown mottling is introduced to the limbs and progresses toward diffuse presentation. Infiltration of brown mottling into the abdomen results in maroon/brown/plum/orange mottling. Tissue collapse and waxy superficial desiccation present with prominent peripheral subdermal adipocere formation. Avian scavenging of left distomedial left leg extends proximally; new avian scavenging is present in the left distolateral arm and bore holes penetrate the right proximal arm and evolve into longitudinal tissue removal across PMI. All limbs present superficial avian scratching and peripheral matrix disturbance is sufficient to result in pseudoburial of the right arm.
25-28	768 - 471 ˚C PMI 100-171 Days	TBS 27-28 were not observed. Third generation body-diffuse stained-glass tissue cracking and sloughing exposes deep maroon tissue discoloration. Discoloration evolves across each body segment with increase in PMI. The abdomen and proximal thighs present maroon/rose/orange mottling that advances toward lateral orange/gold, the chest presents diffuse golden/yellow that disseminates into the cranium and shoulders. Following a marked decrease in ambient temperature and subsequent snow overburden, a diffuse brown/gold discoloration is revealed. Subdermal lipid cell expansion is visible in the abdomen. Tissue collapse is characterized by waxy, pliable, interstitial adipocere formation in the overlying dermis. Subdermal adipocere aggregates remain prominent in the lateral chest and knees. Avian motivated tissue removal extends the length of the left arm with new scavenging of the waxy adipocere deposit in the right knee. Voracious avian scavenging across this period results in complete skeletal exposure of the arms and distal

		legs; exposed bone presents maroon/rose discoloration within the osseous infrastructure.
29-35	459 – 1129 ˚C PMI 172-321 Days	TBS 29-30 were not observed. Body passively displaced downslope following a period of frenetic scavenger activity. Prominent erosion line in soil. Visibility occluded by snow overburden, but persistent avian scavenging is evidenced by avian tracks in the snow and bore holes containing ribboned tissue. One brief period of snowmelt reveals extensive destruction of the remaining tissue layers, which are perforated and shredded and resemble torn fabric. Spring snowmelt reveals complete skeletonization, trabecular mining, disarticulation, and displacement downslope. A canid scavenger gains access to the cage in mid-summer (June 27, 2022), resulting in the destruction and removal of skeletal elements and moderate commingling of donors TB21-104 and TB21-105 in the southwest corner of the cage.
Terminus	TBS 31 PMI 321 Days ADD 1129 ˚C	Due to the extent of skeletal scavenging and displacement, Donor TB21-104 is removed from the research facility for maceration and skeletal curation.

Table 5-14: Trajectory of decomposition - Donor 21-105

Donor TB21-105: Placement Date: 10/15/2021; Placement TBS 3; Pre-placement PMI 18 Days; Pre-placement ADD 55 ℃		
TBS	**ADD/PMI Range**	**Observed Changes**
3-6	3 – 64 ℃ PMI 1-21 Days	TBS 4-5 were not observed. Donor fresh at placement. Several small areas of skin slippage/skin irritation/superficial abrasions due to hospitalization and field placement. Striae distensae diffuse on abdomen. Tissue quality changes with progression of PMI and existing defects (proximal arms, right medial thigh, left lateral thorax) show early color change.
7-10	66 - 69 ℃ PMI 22-23 Days	TBS 7-9 were not observed. Distal limbs present early maroon/orange color change, cheeks present orange, and abdomen presents orange discoloration within striae distensae. Avian scat widely and heavily dispersed and is present on all body surfaces, scratch marks visible in superficial dermis, and left ear is partially removed.
11-14	73 – 119 ℃ PMI 24-33 Days	TBS 12 & 14 were not observed. Drying of all small edges (nose, lips, fingers, toes, and all membranous structures). Face maintains fresh quality peripherally; patterns of color change are central and include vibrant orange cheeks, maroon periorbital tissue, and circumscribed areas of orange tissue discoloration. The scavenged ear presents vibrant maroon/rose discoloration. Dramatic color change in distal arms and legs characterized by vibrant maroon/orange mottling; proximal legs present diffuse orange color change. Color change in proximal and distal limbs remain distinct but begin to bridge with advancing PMI. The thorax presents numerous circumscribed areas of orange discoloration that expand with cumulative PMI but fail to coalesce. New areas of superficial avian scratching are present on the thorax and are associated with distinct patterns of color change (vibrant orange on the chest/vibrant maroon on the abdomen). New bore holes are present in the right distal arm and the right eye is removed. Differential decomposition/tissue island formation in the right and left legs and fluid bloat in the right and left hands and feet.
15-19	121 – 177 ℃ PMI 34-54 Days	TBS 18-19 were not observed. Face presents increasingly diffuse orange color change centrally, and maroon peripherally. This trend advances toward deep maroon/plum in the forehead, periorbital tissue, and peripheral tissue, while orange discoloration is maintained in the cheeks. Tissue at ground-body interface presents deep maroon discoloration. Color change in the trunk coalescing with peripheral areas of fresh tissue retention. The abdomen presents maroon color change while chest maintains circumscribed areas of orange color interrupted by fresh tissue. The right and left arms present deep plum

		discoloration. Distal legs present deep diffuse maroon anteriorly, and vibrant maroon/plum mottling posteriorly. New avian scavenging in the right shoulder reveals underlying lipid/adipocere tissue that trends toward orange discoloration across time. Expansion and coalescence of existing bore holes in the right and left arms through the introduction of new bore holes. Scavenging of muscle and tissue of the right lateral face, right distal arm, and longitudinally in left arm. Circumscribed areas of adipocere formation in left leg, lateral thorax, and shoulders. Interstitial adipocere formation maintains appearance of fresh tissue in the thorax. Fluid bloat retained in hands and feet. First phase skin sloughing with shattered glass appearance initiated in the abdomen, inguinal region, and the length of the legs.
20-22	174 – 176 ˚C PMI 55-63 Days	TBS 21 was not observed. Superficial drying of epidermis characterized by waxy desiccation; soft tissue palpated in dermal layers beneath. Face presents prolific drying and sloughing of epidermis with concomitant second-generation maroon color change. Hands and feet present rose discoloration. Abdomen presents maroon/rose color change; chest maintains circumscribed areas of orange discoloration with coalescence over time. Diffuse areas of tissue sloughing result in second generation vibrant orange color change. Proximal legs present subdermal adipocere aggregates that vary in size and density. Avian scavenging intensifies with advancing PMI, resulting in the reflection of tissue and removal of muscle from the left arm, and of the deep muscle in the right shoulder. Prolific tissue sloughing continues to advance in the lower abdomen, inguinal region, and legs.
23-24	180 - 13 ˚C PMI 64-108 Days	TBS 23 was not observed. All aerial facing surfaces present notable superficial, pliable, waxy desiccation. Subdermal tissue collapse observed in all body sections. Second generation cranial color change intensifies to deep maroon. Abdominal discoloration is diffusely orange/maroon. Chest retains areas of 'fresh' tissue interrupted by circumscribed areas of orange discoloration that advances to coalescence and intermingling of new rose discoloration. Early bridging between abdominal and chest discoloration. Color change homogenizes to a diffuse golden yellow/orange following first major snow fall. Anterior tissue surfaces maintain golden yellow with pronounced capillary marbling; posterior body maintains deep maroon/plum color at ground-body interface. Subcutaneous aggregates of adipocere formation are prominent in the lateral glutes, proximal legs, and scrotum. Persistent avian scavenging results in skeletonization of the right hand and the length of the right arm. Muscle mining progresses in the right shoulder resulting in exposure of

		red 'fresh' muscle pulled from anatomical orientation. Proliferative tissue sloughing advances with cumulative PMI.
25-28	10.10 - -124 ˚C PMI 109-129 Days	TBS 26-28 were not observed. Chest maintains golden yellow discoloration, abdomen, and proximal legs diffusely vibrant orange. Heavy avian scratching and disruption of peripheral matrix results in pronounced pseudoburial of limbs. New avian scavenging is evident in reflection of facial tissue, tissue removal with subsequent ribboning in the distal legs, boring and consumption of subdermal adipocere aggregates in proximal legs, and new bore holes in inguinal region, left shoulder, and chest.
29-35	-137 – 534 ˚C PMI 130-279 Days	Body passively displaced downslope by scavengers. Complete pseudoburial of right arm with extensive adhesion of dirt to the cranium and neck following period of snow overburden. Prominent erosion line in soil. Right arm reduced to bone and substantial tissue removal in the left anterolateral thorax and left proximal leg results in skeletal exposure and displacement. Visibility occluded by snow overburden, but persistent avian scavenging is evidenced by avian tracks in the snow and bore holes containing ribboned tissue. Spring snowmelt reveals complete skeletonization, trabecular mining, disarticulation, and displacement downslope. A canid scavenger gains access to the cage in mid-summer (June 27, 2022), resulting in the destruction and removal of skeletal elements and extensive commingling of donors TB21-104 and TB21-105 in the southwest corner of the cage.
Terminus	TBS 31 PMI 279 Days ADD 533 ˚C	Due to the extent of skeletal scavenging and displacement, Donor TB21-105 is removed from the facility for maceration and skeletal preservation.

Table 5-15: Trajectory of decomposition - Donor 21-106

Donor TB21-106: Placement Date: 10/25/2021; Placement TBS 3; Pre-placement PMI 24 Days; Pre-placement ADD 73 ℃		
TBS	**ADD/PMI Range**	**Observed Changes**
3-6	ADD 3 -109 ˚C PMI 1-34 Days	TBS 5 was not observed. Tissue discoloration characterized by faint pink/maroon blush in face, fingertips, and abdomen that modestly deepens in color and expands in breadth with increase in PMI. Minor abdominal bloat.
7-10	ADD 112 - 137 ˚C PMI 35-40 Days	TBS 8 & 10 were not observed. Maroon discoloration in the face advances to diffuse maroon blush most prominent in forehead. Hands and feet present deeper maroon blush that begins to radiate up distal arms and legs. Minor abdominal bloat with associated slight green discoloration and marbling. Drying of lips, nose, ears, and distal manual/pedal phalanges.
11-14	ADD 138 -149 ˚C PMI 41-45 Days	TBS 13-14 were not observed. Face retains diffuse maroon blush most prominent in forehead. Chest presents maroon blush that radiates into green discoloration beneath the ribs. Small, circumscribed areas of maroon and orange color change are present on abdomen, arms, and legs. Post-bloat abdominal collapse and marbling in neck and abdomen. Heavy dispersal of avian scat on all body and cage surfaces.
15-19	ADD 154 -169 ˚C PMI 46-68 Days	TBS 15 & 18-19 were not observed. Face presents diffuse maroon blush that deepens with advancing PMI; cheeks present vibrant orange discoloration. Circumscribed areas of color change beginning to form on chest, followed by diffuse orange blush; extant areas of circumscribed color change beginning to coalesce in proximal legs. Abdomen retains green discoloration with subsequent presentation of maroon discoloration that advances to mottled maroon/orange. Distal arms and legs diffusely maroon, color change fades into maroon/orange ombre in proximal arms/legs. Tissue associated with posterolateral surfaces and at ground-body interface presents deep, vibrant maroon discoloration. Tissue islands begin formation and reach prominence in the proximal legs. Adipocere formation in defect of proximal right arm. Proliferative facial skin sloughing. Avian scavenging of distal right and left arms and left pectoral muscle characterized by removal of superficial dermis and deep muscle mining. Persistent scavenging results in skeletonization of right and left distal arms. Superficial avian scratching on proximal legs and thorax.
20-22	ADD 166 - -141 ˚C PMI 69-126 Days	TBS 21-22 were not observed. Face presents diffuse plum discoloration following proliferative tissue sloughing. Circumscribed areas of deep plum discoloration present on arms, legs, and abdomen. Distal legs

		present maroon/orange ombre that radiates into diffuse vibrant orange discoloration of the proximal legs with advancing PMI. Chest and abdomen present diffuse, vibrant orange discoloration. Chest discoloration advances to diffuse maroon that bridges into maroon and eventual deep purple discoloration of the shoulders. Shoulders and chest present avian scratching. Arms present retracted tissue, drying of ribboned tissue, and exposure of the left humerus following persistent avian scavenging. Slope wash results in the downslope 'combing' of the beard and hair.
23-24		TBS 23-24 were not observed.
25-28	ADD -154 - -82 ˚C PMI 127-228 Days	TBS 25-26 & 28 were not observed. Tissue discoloration is diffusely mottled umber/pale yellow. Scavenging persists in all body sections resulting in almost complete removal of tissue of head and neck. Tissue removal associated with the right and left shoulders advances into chest and lateral thorax resulting in additional rib exposure, and exposure of pink muscle tissue. Several bore holes are introduced to the inguinal region, and distal legs with concomitant muscle mining.
29-35	ADD -69 - 2008 ˚C PMI 229-401 Days	Tissue discoloration is predominantly umber with retention of areas of pale yellow. Persistent avian scavenging results in complete skeletonization of the head, neck, right and left arms and right and left distal legs with subsequent trabecular mining. Proximal legs are skeletal but retain overlying waxy desiccated tissue as a result of muscle mining. All exposed skeletal elements present fresh, greasy quality that advances to drying and bleaching of distal skeletal elements. Thorax retains tissue with waxy, pliable, adipocere quality that advances to drying and shrink wrapping of ribs, with subsequent tissue loss resulting in exposure and eventual breakage of anterior ribs. Slope wash is persistent, resulting in the tilting of the cranium downslope, peripheral pseudoburial, and substantial infiltration of mud and debris in the head, neck, and thorax. Hair mat separation and eventual loss are followed by movement of the hair mat downslope.
Terminus	TBS 31 PMI 401 Days ADD 2008 ˚C	Donor TB21-106 remains in the research facility; 'terminal' data refers to the data presented at the end of the study period.

5.4 Conclusion

Qualitative assessment of intracohort incidence of categorical traits was considered along two analytical lines: (1) the TBS model's 'classic' descriptions of decomposition change; and (2) high-altitude specific descriptions of decomposition change. Both models were assessed using the same criteria. Each categorical change was scored as present (1) / absent (0) on each data day, facilitating correlation between each trait and ADD. An 80% threshold for intracohort trait presentation was established; traits failing to meet the 80% threshold were rejected from future model building. Donor specific point of first presentation was established for each trait and presented as a cohort range. The range is presented to: (1) establish earliest/latest point presentation; and (2) establish the range of ADD within which a categorical trait first presents. Categorical traits possessing a wide range of presentation (i.e. across a broad range of ADD), are less likely to serve as a strong temporal marker and are therefore less likely to benefit future predictive model development.

Within its intracategorical descriptions, the TBS model uses six 'classic,' descriptions of decomposition change: skin slippage, purge, specific patterns of soft tissue color change, marbling, bloat, moist decomposition. With the exception of moist decomposition, each of the 'classic' categories failed to meet the 80% threshold. While moist decomposition presented in 83% of the sample, presentation was across a broad range of ADD (450 – 3572 ADD^C), suggesting that it does not possess the temporal specificity necessary to meet the criteria for future model building.

Seven unique categorical traits were identified in the first year of study, the suite of which is hypothesized to be unique to high-altitude decomposition. Cohort wide incidence and prevalence of each trait was tested in the second year. These categories include: (1) orange or maroon dominant trajectory of soft tissue color change; (2) adipocere formation; (3) fluid bloat; (4) tissue island formation (localized differential decomposition); (5) skin sloughing; (6) pseudoburial; and (7) slope roll. Four additional categorical changes, including: (1) limb float; (2) effervescence; (3) capillary marbling; and (4)

snow metamorphism, creep, and ice accretion were isolated for future study. With the exception of slope roll (67% sample presentation), all traits met the 80% threshold. However, both pseudoburial (600 – 4300 ADD^c) and slope roll (1355 - 10142 ADD^c) presented across a broad range of first point presentation. Because these categories are highly sensitive to donor-environment interaction and lack the necessary temporal specificity, both are rejected from future model building but are retained as important components of the local taphonomic profile.

CHAPTER 6

RESULTS: FORENSIC ECOLOGICAL PROFILE - SCAVENGING

6.0 Results: Invertebrate and Vertebrate Behavior

Understanding local scavenger behavior both by individual species and as the sum of interacting groups (scavenger guilds) is critical to the environment specific forensic ecological profile. Scavenger activity interrupts the death or deposition scene and results in soft tissue and skeletal displacement and loss. This behavior resonates down the analytical chain as it limits the scope of environmental and biological evidence available to the analyst both on scene and in subsequent skeletal analysis. Longitudinal controlled study of environment specific rate and pattern of human decomposition affords the appended opportunity for controlled study of associated scavenger behavior. Because the structure of scavenger guilds and the behavior of individual species is heavily influenced by local environmental variables, region-specific study is pivotal. Among the most prominent variables at high-altitude are protracted overwintering resulting in limited mobility with concomitant reduction in home range size, scarce resources, and metabolisms slowed by physiological stress.

The scavenger cages used in this study precluded access to human remains by large-bodied scavengers. Rather than constitute a limiting factor, this allowed small-bodied vertebrates the opportunity to proliferate as apex scavengers, and facilitated high-resolution study of their behavior. Because many small-bodied species cooperatively scavenge, their scavenging behavior has typically and necessarily been understood in sum (e.g. 'rodent' or 'avian' behavior), as cooperation precludes species-specific description of scavenging pattern and behavior. Further, the taphonomic signatures of small-bodied scavengers are often overprinted by those of more destructive, larger-bodied vertebrates, adding complexity to pattern elucidation. As such, emphasis in this study was placed on intraspecies continuity in behavior, and the temporal, anato-spatial, and archetypical presentation of osseous and

soft tissue change, summarily yielding a higher resolution model of small-bodied scavengers at high-altitude.

Four primary scavenger groups were observed throughout the course of this study. Insect identification was limited to family. Vertebrate identification extended to genus and species. Primary scavenging groups included invertebrates: (1) Dipterans (blow flies; *Calliphoridae*); and (2) Coleopterans (carrion beetles; *Silphidae*), and vertebrates (1) black-billed magpies (*Pica hudsonia*); and (2) bushy-tailed woodrats (*Neotoma cinerea*; commonly referred to as packrats). Additionally, the presence of red-tailed fox (*Vulpes vulpes*), and an unidentified small-bodied canid species (identified by morphology of osseous defects) were each noted on one occasion, respectively.

6.1 Insect scavenging

Dipteran oviposition and larval development was observed in six donors (50% of cohort); proliferative colonization was limited to three donors (25% of cohort). Coleopteran larval colonization was observed in five donors (42% of cohort). Family identification indicated the presence of blow flies (*Calliphoridae*), and carrion beetles (*Silphidae*). *Calliphoridae* larvae and *Silphidae* grubs presented non-linearly and demonstrated an overall lack of reproductive and competitive success. For clarity, larvae will be used to refer to both immature Dipterans and Coleopterans when discussing patterns in sum. Larval development was characterized by opportunistic, punctuated colonization events. Oviposition occurred in moist and protected areas of the body, including oral, otic, and optic cavities, axillary and inguinal regions, within autopsy incisions and bullae, and beneath tissue layers separated by enzyme excretion. This pattern is widely reported and an arguably universal adaptation, as these sites structurally provide: (1) protection from environmental elements and scavengers; (2) a moist environment integral to early development; and (3) a closed environment that promotes maintenance of the clustered infrastructure of oviposition aggregates (Byrd & Tomberlin 2020). Modes of bodily larval colonization progressed in anticipated ways (e.g. diffuse migration under moisture rich and protective superficial tissue layers).

However, a unique pattern of preferential migration from the body surface to the posterior body and peripheral ground-body interface was most typically observed (Figure 6-1 & 6-2). The catalyst for this behavioral adaptation is hypothesized to be a safety seeking mechanism, as the ground-body interface affords a measure of protection from scavengers and deleterious weather patterns. Despite behavioral plasticity, the interaction between developing larvae and several environment specific variables precluded the overall success of both Dipteran and Coleopteran reproductive and developmental success.

Two primary factors limited successful larval colonization: (1) avian scavenging; and (2) local atmospheric patterns. While avian species were observed scavenging larvae, this hazard is not considered unique, as scavengers present a threat to developing and colonizing larvae in most (and arguably, all) environments. Of greater consequence were local weather patterns associated with high-altitude summers. Insects and their offspring are poikilothermic, making their development highly sensitive to environmental variables. The most critical of these variables are temperature and moisture. While cursory consideration of warm summer temperatures and moderate to high humidity suggest ideal conditions for larval development, an overall inaccurate atmospheric picture is painted. High-altitude summers are characterized by dramatic punctuated weather events, including hailstorms, violent thunderstorms, high winds, and wildfires producing acrid, atmosphere dense smoke. Adaptive mechanisms observed at high altitude were primarily demonstrated by colonization site. While Dipteran oviposition and early larval development was often successful, reproductive and developmental success was interrupted by punctuated, dramatic atmospheric and environmental events, resulting in rapid death of larval colonies and the impediment of overall reproductive success. Rapid colony eradication was distinguished from typical maggot migration by time from oviposition to eradication, and majority instar stage at the time of eradication. For example, TB20-106 presented fly oviposition (PMI 2 Days), followed by sparse colonization of first instar larvae in the autopsy incised thorax (PMI 3 Days). The

following day, antagonistic thunderstorms persisted throughout the morning. When observed that afternoon, lifeless early instar maggots were visible in the thorax and in the surrounding environment; no subsequent maggot activity was observed.

Scavenging larvae constitute a formidable source of soft tissue destruction in many – but not all – environments, as demonstrated by environmentally mediated colony eradication. *Calliphoridae* larvae were observed early in the postmortem interval and associated with separation and enzyme catalyzed dissolution of the epidermis. Due to frequent colony eradication, they were not major progenitors of tissue loss. The morphological impact of their presence was primarily manifest in the widening of colonized body cavities, such as the nares, following migration or death. *Silphidae* grubs were observed during advanced decomposition (TBS 22-24) and scavenging resulted in a distinct series of tissue perforation ranging in size from 1-5 millimeters (Figure 6-3). Because perforations are the result of enzymatic feeding, the edges of tissue defects are morphologically smooth. This lends morphological distinction, making *Silphidae* defects identifiable from alternative sources of tissue perforation, such as avian scavengers and environmental exfoliation. Anato-spatially, perforations were most densely distributed in body segments characterized by thinner dermal structure, such as the face and superior chest. Perforations were initially circumscribed, followed by increasing coalescence across time, mediated by mechanical properties such as environmental exfoliation, expansion and retraction of desiccated tissue, movement of body sections, and the behavior of subsequent scavengers. Coalescence resulted in 'peekaboo' exposure of underlying skeletal elements and promoted their premature weathering.

Figure 6-1: Left - Prolific maggot colonization at the ground-body interface. **Right –** detail of colonization. Note the almost complete lack of thoracic colonization, which provides optimal environmental conditions (moisture, nutrient dense easy to digest viscera, and tissue folds to entrap enzyme secretions and promote tissue dissolution) for development.

Figure 6-2: Left - Facial colonization by mature *Silphidae* larvae; note the density of colonization in the hair, and tissue perforations subsequent to scavenging. **Right -** Prolific grub colonization between the legs at the ground-body interface.

Figure 6-3: Top – Mild loss of orbital tissue following *Silphidae* scavenging. **Bottom –** Advanced tissue loss with coalescence of tissue perforations resulting in aggregate areas of tissue loss and 'peekaboo' exposure of underlying skeletal elements (approximately 30 days of activity, TBS 22-23, PMI 100-129).

6.2 Avian scavenging

In a porcine pilot study, turkey vultures (*Cathartes aura*), ravens (*Corvus corax*), and black-billed magpies (*Pica hudsonia*) were both directly and indirectly (via game camera) observed scavenging cooperatively (Baigent *et al.* 2019). While cooperatively scavenging, species specific patterns of soft tissue and osseous change could not be discerned. The introduction of scavenger cages precluded access to human remains by the larger bodied ravens and vultures, allowing black-billed magpies to radiate. Magpies were observed early in the postmortem interval (within 1-3 days of donor placement); their presence persisted through advanced decomposition and skeletonization. Cage proliferation was typically achieved in solitude. Succession and progression were characterized by a period of intraspecies observation (learning), group proliferation (2-7 individuals), squabbling, and ascendency of a solitary scavenger periodically interrupted by small groups (2-3 individuals).

6.2.1 *Magpie (Pica hudsonia) scavenging*

Magpies were prolific progenitors of tissue removal. Their scavenging persisted throughout the year but was most voracious throughout the fall and winter. Both primary pattern and mode of tissue removal were distinct, as were the passive byproducts of their behavior. Primary scavenging patterns included: (1) boring; (2) muscle mining; (3) longitudinal tissue peeling; (4) ribboning of connective tissue; (5) trabecular mining; and (6) generalized skeletal destruction. Additionally, a propensity for anato-spatial focal scavenging was observed before advancement to a novel anato-spatial focal source was undertaken. Passive byproducts of avian scavenging included: (1) peripheral soil excavation; (2) beak raking and superficial talon stamping; (3) pseudoburial; and (4) slope roll.

6.2.1a. Boring: Magpie boring was associated with the project of dermal excavation, snow clearance, and secondary food sourcing. Magpie induced bore holes are distinct from larval *Silphidae* perforations in size and morphology. Larval *Silphidae* perforations are small (1-5 mm) and present smooth organized borders, while magpie bore holes are larger (15-25 mm) and

distinguished by irregular 'tattered' edges. Boring was accompanied by ribboning, the byproduct of peeling muscle from dense connective tissue. This resulted in the curling of connective tissue as it was forcibly pulled through the beak. Throughout the winter months, snow boring was observed as a means of accessing tissue underlying snow overburden. Snow boring, tissue boring, and concomitant ribboning are presented in Figure 6-4. In addition to soft tissue boring, bore holes were observed in body adjacent matrices, introduced as migrating maggots, worms, or other burrowing insects were opportunistically sourced (Figure 6-5). Matrix boring is considered an important taphonomic change, as substrate focused boring bears resemblance to projectile defects that might be mistaken for environmental data pertinent to scene investigation and interpretation.

6.2.1b Muscle Mining: Boring was independently categorized due to variation in morphology and underlying behavioral motivation. Magpie boring was most prominently associated with the project of dermal excavation to access underlying musculature. Bore holes typically presented focally, followed by: (1) a tightly clustered series with eventual coalescence of defects as excavation of large-bellied muscle groups (e.g. rectus femoris) was pursued; or (2) broad distribution as smaller flat and fiber-complex muscle groups (e.g. rectus abdominis) were foraged (Figure 6-6). A time series of game camera photographs present the active project of muscle mining (Figure 6-7). The pulling of superficial tissue, removal of deep tissue plugs, and insertion of the head into tissue cavities demonstrate that muscle mining is a focused, goal-oriented enterprise.

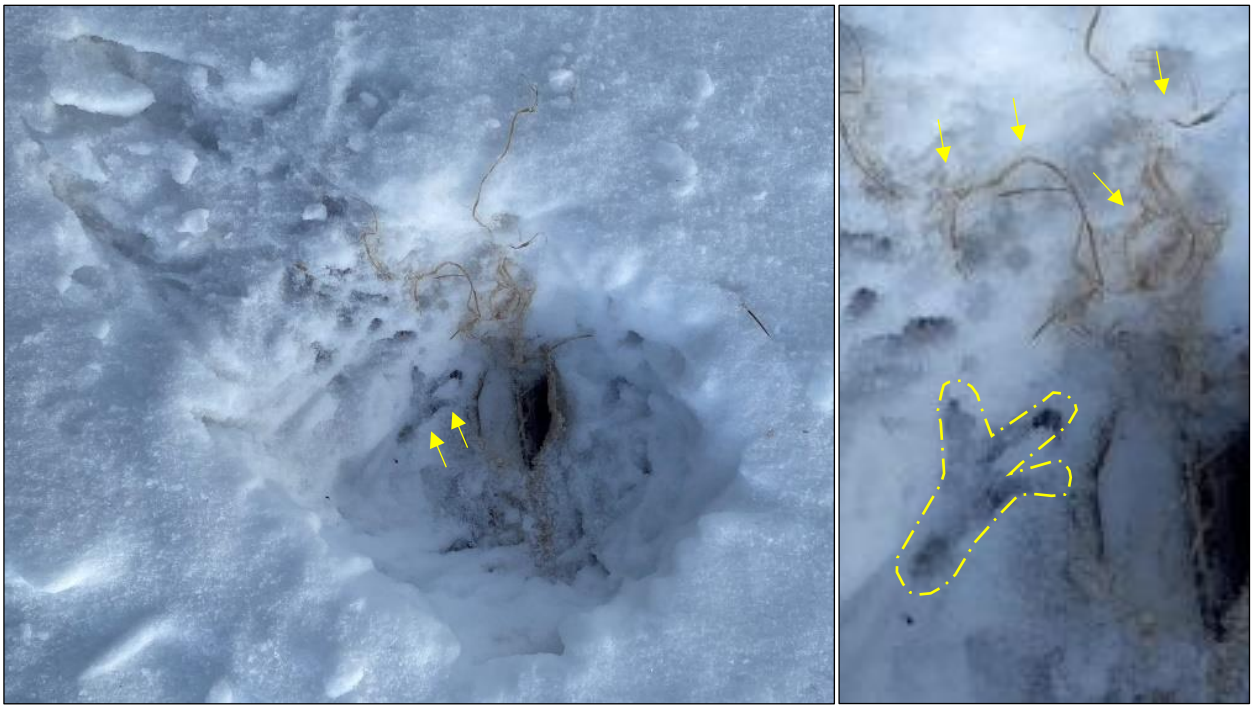

Figure 6-4: Left – Magpie excavation of snow overburden followed by snow boring to reach underlying soft tissue and consequent ribboning. Note anisodactyl tracks in snow surrounding the bore hole. **Right –** Detail of bore hole, ribboning (yellow arrows), and avian track in snow (yellow outline).

Figure 6-5: Matrix boring (indicated by arrows) - bore holes in body adjacent matrices, introduced by magpies scavenging secondary food sources such as migrating maggots, burrowing insects, and worms.

Figure 6-6: Magpie boring. **Top** – Tightly clustered series of bore holes in left proximal leg with coalescence. Coalescence characterized mining of large-bellied muscle groups. **Bottom** – Single bore hole (adjacent to the umbilicus) in abdomen, associated with the mining of flat and fiber-complex muscle groups.

Figure 6-7: Muscle mining. The top row, left to right presents (1) Magpie pulling epidermis to gain access to underlying muscle; (2) the removal of section of muscle placed on donor's forearm; and (3) insertion of the head into the defect cavity. Bottom row left to right presents a corresponding focal image of each step in the series.

Advanced muscle mining (scavenging undertaken following majority clearance of musculature) was associated with advanced decomposition and desiccated tissue. In this phase, pocket searching was undertaken. Pocket searching is characterized by the large-scale project of tissue tearing, a campaign undertaken in search of additional food stores. In this stage, existing bore holes fortified by tissue desiccation served as a beak anchor, creating the tension necessary to facilitate lateral tissue tearing. The result is desiccated tissue that presents a series of small linear tears that progress to large, coalesced tears, giving desiccated tissue an overall dramatically 'tattered' appearance (Figure 6-8).

Figure 6-8: Pocket searching - lateral tissue tearing giving the appearance of 'tattered fabric,' following prolific avian scavenging.

6.2.1c Longitudinal Tissue Peeling: Longitudinal tissue peeling was observed in both fresh and waxy desiccated tissue and was characterized by the sequent peeling of strips of tissue from the limbs resulting in a longitudinal series of ribboning (Figure 6-9 & 6-10). Longitudinal tissue removal was focal, and acutely anato-spatially specific. Tissue peeling began with boring and tissue plug removal. As time progressed, tissue defects became sufficient in size to allow the magpie cranial insertion into the body cavity. As access increased, tissue peeling became more prolific but remained highly focal. Once the project began in a specific body segment (e.g. the distal arm), focus remained on

that body segment until the tissue was cleared. The second generation of scavenging did not begin until the primary segment was devoid of tissue, and a second focal area was pursued. Overall, the pattern of tissue peeling trended toward body-segment specific and circumferential, though tissue may be left at the ground-body interface. Summarily, longitudinal tissue peeling was the primary precipitator of skeletonization of the limbs, rendering the campaign a major component of the taphonomic profile.

6.2.1d Ribboning of Connective Tissue: Ribboning of connective tissue was a consequence of boring, muscle mining, and longitudinal tissue removal. Ribboning is the result of mechanical extension of collagen dense connective tissue as softer water and protein dense muscular tissue was harvested. In the process of pulling skeletal muscle from connective tissue, the connective tissue is forcibly raked across the beak, interrupting the structural integrity of associated fascia, ligaments, and tendons. Much like pulling ribbon across a scissor blade, when pulled across the lateral edges of the mandibular bill, connective tissue is curled. Exposure to aerial elements results in drying and maintenance of the curled connective tissue that bears a distinct resemblance to curled ribbon (Figure 6-11). Ribboning is a unique feature of magpie scavenging that has the potential to be regarded as diagnostic of avian scavenging.

Figure 6-9: Time series game camera capture of magpie mediated longitudinal tissue removal.
Top to bottom (1) bore holes in arm; (2) insertion of head into defect (muscle mining); (3) longitudinal tissue removal with consequent ribboning; and (4) focal tissue removal advancing to skeletal exposure.

Figure 6-10: Focused, circumferential, longitudinal tissue peeling from distal legs while proximal tissue remains uninterrupted. Note the presence of tissue at the ground-body interface and ribboning.

Figure 6-11: Focused image of longitudinal ribboning resulting from the mechanical displacement of structurally dense fascia, ligaments, and tendons subsequent to the removal of muscle by scavenging magpies.

6.2.1e Generalized Skeletal Destruction: Magpie motivated skeletal destruction is broadly categorized as: (1) punctuated; (2) chaotic; (3) focused; and (4) passive. While categorically defined, they are behaviorally intercalated, and will be presented in sum. Magpies tended to scavenge individually or in pairs. The measured, relatively organized project of soft tissue removal is evident in the longitudinal pattern of peeling and the focused specificity of a body segment. When multiple magpies were present, intragroup competition was apparent in wing flapping, swooping, and

pecking. Concomitantly, soft tissue was chaotically removed during rapid swoops, resulting in passive introduction of skeletal defects. Flat bones were the most common site of passive skeletal destruction, most frequently observed in rib ends, the iliac fossae, and the nasal and orbital osseous complexes (Figure 6-12). Osseous destruction was restricted by architecture due to the biomechanical limitations imposed upon scavenging breadth by beak morphology. Because magpies were rarely observed scavenging in groups, these chaotic encounters are considered temporally punctuated events.

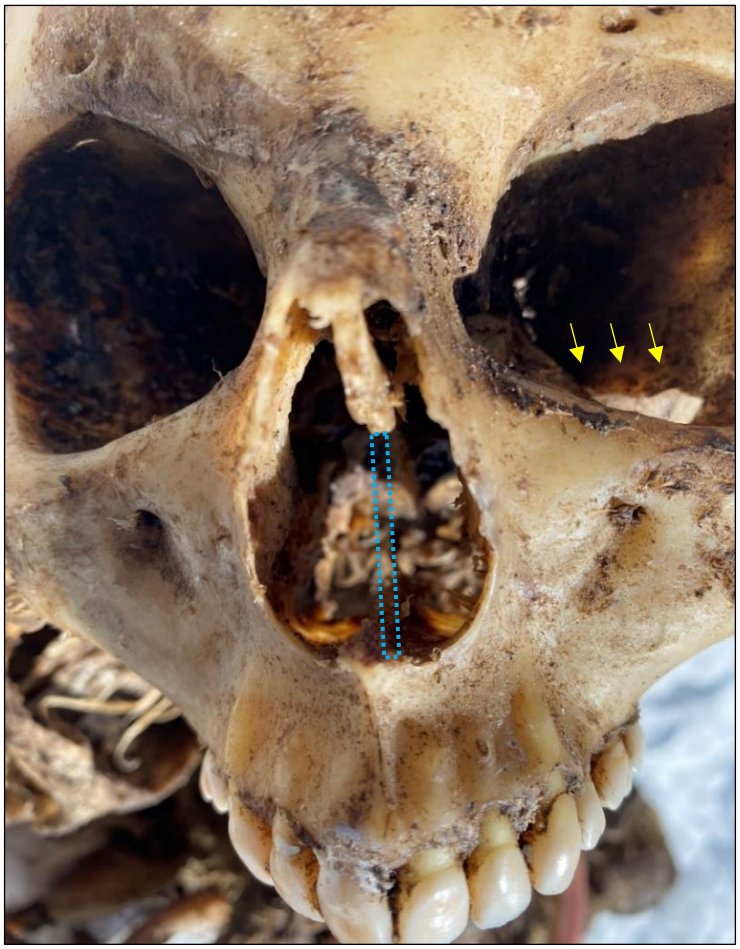

Figure 6-12: Passive skeletal destruction in the optic and nasal osseous complexes following chaotic avian scavenging. Yellow arrows indicate fracture of the maxillary and sphenoidal orbital plates; blue outline indicates breakage of vomer's perpendicular plate.

Rib end fracture was characterized by both focal and passive modes of destruction. Focal destruction was characterized by the clamping of the beak around the visceral and parietal rib surfaces and using oppositional force to snap the rib end off the body. This resulted in disorganized transverse, oblique, and wedge fractures (Figure 6-13). Similar morphology was passively motivated by the removal of desiccated thoracic tissue that maintained its intimate relationship with the underlying ribs. As avian scavengers worked to remove overlying tissue, lateral force was applied, introducing compressive force to the parietal surface, and tension with concomitant failure to the visceral surface. When decomposition of connective tissue was sufficient, passive interruption of the costovertebral joint occurred, resulting in disarticulation, and/or displacement of the ribs or the sternal complex. Flat bone destruction observed in the os coxae and in the nasal and orbital osseous complexes also appeared to be the byproduct of soft tissue scavenging and most typically presented as punctures within the orbital complex and iliac blades, transverse fracture of the vomer's perpendicular plate, and crush fractures of the nasals.

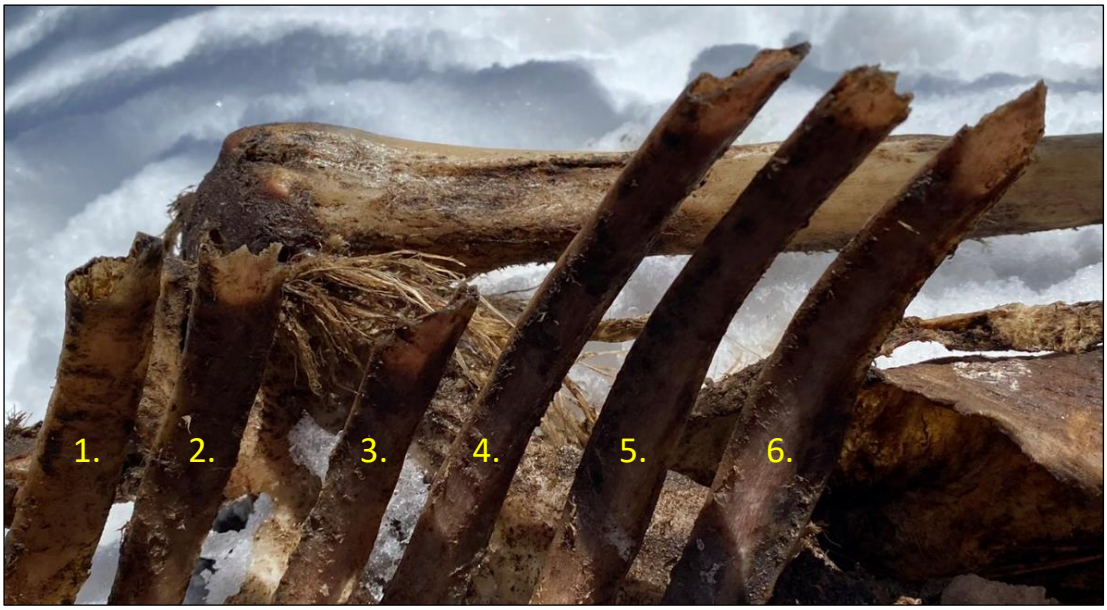

Figure 6-13: Individual with a series of magpie derived rib fractures resulting in several fracture types. Numbers correspond to fracture type: 1, 2, & 5 transverse crush; 3 & 4 oblique fracture; and 6 butterfly fracture. All fracture types present frayed, disorganized edges.

6.2.1f Trabecular Mining: Trabecular mining was only observed among scavenging magpies and was temporally associated with overwintering and early spring. Trabecular mining occurred when tissue removal was sufficient to result in moist skeletonization, facilitating the exposure necessary for compromise of cortical surfaces. Trabecular mining follows a consistent pattern in location and morphology, and only occurred after complete skeletonization. This pattern is therefore regarded as focal scavenging and an extension of anato-spatial specificity. The pattern of trabecular mining mirrored that of boring and muscle mining. Trabecular mining was characterized by focal cortical destruction and removal of underlying trabeculae, likely in an effort to access the associated bone marrow. Trabecular mining occurred in circumscribed areas of trabecular density, such as the distal femora and the vertebral bodies. Summarily, trabecular mining took two primary morphological forms: (1) complete removal of trabeculae with maintenance of an organized border and overall structural integrity of the surrounding cortices; and (2) wide breadth cortical destruction followed by removal of deep trabeculae resulting in a wide conical defect that may advance to complete transverse penetration of bone, with a disorganized and undercut edges. Figure 6-14 presents the two variants of trabecular mining. While trabecular mining is a form of skeletal destruction, it is afforded categorical distinction due the morphological specificity of the associated defects.

Figure 6-14: The two morphological forms of trabecular mining: **Top** – Inferior T5, removal of trabeculae with maintenance of an organized border; and **Bottom** – distolateral femur, wide breadth cortical destruction that advanced to complete transverse penetration and disorganized undercut edges.

6.2.2 Passive Byproducts of Magpie Scavenging

Passive byproducts of magpie scavenging are the biological and environmental changes that occur peripheral to the focused project of scavenging. Identified categories include: (1) peripheral matrix excavation; (2) avian pseudoburial; (3) beak raking, superficial talon scratching, and talon stamping; and (4) avian induced slope roll. These changes serve as indicators of magpie presence and inform the overall composition of the scene-specific taphonomic profile.

6.2.2a Peripheral Matrix Excavation: Peripheral matrix excavation or soil scratching was invariably observed throughout the course of magpie scavenging. Matrix excavation is characterized by both active and passive disruption of the peripheral matrix by the avian beak and talons (Figure 6-15). Passive disruption occurred as magpies walked, flapped, and swooped around the body, disturbing the peripheral matrices. In extreme incidences, peripheral matrices were disturbed in radiations extending as far as 60-centimeters from the body. The resultant dark, upturned matrix gave the misleading appearance of a moist decomposition island. Active peripheral disruption was the result of matrix excavation in pursuit of shed lipids and secondary food sources such as maggots, worms, and insects.

6.2.2b Avian pseudoburial: Avian induced pseudoburial resulted from bioturbation of surface matrices through active scratching and digging into the soil adjacent to the body, or passive tilling of surface matrices throughout the exercise of scavenging. The result was partial or complete burial of a body surface associated with the site of soil disturbance. Burial was typically shallow depth (3-5 mm) but sufficient to obfuscate the affected body section. Matrix excavation and pseudoburial are presented in Figure 6-15.

Figure 6-15: Passive matrix excavation, note disarray of matrix between legs with discernable anisodactyly (avian) footprints. Upturned dirt adheres to greasy bone, obscuring its presence in the environment.

6.2.2c Beak raking, Superficial Talon Scratching, and Talon Stamping: Beak raking, superficial talon scratching, and tissue stamping are cosmetic defects introduced to the epidermis.

Beak raking resulted in linear, parallel striae of various length, resulting from both the collection of insects and failed attempts to puncture the epidermis with the cuspidate apex of the beak (Figure 6-16). *Superficial talon scratching* resembled beak raking in its superficial, non-penetrative morphology, but was distinct in disorganization. While beak raking resulted in organized linear striae, talon scratching was characterized by a disorganized, precipitous cluster of linear defects (Figure 6-16). *Talon stamping* was observed in advanced decomposition, when subcutaneous adipocere formation was sufficient to provide a gelatinous matrix within which a partial impression of the anisodactyl foot may be visible (Figure 6-17).

Figure 6-16: Left - Beak raking; note organized linear, parallel striae. **Right** - Superficial talon scratching; note disorganized clusters of multidirectional striae.

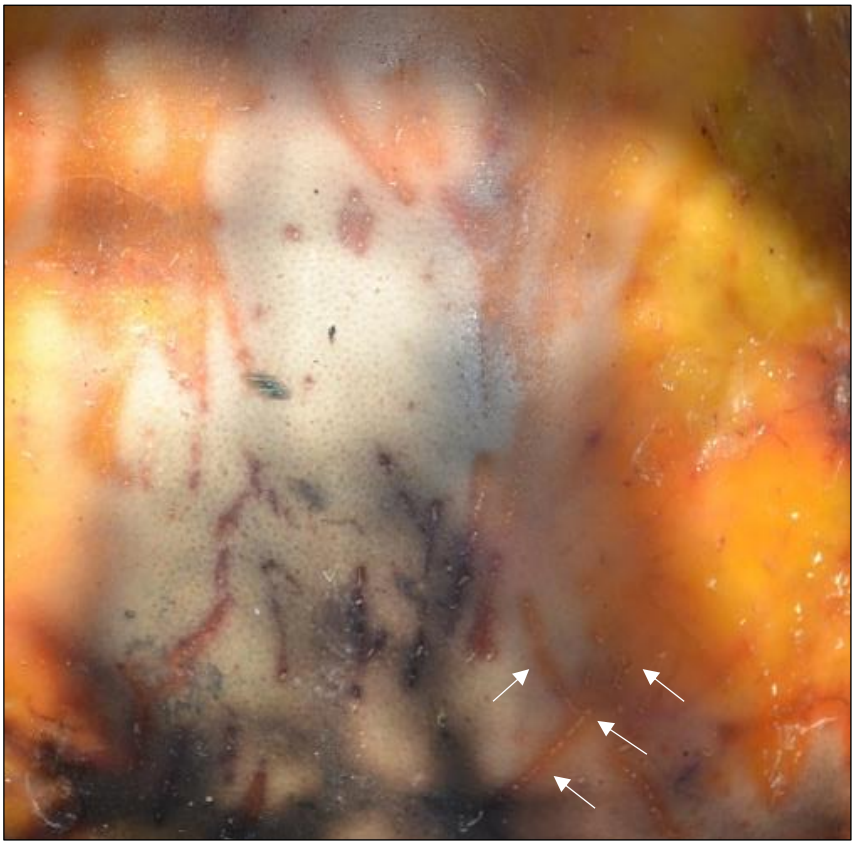

Figure 6-17: Series of partial imprints of anisodactyly (avian) foot stamped in gelatinous matrix of subcutaneous adipocere; almost complete imprint indicated by arrows.

6.2.2d Avian induced slope roll: Slope roll describes the mode and pattern of transport (movement) of human remains through the environment across time. Avian induced slope roll was most typically the result of passive disturbance of small bones and bone fragments while engaged in the primary task of tissue removal. However, in advanced decomposition magpies were observed promoting skeletal disarticulation while performing the task of trabecular mining and were responsible for calculated removal of smaller skeletal elements.

6.3 Packrat Scavenging

Like magpie scavenging, packrat scavenging was observed throughout the year, but voracity increased markedly in late fall and early spring. Packrat scavenging began in early to intermediate decomposition. In general, their scavenging temporally proceeded magpie scavenging and presented on a smaller anato-spatial scale. Both magpie and packrat scavenging accelerated as postmortem interval increased. The anato-spatial scale of packrat scavenging increased markedly in intermediate to advanced decomposition, when waxy desiccation facilitated the removal of larger soft tissue sections. The incidence and prevalence of scavenging by individual packrats could not be assessed, as identification of individuals by morphological traits was beyond the scope of this study. While packrats could not be individualized, they are a behaviorally solitary species and co-scavenging was never captured or observed. Packrat middens were observed both adjacent to, and within individual donors, a pattern highly suggestive of individual, habitual scavenging (Figure 6-18). Packrat home range is classified as radial and their activity extends 15.25 meters within the radial range (Whitford & Steinberger 2010). Middens were distributed throughout the site at a minimum distance of 50 meters apart. Primary modes of packrat scavenging included: (1) opportunistic exploitation of unique resources and lipid dense diet; (2) resource-centric shelter; (3) superficial tissue removal and skeletal gnawing; and (4) territorial resource defense.

6.3.1 Opportunistic Exploitation of Unique Resources and Lipid Dense Diet: Unique resources are defined as those not expected to regularly present within an ecological niche. Packrats cyclically exploited adipocere formation within defects in human tissue, indicating preferential selection of the lipid dense food source (Figure 6-19). While animal carrion possesses the physiological potential for adipocere formation, fundamental differences in lipid structure between humans (phospholipids, sterols, and triglycerides) and animals (triacylglycerols) make the content of each source distinct. In accordance with a propensity for adipocere, packrats displayed a predilection for the lipid layer exposed at the tissue interface of autopsy incision (Figure 6-20). The selective avoidance of intimately associated fresh dermal tissue observed throughout the course of lipid layer scavenging demonstrates a preference for lipid dense tissue types.

Figure 6-18: Game camera timeseries of packrat pedal scavenging in the early postmortem interval (PMI = 5 days). Visits were observed nightly and lasted 3-6 hours.

Figure 6-19: Adipocere formation within tissue defect (frames 1-4 and 6-8), followed by packrat scavenging of lipid dense adipocere (frames 5 & 9). This behavior was repetitive, as adipocere cyclically formed within the same defect and was repetitively scavenged.

Figure 6-20: Preferential exploitation of the adipose layer at the tissue interface of an autopsy incision. Note the release of autopsy sutures subsequent to scavenging, encouraging longitudinal advancement of lipid layer consumption.

6.3.2 *Resource-centric shelter:* Packrat middens were constructed both directly adjacent to, and within cadavers. Intra-corpus midden construction was limited to advanced decomposition, post visceral desiccation. Midden construction began in the fall and the waxy desiccated tissue characteristic of intermediate to advanced decomposition served as both shelter and a lipid dense food source ideal for overwintering. While shelters constructed directly adjacent to, or within a donor indicated a packrat's presence and spatial location, packrat presence and movement was secondarily monitored throughout

the winter by burrow construction and tracks in the snow. Tracks were opportunistically observed during weekly site visits (Figure 6-21). One consistent and persistent travel route was observed following the same course. The route originated in a grove of trees on the west slope, followed the length of fallen logs until an open expanse of snow field was traversed to reach the perimeter of cage number five (closest to the tree stand). Tracks were observed around the perimeter of the then empty cage before traveling south to circle the perimeter of a second empty cage, before finally reaching cage number four. Cage number four and the snow within contained packrat tracks, scat, and burrow holes. The return path followed the route of entrance and terminated imperceptibly in the original tree stand. In the spring, a packrat midden was located in a tree at the eastern face of the grove. The repetitive circling of two empty cage perimeters suggests that the packrat recognized a resource rich change in the environment. Examples of the three packrat midden types observed throughout the course of this study are presented in Figures 6-22 & 6-23.

Figure 6-21: Packrat tracks in the snow traveling north and returning south. Directionality is determined by linear impressions in the snow resulting from a dragging tail bisecting footprints (Halfpenny 2015).

Figure 6-22: Left – Packrat midden constructed against the wall of cage one. **Right-** Packrat midden in tree central to cages six-eight.

Figure 6-23: Early phase packrat midden construction, right lateral shoulder of desiccated donor TB20-105.

6.3.3 Superficial tissue removal: Superficial tissue removal was characterized by: (1) layered peeling of the epidermis from the dermis and the dermis from the hypodermis where tissue removal terminated; (2) peeling of tissue layers from superficial bone; (3) peeling of dense waxy layers of superficial tissue from the hands, feet, and face; and (4) consumption of deep tissue during intra-corpus overwintering. Fresh tissue scavenging was limited to removal of tissue layers from superficial bone, and ridge gnawing. Removal of tissue layers from superficial bone was often attendant to skeletal displacement of the metacarpals/metatarsals and manual/pedal phalanges induced by fluid bloat. Once exposed, osseous scavenging of the cortical borders escalated to complete removal of intermediate and distal phalanges (Figure 6-24). Ridge gnawing, characterized by longitudinal nibbling of soft tissue associated with an anatomically graspable edge was also observed and was unique to early decomposition.

Figure 6-24: Fluid bloat in right foot with tissue removal and small scall skeletal exposure of the first metatarsal (MT1) and pedal phalanges. Note the active and pronounced fluid loss in the area of MT1 and the proximal first pedal phalanx, resulting from loss of the tissue that typically acts as a retentive barrier in fluid bloat.

Tissue peeling was most prolific during advanced decomposition when tissue quality was characterized by waxy and dry desiccation. Temporally, layered tissue removal and peeling of tissue layers from the hands, feet, and face were associated with winter and early spring (Figure 6-25). The associated seasonal influx of moisture resulted in rehydrated, pliable tissue, and compromise of the intimate relationship between tissue layers by moisture infiltration. The plantar surfaces of all donor feet were voraciously scavenged throughout the winter, leaving them largely devoid of tissue in the spring. Plantar tissue removal did not result in perceptible skeletal involvement, indicating that scavenging was directed toward the calcaneal and metatarsal fat pads. As was observed among scavenging magpies, packrats demonstrated a propensity for repetitive exploitation of a focal anatomical region. However, packrat scavenging was smaller in scale and guided by the presence of lipid dense tissue.

Figure 6-25: Packrat tissue scavenging. **Left –** Layered tissue peeling of the abdomen (separation of waxy desiccated epidermis from dermis). **Right –** peeling of plantar tissue. A lack of skeletal involvement suggests that scavenging was directed toward the calcaneal and metatarsal fat pads

6.3.4 Territorial Resource Defense: Packrats are classified as a solitary and territorial species. As such, they are small but prolific scavengers, if they retain access to a desired food source. Aggressive territorial behavior was observed in the field on one occasion, when an attack was levied during data collection in a cage adjacent to a large midden. The resultant injuries were limited to pride and superficial scratches (Figure 6-26). While innocuous in appearance, packrats should be considered a potential threat to practitioner safety throughout field search and recovery operations.

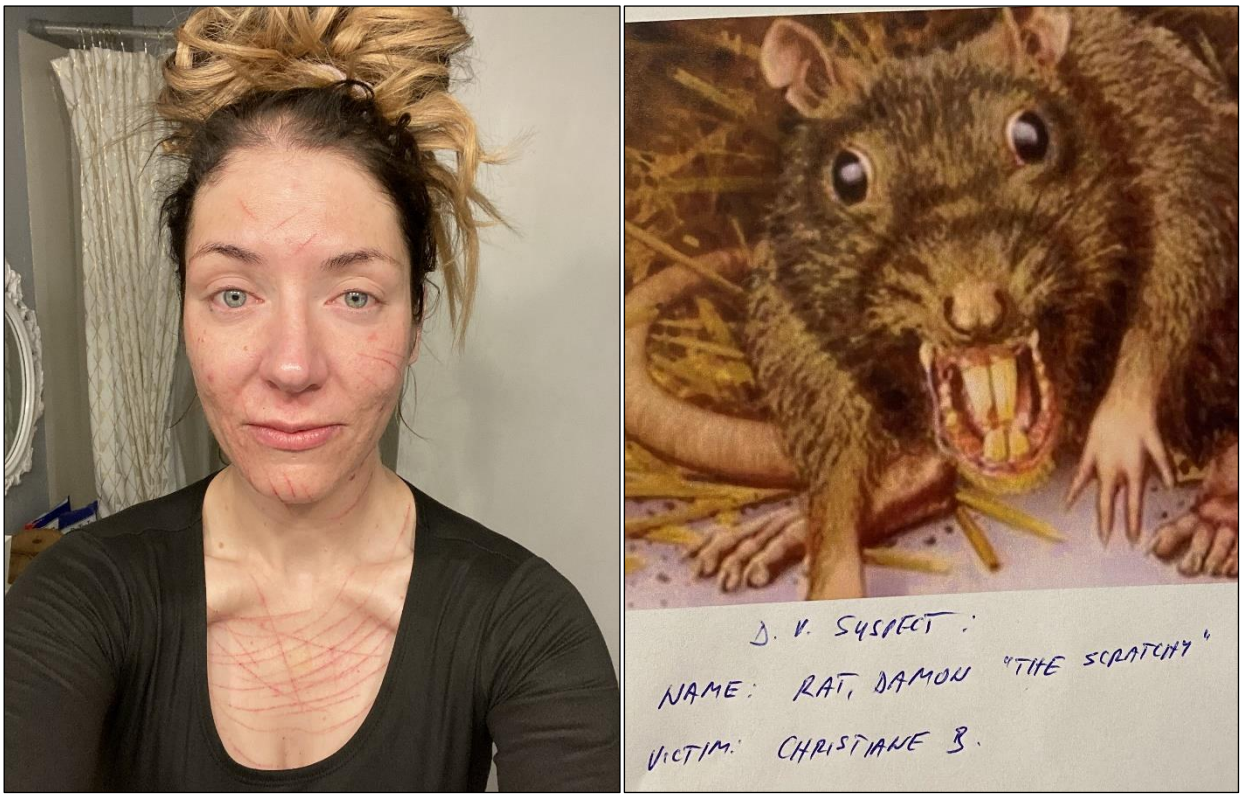

Figure 6-26: Left - The aftermath of a packrat's display of aggressive territorial behavior. **Right** – Law enforcement response, Sheriff McGraw, Park County Sheriff's Office.

6.4 Small Bodied Canid Scavenging

Despite the installation of subterraneous galvanized steel DigDefense panels, two cages were intruded upon by a small-bodied canid on two occasions. In the first incident, game cameras captured images of a red-tailed fox within cage seven. A game camera failed to capture images in the second incident. As a result, species identification was limited to defect morphology in bone, which included conical punctures, epiphyseal crushing, and removal of the manual and pedal osseous complexes

(skeletal complexes larger and more substantial than those manipulated by scavenging magpies and packrats). Both breaches occurred in mid- to late-summer (June and August, respectively).

6.4.1. Canid Incident #1: June 2022

A burrow associated with an approximate 35(L) x 25(H)-centimeter gap in the tines of a DigDefense panel was observed at the base of cage seven, containing donors 21-103 and 21-104. An adjacent game camera captured images of a red-tailed fox (*Vulpes vulpes*) inside of the cage (Figure 6-27). Prior to canid entrance, both donors were skeletal and displaced downslope following prolific magpie scavenging. Skeletal defects observed following canid activity included crushing and removal of the epiphyses of long bones, conical punctures in bone, and loss of numerous skeletal elements, including the skull, long bones, and articulated cervical vertebrae I-VII. A subsequent field search resulted in recovery of the skull and articulated vertebrae approximately 50 meters upslope and east of the cage, a fragment of a distal right radius approximately 33 meters southeast of the cage, a right humerus with proximal and distal epiphyses removed approximately 25 meters northwest of the cage, a left ulna with proximal and distal epiphyses removed approximately 16 meters north of the cage, and several rib fragments in a wash associated with the southwest corner of the cage (Figure 6-28). Based on overall condition and scene investigation, the fragments recovered from the wash were attributed to avian scavenging and slope roll. The majority of both skeletons remained caged, but disturbance was sufficient to result in a complex of comingling in the southwest corner of the cage.

Figure 6-27: Game camera capture of a red-tailed fox (*Vulpes vulpes*) inside of cage seven during canid incident #1.

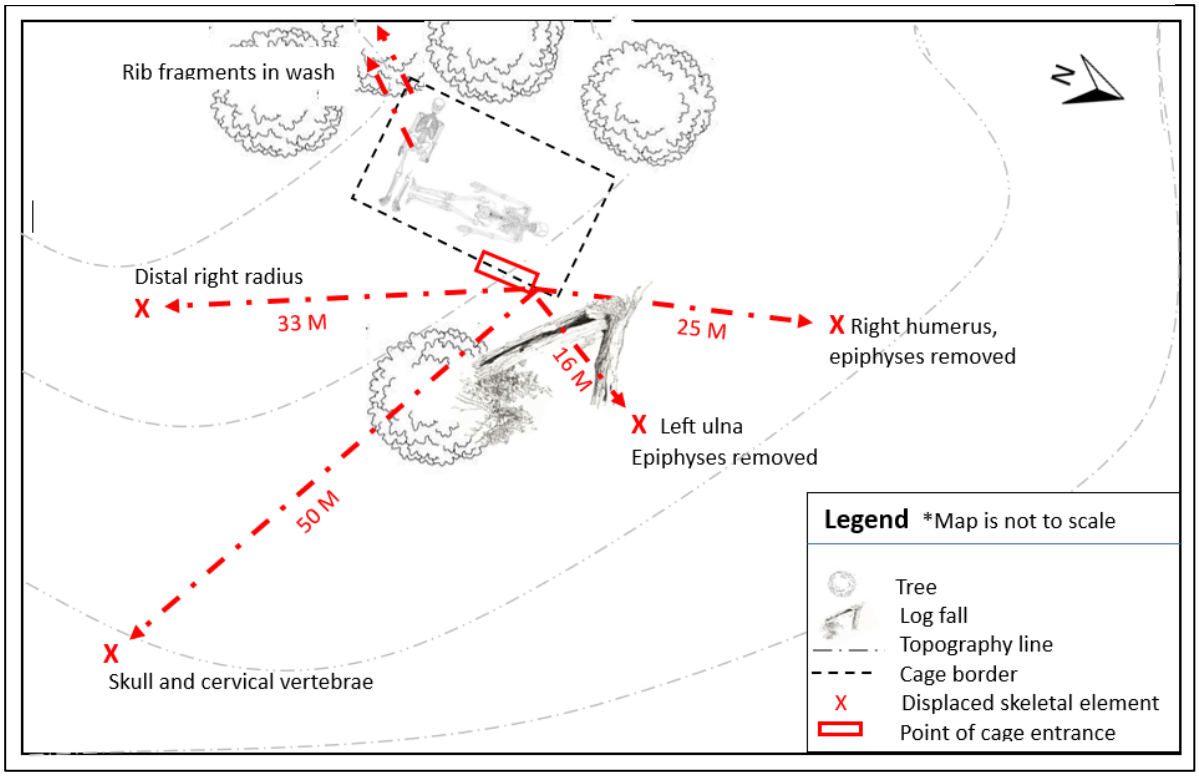

Figure 6-28: Distribution of skeletal elements removed from cage seven during canid incident #1.

6.4.2 Canid Incident #2: August 2022

A burrow associated with an approximate 30(L) x 25(H) centimeter gap in the tines of a DigDefense panel was observed at the base of cage two, containing donors 20-103 and 20-104. Prior to canid interference, 20-103 presented desiccated tissue and skeletal exposure of the: mandibular body, right lateral craniofacial region, anterior cervical vertebrae, left hand, right and left ischiopubic rami, and the plantar surfaces of the right and left feet. Taphonomic skeletal change was limited to subaerial bleaching. Post canid interference 20-103 presented: (1) inferolateral displacement of the right arm; (2) disarticulation of the left humerus and radio- and ulno-humeral joints; (3) superolateral abduction of the proximal left humerus; (4) displacement of the left radio-ulnar complex and the left hand resulting in new skeletal exposure; (5) dramatic lateral abduction of the right leg resulting in a 90˚ angle between the leg and the trunk; (6) tissue displacement resulting in new skeletal exposure of the right and left femora, the lower thoracic vertebrae, the lumbar vertebrae, the right and left os coxae, and right ribs 9-12; (7) torsion of the distal left leg with force sufficient to result in separation and removal of the pedal phalanges (these elements were not recovered). Prior to canid interference, 20-104 retained waxy desiccated tissue on the majority of all body sections. Skeletal exposure was limited to circumscribed areas of the mandible and maxillae, the distal arms, and the dorsal and medioplantar aspects of the right foot. Post canid interference 20-104 presented: (1) tissue removal of right lateral chest and midline resulting in exposure of the manubrium and desiccated anterior longitudinal ligament; (2) complete skeletonization of the right and left distal arms and partial exposure of the left proximal humerus due to tissue displacement; (3) complete removal of the right and left hands with concomitant crush fractures of the right and left distal radial and ulnar epiphyses; and (4) longitudinal peeling of waxy desiccated tissue resulting in skeletal exposure of the left medial tibia and foot. Figures 6-29 and 6-30 present pre- and post-canid interference of 20-103 and 20-104, respectively.

Figure 6-29: Donor 20-103 **Left –** pre- canid scavenging. **Right –** post-canid scavenging.

Figure 6-30: Donor 20-104 **Left –** pre- canid scavenging. **Right –** post-canid scavenging.

While large-bodied scavengers were barred access to donors by scavenger cages, infiltration by two medium-bodied canids demonstrates the extent of scene interruption and skeletal disturbance and destruction achieved in a short span of time. This is demonstrative of the rapidity with which the taphonomic signatures of small-bodied scavengers may be overprinted. While holistic profiles of interspecies scavenging are critical to study of the local environmental, rapid overprinting underscores the need for scavenger studies designed to segregate small-bodied groups to best understand individual mode and trait presentation.

6.5 Conclusion

Understanding local scavenger behavior both by individual species and as the sum of interacting groups (scavenger guilds) is critical to the environment specific forensic ecological profile. The use of scavenger cages in this study precluded access to human remains by large-bodied scavengers. This exclusion allowed small-bodied scavengers to radiate, facilitating high-resolution, categorical description of their behavior. Four primary invertebrate and vertebrate scavenging groups were observed in this study. These included: Dipterans (blow flies; family *Calliphoridae*), Coleopterans (carrion beetles; family *Silphidae*), magpies (Pica hudsonia), and bushy-tailed woodrats (*Neotoma cinerea*; commonly referred to as packrats). Additionally, the presence of red-tailed fox (*Vulpes vulpes*), and an unidentified medium-bodied canid species (identified by morphology of osseous defects) were each noted on one occasion.

Invertebrate identification was limited to family and indicated the presence of blow flies (*Calliphoridae*), and carrion beetles (*Silphidae*). Scavenging by larvae was observed within both groups. While typically prodigious scavengers, both groups were highly sensitive to atmospheric variables and vulnerability to avian scavengers. Attempts to adapt included migration to the ground-body interface. However, behavioral plasticity was insufficient to overcome exogenous variables and reproductive and developmental success was limited.

Magpies and packrats were the most prolific scavengers in this study. Both groups were active throughout the year but voracity increased markedly in the late fall and throughout overwintering. Fresh tissue scavenging was observed among both groups, but species-specific predilection for tissue type diverged. Several categories of magpie scavenging cascaded from the guided project of transdermal tissue boring, longitudinal tissue peeling, and muscle mining. Conversely, packrats pursued lipid dense tissue, adipocere, and thin tissue overlying bone. Several categorical scavenging traits were attributed to each group as a result of their segregation from larger-bodied scavengers. Tenacity among medium-bodied canids resulted in two punctuated scavenging events characterized by skeletal disarticulation, destruction, and dispersal. In concert, the scavenger guild observed in this study cannot be considered representative of the region due to limitations associated with access. However, this study yielded rare, high-resolution profiles of the scavenging behavior of two often underappreciated, under observed, and often overprinted small-bodied groups.

CHAPTER 7

RESULTS: FORENSIC ECOLOGICAL PROFILE – DEMOGRAPHIC, CULTURAL, AND CASE STUDY DATA

7.0 Results: *Population and Land Use Data*

7.1 Population Demographics (US Census Bureau 2022; censusreporter.org 2023)

Park County (PC) has a population of 17,834 residents and a landmass of 2193.5 square miles with a distribution of 7.9 people per square mile. Fifty percent of the population is 50 – 80+ years of age; the median age is 51.3. The 50-59 age group has the greatest populous (20%) followed by group 60-69 years (18%). When compared to the population of Colorado (CO), and the United States (US), the most populous age groups in Park County diverge appreciably (Age 50-59 PC 20% / CO 12.5% / US 13%; Age 60-69 PC 18% / CO 11.2% / US 11.7%). Park County is conservative; 56.9% or residents voted for the Republican Party in the last Presidential election versus 39.9% Democratic. The County is relatively balanced in the distribution of sex (47% Female / 53% Male). A highly significant disparity in race and ethnicity is observed. County residents are 91% White; followed by Hispanic (7%), Asian (1%), and Native (1%) populations. The foreign-born population is 1.6%, well below the national average of 13.6%. Concomitantly, 97% of the population reports speaking 'English only' at home. The highest level of education presents a bell curve (no degree 3%; high school degree 25%; some college 39%; bachelor's degree 23%; post-graduate degree 10%). In county veteran status is 10.6%, exceeding both Colorado (8.3%) and National (6.9%) averages.

There are 7169 reported households with an average of 2.4 persons per household. Married couples constitute 75% of household type, followed by non-family (16.5%), female householder (4.8%), and male householder (3.5%). There are 14,049 housing units in the county, 49% of which are vacant. However, 'vacant' denotes a fully uninhabited property, which fails to accurately describe the housing structure in Park County. Vacation property data analytics company AirDNA named the county seat of Fairplay as the only top-tier location in Colorado for short-term rental purchase (airdna.co 2022). Rather

than reflect ‘vacancy,’ this figure is a better indicator of the number of residents displaced by the local influx of real estate investment in short term property rental. Further supporting this model is the 7000 available vacation rentals in Park County, reported by short-term rental conglomerate Vrbo (2023). As a possible outcome of the housing shortage, geographic mobility was low; 91% or residents remained in the home they occupied one year prior to census, with in-migration limited to 8% of the population.

Of important note, census data reflects the demographic data of those willing to submit to census interview. Park County has a large ‘invisible population,’ primarily composed of single men who have purchased land in remote areas of the county and live off grid. This population, referred to locally as “bucket shitters,” and “the Hartsel homeless,” live in non-traditional housing, including recreational vehicles (RVs), converted tough sheds, converted shipping containers, subterraneous cinderblock shelters, or a synthesis of several different creatively assembled shelter types. Many lack power, an incorporated heat source, and a reliable form of communication (i.e. those that have cellphones live remotely by design and lack cellular service while out of cell tower range). This population constitutes a fascinating subdivision of the local population that is both highly individualized in practice, but culturally collectivized in by their non-traditional lifestyle. The pejorative monikers assigned to the group demonstrate the contempt held by the dominant population, and reenforces their standing as a distinct cultural group through exclusion by informal sanction. The town of Hartsel is located in south central Park County approximately 19 miles from the county seat and is demonstrative of this trend. Figure 7-1 presents Google Earth images of a sample of the landscape containing RVs on several privately owned plots of land. While a distanced but aggregate community is presented, this does not reflect the norm. Remotely located homesteads on larger parcels of land better fit the cultural profile, but are more

difficult to locate and capture using satellite imagery due to their intentional camouflage within the landscape.

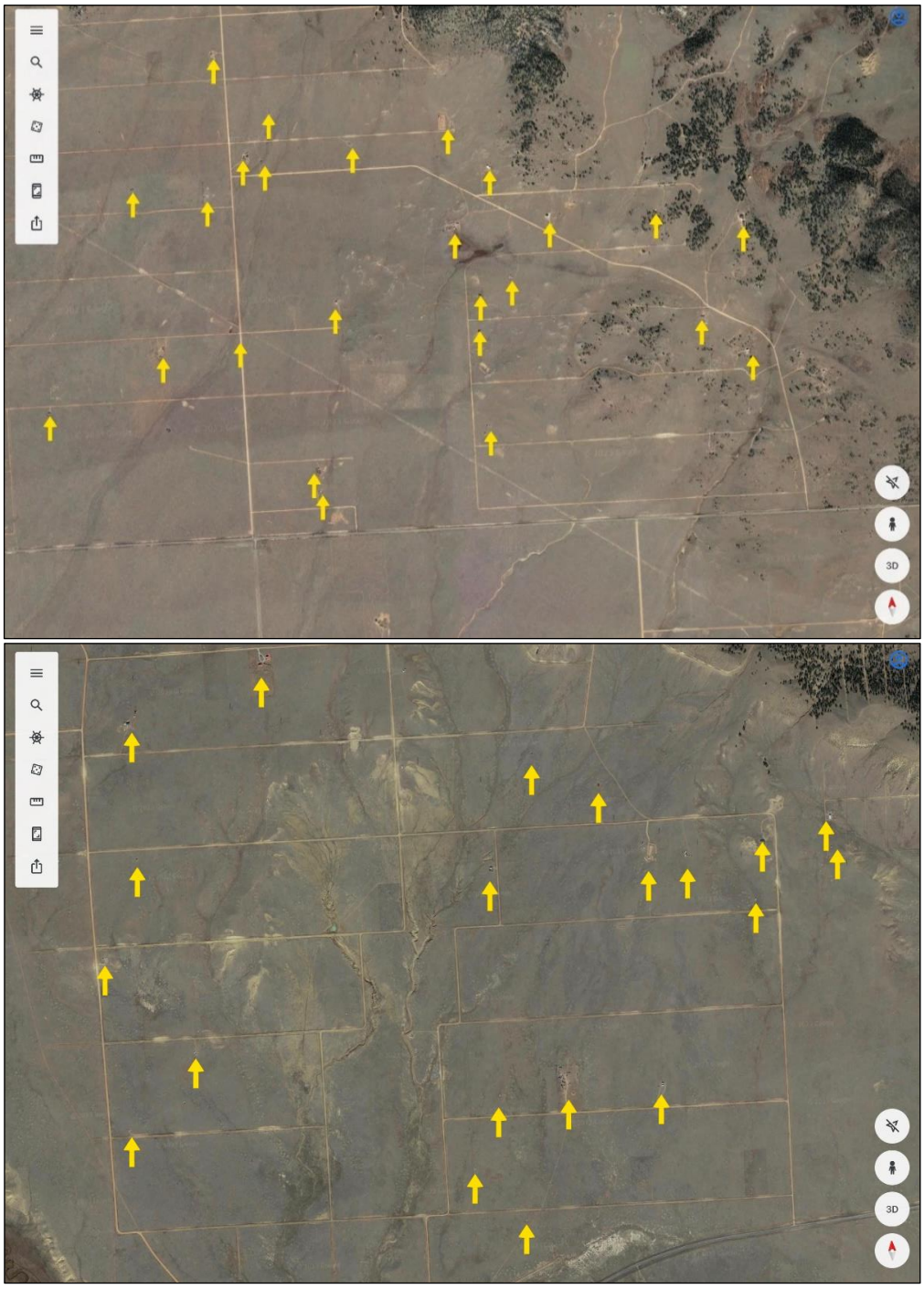

Figure 7-1: Satellite imagery of land samples outside of the town of Hartsel. Homesteads indicated by arrows. Referred to locally as “bucket shitters,” and “the Hartsel homeless,” these individuals constitute one of Park County’s ‘invisible’ populations and compose a distinct cultural group not reflected in census data (www.google.com/maps/place/Hartsel,+CO+80449/@39.0213471,-105.7973724,538m/data).

7.2 Land Use

Park county has a landmass of 2166 square miles; 59% of the region (1278 square miles) is composed of federal and state lands. The primary zoning designations are: (1) conservation and recreation; (2) agricultural; and (3) residential (parkco/183/planningandzoning 2024). A map depicting the distribution of the three categories is presented in Figure 7-2. Between 2010 and 2019, development has increased 3.34% and impervious surface area (a measure of square feet of horizontal surface covered by buildings and other water impenetrable surfaces) has increased by 16.74%. Conversely, a moderate increase in forested area (0.75%) and wetlands (1.05%), paired with a decrease in total agriculture (-17.69%) suggests that development has encroached on agricultural land, as opposed to natural land (MRLC 2022).

The primary mode of county ingress and egress are two State highways (HWY 9 / HWY 285). The county is primarily composed of graded, unpaved county roads yielding access to a complex series of private and residential roads in various states of repair and passability. The highway infrastructure is presented in Figure 7-3. The map of primary roadways does not adequately represent the complexity of Park County's transportation infrastructure. The National Forest Service (NFS) provides seven road designations within the county, including: (1) roads open to highway legal vehicles; (2) roads open to all vehicles; (3) trails open to vehicles 50" or less in width; (4) trails open to motorcycles only; (5) seasonal designation (i.e. roads formally closed due to hazardous winter conditions); (6) interstate; and (7) highways (US, state, county, other). An NFS generated roadway map is presented in Figure 7-4 (NFS 2022). It is recognized that the resolution of the map presented is not sufficient to convey the finite details and distinguishing features of each roadway type. However, when compared to the roadway infrastructure provided by the county's GIS system, the complexity of the local road infrastructure is apparent, and it is evident that important data pertaining to land use is lost. Despite extant maps provided by the NFS, trails may become obstructed, overgrown as a result of infrequent use, informally

rerouted, and/or signage and route markers obscured or intentionally removed. Due to their complexity and the potential for several variables to interfere with their use, knowledge of these roads, the rules associated with them, modes of access, and proficiency in their use is reasonably presumed to be limited.

While the county presents complexity in roadways, public transportation is insufficient to meet the needs of a broadly distributed population. The Summit Stage Park County Commuter is the only commuter transit bus available to residents. Rather than facilitate intra-county transport, the commuter line provides transport from Fairplay to the adjacent tourist dense Summit County (Summit County Stage 2024). Summit County is an internationally recognized vacation destination owing largely to its infamous ski destinations, including Breckenridge, Keystone, Arapahoe Basin, and Copper Mountain. As such, the financial disparity between Summit and Park County is palpable. In 2021, Park County's annual revenue was $1,685,000 (https://parkco.us/625/Financials 2022), in sharp relief to Summit County's partially reported revenue (January – October 2022) of $8,600,000 (Tann 2022). The free commuter bus is limited to four stops: Fairplay (Park County), Alma (Park County), Blue River (Summit County), and Breckenridge (Summit County). The bus runs between 6:45 AM and 6:58 PM. By design, the service was established to provide transportation of Park County's workforce into and out of Summit County to support the labor demands associated with their robust hospitality industry.

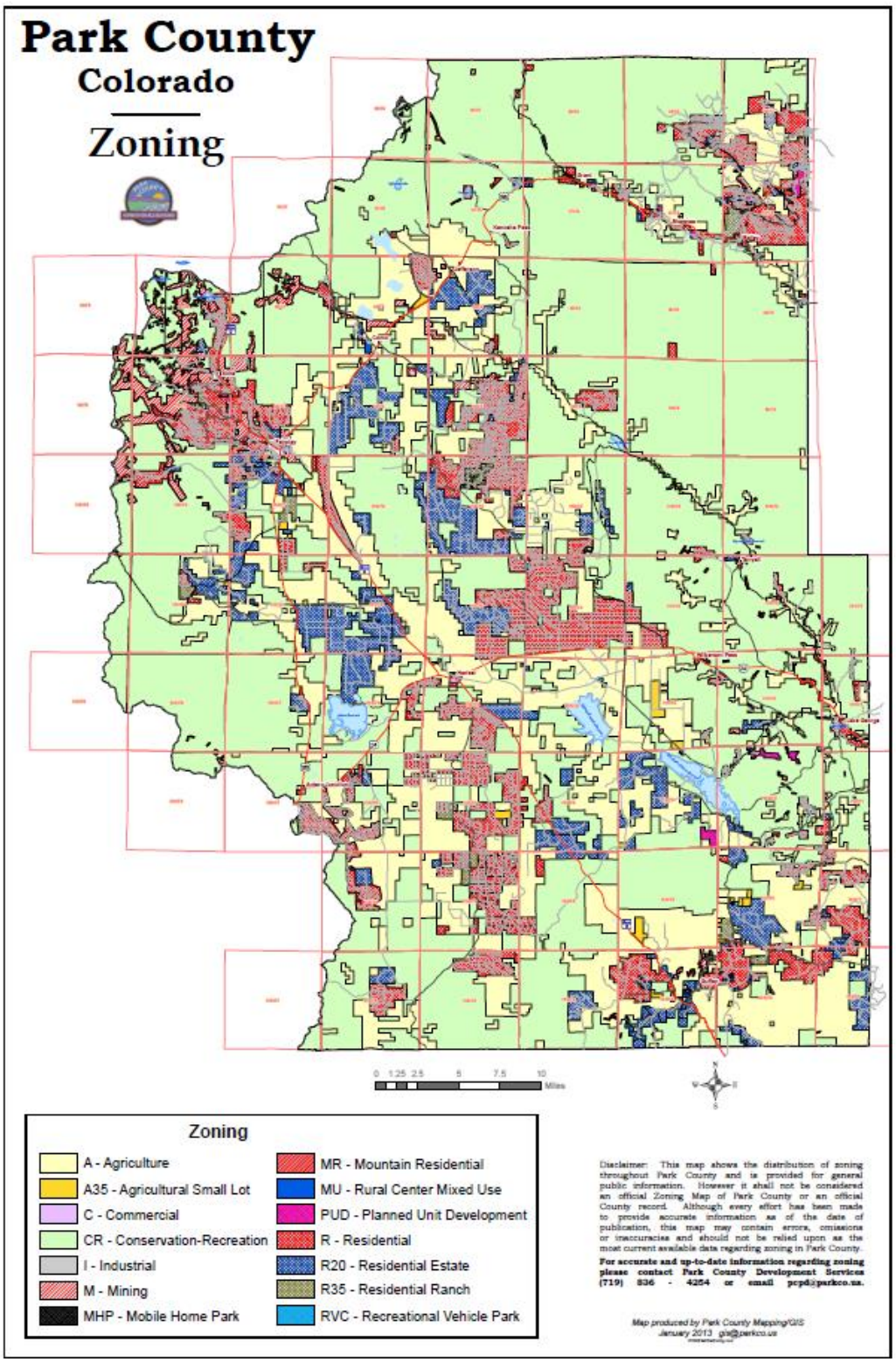

Figure 7-2: Distribution of Park County's primary zoning designations: (1) conservation/recreation (green); (2) agriculture (yellow); (3) residential (red) (https://parkco.us/DocumentCenter/View/1288/Park-County-Zoning-2013?bidId=)

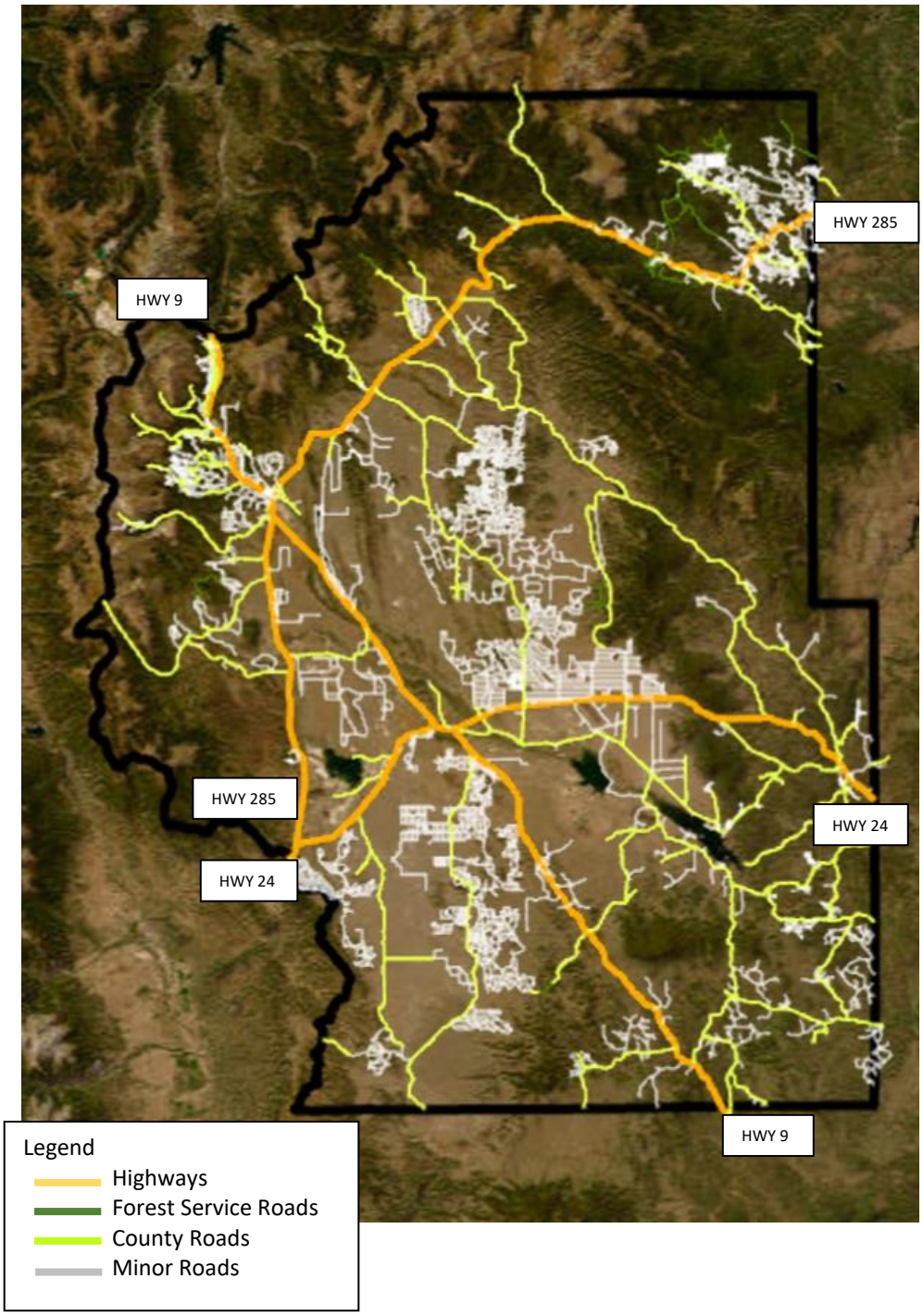

Figure 7-3: Park County's primary roadway infrastructure: (1) State highways (orange); (2) forest service roads (dark green; upper right) County roads (light green); and (3) minor/private roads (gray) (https://maps.parkco.us/).

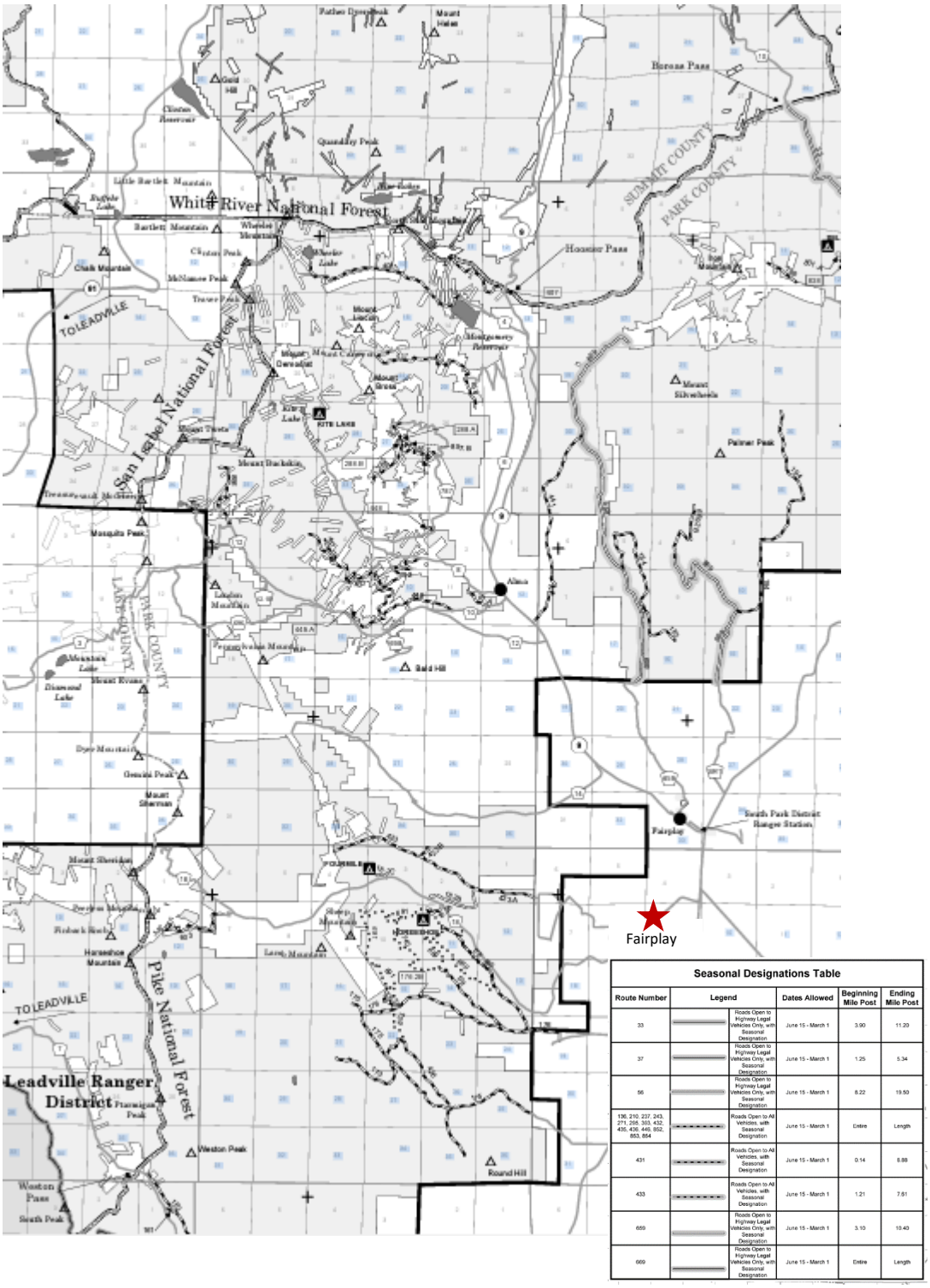

Figure 7-4: Low-resolution map of seven roadway designations, as defined by the National Forest Service (2022), depicting overall 'hidden' complexity of Park County's roadways. The northwest half of map is presented to increase resolution (Fairplay indicated by red star). Complete higher-resolution map accessible at https://www.fs.usda.gov/detail/psicc/maps-pubs/?cid=stelprdb5177824.

7.3 Local Cultural Trends

A search of published literature related to local culture yielded 21 publications specific to the rural Colorado Rockies. The goal of the literature review was to cull data specific to the local environment (the rural Colorado Rockies). Therefore, the citations presented are in no way reflective of the depth or breadth of the body of literature related to these topics. However, the literature review is concerned with the identification of local cultural themes and was therefore intentionally limited in scope. The literature review yielded six cultural themes (Table 7-1). These themes include: (1) racial disparity in recreational land use; (2) variation in culture observed between longtime and incoming residents; (3) the impact of environment on local culture; (4) the effect of cannabis on local culture; (5) predominant land and associated modern tool use; and (6) local recreation. These categories both present the opportunity to identify and understand cultural themes, as well as identify cultural themes that have not been described in academic literature.

Table 7-1: Categorized local cultural themes identified in this study, by source.

Cultural Theme	Publications
Racial disparity in Recreational Land Use	Erickson *et al.* 2009
	Stodolska *et al.* 2020
	Rice *et al.* 2022
	Theriault & Mowatt 2020
Variation in culture observed between longtime and incoming residents	Smith & Krannich 2000
	Graber 1974
	Park *et al.* 2019
	Stokowski 1996
The impact of environment on culture	Sibley 2002
	Holtkamp *et al.* 2018
	Rolston 2008
The effect of cannabis on local culture	Berman 2021
	Bushan 2015
	Reed 2021
Predominant land and (modern) tool use	Consumer Product Safety Commission (2021)
	U.S. Forest Service 2018
	Pearson 1994
	US Department of Agriculture 2021
Local Recreation	Colorado Parks and Wildlife 2022
	South Park Heritage 2022
	Parkcounty.gov 2020

7.3.1 Racial Disparity in Recreational Land Use

Park county has a landmass of 2166 square miles, 59% (1278 square miles) of which is composed of federal and state lands that attract more than 640,000 visitors annually (parkco.us 2020). Park County is primarily White (91%) followed by Hispanic (7%), Asian (1%), and Native (1%) populations (US Census 2022). This fundamentally informs the degree of intra-county diversity. However, additional power regarding local patterns of population-based land use is derived from ethnography concerned with recreation along 'racial' lines. Racially motivated patterns of land use informs transient (visitor) demographics that cannot be derived from census data, as well as elucidate the historic and sociopolitical roots of informal land use sanctions that inform modern patterns of rural region avoidance by people of color (POC). The synthesis of modern cultural configuration and historic boundary construction yields a higher resolution image of the racial homogeneity characteristic of both local and transient tourist populations, while similarly identifying barriers that may preclude engagement with the rural environment for criminally motivated activities.

Rocky Mountain National Park reports that 91% of park visitors identify as White, while visitors identifying as Black constitute a disproportionate 3.8% of annual visitors, a structure that bears resemblance to Park County's population demographics (Erickson *et al.* 2009). Racial disparity in the avoidance of recreation within Rocky Mountain national parks is further documented within Black, Asian, and Latinx populations (Stodolska *et al.* 2020). Four pervasive models are used to describe the relationship between ethnicity and choice in recreation: (1) the discrimination hypothesis; (2) the cultural assimilation hypothesis; (3) the marginality hypothesis; and (4) the ethnicity hypothesis. The perceived discrimination hypothesis suggests that choices surrounding when and where to recreate are informed by discrimination experienced by members of a racially defined population. An emphasis is placed on the contemporary modes of discrimination that individuals may experience while in a park, such as othering, a feeling of unwelcomeness, and the perception of heightened levels of scrutiny

directed toward visiting POC populations by the dominant group. The cultural assimilation hypothesis suggests that the decision-making process associated with park access and use reflects the characteristics of the dominant culture. This is an interesting proposition when the local population (91% White) is compared to the local visitor population (91% White). Assimilation is predicated on the theory that as individuals adopt and adapt to dominant cultural values, beliefs, and behavior, their recreational patterns increasingly mirror those of dominant society. The marginality hypothesis asserts that minority recreation patterns are created and perpetuated by inextricable patterns of historicity and structural violence. The result is modern cultural configurations characterized by limited financial resources related to historical patterns of limited social and physical mobility imposed by discriminatory wage gaps, access to leisure time, and structure of leisure time (Rice *et al.* 2022; Erickson *et al.* 2009; Theriault & Mowatt 2020). Cost, lack of knowledge of opportunities, transportation, time, programs and facilities, and safety concerns may all serve as barriers to access (Stodolska *et al.* 2020). The ethnicity hypothesis (Washburne 1978) is a higher resolution rendition of assimilation theory, in which differences in norms, value systems, and culture specific definitions of "leisure" inform patterns of participation in outdoor recreation.

Drawing on Bordeau (1977), Erickson *et al.* (2009) provide a more holistic theory of racially motivated patterns of park use based on cultural capital and habitus. Cultural capital describes the sum of sociocultural resources (e.g. social, cultural, and historical knowledge), expressed in embodied, objectified, and institutional forms. Embodied cultural capital describes the individual's perception of the world based on the sum of internalized acculturation - what Geertz (1973) describes as self-constructed invisible webs of meaning within which the individual is suspended. Objectified cultural capital describes the possession of cultural objects (art, media, literature, etc.) that serve to perpetuate the embodied form. Erickson *et al.* (2009) offer the example of the technical equipment necessary to participate in certain forms of outdoor recreation as a form of objectified cultural capital that may serve

as a barrier to access in outdoor recreation. More than just 'things,' objectified cultural capital possesses cultural agency in its ability to define the 'haves' and the 'have nots.' Institutionalized cultural capital are formalized, culturally relevant benchmarks denoting success - such as degrees or certificates earned – that further serve to socially stratify. Critical to the concept is that all forms of cultural capital are inter- and intra-generationally heritable, and may be taught or obtained through life experiences, meaning cultural capital is both historically constructed and mutable. In this way, the embodied, objectified, and institutional are paradoxically inherent but dynamic and serve to collectivize and distinguish cultural groups, most typically along 'racial' lines (Yudell 2014). *Habitus* is the performative state of cultural capital, characterized by the often subconscious, "natural," and "appropriate" mode of conduct or action by group members within sociocultural context. Summarily, the decision to "act" (habitus) is directly related to cultural capital and serves as an explanatory model for racially based modes of recreation as a whole, and park use in particular.

The cultural capital/habitus model offers explanation of the mechanisms by which racially derived patterns of recreation are established and propagated. When considered in conjunction with environment perception theory, a deeper understanding of perpetuation is gained. Human perception of the environment is an ongoing project brokered by skills incorporated into the human organism through practice and training in the environment (*sensu* Ingold 2000). Since practice catalyzes changes in proficiency, perception of the environment is an ongoing, dynamic project with historic, spatial, and temporal relevance. However, if habitus dictates and fosters avoidance (as is described within Black communities), proficiency and perception do not have mode for change, social capital is not gained, and proficiency remains (largely) inert.

The root of practiced avoidance of National Park recreation by POC was studied by Erickson *et al.* (2009) through a series of 36 semi-structured interviews. The authors identify historical, linguistic, and cultural factors as the roots that foster persistent avoidance. The authors argue that institutional

racism formally sanctioned by Jim Crow segregation laws and informally sanctioned through normalized patterns of performative and sociocultural racial subordination limited the spatial mobility of black communities. This cultivated a warranted fear of traveling outside of one's social and environmental sphere out of concern for physical safety. Often taken for granted in modern context is that this "history," is not a discrete unit of behavior encapsulated in time. Rather, it is a dynamic multilinear complex of systemic events that evolve into modern cultural context and therefore cannot accurately be categorized as "the past." Formally sanctioned laws supporting segregation persisted into the early 1970s, while informal sanctions fostering racial barriers persist in modern cultural context. The composite product is a paucity of generational distance from the lived experience of Jim Crow law, the effects of which are variably maintained by the persistence and lived experience of informal social sanctions propagating racial barriers. The exchange of intergenerational discriminatory knowledge draws on past and present to function as a preservation barrier, as demonstrated by an interlocuter presented by Erickson *et al*.:

> "In the 60s and 50s discrimination was still so tolerant that your best thing was survival. Your best thing was just walking into JC Penny's and getting accepted there. So you know, why do I want to branch out? Plus you know they are always quoting the fear, you know if I go out of the bounds of the city limit, no telling what I'm going to run into. I may be running into acreage, I may be running into something that doesn't want to relent. Some kid, some minority person for the sake of it, to just go out of say south (Denver) is not safe." (2009: 538)

Shared knowledge for benefit of the perceived - and the real - safety of both the individual and the group constitutes cultural capital and explains why multigenerational boundary maintenance and park avoidance is a critical cultural component.

Intergenerational boundary maintenance is further evident in linguistic use. Historically, as members of the Black community migrated out of southern agricultural communities and into the urbanized north, the process of othering "the country" and "the woods" was undertaken. In a study of the Western Apache, Basso (1970: 1988) demonstrates that communication is highly culturally relative and contains structures of exchange that necessitate deep knowledge of the landscape, historicity,

myth, and cultural mimesis to negotiate interaction. He argues that entanglement with the environment suggests that landscape focused statements may contain indexical messages about the social position of individual social actors, and the relationship between interlocuters. He uses Apache place-naming to explore these relationships and effectively demonstrate that rather than constitute practical/utilitarian symbols, placenames contain social capital. Under Basso's model, "the country" or "the woods" does not refer to a specific place but serves as an ingroup referent to a suite of cultural capital. In this case, these terms draw on historical references to negatively connotated cultural markers associated with the outdoors, such as slavery and clandestine wilderness lynchings (Stodolska *et al.* 2011). The freedom and economic opportunity afforded by urbanism further reinforced the symbolic view of "the country" or "the woods" as a source of individual and economic oppression, and the association of the outdoors with an antiquated and impoverished way of life.

> "Yea, nature walks. That's not a big thing for us. That doesn't do it for us. We're not as really into the preservation of land. But we do not embrace and we do not have an innate or historical appreciation for it…what you call forest, we call woods…the ideology of the woods came out of the Deep South and there was nothing about…it was not good in those kinds of surroundings. Black people was forced to make do in those types of environments, but also they are often associated with outhouses, didn't have inside plumbing. The belief in the South was sometimes fear of going out in the woods...there were a lot of stories of blacks being hung, their bodies being found hung from trees and things like this. So there's not anything comfortable traditionally in African-Americans' mind, in my opinion, about what we would call the woods and you would call the forest." (Erickson *et al*. 2009: 539).

These linguistic referents serve to reinforce cultural barriers, within which 'the outdoors' serves to demarcate "White culture," and is therefore inherently *not* "Black culture." The indexical message not only reinforces that "the woods" are a dangerous place but serves to further define social position of individual social actors, and the relationship between interlocuters within the Black community. The cultural implication of othering the outdoors is not limited to spatial barriers. As an index for "White culture," social barriers are erected and maintained among members of the Black community, where participating in outdoor activities carries the inherent risk of adapting "White culture" to the perceived

effect of rejecting “Black culture.” Summarily, an understanding of the historic, linguistic, ritual, and symbolic modes for the ‘othering’ of the outdoors does not just inform the propensity for POC to recreate in the Rocky Mountains but informs the propensity for racially defined groups to engage with the outdoors in any context. While ‘recreation’ functions as an important analytical referent, it further serves to inform the deeper composite historical and cultural trends by which modes of modern engagement with the environment are constructed.

7.3.2 Variation in culture observed between longtime and incoming residents.

While the mobility of POC remains limited, ease of inter- and intra-region travel, and high amenity values have resulted in overall greater cultural admixture and fluidity within the contemporary Rocky Mountain west. A prominent wave of in-migration began in the 1990s, resulting in regionally unprecedented demographic, economic, and sociocultural transformation (Smith & Krannich 2000). Rather than serve to culturally homogenize the region, studies of changing rural communities suggest substantial disengagement between longer-term residents and newcomers. In an early but still prominent ethnography performed in the Colorado Rockies, Graber (1974) identified disparities in the attainment of higher education as foundational to divergence in world view between longer-term residents (50% attainment) and newcomers (72% attainment). Graber suggests that conflict arises from the dualistic presumptions that longtime residents possess significantly lower levels of education, and incoming residents lack the practical knowledge critical to survive the arduous environment. Push factors catalyzing the movement of incomers included urban pollution, economic competition, and disillusionment associated with the anonymity and impersonality of urban communities. Pull factors included quality of the physical environment, perceived benefits of the rural sociocultural environment, and the romanticized notion of the indexical ‘west’. Differences between longer-term residents and newcomers were manifest in local sociocultural goals, such as the mobilization of support for historic

preservation initiatives among newcomers, interpreted as an attempt to associate and align the group with the region by imposing false historicity.

In a more recent study, Smith and Krannich (2000) identified six categories of divergence between the two groups. Incoming residents expressed more concern than longtime residents over excessive economic development, and the importance of tourism. Conversely, longtime residents expressed concern over preserving existing values and way of life, limiting population growth, the importance of increasing economic opportunity, and concerns associated with the impact of economic development on quality of life. However, the authors conclude that the expectations of substantial differences in attitude between longer-term residents and newcomers of the rural Rocky Mountains toward environmental concern, population growth, and economic development were unfounded. When divergent attitudes were present, longer-term residents were more strongly in support of implementing structural limitations on population growth and economic development than newcomers. This divergence was manifest in patterns of intracommunity sociocultural isolation and boundary maintenance.

The results of the two studies constitute a temporal gradient that may reflect the long-term outcome of sociocultural admixture between the two groups. Newcomers occupy a liminal space in which they are socially suspended between two communities, (*sensu* Turner's [1969] proverbial 'the betwixt and between'). As once newcomers are longitudinally integrated into the community they are socially transformed into longer-term residents; concomitantly, sociocultural change is affected to accommodate the new social space. Summarily these studies support the notion that a cultural gradient exists between adjacent urban and rural communities. The poles are occupied by the maintenance of local sociocultural patterns, while the gradient is occupied by spatially and temporally oriented patterns of cultural maintenance and admixture.

While the temporal gradient suggests an abatement in intergroup tension, structural changes to the economy and housing market in rural mountain towns following the COVID-19 pandemic have encouraged renewed tension. In a joint study conducted by the Colorado Association of Ski Towns and the Northwest Colorado Council of Governments, 4700 long-term (10+ years of mountain residency), fulltime (present greater than six-months annually), part-time (present less than six-months annually), and newcomer (present full- or part-time within the past two years) residents were surveyed to assess the impact of the pandemic on the economic and demographic structure of the rural Colorado Rockies. The result was the Mountain Migration Report (2021), which found that the pandemic precipitated rapid change in social, economic, and housing infrastructure that served to breed social tension. The findings of this study were intimated by cross-sectional data derived from the US Census Bureau (2022), AirDNA (airdna.co 2022), and Vrbo (2023) which demonstrate that of the 14,049 housing units in Park County, 49% (approximately 7000) have been monopolized by real estate investors interested in acquisition of a second home outside of urban centers and/or in housing dedicated to short term property rental. Both longtime and incoming residents have been displaced by the monopoly of real estate investment, which has served to decrease the inventory of available housing, creating scarcity that has dramatically increased the cost of long-term rentals. This problem is intensified by low wages associated with the customer service-based economy of mountain towns, the labor force of which is largely composed of longtime and fulltime residents expected to “be grateful” for the economic growth that paradoxically serves to alienate them. Conversely, approximately 60% of newcomers and 70% of part-time residents work remotely for an out-of-county employer and are therefore sheltered from the economic restraints imposed on members of the local economy. This creates a disparity between the economic barriers encountered by each group, further serving to intensify the project of othering (Mountain Migration Report 2021).

Rapid changes in the socioeconomic infrastructure have served to propagate tension between longtime/fulltime residents and part-time/newcomer residents. The adjacent towns of Breckenridge and Fairplay serve as a case study in the structure and function of this tension. While only 23 miles outside of rural Fairplay, Breckenridge is an internationally renowned tourist destination famous for winter recreation, dining, shopping, multimillion dollar residences, and wealthy vacationers. The two towns are separated by Hoosier Pass, which serves as a geographic and cultural barrier between the two towns. While Breckenridge describes Fairplay as "the funky, fun, charming next-door neighbor of Breckenridge," and "Breckinridge's favorite neighbor," (Girvin 2023), Fairplay's local culture suggests that the affection is unilateral. Breckenridge is widely regarded as the catalyst for the surge in local real estate investment, where part-time/newcomer residents priced out of Breckenridge's (multi)million-dollar real estate market opt to purchase in nearby Fairplay, and short-term property rentals support Breckenridge's tourist overflow. While Fairplay's infrastructure supports Breckenridge tourism, the lack of reciprocity has generated an air of local animosity. While housing and affordable cost of living are forfeited by residents of smaller mountain communities, the majority of tourism revenue is seen in adjacent 'destination' communities (Mountain Migration Report 2021). The inequitable structure of this relationship has created an undertone of derision for part-time/newcomer/tourist populations within the local community, many members of which assume that visitors possess an air of entitlement and a disregard for the local community and environment.

The rapid change in sociocultural, political, and economic infrastructure catalyzed by the pandemic catastrophized social identity for many people around the world. As social roles, routines, responsibilities, and interactions were effectively altered by the formal and informal sanctions fostering social distancing and quarantine, individuals experienced alienation from culturally constructed identities, resulting in social role disruption and crisis of 'self' (Liu *et al.* 2021). While longtime/fulltime residents accustomed to rural living were arguably more adequately equipped to endure isolation, they

were not immune to the cataclysmic (bio)cultural disruption imposed by the pandemic. While the 'crisis of self,' constituted micro (individual) and macro (cultural) schism, rather than serve to undermine cultural ontogeny, the agitation yielded liminal space within which cultural transformation had the potential to occur.

van Gennep (1960) proposes liminality as a theoretical model for understanding cultural rites of passage, conceived as distinct phases arranged in three subcategories: (1) rites of separation; (2) rites of transition; and (3) rites of reincorporation. The initial phase is both signaled and defined by the shedding of one's existing social status and roles. This separation from a previously recognized cultural form facilitates passage into liminality, a transitional phase defined by a socially isolated position adjacent to, but external from the cultural body politic. As negative rites, taboos are drawn upon to construct a barrier between the individual in transition, and the collective. Within the infrastructure of the pandemic, taboo was derived from formal and informal sanctions encouraging social distancing and quarantine, creating both literal and figurative isolation of the individual from the body politic. The creation of a culturally void interface between the individual and the collective constitutes a phase of uncertainty and danger, but also presents an opportunity for creative innovation. Passage through the cultureless chasm is typically negotiated by designated ritual and a culturally ascribed authority figure. Successful passage through the transitory phase yields a new cultural identity and status defined by attendant expectations and responsibilities. Reincorporation is mediated by the rigorous performance of circumscribed ritual which serves to reconcile the dissonance attendant to the transition phase and incorporate the transformed body back into the body politic.

Turner (1967) defines society as a structure of positions within which the 'self' is understood through individual orientation within the structure. The construction of individual identity is a dynamic and ongoing project guided by inside images and outside perceptions of 'self' which may be modified and adapted to accept, resist, affect, or otherwise negotiate social demands. Images of self are reflected

in an amalgam of meaningful symbols and narratives digested and embodied by the individual, and reciprocally shared with the world. Liminality constitutes the fracture of the individual from the structure, yielding an unranked, interstitial position. In their shared inhabitation of interstitial space (regardless of the catalyst for fracture), liminality creates a temporary community of cultural outsiders. Turner famously described the liminal state as an experience that is "neither here nor there…betwixt and between the positions assigned and arrayed by law, custom, convention, and ceremonial" (1969: 96). Turner suggests that the culturally unbound individual is passively integrated into a *communitas* of individuals who, for any myriad of reasons, are also experiencing a social untethering. Members of *communitas* may seek to socially align in *liminoid* spaces – small, dynamic, culturally, and temporally bound social spheres that serve to temporarily collectivize individuals in a shared social sphere.

Conceptualizing the sociocultural upheaval catalyzed by the pandemic within the framework of liminality yields the following process: (1) rites of separation are defined by the formal and informal sanctions that served to physically remove the 'self' from internalized cultural context, resulting in social role disruption; (2) rites of transition are defined by the renegotiation of self and reformation of group identity often informed by individual coping mechanisms adapted to negotiate the fracture and (re)alignment with a cultural group nested within a shared sphere of experience; and (3) rites of reincorporation are defined by the relaxation of the formal and informal sanctions fostering fracture, restructuring newly formed and newly integrated individuals and social groups into a reformed cultural collective expected to be both locally and globally relevant. Locally, rapid changes in the socioeconomic infrastructure served to propagate tension between longtime/fulltime residents and part-time/newcomer residents. Thus, rites of reincorporation were achieved through the construction of temporal and geographic barriers that served to re-collectivize individuals into a 'local' population, the configuration of which was defined and legitimized by time spent in the local environment. The reincorporation process is mediated by the rigorous performance of circumscribed ritual which affords

the individual the opportunity to demonstrate group identity and identify cultural interlocuters. 'Ritual' serves to reconcile the dissonance attendant to the transition phase and incorporate the transformed body back into the body politic. In Fairplay, rituals are observed in activities that serve to maintain the temporal and geographic boundaries that serve to legitimize members of the 'local' population.

While ritual constitutes the ostentatious, performative aspect of cultural reconfiguration, symbols serve to communicate, perpetuate, and reinforce the values of the reimagined politic. Turner (1967) argues that symbols are temporally relevant cultural units that possess agency. While the performance of ritual constitutes distinct phases that serve to socially acclimate the group to internal change and adapt to their external environment (both cultural and physiobiotic), the ritual symbol becomes an agent of social action. Within the relevant and appropriate context of action, the symbol serves as a dynamic entity associated with both individual and collective interests, purposes, goals, aspirations, and ideals which may be explicitly formulated or inferred from observed behavior.

Microaggressions expressed toward the tourist population serve to ritualistically collectivize 'locals,' rely heavily on symbolism, and are most typically enacted on the highway and within the natural environment. This phenomenon is explained by the local infrastructure. Because tourists largely use Fairplay as a bedroom community - commuting in to sleep, commuting out to recreate - and because Fairplay's rural location necessitates that locals spend a significant amount of time on the highway, the majority of interaction between 'locals' and the part-time/newcomer/tourist population occurs on the road, rendering 'the highway' an important cultural stage. Further, because of its rural location defined by a harsh high-altitude environment and expansive wilderness, Fairplay's natural environment constitutes a critical cultural arena used to define the 'other' and collectivize the 'local.'

Symbology derived from the environment and exercised along the highway is evident in popular bumper stickers and the use of license plates, both of which serve as referents to communicate cultural assumptions and reinforce the 'local' versus 'newcomer' barrier. 'Breckenridge' as a temporally relevant

cultural complex, is collectively envisaged as the antithesis of local values and ideals. Because it is characterized by the wealth and tourism that are perceived to be the root of Fairplay's socioeconomic subordination, 'Breckenridge' as a geographic location is redefined as an entity with social agency and therefore a forum for rebellion. Popular bumper stickers and t-shirts sold in Fairplay and the neighboring town of Alma state, "don't Breckenridge my Fairplay," a sentiment further expressed through the repurposing of a popular bumper sticker picturing a burro next to the phrase "get your ass over the pass." In its original conception, the bumper sticker was a double entendre referencing the town's popular 'Burro Days,' an annual festival honoring the critical role burros played in the region's historic mining operations. A major component of the festival is the burro race, in which athletes paired with a trained burro run a 29-mile circular course from Fairplay to the top of Mosquito Pass, thereby getting their ass, over the pass. While a longstanding popular joke, the bumper sticker, and its meaning have been readapted within local cultural context to: (a) refer to the practice of Fairplay residents working in Breckenridge's tourism industry rushing back over Hoosier Pass to escape the part-time/ newcomer/tourist population; and (b) act as a not-too-subtle invitation for the part-time/ newcomer/tourist population to depart Fairplay by way of Hoosier Pass toward Breckenridge, or Kenosha Pass toward Denver.

Similarly, with an influx of in-migration and visitation from out-of-state residents, license plates constitute a core index for symbolic othering, and serve to communicate opposition to the perceived value system of the relevant state. The political climate associated with individual and group response to the pandemic served to reorient individuals into (often emotionally charged) liminoid spaces. In a study of suboptimal vaccination coverage, Sah *et al.* (2021) identified Florida and Texas as the primary progenitors of COVID-19 variants, a trend attributed to vaccination incidence below the national average. In a study of the psychological roots of vaccination resistance, Hornsey *et al.* (2018) dispel the assumption of vaccination resistance as a correlate to socioeconomic status or educational level. While

independent of education and socioeconomic status, a survey of 5323 participants across 24 countries yielded four primary traits observed among vaccine resistant individuals. In order of magnitude, antivaccination attitudes were highest among those who (1) were strong adherents to conspiratorial thinking; (2) were highly reactive and sensitive to perceived impingement on personal freedom; (3) reported high levels of sensitivity and disgust toward corporal pollution; and (4) had strong individualistic/hierarchical worldviews (*ibid*). Throughout the pandemic these traits organized cultural subsets, producing a gradient of personal and cultural identification often expressed along party lines. Voters in Texas and Florida supported increasingly exclusive legislation that served to formally and informally sanction infringement upon free speech, and the rights of immigrants, POC, women, and the LGBTQIA+ community. Anti-minority violence and sentiment became so dangerous in Florida, both domestic (NAACP 2023), and international (GCT 2023) travel warnings were issued categorically identifying Florida as 'dangerous' and warning against travel to the state. Similarly, the volume of recent legislative change in Texas targeting women's reproductive rights, freedom of speech, climate change, and LGBTQIA+ rights have informally designated the state as unsafe for a sphere of both residents and travelers (Pilkington 2023).

While formal advisories and the political climate warned against travel to Texas and Florida, Texas and Florida residents were among the top three states traveling to Colorado (Denver Travel Bureau 2022). While Park County skews conservative (56.9%), local sentiment toward Florida and Texas travelers suggests that the "local" versus part-time/newcomer/tourist population identity eclipses the importance of political identity. License plates serve as a conspicuous index for non-local visitors and the cultural value assigned to disparaging a state discerned from the homogeneity of disdain attached to referents. Owing to the depiction of two oranges on the Florida license plate, the pejorative phrase "double orange douche bags" is commonly conjured to refer to the vehicle's occupants, who are expected to drive below the posted speed limit, assert a dangerous monopoly on the road while viewing

the landscape, and pose a threat to pedestrians in fulfillment of their own vacationing needs. Similarly (while observably less imaginative) the phrase “juuuuuuust…fuck Texas,” or its variant “just…fuuuuuuck Texas” is a common response to Texas license plates, vehicles driving slowly in the left passing lane (used regardless of geographic origin), and large diesel trucks that “roll coal” (i.e. diesel trucks modified to intentionally emit dense black exhaust; used regardless of geographic location).

While seemingly gratuitous, continuity in application among and between users, and situational awareness in application of the phrases demonstrate social agency that transcends simple profanity. While simple in form, continuity in the application of the Texas referent demonstrates the unique use of phonemes to elevate the conspicuousness of the phrase, thereby serving to formalize its use as an ingroup marker between interlocuters. Using language modification observed among Cuna children playing word games, Sherzer (1970) demonstrates that rather than constitute an impoverished understanding of language models, the manipulation of phonemes represents a deep knowledge of linguistic tools and their manipulation, and the reflexivity of language. Webster (2018) expands on this in consideration of the effect of performance and phoneme manipulation on the translation and variable understanding of Navajo poetry. In one of many examples, Webster describes a poem in which the use of the sound -*chx*- -- achieved by the combination of the voiceless palatal affricate <ch> and a velar fricative <x> -- is used to create meaning in its performance. The combination results in a repetitive rhyme derived from the consonant cluster, however all forms of the consonant cluster employed in the poem can also appear in spoken and written discourse without the velar fricative <x>. This leads to the conclusion that -*chx*- is a critical expressive feature of the poem in the sound that it generates, but is not necessary in ‘proper’ form. This, Webster convincingly asserts, demonstrates the manner in which presentation yields insight into attitudes toward characters without changing semantico-referential meaning. Similarly, consistent application of the UH /ʌ/ vowel in “juuuuuuuuuuust” and “fuuuuuuuck” represent continuity among users and elevates the phrase from

simple profanity to intentional, stylized presentation designed to evoke deeper webs of narrative which serve to unify language communities and efficiently facilitate the sharing of more complex narratives.

7.3.3 The Impact of Environment on Culture

Fundamental differences in patterns of local culture attributed to mode of interaction with the local environment have been observed and documented between urban and rural Rockies cultural groups (Sibley 2002). Rural communities are associated with lower population density, homogeneity in language, culture, and customs, agriculture-based subsistence, close contact with nature, and slower means of communication (USDA 2019). Urban communities tend to embody the nature versus culture ethos, where the relationship between the individual and nature is largely limited to the taming of nature (e.g., cultivated landscapes and an emphasis placed on capitalist progress at the expense of the natural environment). In contrast to the nature/culture dominance model, Rolston (2008) argues that rather than eclipse the natural environment, the presence of urban focus (the zone where arts and achievement overshadow environment) exists in tandem with wild and spontaneous nature (the events that take place in the absence of humans) in rural communities. This paradox results in a synthetic or hybrid cultural configuration where both nature and culture are simultaneous foci. Nature is redirected into cultural channels, resulting in the embodiment of both paradigms. The result is a cultural group in both passive (embodied) and active (performative) but always dynamic engagement with nature. This has the effect of shaping local patterns of values and traditions, shared knowledge, symbolism, tool production and use, and political and social economy. In his search for the 'code of the West,' Sibley (2002) concludes that while elusive, the ethos of the rural west is centered upon a paradoxical relationship between individualism and community. Individualism is based on the expectation of hard work for individual and familial resources within the closed family unit. However, active engagement between community members is a necessity for surviving the harsh environment, facilitating bonds, and maintaining a cultural network across the rural landscape. The sum of these arguments is defined by

Ingold's (2000) environment perception theory, the thrust of which emphasizes the ongoing project of skill acquisition which serves to reorient an individual within an environment across time and space. In this framework, intracultural opposition creates novel opportunity for skill acquisition thereby yielding reorientation understood as spatially and temporally relevant cultural aptitude and catalyzing cultural change. Rather than constitute schismogenesis, seemingly paradoxical relationships between nature and culture, individual and community, constitute liminoid spaces within which change in proficiency and cultural configuration may occur. Because the 'raw data' (local cultural configuration and physical environment) are relevant, the output is a spatially, temporally, and geographically unique cultural configuration. Thus, rather than represent a community 'more aligned with nature' (and subsequently devoid of culture), rural Rocky Mountain communities represent a unique nature-culture relationship based on innovation performed within unique liminoid space.

This concept is reinforced by distinct linguistic differences observed between Rocky Mountain and Southwest populations, attributed to local environment and the impact of topographic boundaries. Holtkamp *et al.* (2018) assert that – while the Rocky Mountains and the Southwest are iconic American regions – their broader 'cultural knowledge' is largely limited to romanticized narratives created and perpetuated by popular media. As a result, the respective local culture of both regions remains relatively underexplored. Toward an understanding of cultural geography, a vernacular mapping approach was applied to investigate cultural distinction between Rocky Mountain and Southwest populations through language use. Just as Basso (1988) described the use of placenames by the Western Apache to evoke deeper webs of cultural narrative, Holtkamp *et al.* propose the application of vernacular mapping to display the spatial distribution of toponyms in order to assess their degree of regional and cultural distinction (2018). The results demonstrate that the distribution of culturally relevant feature names share a positive relationship with the Southwest and Rocky Mountain regions as defined by physiographic characteristics.

Locally, place-naming relies on geographic characteristics to reinforce the cultural boundaries that exist between local and newcomer populations. The landscape to the east of the Rockies is colloquially referred to as the "Great Plains," a region characterized by expansive flatlands and farming operations. In contrast to the capricious landscape that defines the Rocky Mountain region, the homogenous landscape to the east is regarded as 'simpler,' a characteristic symbolically bestowed upon associated newcomers and tourists. This sentiment is linguistically referenced through application of the phrase, "fucking flatlander," popularly applied by locals to out-of-region actors in response to a display of cultural incompetence, or a perceived slight, thereby using landscape to evoke a referential group characterized by incompetency within the environment. "Incompetency" is not a reference to a particular skillset, but rather serves to communicate a symbolic suite of characteristics that distinguish the "local" from the "newcomer" and their presumed incompetence within the local landscape antithetic to the eastern plains. Use of the phrase may be inverted and applied in jest when both interlocuters are local residents and one actor performs a minor cultural transgression, such as spilling a beer, or tripping while walking in the woods. Both the direct and inverted form serves to: (1) culturally orient interlocuters through a display of social and geographic competency derived from a shared understanding of the complex narrative imbued in the phrase; (2) politically and morally align the group through recognition of orientation, and agreement with it; and (3) communicate a complex narrative about the locally ascribed subordinate position of outsiders, characterized by shared frustration with the cultural, political, and economic change attributed to their presence, and the shared desire to rebel against that pressure.

7.3.4 *The Effect of Cannabis on Local Culture*

The 2012 passage of amendment 64 and subsequent legalization of marijuana in Colorado dramatically altered perceptions of drug use, regulation, tourism, and sociocultural transition. However, passage of amendment 64 was also a source of political ire and heavily debated along party lines. The

amendment passed with 55% voter support, largely attributed to an increase in younger, liberal voter turnout (Reed 2021). Colorado's rural, conservative, and aging populations largely maintain a stance of opposition to the legalization of marijuana; paradoxically, rural regions are highly correlated with illegal marijuana grows. The Colorado Bureau of Investigation's (CBI) Illicit Market Marijuana Team (IMMT) was established to identify and dismantle illegal grow operations and is foundationally focused on rural communities (*ibid*). When compared to urban regions, the rural regions of the Colorado Rockies demonstrate less approval of legalization, resistance to its economic benefits, uphold stricter regulatory laws for the cultivation and sale of marijuana, and advocate against marijuana tourism (Berman 2021). Resistance to marijuana growth is a case study in the tensions that arise between both longtime and in-migrating residents. The conservative, aged demographic, and closed community structure of Park County - where a cultural emphasis is placed on preserving existing values and way of life, limiting population growth, and concerned with the impact of economic development on quality of life – stand in stark contrast to the progressive legalization of once illicit substances (Smith & Krannich 2000).

While longtime residents hold (or are presumed to hold) a conservative stance on marijuana cultivation and sale, consideration of the cultural ethos surrounding marijuana along broader generational lines creates an increasingly complex picture. Fairplay is host to a small but prominent community of artists demographically consistent with longtime residents, but culturally and politically divergent from the population norm. Six miles north of Fairplay, the small town of Alma (North America's highest incorporated town) is an artist enclave with a population of 275. The town takes great pride in both its geographic and cultural distinction. Originally named after the local grocer's daughter, today the town seeks to align its name with the Spanish translation of Alma, meaning "soul" (townofalma.com 2023). The town's website boasts the unofficial motto "everyone is accepted as long as he accepts all in return," and the small community attracts a diverse population of both newcomers and longtime residents. In contrast to Park County's greater resistance to marijuana cultivation and sale,

the residents of Alma consented to legal marijuana sales on the first day of legislation enactment (Aguilar 2022). This stands in stark contrast to the "rural resistance," upheld by rural Colorado towns as recently as 2022, and hints at the structure of the region's outlier communities. Just as the "Hartsel Homeless" compose an 'invisible' fringe community, those in support of marijuana cultivation and sales further serve to demonstrate the cultural complexity of a region that has long been homogenized as 'rural and conservative.'

7.3.5 Predominant Land and Associated Modern Tool Use

Agriculture composes one of three primary zoning designations in Park County (parkco.us 2023). As such, modes of cultural capital and local patterns of tool use may be derived from the actions displayed and embodied by the agriculture community. Additionally, values and actions emphasized within agricultural communities serve to inform and better understand the increasingly complex local cultural configuration. In 2010, Park County Commissioners approved the passage of resolution number 30-2010, the *Right-to-farm and Ranch policy* (parkco.us 2023). The Right-to-farm and Ranch law was passed to protect farmers and ranchers from complaints and nuisance suits issued when agricultural activities encroached upon neighboring land. The catalyst for the bill was increasing concern over part-timers and newcomers asserting their value system upon the landscape with an emphasis placed on maintaining the romanticized purity of the land. Twelve years after the resolution's passage, the region's pride and economic emphasis on agriculture is 'writ large' across the landscape in the repetitive display of signage declaring Park County as "proud to be a right-to-farm and ranch county." The spatial repetition of this phrase represents more than a simple assertion of a subsistence pattern. The statement and its display acts as a form of resistance to increasing (assumed liberal) scrutiny of the environmental impact of farming and ranching operations. This further serves to assert the region's conservative values to the county's annual 640,000 visitors, and orient the core community as aligned through subsistence, practice, and belief.

From a practical perspective, agriculture is associated with a suite of tools with which a percentage of the population are presumed to own and demonstrate proficiency in use. The cattle and beef cow industry is the focus of agricultural practice in Park County (Meyer 2021). The foundation for understanding local allegiance to agriculture is easily located on the county's website, which unequivocally states that if you live next to a ranch, you should expect "noise from tractors, dust from animal pens, odor from animal confinement and manure, water seepage from irrigation, and use of herbicides and fertilizers" (parkco.us 2022). Cattle and beef cow ranching are associated with the ownership and operation of heavy equipment such as backhoes, tractors, plows, skid steer loaders, multi-terrain loaders, mini hydraulic excavators, off highway vehicles (OHVs), and all-terrain vehicles (ATVs). Less technical equipment includes livestock trailers, water supply systems, feeders, and manure spreaders. Ranches are typically associated with additional livestock, with an emphasis placed on dogs and horses to aid in the demands associated with pasture transfer, cattle rounding, and tracking herd strays. Outside of the ranch, agriculture-centric activities such as the annual Park County Fair and Stock show are highly anticipated and heavily attended. These events spatially monopolize the county seat and serve to collectivize the community and informally maintain a cultural orientation toward agriculture-based value practice.

7.3.6 Local Recreation

Local recreation informs patterns of land use both among the local population, and the transient tourist population. The greatest landmass in Park County is zoned as conservation and recreation (federal and state parks). The county has more territory above 9000 feet than any other county in the state making it a unique destination for recreationists. The rugged and diverse landscape attracts more than 650,000 visitors a year and informs habitual land use patterns among residents. Camping and hiking attract crowds that tend to recreate along well-established trails and within established or often used campgrounds (Powell & Mitchell 2012). Primitive camping is permitted within State and National

Forests where site stays of up to 14-days are sanctioned. Though not always competent to do so, those willing to venture deeper into National and State parks tend to engage in more extreme wilderness activities. Backpacking, rock climbing, rappelling, bouldering, caving, winter camping, ice camping, ice climbing, snow machining, and distance snowshoeing/backpacking is a short list of activities popular in backcountry engagement. Just as the vastness of the landscape fosters unconventional housing, it supports habitual but transient site use by those familiar with the wilderness.

As previously demonstrated, in addition to its primary roadway infrastructure, NFS provides seven road designations within the county and a complex mapping system to facilitate their use. Among the designations are trails open to vehicles 50" or less in width. Off highway vehicles and all-terrain vehicles are popular among both residents and visitors and comprise the greatest percentage of vehicle thefts within the county (Park County Sheriff's Office Detective Wendy Kipple, personal communication). The NFS mapping system presents a complex system of trails, many characterized by passage limited to ATVs. The United States Forest Service and Department of Agriculture provide periodic regional statistics on the demographics of ATV use (Topping *et al.* 2021). The most recent study demonstrates that: (1) the western region (defined in the study as Arizona, Colorado, Idaho, Montana, Nevada, New Mexico, Utah, and Wyoming) has an exponentially larger population of ATV users than the North, South, Midwest, and Pacific regions; and (2) Colorado's OHV/ATV rider participant population is among the top ten states in the country. Figure 7-5 presents the OHV/ATV participant population by state and highlights regional distinction in OHV/ATV use. Despite the disproportionate population of OHV/ATV riders in the state, and despite the complex, rugged, and vast terrain in the region, the Consumer Product Safety Commission (CPSC) reports that Colorado is number 28 of the 50 states reporting cases of injury and death sustained throughout the course of ATV use (2021). This lack of injury statistic suggests proficiency in use is proportionately greater than the at-risk population – although failure to report cannot be discounted.

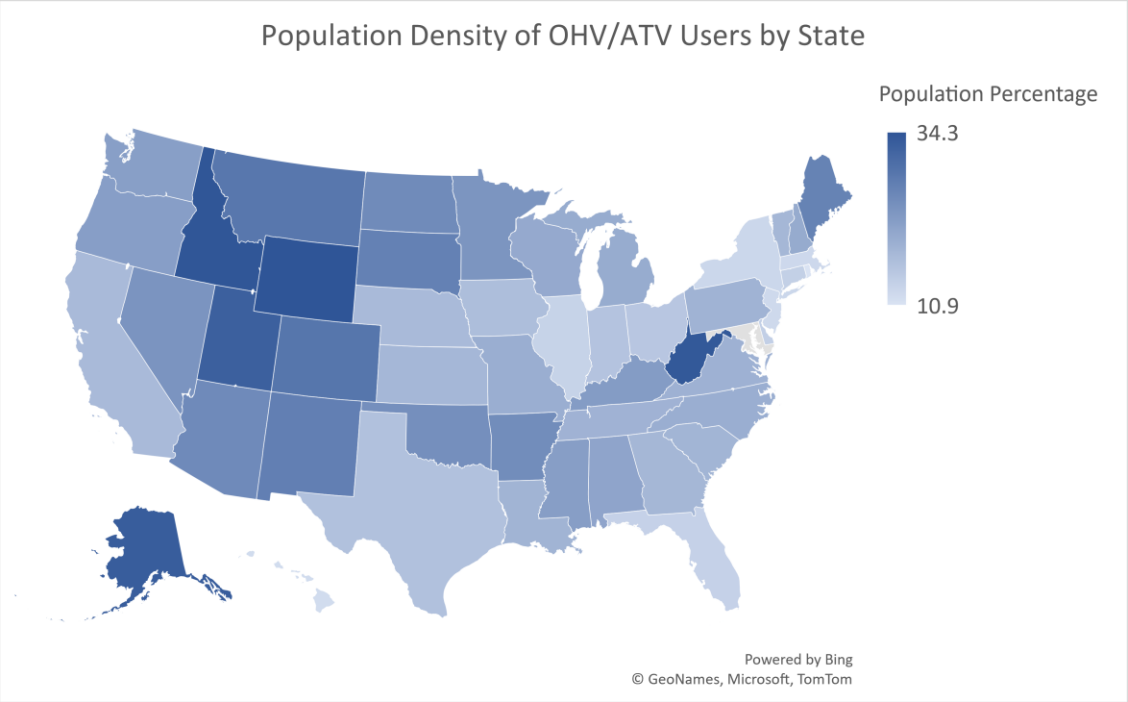

Figure 7-5: Heat map depicting the percentage of OHV/ATV users by state. Note the disproportionate population use density in the Western Region - defined as Arizona, Colorado, Idaho, Montana, Nevada, New Mexico, Utah, and Wyoming (based on data provided by Topping *et al.* 2021).

An equally if not more popular form of summer recreation exploits the region's five artificial waterways. The 2021 Park County profile reports that the county's five storage reservoirs (Antero, Eleven Mile, Tarryall, Spinney, and Montgomery) are important wildlife and aquatic recreation areas that attract more than 500,000 people every year. The waterways are popular fishing, boating, camping, and wildlife viewing areas but are a seasonal attraction; visitor density is greatest in the spring and summer and sites are frequented by both local and tourist populations.

In the fall, the landscape is monopolized by an influx of local and visiting hunters. Hunting is authorized by permit only; the type of animal hunted, the region hunted, and the type of projectile used are established and policed in accordance with a five-year schedule issued by Colorado Parks and Wildlife (2022). For example, deer and elk hunting is permitted in the I25 and GMU 140 region by archery (September 1-September 30), and muzzle loader (September 9 – September 17). In the plains region they may be hunted by archery (October 1 – December 31), muzzleloader (the second Saturday in

October for nine days following), and rifle (the Saturday of the last full weekend of October and run for 11 days). Elk, moose, pronghorn, mountain lion, and black bear hunting seasons all follow the same specificity in weapon type, and season. Hunting season affects seasonal mobility and land use, both among the local and visiting populations. The local population (both hunters and non) are privy to the zones most highly exploited by permitted and illegal hunters. Local recreation is curbed, and patterns of land use altered by the presence of the large hunting population. Colorado is an open carry state, and within the top ten states with the highest percentage of concealed carry permit holders, Colorado is number seven (USCCA 2022). While firearms are a familiar site within the county, some firearms owners capitalize on the fall firearm traffic and establish shooting ranges on private property, an act informally sanctioned, "as long as people are responsible" (Sheriff Tom McGraw, personal communication). Summarily, local residents become reticent to enter the environment, and uncalculated risks may be unintentionally taken by those unfamiliar with the landscape.

7.4 *Results: Case Studies*

Seven case studies meeting the study criteria were randomly culled from the PCCO case repository. All cases presented have been resolved through investigation and when relevant, litigation. Cases are presented in random order; names have been redacted and biodemographic data reported do not extend beyond the data reported in Coroner press releases and in the media. The specific case year has intentionally been obscured. A summary of the informant type (individual reporting the presence of a decedent), the month of discovery, cause and manner of death, and a brief site description are presented in Table 7-2.

7.4.1 *Case Study #1*

Manner of death: Homicide

Cause of death: Multiple postcranial gunshot wounds (GSW)

Decedent biodemographics: 45-year-old white male

Identification method: DNA

Description of remains: Partial skeletal remains (cranium, mandible, first cervical vertebra).

Reporting Party: Hiker

Month of discovery: July

In July, a recently hired off-duty Department of Wildlife Officer embarked on a "random," off trail hike. This hike was part of a series he had undertaken throughout the county to familiarize himself with - and increase proficiency in - the local landscape. While climbing a steep slope, he observed what appeared to be human bone (Figure 7-6). PCCO responded and determined that the skeletal remains were human. Subsequent osteological analysis identified the subject as an adult white male and identified perimortem fracture in both the cranial base, and in the first cervical vertebra, both highly suggestive of traumatic injury.

The deposition site was approximately two miles from the closest county road. Skeletal elements were located within a 200-yard scatter on a moderate to steep slope. A 5.5-acre area line search was undertaken by 15 search team members, including members of the Park County Sheriff's Office (PCSO), PCCO, Park County Search and Rescue (PCSAR), Colorado Forensic Canines (CFC), and two forensic anthropologists. Two packrat middens were located during the search and were deemed of investigative interest due to the rodent group's well documented proclivity for incorporating skeletal remains into their nests. In this case, neither midden yielded any additional skeletal remains. Two swatches of denim fabric were recovered from two rodent holes unrelated to the middens.

The subject was identified through DNA analysis and a brother was identified and located in an out-of-county city. An investigative interview revealed that the brother (now suspect) had a complex and often violent relationship with his family. It was further revealed that when the brothers were young, the family often spent time hunting and fishing in the wilderness area where the skeletal remains were recovered. An investigation of the suspect ensued, resulting in his eventual arrest. While incarcerated in county jail, the District Attorney's Office offered a plea deal in exchange for a confession. Under the terms of the plea, the suspect admitted to shooting the decedent multiple times in the chest, dismembering the body, and disposing of the head in the wilderness area of discovery. The postcranial body was disposed of at a second, out-of-county site, approximately 70 miles southwest of the cranium's deposition site, in an outdoor area proximal to the suspect's home. Subsequent searches of the identified area were unsuccessful, and the postcranial remains were never recovered.

Figure 7-6: Left - Overview of landscape; **Right -** human cranium *in situ*.

7.4.2 *Case Study #2*

Manner of death: Accidental

Cause of death: “Undetermined due to backcountry circumstances.”

Decedent biodemographics: 43-year-old white male

Identification method: DNA

Description of remains: Body in advanced state of decomposition

Reporting Party: Search and Rescue Hiker

Month of discovery: July

In July, Park County Dispatch received a call regarding a missing party who had reportedly traveled from the Denver Metro Area to rock climb in the Lost Creek Wilderness area. The Lost Creek Wilderness is characterized by extremely steep and rugged terrain composed of dramatic rock spires, boulders the size of a single-family residence, and jagged granite outcroppings (Figure 7-7). When the subject failed to return at the expected time, friends became concerned and filed a report with the PCSO. Approximately one month after the report was filed, in one of many search missions undertaken in the case, a PCSAR team converged on an area where the subject was suspected to have been climbing. Upon detecting the scent of decomposition, one PCSAR member broke from the team. The PCSAR member – described as “a hardcore outdoorsman” - traveled four miles from the defined search area to locate the scent source. Upon reaching the source area, massive boulders occluded line of site, however a small cave entrance was located and identified as the source of the scent. The cave was located at the site where the “Lost Creek,” diverts subterraneously and traverses a series of geological formations of unknown path and distance. The depth of the cave was unknown and was crosscut by the underground river. The subject’s body was observed on a sandbar located on the opposite side of the river from the cave entrance. Advanced decomposition and prolific maggot activity were observed (Figure 7-8).

PCCO deployed the following day, supported by three regionally local law enforcement agencies, two search and rescue teams, and 11 horses used to transport equipment and carry key recovery team personnel (Figure 7-7). During the eight-hour hike across steep and treacherous terrain, three members of the search team sustained injuries sufficient to necessitate their return to the staging area; one member required hospitalization as the result of a fractured fibula. One horse was fatally injured. Upon reaching the site, it was determined that the unknown depth of the cave and the high potential for the river to possess a dangerous undercurrent made ingress through the cave entrance too dangerous. A point of entry was identified in the roof of the cave, and two SAR members rappelled 40-feet to the base of the cave. The safest landing site did not allow access to the decedent and the SAR members were forced to ascend. It was determined that recovery would require two rescue team members to climb into the four-feet-deep water with unknown current while negotiating a low jagged granite ceiling. The SAR captains from both agencies advised that recovery was too dangerous and would require special equipment not present on scene. A SAR team member and cave system expert advised that the danger associated with recovery outweighed the necessity.

A field solution was devised to mitigate the danger presented to the recovery team and satisfy the necessity for the decedent's scientific identification. A tissue sampling device was fashioned from a sterile surgical blade affixed to a five-foot pole. The pole was extended over the river and a tissue sample was collected to facilitate a positive identification via DNA testing. DNA results confirmed the identity of the missing rock climber. The family was notified and advised of the danger associated with recovery. They declined to put any member of SAR in danger and expressed their support of the decedent remaining in his "natural tomb," within the wilderness that he loved.

This resolution was short lived – shortly after the decision was made for the subject to remain in the wilderness, a privately funded "extreme recovery team," contacted PCCO and asserted their ability to perform the dangerous recovery. After scouting the site, a team of four recovery specialists were

transported via helicopter. Upon arrival, the pilot rested one skid on a tall granite spire and team members disembarked the aircraft onto a small platform at the apex of the spire. A 45 meter line was dropped and recovery team members and a cargo net containing equipment were individually transported via longline to the body recovery site. The team donned full body dry suits and used webbing to maneuver the decedent onto the sandbar, where he was transferred to a mesh water bag, floated across the water, and maneuvered out of the cave. Following successful recovery, the decedent was affixed to the longline and flown to the closest major road, where PCCO took possession of the body. Autopsy did not reveal injury sufficient to determine cause of death. Manner of death was designated as accidental; cause of death was "undetermined due to backcountry circumstances." The decedent was released to his family for final disposition following autopsy.

Figure 7-7: Left - Overview of landscape; **Right -** packhorses carrying equipment to the remote scene.

Figure 7-8: Left - Overview of cave entrance among boulders (indicated by arrow); **Right -** detail of cave entrance through which the body was visible but unreachable.

7.4.3 *Case Study #3:*

Manner of death: Suicide

Cause of death: Alcohol and oxycodone toxicity

Decedent biodemographics: 33-year-old white male

Identification method: Fingerprints

Description of remains: Body in advanced state of decomposition with extensive animal scavenging.

Reporting Party: Hikers

Month of discovery: July

In July, a group of campers departed their campsite in anticipation of a remote, backcountry hike. Approximately one-hour into their hike, the group observed a small campsite on a distant ridge. They proceeded in the general direction of the site with no intention of approaching the encampment. Upon reaching a distance sufficient for observation of the details of the encampment, a tent was noted to be partially collapsed and the site in a general state of disarray. Concerned for the safety of the camper, the hikers approached and observed the partially scavenged remains of an adult male in an advanced state of decomposition (Figure 7-9).

Park County Dispatch was alerted and PCCO deployed to the scene. Upon arrival, a collapsible two-rod arch-bow system tent was observed. Both rods were splintered, undermining the structural integrity of the tent, resulting in its partial collapse. The decedent was observed three meters from the entrance of the tent. Advanced decomposition was characterized by loss of tissue composition, adipocere formation, and residual evidence of vibrant maroon and orange tissue discoloration in the thorax and limbs. The right leg was largely devoid of tissue and bear scat was present in the immediate vicinity, indicating the presence of a scavenging black bear (*Ursus americanus*; Figure 7-9).

The coroner's report noted that the campsite overlooked "an idyllic mountain scene" (Figure 7-10). The tent contained two one-liter bottles of whisky, each partially consumed, a vape pen, wallet,

utility knife, cellphone/battery/charger, an airsoft pellet gun with pellets, a cooking kit, shovel, hammer, first aid kit, camp stove, iodine tablets, coffee pot, and a notebook containing passages conveying suicidal ideation, depression, and life regrets.

A presumptive identification was made using a driver's license located in the decedent's wallet; identification was scientifically confirmed by fingerprints. The decedent was identified as a man from the eastern plains of Colorado, reported missing three months prior to his recovery.

Figure 7-9: Left - Relationship between decedent (indicated by arrows) and collapsed tent; **Right -** detail of decedent presenting advanced decomposition and bear scavenging of right leg.

Figure 7-10: View from the decedent's tent, described in the coroner's report as "an idyllic mountain scene."

2.4.4 *Case Study #4*

Manner of death: Accidental

Cause of death: hypothermia following accidental fall

Decedent biodemographics: 75-year-old white female

Identification method: Fingerprints

Description of remains: Fresh/very early decomposition

Reporting Party: Search and Rescue

Month of discovery: August

In August, a 75-year-old woman and her long-time 85-year-old hiking and camping companion embarked on a hike to a remote, moderately wooded campsite in the Lost Creek Wilderness area of Park County. The pair frequented the site, reportedly camping at this location for days at a time across numerous trips. Carved benches, a tent pad, hummingbird feeders and suet cage, hanging canvas storage bags, and permanent equipment lines fashioned from tree branches indicated habitual site use. The site was noted to be exceptionally clean; no trash or debris were present. Homogeneity of ground surface duff was suggestive of focused site curation. The subject's companion was described as "fastidious about nature," and insistent that it be kept "intact and untouched" (Figure 7-11).

Figure 7-11: Left - Overview of local landscape, note the series of large and complex rock outcroppings. **Right -** overview of the couple's curated campsite, note hummingbird feeders in foreground, hanging blue canvas bags, and tent pad delineated by green rolled up tarps.

As the pair approached the site, the subject expressed physical discomfort and stated that she needed to stop and rest. She encouraged her companion to proceed to camp to begin setting up. Those close to her described her as an avid hiker in excellent physical condition, so her request for a brief rest was not regarded as cause for concern. Despite her excellent physical condition, “memory issues,” were reported by case informants. Despite cognitive decline, she was compliant with her pharmaceutical regimen and her condition was regarded as mild. When she failed to reach camp within the time expected, her companion returned to her last location, but she was no longer present. He searched the area but was unable to locate her. Due to the remote location of the site, the lack of cellular service, and concern that the subject may have injured herself and would return to find an empty camp, he made the decision to spend the night in their encampment, with the hope that she would return.

When she failed to return by the following morning, her companion packed out of the site and hiked until he reached an area of cellular service, enabling him to report her missing and request emergency services. PCSAR and the subject’s son responded to the scene. After a brief search, the subject was located approximately 30 meters from the campsite. She had sustained a 10 meter fall into a boulder lined ravine following an apparent attempt to drink from an adjacent river (Figure 7-12). Her companion had expressed concern over her approaching the river in the past due to the steep embankment, slippery rocks, and high flow rate. His concern was sufficient to result in him “banning her" from water collection while they camped. The decedent was wedged in a partially flexed position between granite boulders at the base of the ravine. She was unclothed with the exception of a pair of jean shorts pushed down to her ankles. Descent into the ravine was considered too treacherous to be undertaken by the PCSAR team. However, dissenting members made the decision to rappel into the ravine and attempt recovery. The mission was successful; the decedent was wrapped in a heavy nylon recovery net and lifted to ground level by a block and tackle pully system manually hoisted by PCSAR team members. She was then airlifted from the site via helicopter and longline and transferred to the

coroner at the closest accessible trailhead (Figure 7-13). Autopsy failed to uncover traumatic injury sufficient to explain cause of death. Death was attributed to hypothermia following an accidental fall.

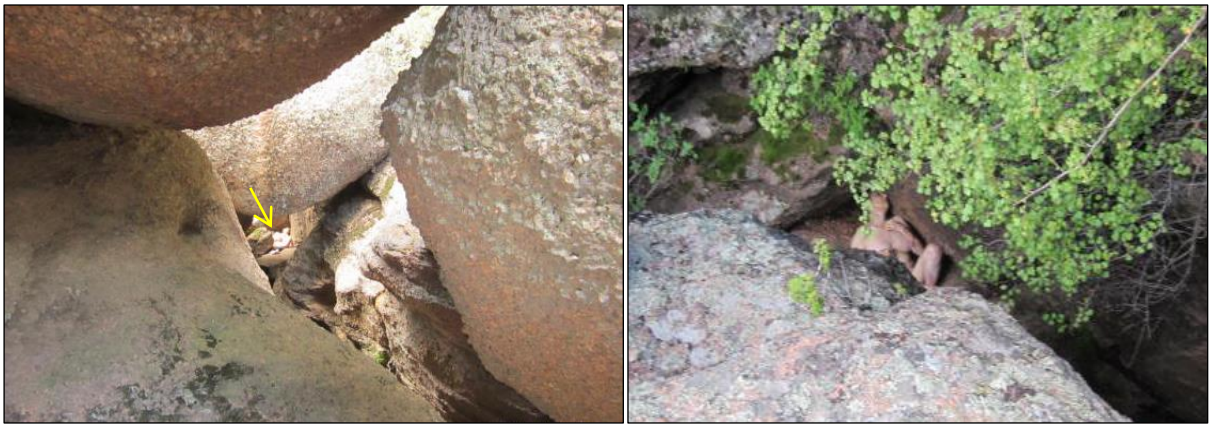

Figure 7-12: Left - Overview of boulder lined ravine into which the decedent sustained a 10 meter fall (decedent indicated by arrow); **Right -** detail of decedent *in situ*.

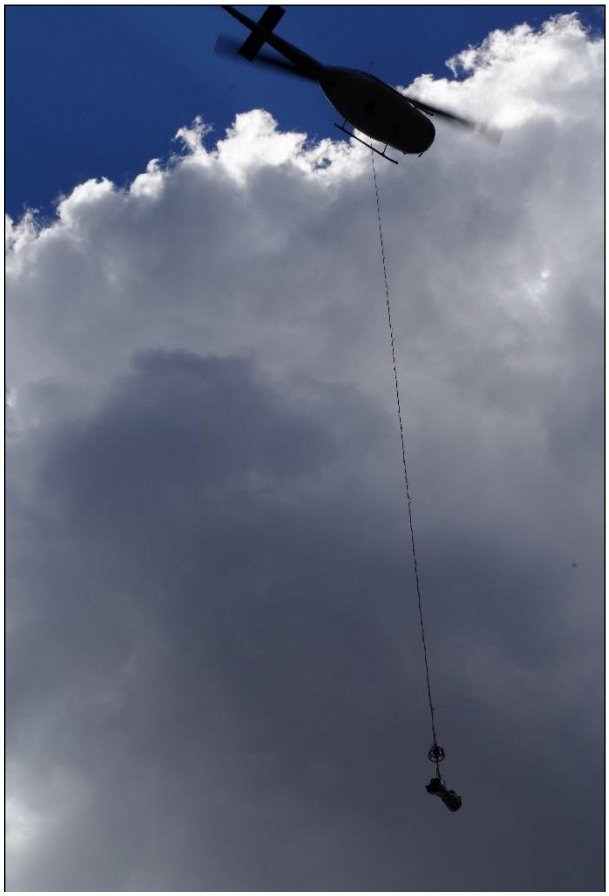

Figure 7-13: Removal of decedent from rock ravine via helicopter and longline, demonstrating the danger and complexity associated with backcountry field recovery.

2.4.5 *Case Study #5*

Manner of death: Suicide

Cause of death: Massive head trauma following GSW to face

Decedent biodemographics: 61-year-old white male

Identification method: DNA

Description of remains: Skeletonization with extensive animal scavenging and skeletal displacement.

Reporting Party: Mushroom hunter

Month of discovery: August

In August, a mycophile hunting in a remote location of National Forest Service land happened upon what appeared to be a partially concealed shelter. Upon closer investigation, he observed what he believed to be human bone scatter. He notified Park County Dispatch; PCSO and PCCO responded to the scene. Upon arrival, a bunker was observed. The bottom 125 centimeters of the structure were subterraneously sunken into a hand excavated pit. The top 60 centimeters of the structure consisted of hand-hewn log walls and a sloped log roof covered with a tarp, soil, and tree boughs (Figure 7-14). The slope of the roof met a log door wrapped in trash bags. Inside the shelter, vertical log walls were lined with foil emergency blankets and hand-hewn shelves containing personal items (Figure 7-14). An adjacent subterraneous structure composed of small logs contained three Everlast batteries wired together and attached to an inverter and a solar box; two solar panels were subsequently located six meters upslope (Figure 7-15). Several personal items, including preserved food, clothing, a 410 shotgun, air rifle, .22 rifle, flare gun, crossbow, pelican case of ammunition, and rocket motor with fuse altered to explode were located within the shelter. The renewable power source, shelter floor plan, and the sum of material contents within suggested fulltime occupancy.

The interior of the shelter had been ransacked; bear scat, packrat scat, and packrat nests were observed throughout (Figure 7-16). The outdoor scene was characterized by a heavily wooded landscape

and defined by the approximate 100 meter x 100 meter scatter of heavily scavenged human skeletal remains (Figure 7-17). Additionally, highly fragmentary human remains were located inside of the shelter within the top layer of disturbed soil, and within packrat nests (Figure 7-18). An aggregate of small cranial bone fragments was identified in proximity to the east wall, which contained a now dry, unknown liquid substance, the color and morphology of which were consistent with high-velocity blood spatter.

Paperwork containing information with the potential to inform decedent identity, and a functional, late-model cellphone were located while sifting topsoil within the shelter. Analysis of the cellphone's data indicated that all incoming phone calls were sent to voicemail, then batch reviewed once every two weeks. A text message sent by the subject in October stated, "I'm going off grid," to which the recipient responded, "which grid?" The subject did not respond and the exchange ceased. The cellphone was last used in November of the same year. The lead provided by the paperwork in the shelter directed investigators to family members, who had not had contact with the decedent in over five years. A comparison of familial and decedent DNA yielded a positive match. Subsequent osteological analysis identified the cause of death as high-velocity projectile trauma to the anterior cranium. Manner of death was suicide.

Figure 7-14: Left - Exterior of partially subterraneous, hand-hewn log structure. Note the entrance (photo left), and the earthen mound occluding the structure's visibility (photo right). **Right -** Interior backwall of the structure (following removal of personal items and items of evidence), note hand-hewn log ceiling and wall with subterraneous, hand excavated extension. Personal protective equipment was donned due to the volume of rodent scat.

Figure 7-15: Subterraneous power source composed of log frame and hatch wrapped in tarp containing three Everlast batteries wired together and attached to inverter and a solar box. Two solar panels were subsequently located six meters upslope.

Figure 7-16: Left - Overview of landscape which served to further camouflage the log structure; **Right -** partial extent of exterior skeletal scatter, indicated by blue and pink pin flags.

Figure 7-17: Left - Interior of shelter prior to removal of personal items and items of evidence, note hand hewn cot, foil wrapped walls, numerous personal items, and disarray caused by large-bodied scavenger; **Right -** interior of shelter facing entrance following removal of personal items and items of evidence, note organization of interior infrastructure and one of many small shelves built to hold personal items.

Figure 7-18: **Left -** Skeletal remains recovered from base of interior east wall, note highly fragmentary nature, attributed to high-velocity projectile trauma and rodent scavenging; **Right -** detail of cranial fragments presenting rodent scavenging, variably nested in layered, dense packrat scat.

7.4.6 *Case Study #6*

Manner of death: Homicide

Cause of death: Massive projectile trauma to posterior cranium

Decedent biodemographics: 29-year-old white male

Identification method: DNA

Description of remains: Advanced decomposition, partial skeletonization

Reporting Party: Anonymous informant

Month of discovery: August

In August, an informant contacted PCSO with an anonymous tip stating that his girlfriend - heavily under the influence of alcohol - had recently confessed to the murder and burial of an ex-boyfriend. While recounting the story, the suspect identified her brother as the shooter. When questioned, the siblings confessed. Despite their confession, the two maintained that the shooting occurred in self-defense as the victim attempted to force entry into the late model Winnebago the three shared on a rural property outside of Fairplay. The decedent was reportedly buried adjacent to the Winnebago after sustaining two gunshot wounds to the head. Following the incident, the siblings vacated the rural property and departed Fairplay to stay with friends and family in the Denver Metro Area. However, citing their fear of the grave's shallow depth and subsequent disinterment by scavengers, the pair returned to the scene within the week to excavate the grave. Following disinterment from the primary burial site, a secondary grave was hand excavated to a reported one meter depth. The suspects directed PCSO Detectives to the burial site and anthropologist response was requested.

Upon scene arrival, the Winnebago was found to be inhabited by packrats and in an advanced state of disrepair. The reported burial site crosscut an approximate 35˚ slope; the overlying matrices appeared undisturbed (Figure 7-19). Three downed and partially decomposed logs were placed parallel

to one another at surface level, overlying the interment site. Excavation began in the compact, clay based, granite dense matrices and proceeded slowly due to the logistical problems associated with excavating difficult substrate on a steep slope. After two days of excavation, the reported one meter grave depth was reached; no physical or environmental evidence for interment was observed (Figure 7-20). The female suspect was escorted to the scene for questioning; when faced with the excavation, she began to cry and advised investigators that they "had to dig deeper."

Due to the practical difficulty associated with excavation, doubt began to grow among investigators that an individual would be capable of manually excavating a grave beyond the reported one-meter depth. As a result, the decision was made to proceed with a backhoe. The exhumation site was expanded to a five meter by five meter area; anthropologists sighted the excavation bucket from two different vantage points as excavation progressed (Figure 7-21). After three hours of excavation, doubt surrounding the grave depth continued to grow. Sunset approached and the decision was made to cease operations based on the presumption that the informants were mistaken, or were lying about the gravesite location. Shortly after the decision was made, the backhoe unearthed the toe of a boot (Figure 7-22). Hand excavation resumed the following morning. Stratigraphic excavation to a two meter depth revealed the decedent lying in a flexed position on the frost line (Figure 7-23). The remains were heavily saponified but maintained circumscribed areas of tissue presenting a vibrant orange discoloration. The male suspect subsequently admitted to using methamphetamines and a pickaxe to manually excavate the deep grave across the span of a week. Autopsy revealed two gunshot wounds to the back of the head, contradicting the claim of self-defense. Both brother and sister were tried and convicted of murder.

Figure 7-19: Left - Overview of the scene environment and the slope within which the decedent was buried; **Right -** example of the Winnebago (non-traditional housing) the suspects shared with the decedent on the remote scene. The Winnebago was found to be inhabited by packrats at the time of scene investigation.

Figure 7-20: Left - Hand excavation of suspected grave area through one-meter of compact, granite-dense matrix; **Right -** example of granite density in upturned matrix.

Figure 7-21: Left - Backhoe negotiating the steep landscape after requested by anthropologists to excavate the difficult terrain. **Right -** excavation of what would expand to a 5m x 5m exhumation site. Note size and density of granite occlusions.

Figure 7-22: Left – Sole of boot (yellow circle) approximately two-meters below surface level within the 5m x 5m exhumation site. **Right -** Hand excavation revealed a second boot and the contour of a body in flexed position.

Figure 7-23: Left - Full body contour and body position revealed following hand excavation; note vibrant orange discoloration of calotte (yellow circle) and adipocere aggregate (yellow arrow). **Right -** removal of the decedent revealed heavily saponified remains and additional vibrant orange discoloration of the frontal region (yellow arrow).

7.4.7 *Case Study #7*

Manner of death: Suicide

Cause of death: Mechanical asphyxiation by hanging

Decedent biodemographics: 19-year-old white male

Identification method: DNA

Description of remains: Waxy desiccation/partial skeletonization.

Reporting Party: Off trail hiker

Month of discovery: May and July

In May, a class of second graders accompanied by two teachers and their school principal embarked on a hike along the Colorado Trail. As the group followed the trail, they came upon what appeared to be a skeletal human arm with residual soft tissue, scavenged scapula, clavicle, and hand articulated (Figure 7-24). The PCCO responded and requested anthropologist support. The arm was identified as human. Despite disarticulation from the body, the bones presented relatively little evidence of scavenger behavior. Subsequent area searches failed to yield additional human remains.

In July of the same year, a couple was hiking a remote section of the Colorado Trail approximately three kilometers from the site of the recovered arm. An argument caused the male party to venture off trail. Because he was wearing homemade moccasins that made it difficult to traverse the rugged terrain, the male party traveled a series of game trails until he happened upon the heavily scavenged, desiccated, and partially skeletonized remains of a young adult male. Upon discovery, he "began screaming," for his girlfriend, who guided the pair back to the trail. Park County Dispatch was alerted following the couple's return to cellular service range; PCCO responded.

Despite the remote location of their hike, the couple was not carrying any form of navigational equipment, necessitating that they lead responders to the recovery site. Despite the circumstance, the couple continued to argue, detracting from their ability to focus as they led investigators to the scene.

Fortunately, the pair had the foresight to mark the area where they broke trail with a cairn. A series of game trails were followed without the couple's direction until the decedent was located. Upon scene arrival, the responding deputy observed the decedent lying supine at surface level with a ligature around the neck (Figure 7-25). The opposing end of the rope was knotted around a small, one kilogram rock used to wrap the rope around an overhead tree branch (Figure 7-26). The body was partially skeletal but maintained tissue in the legs, feet, and cranium, and a head of long blond hair. The left arm was missing postmortem. The remaining soft-tissue was characterized by interstitial adipocere formation, waxy desiccation, and umber discoloration (Figure 7-27). Inactive maggots were affixed to ceraceous tissue that presented latticing consistent with larval consumption. Due to the remote location and difficulty of the terrain, it was not logistically possible to carry the decedent out of the park. The narrow width and complexity of the trail would not allow passage of a full-sized vehicle, necessitating transport by ATV. A team of operators deployed on two ATVs. The lead ATV carried a driver and a trail sighter, the second ATV carried a driver, the deputy coroner, and the decedent.

In October of the previous year, a 19-year-old male was reported missing after leaving his home in Nebraska following an argument with his parents. The decedent was subsequently traced to the Denver Metro Area using credit card data, where he was observed on surveillance camera purchasing a backpack, rope, and basic outdoor supplies. The following spring, his car was discovered in a trailhead parking lot. A cellphone recovered from the vehicle contained an unsent text message, the contents of which read like a suicide note. Based on his distinctive long blond hair, the decedent was presumptively matched to this missing person report. A comparison of familial and decedent DNA yielded a positive identification.

Figure 7-24: Left - Overview of human arm recovered from a length of the Colorado Trail (indicated by yellow pin flag). **Right –** Coroner photograph of arm with residual soft tissue, scavenged scapula, clavicle, and hand articulated.

Figure 7-25: Left – Scene overview. **Right –** Overview of decedent *in situ*.

Figure 7-26: Left - Overview of rope wrapped around overhead tree branch. **Right –** Coroner photograph of rock knotted with rope, cut during investigation to preserve the knot.

Figure 7-27: Left – Detail of heavily scavenged thorax; note cervical ligature, absence of left arm, and retention of ceraceous cranial tissue and long blond hair. **Right –** Ceraceous decomposition island following body removal.

Table 7-2: Summary of case study data by case study number, informant type, suspected month of death, month of discovery, manner of death (MOD), cause of death (COD), and a brief summary of site details.

Study ID	Informant	Month of Death	Discovered	MOD	COD	Site Details
Study 1	Hiker	May, prior year	July	Homicide	GSW to chest	Backcountry slope - off trail
Study 2	SAR	June	July	Accidental	Backcountry circumstances	Backcountry cave - off trail
Study 3	Hiker	April	July	Suicide	Alcohol and oxycodone toxicity	Backcountry camping
Study 4	SAR	August	August	Accidental	Hypothermia following a fall from a height	Backcountry camping
Study 5	Mycophile	November	August	Suicide	Massive head trauma following GSW to face	Backcountry - non-traditional dwelling.
Study 6	Anonymous	May, prior year	August	Homicide	Massive head trauma following two GSWs to posterior cranium	Burial on private property - non-traditional dwelling
Study 7	Hiker	September, prior year	July	Suicide	Mechanical asphyxiation	Backcountry grove of trees – off trail

7.5 Conclusion

A four-point approach to integrating local modes of human behavior into the forensic ecological profile was undertaken in this study. These data divisions included: (1) census data; (2) land use data; (3) ethnography; and (4) case study. Census data revealed a population primarily composed of older, white, conservative, males with a higher than state- and national-average veteran population. Housing data demonstrate that 49% of the county's housing is vacant. Rather than denote non-occupancy, these data are reflective of the region's post-COVID surge in real estate investment. This surge has failed to benefit the local community, as investment has largely been made in pursuit of short-term vacation rental ventures. This discrepancy has resulted in a local housing crisis that has served to create tension between longtime residents, newcomers, and short-term visitors.

Land use data demonstrate that housing is tertiary to the county's overall zoning infrastructure. Primary is designation of 59% of the region as federal and state land, followed by agricultural use, and residential zoning, respectively. Cursory consideration of the county's transportation infrastructure reveals a simple framework of three state highways bisected by county roads. However, consideration of National Forest Service roadway designations reveals a complex infrastructure of roadways governed by seasonality and vehicle type. This complex infrastructure variably yields access to the county, based on user experience and degree of familiarity with local landscape. Cultural patterns of road use further inform the complexity of relationships between longtime residents, newcomers, and short-term visitors as social tensions are enacted through symbolic use of the highway.

Six cultural trends, including: (1) racial disparity in recreational land use; (2) variation in culture observed between longtime and incoming residents; (3) the impact of environment on culture; (4) the effect of cannabis on local culture; (5) predominant land and modern tool use; and (6) local recreation were isolated using extant ethnographic study. Summarily, these categories give structure to the county's transient tourist population, provide deeper insight into intra-community sociocultural

infrastructure, and inform modes of in group signaling. Finally, a subset of the Park County Coroner's Office case data were sampled. These cases serve to supplement the practical data lost in empirical, controlled study. Summarily, the four-point integration approach served to broadly inform the structure of local cultural mimesis, although future study will benefit from a more precise integration model.

CHAPTER 8

DISCUSSION AND CONCLUSION

8.0 *Quantitative Analysis: Tests for Reliability*

Intraobserver error was assessed using Spearman rank correlation and demonstrated a strong positive correlation between the originally assigned TBS, and the subsequently rescored TBS ($r_s(8) = 0.85$, $p = 0.004$). Conversly, interobserver error – assessed among fifteen observers using Krippendorff's alpha – demonstarted minimal agreement among observers ($\alpha = 0.26$, $p = 0.0001$). These results are contrary to those presented by Dabbs *et al.* (2017). In a study conducted among sixteen observers, the authors assessed application of the TBS model to digital color photographs substituted for *in situ* field observation of human decomposition. Concordance in TBS assignment was high among observers, indictating that digital images are an appropriate substitute for field observation, when necessary. The difference in outcome between the two studies may be attributable to several factors. While the structure of the study cohorts were similar (experience level beginner/intermediate/advanced, and education level Bachelor's/Master's/PhD), the Dabbs *et al.* study cohort was drawn from three primary institutions: (1) Southern Illinois University Carbondale (CFAR), Southern Illinois; (2) Colorado Mesa University's Forensic Investigation Research Station (FIRS), Western Colorado; and (3) Sam Houston University (STAFS), Southeast Texas. Conversely, this study cohort represented five different broadly distributed academic and professional instiutions. While the reported experience level of participants in the Dabbs *et al.* study could be reasonably affirmed, this study relied on the veracity of participant statements so the true level of participant training and experience could not be assessed.

A more compelling basis for the divergence in study results is the regionality of CFAR, FIRS, and STAFS. Early phasic and categorical models developed to describe the trajectory of human decomposition were largely limited to arid environments (Galloway *et al.* 1989; Galloway 1997; Rhine & Dawson 1998), and the woodlands of eastern Tennessee (Bass 1997), both of which share regional and environmental continuity with CFAR, FIRS, and STAFS. Galloway (1989 & 1997), in particular, served as

the foundational basis for the categorical changes described in the TBS model. While environment specific divergence from the categorical change presented in the TBS model is expected – and has been demonstrated in Western Colorado by Connor *et al.* (2019) - regional proximity between the study facilities and the foundational work suggests a high potential for overlap in some aspects of gross decompositional change. The high-altitude environment that served as the geographic basis for this study shares few characteristics with extant studies and throughout the course of study, yielded a unique suite of categorical change that were not encapsulated by the TBS model. Rather than undermine the results reported by Dabbs *et al.*, the lack of interobserver agreement in this study is consistent with the sum of the study's results: (1) the seriation of categorical change presented by the TBS model (the qualitative aspect) does not reflect those observed at high-altitude; and (2) the TBS regression model (quantitative aspect) does not accurately predict PMI among the high-altitude cohort of human donors. Because the test for interobserver reliability was performed among a cohort of human donors that did not present the same categorical change encapsulated by the scoring matrix, interobserver concordance would be *more* troubling and likely attributable to model mimicry as opposed to true user agreement. Further, given the extreme difference in the high-altitude decomposition process, it is arguable that all observers may be classified as 'beginners,' regardless of reported experience level. Observer inexperience was the primary factor driving disagreement between observers in Dabbs *et al.* (2017). Future study will assess interobserver error using a matrix reflective of the seriation of categorical change identified in this study.

8.1 Quantitative Analysis: Efficacy of the TBS Model at High-altitude

The first goal of this study was to evaluate the accuracy and reliability of the quantitative aspect of the TBS model for estimating PMI in a high-altitude environment. It is important to acknowledge that despite reducing each donor's PMI to less than one year within the high-altitude data set, the original and high-altitude data sets are not composed identically. The TBS cohort is composed of 68 human

remains cases retrospectively observed using case photographs. This method has subsequently been validated in controlled study by Dabbs *et al.* (2017). Each case in the TBS cohort is represented by a point estimate of PMI (the majority of which were established using entomological data), yielding a single TBS score on a single day. The use of entomological data in retrospective estimation of PMI has since been heavily criticized by Moffat *et al.* (2016). The high-altitude cohort is composed of substantially fewer individuals (n = 12), but the data are derived from direct, longitudinal field observation. While differences in cohort size may arguably be a source of error, Moffat *et al.* (2016) cite issues associated with estimated PMI as a major source of error in the original TBS study, leading the authors to argue that the original cohort is more appropriately represented by 15 cases. Factors affecting TBS case removal include: (1) PMI estimation using entomological methods, due to associated inaccuracy; (2) all indoor cases, based on data demonstrating that insect exclusion or inhibition slows decomposition; (3) ADD beyond 3000 due to associated longitudinal skeletonization; and (4) unknown height and body mass. Despite these differences, both study cohorts are represented by comparable PMI, and a similar suite of TBS values (TBS cohort 3-35 / High-altitude cohort 3-31). Despite the greater maximum TBS value in the TBS cohort, the difference is marginal, and the high-altitude cohort is represented by all possible TBS scores less than 32, while the TBS cohort contains missing values. Summarily, while the data sets exhibit minor differences in structure, they maintain continuity in composition.

The TBS model's quantitative approach was independently tested within a cohort of 12 human donors decomposing in a high-altitude environment. This was done by following the study design presented by Megyesi *et al.* (2005). Specifically, the TBS data set in this study was limited to observations made within each donor's first year of decomposition, and subsequent distribution, transformation, and analyses mirrored those performed in the original study. The TBS model did not sufficiently predict PMI in the high-altitude cohort, nor did temperature or PMI alone sufficiently describe the variation in decomposition. In the first step, the distribution of ADD and PMI were individually plotted against TBS

derived from the high-altitude cohort. Neither distribution was linear, and the overall trend demonstrated a rapid early climb in TBS scores, followed by a persistent, slow-moving plateau. These results are consistent with those reported in extant TBS model validation studies (Sutherland et al. 2013, Marhoff *et al.* 2016; Connor *et al.* 2019; Dawson *et al.* 2022).

The ADD and PMI data were LOG transformed and TBS squared in an attempt to normalize the data. The relationships between both ADD vs. TBS and PMI vs. TBS were tested using linear regression, and the plots of each test fitted with a regression line. Transformation marginally served to normalize the data. The regression lines suggest that the TBS model is not a correct fit for estimating rate of decomposition at high-altitude. Adjusted R-squared values support the model's poor performance when applied to the high-altitude cohort; Log_{10}ADD vs. TBSSQ (0.42) and Log_{10}PMI vs. TBSSQ (0.54), where ADD^c accounted for 42% of the variance observed in decomposition, and PMI accounted for 54%. This suggests that neither ADD^c nor PMI is a strong predictor of decomposition when regressed against TBS. Megyesi *et al.* (*ibid*) report substantially higher R-squared values for Log_{10}ADD vs. TBSSQ (0.84) and for Log_{10}PMI vs. TBSSQ (0.70), with ADD^c accounting for 84% of the variance observed in decomposition and PMI accounting for 70%. Log_{10}ADD explained greater variation in decomposition than Log_{10}PMI within the Megyesi cohort, leading the authors to conclude that time and temperature served as a better index for predicting PMI than time alone. The inverse was true within the high-altitude cohort where Log_{10}PMI vs. TBSSQ explained greater variation in decomposition than Log_{10}ADD vs. TBSSQ. Because PMI directly reflects time, this suggests that a variable or variables encapsulated by time may serve as a better predictor or predictors than ADD alone.

While these results demonstrate environment specific divergence in the predictive power of the TBS model, they should be considered with caution based on the underlying statistical model applied. TBS fails to meet the definition of a ratio-scale measurement – a quantitative scale within which there is a true zero, and equal intervals between neighboring points – making the application of a parametric

regression model inappropriate. Further, both the raw and transformed ADD data yield heteroscedastic distributions, making application to a model that assumes homoscedasticity inappropriate. While linear regression was applied to the dataset in this study, it was done so to achieve an equitable comparison between the original study design and this study. Future quantitative model building will rely on statistical models in which the parameters are satisfied by the structure of the data.

8.2 *Quantitative Analysis: Atmospheric Variables*

Because PMI (time) accounted for greater variance in decomposition within the high-altitude cohort, the potential for several atmospheric variables to affect the rate and trajectory of decomposition were investigated. First, the distribution of TBS was considered along three temperature scales, ADD^{c}, $ADD^{C>0}$, and ADD^{K}. A general trend in rapid increase in TBS in early PMI, followed by a persistent score plateau was observed across all temperature scales. This pattern was not observed or reported in the original study, likely due to the point estimate structure of the data set, and the paucity of late-stage TBS scores. However, this pattern has been broadly observed and widely reported in longitudinal, environment specific validation studies of the TBS model (Sutherland et al. 2013, Marhoff *et al.* 2016; Connor *et al.* 2019; Dawson *et al.* 2022).

While overall continuity was observed in the pattern (rapid climb followed by plateau) of distribution across all temperature scales, some variation in distribution was observed. Cohort wide distribution of TBS on the ADD^{c} scale demonstrated the complexity associated with score undulation between positive and negative temperature values. Undulation was predictably greatest in the winter months when temperatures dropped into negative values. While undulation on the ADD^{c} scale is temperature based, this is also a period of high precipitation. Baigent et al. (2014) observed a direct relationship between precipitation and score reversal, suggesting that temperature undulation encapsulates several variables that may have a direct effect on TBS scores. Megyesi *et al.* (2005) argue that 0 ˚C be used as the base temperature for the cessation of decomposition based on the idea that

freezing temperatures acutely inhibit biological processes. The authors cite an arrest in bacterial growth as evidence for cessation, but concede that "it is not known at what temperature decomposition processes actually cease" (2005: 5). However, more recent studies demonstrate that the assumption of biological arrest in cold temperatures is overly homogenous and overly reductive. Forbes *et al.* (2014) identify the lack of temperature dependent decomposition studies as one of the primary problems facing modern taphonomy research. In a study of seasonally defined phases of composition, number, and abundance of volatile organic compounds (VOCs) in decomposition odor in outdoor environments, the authors identify an anticipated proportional difference between the rate of decomposition and abundance of VOCs between the winter and summer months. However, while proportionately disparate, a consistent inter-seasonal trend in rapid increase in VOC abundance was observed in two phases. The first peak was observed during active decay, followed by a second peak occurring later in decomposition. While also proportionately divergent, compound class was consistent between the winter and summer seasons. While sulfur-containing compounds, alcohols, and ketones represented the most abundant classes in both seasons, each of the ten compound classes were physically identified in decomposition throughout both seasons. This suggests that, while decomposition slows in the winter months, the process does not completely arrest.

While biological processes are considered paramount in rate and pattern of decomposition, mechanical processes associated with freezing, and their potential impact on the trajectory of decomposition cannot be overlooked. Slow freezing of tissue results in a residual unfrozen medium characterized by channels of decreasing size and increasing solute concentration. Cells entrapped in the channels respond osmotically and shrink within the high solute concentration. While *in vivo* injury resulting from slow freezing has long been attributed to the concentration of solutes or the cellular osmotic relationship, Mazur (1984) presents evidence to suggest that injury is the result of channel morphology. While this, and similar concepts may superficially appear to represent physiological

minutia, they are critical to taphonomic study, where cell death has likely occurred but the underlying passive mechanisms for tissue stress and strain remain active.

While biological processes may slow (and in some cases arrest) when temperature decreases, there is no empirical evidence to support a temperature threshold for absolute arrest, as the TBS model suggests. It is worth noting that the study's quantitative regression analysis relies heavily on LOG transformation, which cannot be applied when negative values are present. The ascribed 0 ˚C base necessitates the conversion of all negative temperature values to 0 ˚C, with the expected effect of eliminating the undulation of TBS between positive and negative values observed on the ADD^c scale. However, the concomitant impact is the removal of associated variables that may have an impact on rate and pattern of decomposition.

In contrast to the Celsius scale, kelvin (K) is the primary unit of temperature in the International System of Units and the primary unit of temperature in engineering and physical sciences. Kelvin is a thermometric scale on which zero coincides with the theoretical absolute zero of temperature, with absolute zero representing the thermodynamic equilibrium state of minimum energy. Dabbs (in press) advocates for the application of the kelvin scale to decomposition studies, citing: (1) ease of conversion from the international standard of Celsius to kelvin ($K=C^o+273.15$); and (2) elimination of the need to assign an arbitrary threshold for the cessation of decomposition, as kelvin is an absolute temperature scale that does not contain negative values. In addition to the cited advantages, kelvin also presents a statistical advantage. As an absolute temperature scale, kelvin eliminates the analytical limitations imposed by data sets containing negative values, specifically, those associated with both mathematical transformation (e.g. LOG transformation/base transformation) and assumption violation in statistical models that do not tolerate negative values. The application of the kelvin scale to the high-altitude data resulted in broader distribution of scores within the TBS 15-25 range. Within the 25-33 range, the sharp angle presented by both of the Celsius scales at the onset of the plateau phase was smoothed, the

structure of the plateau less rigid, and the data are more broadly distributed to the right. Based on both the analytical properties and the observed effect on data distribution, kelvin has the potential to reconcile disparities observed between the ADD^{c} and $ADD^{C>0}$ temperature scales and should be considered in future model building.

In addition to the three temperature scales, the trajectory of TBS by individual donor was plotted against accumulated pressure days, accumulated rain days, accumulated precipitation days, accumulated relative humidity days, accumulated solar radiation days, and accumulated wind speed days. Because it establishes a line through the moving central tendency of the stressor-response relationship, a LOESS curve was fitted to individual donor distribution along each atmospheric variable scale, facilitating visual assessment of the relationship between the two variables. The LOESS curve of each of the atmospheric variables invariably demonstrated that the data are not linear. Overall - with the exception of accumulated rain days - LOESS elucidated strong visual relationships between TBS and each of the atmospheric variables. Multivariate regression analysis using the first-, second-, and third-degree polynomial orders supported the hypotheses generated by observation of LOESS.

As with LOESS observation, multivariate regression analysis demonstrated that - with the exception of ARD - all weather variables explained variation in decomposition almost as well, if not better, than ADD^{c}. That this general pattern was observationally predicted within the data fitted with a LOESS curve demonstrates the power of LOESS in elucidating higher resolution patterns within large data sets. Atmospheric variables were quantitatively assessed using first-, second-, and third-degree polynomial orders. R-squared values associated with the first (linear) explained the least amount of variation, an expected outcome as LOESS demonstrated the parabolic structure of the data sets. However, APD, ASRD, and AWSD explained greater variation than ADD^{c}. This may be due to the potential for greater fluctuation in temperature values at high-altitude when compared to the fluctuation potential of APD, ASRD, and ASWD. Altitude is associated with a suite of atmospheric variables, the

parameters of which are largely defined by elevation, pressure, and oxygenation. Environmental constraints intrinsic to altitude (i.e. the window of potential fluctuation) may be more conducive to tests for linearity.

Atmospheric pressure can be understood as the total weight of air above a unit area at any elevation. While atmospheric pressure is variable, altitude is associated with an overall decrease in pressure, due to a reduction in the availability of air molecules above a given surface. A similar surface at a lower elevation is subject to the pressure created by a substantially greater number and weight of air molecules. As a result, the lower elevation point is subject to greater variability and fluctuation in atmospheric pressure. While APD is not truly linear, increase is constant and at high-altitude, resulting in a relatively small window of potential fluctuation. Reduced fluctuation means a less variable increase in APD over time, which may mimic linearity and explain APD's strength in explaining variation in decomposition at the lowest order.

Solar radiation shares a similar but inverse relationship with altitude. Solar radiation increases with altitude due to the associated decrease in air molecules, ozone, aerosols, and cloud cover. In a study of the effect of altitude on solar UV-A and UV-B irradiance, Piazena (1996) observed a linear increase of the diffuse components in both UV-A and UV-B ranges with altitude. While solar radiation varies seasonally, ASRD is ultimately additive, enhancing the linearity that would perform positively in the first order.

Wind speed is a composite of pressure, temperature, and altitude. The pressure gradient created by a high-pressure area (high air density and pressure) meeting a low-pressure area (low air density and pressure) results in pressure equalization at the gradient interface catalyzing the speed of flow (wind). The result is an increase in wind speed relative to an increase in elevation which carries an innate relationship with pressure. As with APD and ASRD, AWSD is additive and because pressure is a major contributing factor, it may explain variation in decomposition similarly to APD in the first order.

Both the second and third orders are parabolic, and both categories present higher R-squared values when compared to those of the linear model. This is an expected outcome based on the non-linear structure of the high-altitude data set. R-squared values associated with ASRD (0.66) and AWSD (0.65) explained greater variation in decomposition than ADD^c (0.61) in the second order. While the R-squared value associated with APD increased, it failed to rise above that of ADD^c. As previously established, temperature carries greater fluctuation potential than pressure, the fluctuation potential of which is constrained by low levels of atmospheric oxygenation. In this scenario, an overall increase in the explanatory power of APD, but a decrease in explanatory power compared to ADD is logical. The greater fluctuation potential of ADD^c is more conducive to a parabolic fit, while the linearity imposed on APD by environmental constraints is not. However, APD is not truly linear, as is demonstrated by an increase in predictive performance in the second order.

The third order yielded the highest R-squared values across all atmospheric variables, a predictable result based on the complexity of the data structure demonstrated by LOESS. In the third order, the R-squared values associated with ASRD (0.67) and AWSD (0.65) exceeded that of ADD^c (0.64), followed by APD (0.59), ARHD (0.57), APreD (0.50), and ARD (0.10). The explanatory power of ASRD exceeding that of ADD^c is a predictable outcome in the high-altitude environment. Both UV radiation and temperature possess thermocatalytic potential, but elevation has a direct effect on that potential. UV radiation is absorbed by the atmosphere, and a reduction in atmosphere is correlated with an increase in radiation (an approximate 2% increase with every 100 meters of altitude gain). Conversely, as elevation increases, atmospheric pressure decreases, resulting in broader distribution of oxygen molecules, and an overall decrease in temperature - approximately 1.2 degrees Celsius for every 300 meters of elevation gain. Because there is evidence to support the supposition that net decomposition slows, but does not cease, with decreasing temperatures (Forbes *et al.* 2014), there is a logical connection between altitude and a reduction in the explanatory power of temperature.

Despite the inverse relationship between UV, temperature, and altitude, ADD^c remains a strong predictor of the variance observed in decomposition at high-altitude. When considered in higher-resolution, the inverse relationship between UV and temperature is demonstrative of the complexity of relationships that can arise within a microenvironment. In a lower elevation model, UV radiation is absorbed by the lithosphere and heats the troposphere via conduction and convection, resulting in decomposition primarily catalyzed by conduction of a subterraneous heat source. Conversely, both UV and temperature are strong predictors of the variance observed in decomposition at high-altitude. This suggests that decomposition is catalyzed by both radiant (UV) and conductive (lithospheric) heat, resulting in a more complex relationship between heat and the surface area of human remains decomposing at surface level in the high-altitude environment. While a compelling analytical scenario, comparative studies conducted in lower altitude environments are necessary to validate the strength and weight of this hypothesis.

Continuity in the predictive power of wind speed across all orders is superficially surprising. However, a dissection of the components of wind speed yields an explanatory model for the variable's explanatory power. As previously discussed, wind speed is a composite of pressure and temperature (variables sensitive to altitude). In quantitative analysis, ADD^c was a performative intermediary between windspeed and pressure. As a composite of pressure and temperature, windspeed would logically explain a greater percentage of variance in decomposition. However, while 'logical' in *post hoc* consideration, this is more importantly demonstrative of the potential symmetry, and complexity inherent to categorical variables that possess multiple lines of environmental feedback.

While not among the variables with the greatest explanatory capability, R-squared values associated with relative humidity (0.57) and precipitation (0.50) suggest that both are notable predictors of the variance observed in decomposition at high-altitude. Relative humidity is a percentage of the amount of water vapor present in the air, versus the amount needed for saturation at the same

temperature. Similar to the atmospheric variables discussed, altitude shares a unique relationship with relative humidity. On average, moisture availability (relative humidity) decreases with elevation gain. However, this pattern seasonally vacillates, demonstrated by the reflexive nature of humidity to seasonal atmospheric conditions. While temperature decreases with elevation gain, relative humidity seasonally reaches 100% when snowfall is persistent and heavy. The increase in humidity results in an overall reduction of the rate of altitude associated decrease it temperature. While environmental conditions remain overall colder at high-altitude, snow paradoxically provides a measure of insulation as relative humidity serves to reduce the rate of cooling. This pattern both underscores the need for future study pertaining to the effect of snowfall and snow overburden on decomposition, and the problems associated with the assumption of decomposition cessation at 0 ˚C

Like relative humidity, precipitation is highly sensitive to season. This phenomenon may explain why both variables are notable predictors of the variance observed in decomposition at high-altitude, but do not perform as strongly as more regulated atmospheric variables. Precipitation encompasses any product of condensed atmospheric water vapor that falls from the sky as a result of gravitational pull. When water saturation within a portion of the atmosphere is sufficient to result in 100% humidity, water condenses and “precipitates,” (falls) in the form of rain, ice pellets, hail, snow, or graupel. High-altitude environments are characterized by the orographic effect – precipitation that falls when saturated air contacts a landform barrier and is forced to ascend, resulting in contact with low temperatures associated with elevation, resulting in rain or snowfall. Cold temperatures and the lack of atmospheric oxygen molecules are not conducive to moisture retention. As a result, precipitative events tend to be punctuated and substantial. The impact of this phenomenon explains both the relatively high R-squared value of APreD (0.50) and the low R-squared value of ARD (0.10).

Precipitation is categorically comprehensive (it encompasses all forms of hydrogen aggregates), and maintains the potential to be both additive, and cumulative (e.g., snowfall may be added to existing

overburden and cumulate throughout the season). Baigent (2014) demonstrated that score reversal within the TBS model was highly correlated to precipitation. While sensitive to season, the manifold forms lend temporal diversity. Conversely, rain-days at high-altitude are substantial in volume, but are seasonally mediated punctuated events. Based on circumstance – punctuated events characterized by temporal paucity – rain may: (1) lack the frequency necessary to have an appreciable impact on decomposition; (2) lack the power to catalyze the histomorphological change necessary to be detected by a quantitative model; or (3) lack the ability to catalyze the longitudinal histomorphological change necessary to promote mathematical sensitivity and specificity in a quantitative model. While the R-squared values associated with ARD increased across orders, the overall values remained low. Regardless of the underlying rationale, continuity in the inability of ARD to act as a notable predictor of the variance observed in decomposition at high-altitude suggests that future model building will not benefit from the incorporation of ARD.

8.3 *Qualitative Analysis: Efficacy of the TBS Model at High-altitude*

The qualitative approach to the TBS model was tested by isolating the categorical changes defined within the model (skin slippage, purge, specific descriptions of soft tissue color change, marbling, bloat, and moist decomposition) and scoring them as present (1) / absent (0) throughout the trajectory of decomposition. Category specific present/absent scores were summed at the terminus of data collection to establish point presentation and the percentage of the cohort in which each change presented. This study established an 80% threshold for intracohort trait presentation. Traits failing to meet the 80% threshold will be rejected from future model building. Like the quantitative model, the qualitative categories established by the TBS model performed poorly at high-altitude with only one of the six categories of gross tissue change (moist decomposition) meeting the 80% threshold. Because the 'classic' qualitative categories of tissue change were derived from a large body of empirical research,

substantial consideration has been given to why these categories may not present in a high-altitude environment.

8.3.1 *Tissue discoloration*

Pink/white tissue discoloration was the most frequently observed trait (92% of sample). However, because this trait is described in early decomposition and 11/12 (92%) of donors are white, no analytical power has been ascribed to this category, in this study. Gray to green discoloration was observed in one donor (8% of the sample); the point of first presentation was 18 ADD^{c}. Black variably presented in circumscribed areas of color change throughout decomposition, however it did not present as the dominant mode of color change within any donor or along a predictable timeline. Brown (specifically, umber) did present as a dominant color change within the high-altitude cohort, however this was associated with late-stage advanced decomposition, as opposed to a phasic characteristic of early decomposition as presented by the TBS model. Because pink/white is a melanin correlate, brown discoloration did not correspond to equivalent phases of decomposition, green presented infrequently, and black was not observed as a categorical change, all phases of tissue discoloration presented in the TBS model have been eliminated from future use in high-altitude model building.

One donor (20-103) in the high-altitude cohort identified as black; pink to white discoloration was not observed throughout the trajectory of 20-103's decomposition. While a population's rate and pattern of decomposition cannot be derived from a sample of one, the impact of variable melanin concentration on the presentation of soft tissue discoloration does not constitute an analytical leap. While the lack of racial diversity in human decomposition and curated skeletal collections is a well-recognized analytical gap (Winburn *et al.* 2020; Campanacho 2021; Ross & Williams 2021), it is not one that will be easily solved. However, the lack of data does not warrant a lack of discussion. Winburn *et al.* (2020) cite the historically rooted, wholly warranted, and contemporary prominence of distrust for medical and scientific communities within BIPOC communities. This distrust is rooted in unethical

practice associated with undisclosed research, such as the Tuskegee study of untreated syphilis, conducted within a Black male population as late as the 1970's. The authors advocate for educational outreach and complete transparency in research goals, as well as education outlining the practical benefits of this research for community members. While the number of racially diverse pre-registered donors in the William M. Bass donated skeletal collection has increased in recent years (Campanacho 2021), racial disparity within curated collections will not be reconciled rapidly. However, rather than build models 'based on what is available,' model builders relying on variables such as tissue color change must remain cognizant of applying more inclusive terminology, and must reinforce to the user that racial disparity is inherent to a model built within a single population. While this may seem 'obvious' to anthropologists, as the greater law enforcement community begins to adopt and employ our analytical models, anthropologists are duty bound to educate and avoid racial homogenization.

8.3.2 *Moist decomposition*

Moist decomposition followed tissue discoloration in the frequency of observed traits (83% of sample), however the category constituted the widest breadth of first point presentation (842 - 6461 ADD^{c}), was sensitive to score reversal, and most typically presented in the inguinal region, as opposed to diffuse across all body surfaces (though whole-body moist decomposition was observed in three donors). Because warm and moist conditions stimulate decomposer activity, Zhang *et al.* (2008) identify temperature and precipitation as primary instigators of moist decomposition. Precipitation constitutes a complex and dynamic atmospheric variable in the high-altitude Rockies. While overwintering is characterized by heavy snow overburden, snow metamorphism, creep, and ice accretion, spring is typified by a complex aggregate of these variables as melt and runoff create a composite of winter variables resulting in a seasonally dynamic environment. Late spring and summer are defined by North American Monsoons; when local temperature and humidity are sufficient, moisture release may constitute 5-10 percent of a site's annual rainfall within the span of one hour (Cannings 2006). As

previously outlined, temperature and altitude share an inverse relationship, meaning that while precipitation is high, temperatures are low. However, as precipitation increases, temperature also increases due to the insulative nature of atmospheric moisture, but remains low when compared to lower elevations. The impact of this complex relationship on variables such as moist decomposition is unknown and constitutes an avenue of future study.

On the adjacent Western Slope of Colorado, Connor *et al.* (2019) observed a distinct but equally complex relationship between atmospheric variables and moist decomposition. While high-altitude complexity is primarily attributed to seasonal fluctuations in atmospheric moisture, complexity described on the high-elevation plains was attributed to the absence of moisture. The human dermis has evolved to negotiate the complex relationship between *in vivo* thermal homeostasis and the environment. The complexity and breadth of presentation associated with moist decomposition is related to these evolved dermal mechanisms, the properties of which have the potential to remain active postmortem. Transepidermal water loss is largely mediated by the degradation of dermal barrier quality following cumulative protein removal from the stratum corneum (Lu *et al*. 2014). *In vivo* protein synthesis serves to maintain the moisture barrier, a process that cannot be sustained postmortem due to the body's functional loss of ability to synthesize proteins. Protein solubility is a thermodynamic parameter, making postmortem degradation of the protein moisture barrier (and subsequent moisture loss) highly sensitive to the local environment. This phenomenon explains interdonor variation in the presentation of moist decomposition, and the breadth of point presentation of moist decomposition among donors. Because it is reactive to the ambient environment, protein solubility in the protective skin barrier would functionally vary based on the amount of heat available to catalyze protein dissolution, seasonal variability in the transfer of thermal units, *in vivo* barrier composition, and the passive incorporation and evaporation of environmental moisture.

Chemiophysical complexity is dramatized by the physical structure of the dermis. Dermal porosity lends hygroscopic properties postmortem, largely due to the evolved mechanisms of radiant heat transfer and surface diffusion (Kyunghoon *et al.* 2007). Hygroscopy refers to the phenomenon of matter (in this case, tissue layers) attracting and holding water molecules sourced from the surrounding environment via absorption (incorporation into tissue) or adsorption (molecular bonding of water molecules to tissue surfaces). The former promotes longitudinal, dynamic cycles of water absorption and release, while the latter promotes superficial moisture adherence via physiochemical bonds (Lu *et al.* 2014). Summarily, in addition to intrinsic variables such as the protein structure of the moisture barrier, passive environmental variables and their chemiophysical ability to interact with tissue postmortem create a complex composite of variables participating in moist decomposition.

Confounding the application of moist decomposition as a temporal marker for decomposition was the anato-locality observed within the cohort. Moist decomposition most typically presented in the inguinal region. Moist decomposition encapsulates the process of macroscopic purging of fluids catalyzed by the gaseous byproduct of bacterial metabolization (Gill-King 2006). The point presentation of moist decomposition may be explained by underlying continuity in the anatomical mechanisms responsible for *in vivo* pathology in the abdomino-inguinal region.

The abdominal and inguinal regions are bridged by the inguinal canal, a lumen that originates in the inferior abdominal wall and extends inferomedially into the inguinal region. The canal allows passage of anatomical structures from the abdominal wall to the external genitalia (Tuma *et al.* 2022). Clinical significance is derived from weakness in the abdominal wall, resulting in abnormal displacement of abdominal structures such as the intestine. Pathological passage of abdominal structures through the inguinal canal results in an indirect hernia (Öberg *et al*. 2017). Inguinal circumscription of moist decomposition may be the result of gravity and decomposition within the abdominal and intestinal walls. Moist decomposition presented the widest temporal breadth of presentation. Early presentation

may be the result of decomposition of the intestinal walls, resulting in gravity mediated (downslope) displacement of fluids and bacteria to the inguinal region via the inguinal canal. As decomposition advances, loss of structural integrity within both the intestinal and abdominal walls would result in higher volume displacement of fluids and bacteria, further promoting point presentation of moist decomposition. While anatomically derived, this explanation is conjecture, constituting one of many potential explanations for the focal moist decomposition observed in this study. However, it is a compelling example of the intercalated effect of anatomy, physiology, and environment on the rate and pattern of decomposition in a high-altitude environment, and warrants future study.

8.3.3 *Bloat*

Bloat followed moist decomposition in the frequency of observed traits (67% of sample). In establishing the region-specific qualitative decomposition sequence of Colorado's Western Slope, Connor *et al.* (2019) demonstrate that – among five categorical changes – bloat and ADD shared the weakest correlation. This is attributed to a lack of tempero-linear presentation. The trajectory of bloat may be interrupted by rapid desiccation in the summer months or delayed in colder months. Donors placed in the winter months variably presented bloat when temperature increased and became more conducive to microbial activity. As was observed on the Western Slope, high-altitude bloat did not progress in a linear or homogeneous pattern. The range of point of first presentation was 240-2205 ADD^{c}. When bloat did present, it was among donors placed in the spring and summer months (late March – August). As was observed by Connor *et al.* (2019), donors placed in the winter months did not bloat; however, the potential for temperature mediated delayed bloat was not observed within the high-altitude cohort. This suggests that temperatures associated with overwintering at high-altitude were sufficiently low to: (1) diminish the population of the endogenous microbiome (Schwab *et al.* 2014); (2) depress metabolic potential (*ibid*); (3) catalyze anatomical change that prevented bloat; or (4) promote

any combination of these variables, resulting in the post-winter inability to produce the volume of gas necessary to achieve bloat.

8.3.4 *Marbling*

Marbling performed as poorly as bloat in the frequency of observed traits (67% of sample). The range of point of first presentation was 34 - 589 ADD^c, yielding a smaller range of point presentation, but was overall too infrequent in presentation to serve as a reliable temporal marker. Marbling is the result of postmortem staining of the intima of large blood vessels by hemolysis and gravitational settling of blood (Clark *et al.* 2006). A variant of traditional marbling was identified and introduced in this study. Capillary marbling is characterized by the staining of the intima of the network of delicate branching blood vessels that form a complex network between the arterioles and venules. Associated gross tissue change was typified by vibrant orange tissue discoloration with a delicate complex of maroon/rose marbling within. 'Traditional' marbling (staining of large blood vessels) was unreliably observed but was associated with a relatively small temporal window. Conversely, capillary marbling was observed among all donors, but temporal distribution spanned a broad range of ADD. Capillary marbling was categorized as an honorable mention in this study. This category encapsulated changes observed within the study cohort that lacked a strong phasic correlation, or were hypothesized to have an impact on the gross or chemiophysical trajectory of decomposition. These traits were not quantified in preliminary trait discernment and definition. Like traditional marbling, capillary marbling is a poor temporal marker. However, the incidence and prevalence of the phenomenon suggests the potential for informing an unidentified physiochemical cascade of decomposition change at high-altitude and therefore warrants future study.

8.3.5 *Skin slippage*

Skin slippage followed marbling and bloat in the frequency of observed traits, with a dramatic decrease in incidence (25% of sample). When observed, skin slippage was most typically associated with

maggot mass formation, where the secretion of a complex amalgam of digestive enzymes promote debridement mechanisms (Nigam *et al.* 2006). Because maggot mass formation and propagation at high-altitude demonstrated high sensitivity to environmental variables, maggots were unreliable progenitors of skin slippage. In the absence of an arbiter, skin slippage is catalyzed by the release of hydrolytic enzymes by cells lining the dermal-epidermal junction (Clark *et al.* 2006). Enzymes are highly sensitive to temperature and local pH. Denaturation occurs when an enzyme loses its native conformation - the highly specific three-dimensional structure maintained by hydrogen bonds - rendering it unable to bind to a substrate and perform its requisitioned activity (Pegg *et al*. 2006). While temperature mediated denaturation is typically discussed in relation to heat, Georlette *et al.* (2004) outline modes of cold temperature denaturation that have catalyzed the evolution of cold-adapted enzymes. Low temperatures thermodynamically favor hydration of polar and non-polar protein groups. A byproduct of this process is the weakening of hydrophobic bonds critical to native conformation and stability, resulting in denaturation. This process has the potential to physiologically undermine the structure and function of the hydrolytic enzymes responsible for skin slippage, and serves as an important reminder that the potential for cold temperatures to catalyze decomposition should not be minimized. Summarily, the conditions conducive to skin slippage were too environmentally sensitive and specific to yield predictive power, supporting trait elimination from future model building.

8.3.6 *Purge*

Like bloat, purge is the result of endogenous gases; purge was observed in one individual (8% of sample). While bloat is the result of intralumen entrapment of gasses, purge is the result of gaseous discharge. When endogenous pressure is sufficient, gases confined to the gastrointestinal tract provide the pressure necessary to expel aggregate decomposition fluids through peripheral orifices. The poor performance of bloat and deficient performance of purge as temporal markers for decomposition at high-altitude are superficially surprising when considered in clinical context. High-altitude flatus

expulsion (HAFE) is an uncomfortable but benign pathophysiological result of high-altitude. As air pressure decreases, gastrointestinal gases expand; the aggregate gas leads to bloating, discomfort, and necessitate release, resulting in increased flatulence (Anand *et al.* 2006). While the etiology of HAFE should be conducive to both purge and bloat, the incidence of both categorical changes does not support the presumption.

When considered in the context of decomposition, an alternative, and more persuasive explanation is provided by intestinal barrier dysfunction. Studies pertaining to both HAFE and intestinal barrier dysfunction are limited to *in vivo* clinical context. However, as a result of temperature (held constant by *in vivo* homeostatic boundaries), and pressure, HAFE is the byproduct of *in vivo* biophysiological processes. Conversely, the mechanisms of intestinal barrier dysfunction are conducive to a positive feedback system when considered in postmortem context. Hypoxia-induced intestinal barrier injury is clinically defined by multifactorial interruption of the complex physiochemical and biomechanical systems that maintain the intestinal barrier. The intestinal barrier is a complex, semipermeable membrane that facilitates the exchange of nutrients, engages in immune sensing, maintains and restricts the movement of the gut biome, and restricts pathogenic bacteria and molecules (McKenna *et al.* 2022). Barrier disruption is a complex cascade of physiomechanical processes resulting from a loss of cellular oxygenation (as is associated with high-altitude environments, and the postmortem physiological environment). Hypoxia results in the depletion of adenosine triphosphate (ATP), decreased pH, and the proliferation of reactive oxygen species (ROS; molecules derived from oxygen vigorously engaged in intermolecular oxidation), all variables that interrupt barrier integrity. This interruption results in increased barrier permeability, allowing contra passage of luminal contents through the intestinal wall, and bacterial translocation. Additionally, because apoptosis and entosis are tempero-phasic, recruitment and activation of innate immune cells (e.g., resident macrophages, circulating monocytes, Kupffer cells) persists postmortem. Immune cells facilitate the release of

proinflammatory cytokines into the bloodstream, inciting local or systemic inflammatory response (*ibid*). When hypoxia persists, a positive feedback loop promotes atrophy of mucosal layers, further compromising the intestinal barrier. Gram-negative bacteria containing lipopolysaccharides (endotoxins) cross the compromised intestinal barrier and activate resident macrophages to release proinflammatory cytokines, again promoting barrier lysis and instigating molecular death. Summarily, both the translocation of the enterobiome, and the dissemination of proinflammatory cytokines may significantly interrupt the structure of the gastrointestinal tract, the structure of bacterial colonies, and the distribution of the gaseous byproducts of their metabolization. Loss of barrier integrity is highly correlated to deoxygenation, a process that escalates postmortem, suggesting that barrier loss may play a crucial role in absence of gross postmortem change catalyzed by gases.

8.4 *Qualitative Analysis: Categorical Change Observed at High-altitude.*

While the qualitative categorical variables used in the TBS model largely failed to provide a reliable matrix within which to score decomposition at high-altitude, a suite of environment-specific categorical changes were identified and defined. These categories include: (1) an environment-specific pattern and trajectory of color change; (2) skin sloughing ; (3) fluid bloat; (4) tissue island formation (localized differential decomposition); (5) adipocere formation; (6) pseudoburial; and (7) slope roll. The 80% threshold for intracohort trait presentation established to test the 'classic' categories was also applied to high-altitude categories. Traits failing to meet the 80% threshold were rejected from future model building. Six of the seven traits met the 80% threshold. Slope roll was limited to 67% cohort presentation and presented across an exceedingly wide range of point presentation (1355 - 10142 ADD^{c}). Likewise, pseudoburial was overall dynamic and additive, and therefore difficult to quantify. Additionally, the category presented across a broad range of ADD (810 - 4273 ADD^{c}). As a result, both categories were removed as potentiates for future model building. While not valuable as predictors, each category contains critical data regarding the movement and obscurement of human remains in the postmortem

environment. Longitudinally, these data will inform field search and recovery models and are therefore considered important elements of the region's taphonomic profile.

8.4.1 Environment specific pattern and trajectory of color change

Due to the breadth of anato-spatial distribution, and the vibrancy of colors presented, the pattern of tissue discoloration was the most prominent change observed at high-altitude. In the test for interobserver error, 14 of the 15 independent observers provided comments pertaining to the fitness of the TBS model for application within the high-altitude cohort. The most persistent comment (14/14 commenters) referenced color. The most eloquent of these comments stated, "this color situation is making me feel real big feelings." The cause for consternation was the lack of continuity between observed color change, and the descriptive categories within the TBS model. Tissue discoloration phasically and contemporaneously ranged from vibrant orange and/or vibrant maroon, rose, plum, golden, pale yellow, brown, and umber. Circumscribed areas of black, green, and gray also presented asynchronously throughout decomposition.

The distinct seriation of phasic, anato-spatial color change observed within the high-altitude cohort is consistent with both the morphology of the circulatory system, and the local environmental variables that mechanically and physiologically affect decomposition. Cranially, the superficial carotid artery diverges into eight primary branches, four of which (lingual, facial, maxillary, and superficial temporoparietal) comprise the major superficial vasculature infrastructure of the face. The maxillary and superficial temporal arteries form the two terminal branches of the external carotid artery; the dominant facial branches are oriented peripheral to the central face. The chest and thorax are vascularized by the cardiac and pulmonary complexes (chest) and the descending aorta and major organ branches (abdomen). The brachial artery is the primary branch of the arms, which radiates into divergent branches that feed the anterior and posterior compartments of the distal arm. The iliac and femoral arteries form a junction that extends as the primary branch of the legs, which then radiates into

divergent branches that feed the anterior and posterior compartments of the distal legs. An increasingly diminutive network of vasculature radiates into the tissue peripheral to all major vascular structures.

In the high-altitude cohort, early color change presented as a 'blush' orange or maroon and was defined by initial color change in the face, neck, hands, and feet. Each of these anatomical landscapes are peripheral to the core, and are terminally tissue bound when considered in terms of gravitationally mediated fluid gradients. Color change in the head/neck was characterized by discoloration peripheral to the face; the face frequently presented periocular discoloration. This pattern of early color change is consistent with the anatomical location of the major craniofacial vasculature. Color change in the distal limbs may be attributed to the relationship between gravity and fluid gradients, within which no-longer-circulating blood is passively transported by downslope gravitational flow and pools in the tissue bound extremities.

Cranially, discoloration temporally progressed toward diffuse discoloration of the face and neck, increased vibrancy, and prominent discoloration of the nose and cheeks. Postcranially, color change in the distal limbs increased in diffusion and vibrancy. This pattern is consistent with the progressive staining of the surrounding tissue via progressively smaller vasculature (capillaries and anastomoses). Postcranially, the neck, midline chest, and distal arms and legs presented a light shade of orange or maroon that became more vibrant as ADD increased. Concomitantly, the central abdomen presented a focal orange or maroon blush. The second generation of color change mirrors the major vascular system - the cardiac and pulmonary complexes (chest) and the descending aorta and major organ branches (abdomen).

The third phase of color change was characterized by first generation tissue sloughing in the face, resulting in a new phase of color vibrancy. Lateral extension of chest discoloration was observed, resulting in diffusion into the shoulders. Discoloration of the distal limbs advanced to diffuse and vibrant, and began extension into the proximal arms and legs, typically as a vibrant orange or maroon

blush that may be mottled with rose/maroon or rose/orange. The abdomen and lateral chest became more homogenously colored but remained anatomically circumscribed by a bridge of fresh tissue.

The fourth phase was defined by a second generation of prolific facial tissue sloughing resulting in gray/plum discoloration. While the TBS model describes a gray to green discoloration, this phase is associated with very early decomposition. The plum/gray observed in this study presents in intermediate to late-stage decomposition and is foundationally derived from the vibrant orange/maroon that precede it. Tissue discoloration in the proximal arms began to bridge with the lateral shoulders and lateral thorax. Abdominal discoloration presented more diffusely and slowly began to coalesce with the lateral chest and inguinal region. The proximal and distal arms and legs also began to coalesce, resulting in diffuse discoloration of the hands/feet and distal arms/legs with a zone of coalescence in the area of the elbow/knee, fading into a diffuse vibrant orange, maroon, or a mottled orange/maroon/rose in the proximal limbs.

Late-stage color change was defined by complete coalescence in areas retaining fresh tissue bridging and diffuse vibrancy. This was followed by the phasic loss of vibrancy (e.g. areas of diffuse maroon faded to a deep plum, orange faded to a yellow/orange ombre followed by pale yellow) relational to anato-spatial temporality of early color change (i.e. loss of vibrancy began in the face and distal limbs and generally followed the above-described trajectory). Finally, color change advanced to mottled umber, followed by pale yellow, and finally a pale brown.

The pattern of color change and its relationship to the circulatory system are important considerations both because of the distinctive pattern and presentation observed at high-altitude, and because of its hypothesized relationship with a number of the categorical changes observed at high-altitude. Gill-King (2006) provides a comprehensive overview of the chemical and physical interactions that define the trajectory of human decomposition. Within this matrix, the conversion of heme to bile

pigments, and the precipitation and diffusion of hydrogen sulfide (H_2S) within blood vessels and tissue are identified as the primary progenitors of color change.

The conversion of heme to bile pigments involves a cascade of physiological events that serve to remove old and damaged erythrocytes from circulation and recycle iron ions. This process is outlined in detail by (Kalakonda *et al.* 2023) and summarized in simplified form here. Senescent erythrocytes are phagocytized by macrophages in the bone marrow, liver, and spleen. Iron ions are bound by transferrin, a metal binding protein that facilitates transport to: (1) the liver where it is transferred to ferritin for storage, or (2) to locations of hematopoietic bone marrow for production of new generations of erythrocytes. Concomitantly, the heme portion is cleaved into biliverdin (green pigment) for transport through the circulatory system and subsequent conversion to bilirubin (yellow-orange pigment) by biliverdin reductase. Biliverdin reductase reactions occur within the reticuloendothelial system (liver, spleen, and lymph nodes), which produces a tightly compressed structure bound by hydrogen, rendering the molecule essentially insoluble in aqueous solutions at neutral pH. Transport of plasma liberated bilirubin to the liver is facilitated by association with the liver protein albumin. The albumin-bilirubin complex functions as both a transport and corralling mechanism. The albumin-bilirubin complex transports bilirubin to the liver, where pigment-albumin disassociation occurs, followed by hepatocyte uptake, conjugation, and secretion in the form of bile. The binding of albumin further serves to corral bilirubin by limiting the pigment's escape from the vascular space, preventing its precipitation and deposition in tissues. While this physiological cascade appears to be elegantly orchestrated, it is physiologically inefficient - first pass clearance of bilirubin through hepatocytes is approximately 20% - resulting in the release of unconjugated bilirubin bound to albumin into venous circulation.

While the liver constitutes a primary reservoir of bile pigments (to which early abdominal color change has been classically attributed), macroscopic consideration of the physiological cascade of their movement clearly demonstrates that bile pigments are present in varying concentration throughout the

circulatory and reticuloendothelial system. In early decomposition, hydrolases liberated by lysing pancreatic cells attack biliary structures, releasing pigments into circulation and surrounding tissue structures, facilitating their facultative presentation in the overlying dermis. Biliverdin presents along a blue-green spectrum while bilirubin presents along a yellow-orange-red spectrum; pigment presentation is dependent upon oxidation state and local pH. As the local tissue environment increases in acidity, bilirubin is reduced to urelobin which presents along the yellow-brown spectrum. Because pigment presentation is relational to oxidation state, the greater availability of oxygen to superficial tissues typically results in distinct pigment presentation. As decomposition advances, the suite of hemoproteins (e.g. hemoglobin, cytochromes, myoglobin, etc.) undergo degradation throughout all tissue structures, resulting in widespread tissue discoloration.

Hemoproteins are extremely sensitive to oxidation, the relationship of which is directly reflected in their pigment presentation. Foundationally, hemoproteins present along the red spectrum, but tissue oxidation yields specificity. Considering high-altitude tissue color change in the context of myoglobins yields a compelling explanatory model. In a highly oxygenated state, myoglobin (a primary protein in skeletal and heart muscle) presents along a vibrant maroon-red spectrum (oxymyoglobin). When myoglobin is unbound by oxygen (deoxymyoglobin), it presents along a purple-maroon spectrum. Finally, when the iron ion is oxidized (metmyoglobin) it presents along a deep maroon-brown spectrum. Myoglobin is monomeric, making binding non-cooperative (the binding of a ligand does not affect the affinity of a second ligand site), yielding a hyperbolic oxygen saturation curve – as concentration of oxygen increases, saturation occurs and levels off. This demonstrates that myoglobin has a high affinity for oxygen, binds oxygen strongly, and is reticent to release oxygen easily. The *in vivo* chemical interactions that define the hyperbolic oxygen saturation curve are purported to progress to a parabolic curve postmortem, when affinity is physically no longer under physiological control, and subject to exogenous chemical control.

The myoglobin oxygenation cycle is consistent with the pattern and trajectory of tissue color change observed at high-altitude. This trajectory was defined by: (1) phasic color change (due to the additive quality of oxygen binding); (2) ombre and/or mottled color change (a relational gradient of colors purported to be the result of myoglobin's non-cooperative property); and (3) apogetic (phasic increase in diffusion and vibrancy followed by phasic decline in the same properties) purported to reflect the parabolic oxygen saturation curve. The oxygen binding curve is defined by fractional oxygen saturation of the protein (y-axis) and the partial pressure of oxygen in the environment (y-axis). Because the hyperbolic oxygen saturation curve is fundamentally sensitive to the partial pressure of atmospheric oxygen (pO_2), the high-altitude environment – characterized by low oxygen concentration – would spend a protracted amount of time climbing before saturation leveled off and began to decline. This phenomenon provides one explanatory model for the overall consistent pattern of color change among donors (all microscopically sensitive to the fundamental principles of pO_2), the environment specific mode and presentation of color change (macroscopic sensitivity to pO_2), and variable presentation within and between microenvironments (e.g. seasonal availability of elements which may interfere with oxygen saturation postmortem). Summarily - while an oversimplification of the multilinear process of tissue change - this may explain why the predominant spectrum of tissue discoloration at high-altitude is so unique. Lower altitude sites achieve rapid oxygenation of myoglobin due to high concentration of pO_2 and therefore one mode of tissue discoloration (e.g. vibrant maroon or vibrant orange) may never have the opportunity to present. Because pO_2 is a gradient directly related to elevation gain, higher altitude sites may variably present a similar spectrum of color change which may have a temporal (e.g. seasonal) or atmospheric (e.g. barometric pressure affecting pO_2 in the time surrounding death) component.

While the underlying physiological process propagating tissue color change is a relative constant, the pattern and spectrum of tissue discoloration is not constant across microenvironments. Neither the color spectrum, nor the trajectory of color change described in the TBS model was observed at high-

altitude. The systemic distribution of bile pigments and their sensitivity to partial pressure of atmospheric gasses (oxidation) provide a foundation for understanding region specific presentation of postmortem tissue discoloration. Two primary tissue discoloration trajectories were observed at high-altitude: (a) maroon/red/purple dominant, and (b) vibrant orange dominant. The dominant systemic bile pigment (bilirubin) and the degradation of hemoproteins are among the primary contributors to postmortem tissue discoloration, are extremely sensitive to pO_2, and collectively constitute an orange-red-maroon-purple color spectrum that is consistent with the tracts observed in this study. While oxidation is a key component in the trajectory of discoloration (orange dominant versus maroon dominant), the contribution of temperature, hydrogen, and pH cannot be overlooked. However, as a foundational explanatory model, the relationship between bile pigments, hemoprotein oxidation and degradation, and atmospheric pressure provide a compelling index for the local patterns of observed color change.

8.4.2 Tissue sloughing

Considerable space has been dedicated to the underlying physiological and mechanical processes purported to affect local patterns of color change because of their tangential relationship to related, but distinct categories of transformation. Tissue sloughing presented in 'dynamic,' and 'idle' forms. Both modes were invariably associated with observation of color change in the underlying tissue. The processes of sloughing and color change are inferred to be the result of mechanical strain, vasculature, precipitation and diffusion of H_2S throughout blood vessels and tissue structures, and time. In addition to hemoprotein degradation and oxidation, Gill-King (2006) identifies precipitation and diffusion of H_2S within blood vessels and tissue structures as a primary progenitor of color change. Dynamic color change is associated with proliferation of blood vessels by H_2S during putrefaction, followed by progressive diffusion into the extracellular fluid of surrounding tissues. Hydrogen sulfide catalyzes decomposition of hemoglobin, the byproducts of which are responsible for staining vascular

intima, and subsequent staining of surrounding tissues. Gas planes created during tissue proliferation result in cellular separation of once intimate structures, resulting in tissue planes variable in vascular density, with deep layers containing primary, large structure vasculature that decrease in size but increase in density across progressively superficial planes.

The synthesis of hemoprotein degradation and oxidation, the anatomy and physiology of the vascular system and tissue structure, and the formation of tissue planes catalyzed by H_2S diffusion lends insight into contiguous but distinct phases of tissue sloughing and color change. As H_2S diffusion progresses throughout early decomposition and facilitates tissue plane formation, each layer varies in volume of extracellular fluid and density of vasculature from which decomposing, pigment bound hemoglobin may diffuse. 'Dynamic' tissue change is hypothesized to be the result of holistic structural change as the body metamorphizes in form and density. As the body expands and contracts through processes such as fluid loss and bloat, exposed tissue responds mechanically. This process is further complicated by extrinsic factors interacting with tissue, such as cyclical introduction of moisture which increases tissue volume, followed by subsequent drying and retraction through interaction with the atmosphere. When discontinuity in volume and shape of body mass and the most superficial tissue layer(s) is sufficient, mass sloughing occurs, revealing the color change presented by the underlying tissue layer.

Similarly, 'idle' tissue sloughing observed in advanced decomposition is demonstrative of the increasingly finite relationship between tissue approaching desiccation and mechanical stress and strain. While less pronounced in advanced decomposition, tissue remains sensitive to the influence of intrinsic and extrinsic variables. For example, tissue retains hygroscopic characteristics throughout decomposition, facilitating cyclical hydrogen exchange resulting in mechanical expansion and contraction throughout associated phases of hydration and dehydration. Because the body contains overall less fluid volume in advanced decomposition, expansion and contraction potential is limited to the volume uptake

potential of desiccated tissue. While less sensitive to volume change, desiccated tissue is characterized in part by decreased elasticity. The composite of finite expansion and contraction and loss of elasticity make exposed surfaces more vulnerable to uplift and sloughing catalyzed by environmental transport of exfoliant materials. Ultimately dynamic and idle tissue sloughing represent opposite poles of the same spectrum. As the cellular and chemiophysical properties that maintain tissue structure and facilitate chemical exchange between the environment and human remains diminish in capacity across the postmortem interval, physical change is rendered commensurately imperceptible. Like dynamic tissue sloughing, idle tissue sloughing is mediated by separation of tissue layers, however idle tissue sloughing is gradual, facilitating maintenance of the overall structure of a separating tissue layer as it migrates away from the body, resulting in diffuse areas of opacity, followed by a 'shatter event' (likely catalyzed by an environmental exfoliant). The result is tertiary or quaternary phase color change that appears spontaneous, but is the result of gradual uplift followed by the sudden exposure of a new tissue plane.

8.4.3 Fluid Bloat and Tissue Island Formation

Both fluid bloat and tissue island formation (differential decomposition) are purported to be the result of gravity acting on the diffusion of fluid through tissue gradients. Downslope oriented, enclosed tissue structures (hands/feet, neck/cranium) invariably presented fluid bloat. While fluid bloat was a distinct categorical change within the high-altitude cohort, the general relationship between gravity and fluid migration suggests that it may present in any environment within which a sufficient slope is present. However, the possibility of a relationship between tissue characteristic and preservation and high-altitude extrinsic variables acting upon the presentation of a categorical change should not be ignored. Fluid bloat therefore serves as a categorical change, and an exercise in separating 'universal' principles from local aggregate of variables which may make a categorical change unique.

While distinct in presentation, a perceptible pattern of tissue island formation could not be discerned. The trait was invariably associated with or the byproduct of rapid drying of the proximal

epidermis. This suggests a complex relationship between the increased UV exposure associated with high-altitude and the gravity induced movement of fluid through tissue gradients. Just as fluid bloat is the likely byproduct of gravity (a universal variable) and environment (a specific suite of variables), tissue island formation appears to more clearly represent the confluence of universal and environment specific variables. As phasic categories of change, and as potentially representative of the cross-section between universal-local variables, both fluid bloat and tissue island formation warrant future, higher-resolution, targeted study.

8.4.4 Adipocere Formation

Extensive attention has been dedicated to adipocere formation both in controlled study and in case study, yet current knowledge of the mechanism of adipocere formation remains limited and a single accepted model is lacking (Magni *et al.* 2021). Adipocere formation is generally recognized to be the result of interaction between postmortem decomposition of adipose tissue, intrinsic lipases, and enzymatic activity associated with microorganisms colonizing the respiratory and intestinal tracts (Yan *et al.* 2001). Presence of sufficient adipose tissue, moisture, mildly alkaline pH, warm temperatures, bacteria, and overall anaerobic conditions are the widely agreed upon variables conducive to adipocere formation (Clark *et al.* 2006). However, significant debate exists over the mechanisms or interaction between mechanisms governing each category of change. In an impressive review of adipocere research and case study, Magni *et al.* (2021) present three prevailing theories for the chemical mechanism of adipocere formation (fat migration theory, saponification theory, and hydrogenation theory). However, the authors observe that while each of the theories explain some aspects of adipocere formation, all fail to explain all aspects of its development.

In the oxygen depleted postmortem tissue environment, anaerobic microorganisms - the metabolism of which aids in adipocere formation - are afforded the opportunity to flourish. Antecedent aerobic species are of equal importance, as their metabolic activity further depletes tissue oxygen,

creating an environment in which anaerobes thrive. Just as chemical mechanisms are holistically understood but lack theoretical precision, the role of the microorganism is commensurately complex. A multitude of microorganism species are associated with different modes of lipid conversion. *Bacillus subtilis, Staphylococcus aureus*, and *Micrococcus luteus* are all examples of species capable of facilitating the conversion of oleic to hydroxy fatty acids, while species such as *Flavobacterium meningosepticum* and *Micrococcus luteus* are further capable of catalyzing conversion of hydroxy fatty acids to oxo fatty acids (Magni *et al.* 2021). The relevance of conversion minutiae is found in theory surrounding the composition, characteristics, and stabilization of adipocere, believed to be the result of various composites of fatty acids (Takatori & Yamaoka 1977). Additional variables, such as temperature, pH, and presence of H_2O available to influence chemical reactions further complicate a concise understanding of adipocere formation. The implication is that the potential for identifying a 'universal formula' for adipocere formation is tenuous. Rather, the variables within the local environment that serve to foster or arrest the survival of specific bacterial species and facilitate chemical processes may have a greater influence on adipocere formation, stabilization, and degradation than a predictable set of standards.

In their extensive review of adipocere formation, Magni *et al.* (2021) observe that the majority of empirical study has been performed through the use of human analogues (typically pigs), while human data derived from case studies provide point observation of an individual, but lack the benefit of longitudinal observation. Adipocere formation was an unexpected outcome of decomposition at high-altitude. While formation and degradation were superficially documented, the apparent lack of controlled, longitudinal study of adipocere formation within a cohort of human remains suggests that a substantial contribution may be made to the literature through future, directed study.

8.4.5 Slope Roll and Pseudoburial

Human remains are sensitive to postmortem interaction with the environment, regardless of geographic location. However, environmental variables such as local scavenger guilds, terrain type,

vegetation, and patterns of atmospheric change collectively create a local signature for taphonomic change. While variation between cases will almost invariably exist, a macroscopic understanding of the concert of local variables affecting postmortem change is critical to informing both search and recovery efforts and patterns of taphonomic overprinting which may affect subsequent laboratory analysis.

Because the loss of skeletal elements due to scavenging by large-bodied vertebrates and skeletal scatter were a concern, donors were placed in cages that precluded observation of natural patterns of slope roll. However, the length of the cages and the downslope orientation of donors facilitated observation of early movement. The primary catalysts for movement of skeletal elements downslope were (1) the passive result of avian scavenging during both active tissue exploitation and intragroup squabbling; (2) the effect of gravity on the steep slope; (3) the effect of sudden, high-volume rainstorms; and (4) the movement of sediment downslope due to atmospheric variables such as rain, wind, and snow. Holistically, the passive movement of skeletal elements progressed relatively slowly. However, two donors were heavily scavenged and disarticulated by a red-tailed fox during an act of cage security transgression. In this case, skeletal elements were disarticulated and rapidly displaced during the primary scavenging event, and in the weeks following by both small-bodied scavenging vertebrates, and downslope wash. This demonstrates the disconnect that may occur between the parameters necessarily imposed on controlled study and natural circumstance. An attempt to mitigate this disparity was made in preceding scavenger behavior studies performed using pigs as a human analogue (Baigent *et al.* 2019), but future study would benefit from expanding the empirical model to include study of large-bodied scavengers, while maintaining the ethical boundaries associated with both human donors, and local populations at risk for unwanted interaction with human remains.

The type and extent of pseudoburial observed in this study was unexpected when considered in practical case context. Like slope roll, pseudoburial was catalyzed by (1) active; (2) passive; and (3) animal mediated processes. Both passive (adherence of environmental sediment to ceraceous tissue

surfaces), and animal mediated (superficial passive burial as a result of burrowing or scavenging behavior) trended toward mild to moderate concealment of human remains. The impact of each was variably amplified (due to the additive effect of repetitive exposure) or tempered (due to removal of debris by wind, rain, etc.) as PMI increased. The 'active' mode of pseudoburial (movement of surrounding matrix downslope by environmental processes such as transport of soil and rock by gravity and water) proved to be the most dramatic. In several cases, the body acted as an obstacle to downslope movement of debris, resulting in infill of open body cavities and in some cases, complete burial of affected body parts. Greater consideration of this process should be integrated into future outdoor search models and simple excavation of areas containing skeletal elements and environmental signs of slope wash should be integrated into search and recovery protocol.

8.5 Forensic Ecological Profile

A major goal of this project was to establish a holistic taphonomic profile (forensic ecological profile) of the high-altitude Colorado Rocky Mountain Region. This profile was proposed to include atmospheric variables, invertebrate and vertebrate behavior, and local human behavior. Study was achieved through data derived from an onsite weather station, field observation of scavenger behavior, analysis of census, land use, and zoning data, the categorization and interpretation of extant local ethnography, and forensic case study. Because atmospheric variables have been subject to extensive discussion, they will not be presented in repetition here.

8.5.1 Scavenger Behavior

Superficially, the exclusion of large-bodied scavengers may be viewed as a shortcoming of this study, however this afforded the opportunity to observe behavior and taphonomic overprinting specific to small-bodied scavengers. This behavior would otherwise be obscured by the more impactful imprint of large-bodied scavengers. The importance of these data is apparent in cross-sectional analysis of case study, where the presence of avians and packrats was observed, and their scavenging inferred, but

where a lack of data precluded identification of specific behavior that may inform skeletal change or movement of elements through the environment. Additionally, the local case study analysis described the behavior of large-bodied scavengers that could not be observed in this study. This demonstrates the power of the relationship between empirical and case study data. While practitioners are limited to case-specific, point presentation of human decomposition and taphonomic change, these cases and associated specifics are not controlled, yielding data that may be otherwise unobservable in controlled study. Conversely, controlled study provides longitudinal data that the practitioner is not otherwise afforded the opportunity to observe, enhancing the local understanding of decomposition and environmental entanglement. Data derived from both models presents an opportunity to formulate new research questions, devise new study designs, and to develop novel modes of data dissemination. The elegant relationship between research and practice demonstrates the importance of both interdisciplinary study and the need for strong relationships between the medicolegal community, and academics concerned with the forensic sciences.

8.5.2 Census, Land Use, and Ethnographic Data

Demographic data demonstrated a local population that trended toward older, White, male, and conservative. Census data further revealed an almost complete lack of racial diversity among Park County residents (91% White, 7% Hispanic). Concomitantly, ethnographic analysis identified racial disparity in recreational land use. This disparity is demonstrated not only by systemic functional barriers that preclude racial diversity in outdoor recreation, but in many cases, a strong cultural aversion characterized by multigenerational boundary construction and maintenance. This behavior is demonstrative of Ingold's (2000) environmental perception theory, which states, in part, that perception of the environment is an ongoing, dynamic project with historic, spatial, and temporal relevance. Rather than choosing not to engage with Colorado's rural mountainous regions, ethnography performed among Black Colorado residents revealed active avoidance of the region. Ingold (*ibid*) provides a theoretical

framework within which to understand avoidant behavior, as he argues that human perception of the environment is an ongoing project brokered by skills incorporated into the human organism through practice and training in the environment. Historicity that fosters avoidance, and lack of incorporated skills through practice and training result in othering of the rural, natural environment thereby further fostering avoidance. Summarily, theory and data support the conjecture that the local population structure has the capacity to inform the transient population structure, as both are reflective of who is willing to engage with a specific environment, whether in recreation or nefarious activity.

Census data is arguably limited in utility due to the inherent reflection of those willing to participate in data provision. However, census participants constitute a group, and therefore the subsequent data serves to provide a baseline from which to identify divergence. Using census population data as a baseline, the cross-section of census housing data, GIS data, case study, and information provided by members of the local medicolegal community (informal ethnography) revealed a local 'hidden' population composed largely of single white men in their fifties and sixties who have elected to live 'off grid,' in unconventional housing. Known atypical housing ranges in novelty from recreational vehicle (RV) to partially subterraneous, hand-hewn log structure, though there is undoubtedly a broader range of yet-to-be-discovered (intentionally hidden) innovative housing throughout the complex, rural region. Depending on land ownership and use, several formal sanctions – such as zoning and citation laws - exist in an attempt to dissuade off grid housing. Additionally, the local lexicon contains several pejorative referents to the group, indicative of an additive system of negative informal sanctions imposed upon the group. Despite these sanctions, the population both grows and persists. This is one example of a fascinating line of potential study in cultural anthropology identified through the development of the forensic ecological profile in the course of forensic taphonomy investigation. Collectively, this is demonstrative of the unique academic orientation of forensic taphonomy and the potential for the discipline to truly embrace a four-field approach to forensic investigation.

Group closure is not limited to Park County's 'invisible' communities. Cannabis economy revealed a new population within which participants span the spectrum of human behavior from criminal to artistic. Cannabis economy further identified a fissure in the local community, the poles of which are defined by resistance to, and abutment of, cannabis production and sales as a beneficial economic avenue. Baseline demographic data further served to inform local modes of community structure, division, conflict, and resistance. In a seminal ethnography pertaining to Colorado's Rocky Mountain region, Graber (1974) described the nature and structure of conflict between newcomers and longtime residents, a pattern that persists in modern cultural configuration almost 50 years later (Mountain Migration Report 2021). Foundational to modern conflict is a dire lack of housing for local residents, the use of Park County as a bedroom community for neighboring wealthy counties with little economic benefit, and the use of Park County residents as an underpaid labor source. This disaffection is publicly conspicuous in symbolism and language use, and further demonstrated by study of local median rent versus income, limited availability of public transportation with guided access to neighboring wealthy communities, and local housing and vacation rental statistics. Additionally, several of the forensic cases studies presented (involving lengthy, intricate, dangerous, and resource driven recovery missions) involved out-of-county visitors, further serving to demonstrate the unilateral designation of resources devoted to out of county residents and the internal frustration born of the skewed relationship.

The "newcomer" versus "longtime resident" fissure inaccurately portrays homogeneity within the longtime resident group. Those most affected by the housing crisis and labor market belong to younger, less-established generations who grew up in-county, or more typically, migrated to the area and have a residency history sufficient to qualify as a longtime resident. This group tends to lean more liberal and is generally more receptive to perceived beneficial economic change such as cannabis economy. A second group of longtime residents is characterized by multigenerational landowners, most

typically subsisting on agriculture. This community is less affected by concerns associated with the housing and labor markets, but is impacted by social change associated with cannabis culture, environmentalism, land use, and the post-COVID influx of (often urban) “newcomers.” Patterns of land use and subsistence constitute a valuable data source in the construction of the forensic ecological profile and provide the resolution necessary to discern intragroup variation. Zoning, land use, political data, the primacy of agriculture in economic subsistence, and formal sanctions such as the Right-to-farm and Ranch law demonstrate a local allegiance to conservative, ‘traditional,’ values that intentionally situate the community in opposition to (assumed) ‘liberal’ or ‘environmentalist,’ newcomers. While data aids in the general construction of cultural groups, an understanding of primary modes of local subsistence further informs modes of interaction and engagement with the local environment, which includes modes of manipulation.

From a practical perspective, agriculturalism is associated with a suite of tools and heavy machinery, the operators of which are presumed to be proficient. Further, local recreation centers upon varying levels of familiarity with the backcountry, and the use of firearms, boats, snowmobiles, ATVs, and ORVs all of which are associated with unique knowledge of, and relationships with, the local environment. ATVs and ORVs, in particular, are associated with a ‘hidden,’ complex formal and informal infrastructure of backcountry roadways that yield access to largely unknown pockets of the county. Case study analysis demonstrated the use of ATVs, backhoes, and helicopters in search and recovery efforts, the use of which should be regarded as bilateral as those used to recover may in turn also be used to conceal.

8.6 Conclusion

This tripartite study sought to (1) test the qualitative and quantitative aspects of the TBS model in a high-altitude environment to assess the suitability of application in the estimation of local postmortem interval; (2) establish the rate and pattern of human decomposition, isolate and describe

phasic patterns of soft tissue change throughout the trajectory of decomposition, and test seven atmospheric variables to assess the utility of integrating atmospheric data beyond accumulated degree days into PMI estimation in a high-altitude environment; and (3) develop a region specific bioecological profile with an emphasis on the integration of human behavior in a high-altitude environment. Both the qualitative and quantitative aspects of the TBS model failed to perform at high-altitude. Based on the result of these analyses, the TBS model should not be applied to PMI estimation in a high-altitude setting, which necessitates the development of new models to encapsulate the changes observed in the high-altitude environment. Toward that end, five phasic, categorical patterns of gross tissue change were identified in this study, supplemented by two broad categories of taphonomic change. While several of these phenomena have been individually described in a diversity of environments, the suite is unique to the high-altitude environment investigated in this study. Further, an analysis of seven atmospheric variables identified three variables that described the variation in decomposition as well or better than temperature using accumulated degree days. The identification of a phasic suite of soft tissue change and atmospheric variables with predictive power beyond ADD is highly suggestive of future success in region-specific predictive model building. Finally, the aggregate study of local scavenger behavior, census and land use data, extant ethnographic study, and forensic case studies successfully established a foundational forensic ecological profile and fulfilled the goal of encapsulating human behavior, although future study will benefit from a more precise integration model.

The TBS model constituted a groundbreaking addition to forensic taphonomy research that has sparked interest in validation and comparative study across the world. While the model is not appropriate for use in this high-altitude environment, the model's contribution to the discipline cannot be overlooked, as it served as the basis for comparison and identification of unique traits in this study. However, the environment specific inadequacy of the TBS model to predict postmortem interval also cannot be overlooked, and emphasizes the need for high-resolution, environment specific research and

model building. Just as decomposition is environment specific, so is the forensic ecological profile. This study has introduced one, largely desk-based model inclusive of cultural anthropology, used to encapsulate local patterns of behavior. Like all forms of region-specific study, this profile is local and mutable, but serves as a foundation that will benefit from the addition of multidisciplinary study. Summarily, in both the study of rate, pattern, and trajectory of human decomposition, and in behavioral characteristics encapsulated by the local environment, this study underscores the need for holistic, environment specific model building, the units of which will build a collective within which to understand patterns of continuity and divergence.

REFERENCES

Aguilar J (2022). Four Towns Just Said No to Marijuana Sales, But How Strong is Rural Colorado's Distaste for Weed? The Denver Post. https://www.denverpost.com/2022/05/04/marijuana-rural-urban-hooper-election-legal-sales/. Accessed 01/20/2024.

Ahrens CD, Hensen H (2018). Essentials of Meteorology: An Invitation to the Atmosphere. Eighth Edition. Boston, MA, Cengage Learning.

Allaire MT (2002). Postmortem Interval (PMI) Determination at Three Biogeoclimatic Zones in Southwest Colorado. Master's Thesis, Louisiana State University, Agricultural and Mechanical College.

Anand AC, Sashindran VK, Mohan L (2006). Gastrointestinal problems at high altitude. *Tropical Gastroenterology.* 27(4):147-153.

Andrade C (2020). Sample Size and its Importance in Research. *Indian J Psychol Med.* 42(1):102-103.

Armelagos GJ (2011). Histories of Scholars, Ideas, and Disciplines of Biological Anthropology and Archaeology. *Reviews in Anthropology.* 40:107-133.

Baigent CI, Gaither CM, Campbell C (2014). The effect of altitude on decomposition: a validation study of the Megyesi method. *Proceedings of the American Academy of Forensic Sciences.* 20:485-486.

Baigent CI, Connor MA, Dabbs GR (2019). Introducing FIRS-TB40: Scavenger Succession and Progression at a High-Altitude site in Colorado. *Proceedings of the American Academy of Forensic Sciences.* 25:127.

Baigent CI, Agan C, Connor M, Hansen ES (2020). Autopsy as a form of evisceration: Implications for decomposition rate, pattern, and estimation of postmortem interval. *Forensic Sci. Int*. 306(1):1-8.

Baigent CI (2023). Summit County Coroner's Office 2022 Annual Report. Summit County Government Office of the Coroner. https://www.summitcountyco.gov/132/Annual-Reports. Accessed 1/10/2024.

Bailey RG (1995). Description of the ecoregions of the United States. 2nd edition revised and expanded (1st edition 1980) Edition. Misc. Publ. 1391 (rev.). Washington, DC: USDA Forest Service. 108 pages with separate map at 1:7,500,000 https://www.fs.fed.us/land/ecosysmgmt/index.html

Bass WM (1997). Outdoor decomposition rates in Tennessee. In: Haglund W, Sorg M, eds. Forensic taphonomy: the postmortem fate of human remains. Boca Raton, FL: CRC Press; 181–186.

Basso K (1970). "To Give up on Words": Silence in Western Apache Culture. *Southwestern J. of Anthropology.* 26(3):213-230.

Basso K (1988). "Speaking with names": Language and Landscape among the Western Apache. *Current Anthropology.* 3(2):99-130.

Beall CM, Goldstein MC (1987). Hemoglobin Concentration of Pastoral Nomads Permanently Resident at 4,850-5,450 Meters in Tibet. *Amer. J. Physical Anthropology.* 73:433-438.

Berman L (2021). Cannabis Capitalism in Colorado: An Ethnography of Il/legal Production and Consumption. Doctoral Dissertation, University of South Florida. Scholar Commons. https://scholarcommons.usf.edu/etd/8735. Accessed 01/20/2024.

Betz M, Valley M, Lowenstein S, Hedegaard H, Thomas D, Stallones L, Honigman B (2011). Elevated suicide rates at high altitude: sociodemographic and health issues may be to blame. *Suicide Life Threat. Behav*. 41(5):562-573.

Birkby WH, Fenton TW, Andersen BE (2008). Identifying Southwest Hispanics Using Nonmetric Traits and the Cultural Profile. *J. Forensic Sci*. 53 (1):29-33.

Blatter J, Haverland M (2012). Designing Case Studies: Explanatory Approaches in Small-N Research. New York, NY: Palgrave Macmillan.

Bourdieu P (1977). Outline of a theory of practice. Cambridge, NY: Cambridge University Press.

Bushan Aparna. 2015. An Evaluation of the Effects of the Legalization of Marijuana in Colorado and Washington from an International Law Perspective. Can.-USLJ 39: 187-202.

Calcagno JM (2003). Keeping biological anthropology in anthropology, and anthropology in biology. *Am. Anthropologist.* 105(1):6-15.

Campanacho V, Alves Cardoso F, Ubelaker DH (2021). Documented skeletal collections and their importance in forensic anthropology in the United States. *Forensic Sci.* 1(3): 228-239.

Cannings R (2005). The Rockies: A Natural History. New York : Greystone Books.

Census Reporter (2023). Park County Colorado. https://censusreporter.org/profiles/05000US08093-park-county-co/. Accessed 01/29/2023.

Christensen AM (2004). The impact of Daubert: implications for testimony and research in forensic anthropology (and the use of frontal sinuses in personal identification). *J. Forensic Sci.* 49(3):427–430.

Christensen AM, Crowder CM (2009). Evidentiary Standards for Forensic Anthropology. *J. Forensic Sci.* 54(6):1211-1216.

Clark MA, Worrell MB, Pless JE (2006). Postmortem changes in soft tissues. In: Haglund H, Sorg M editors. Forensic taphonomy: the postmortem fate of human remains. Boca Raton, FL: CRC Press. 151–64.

Cleveland WS (1979). Robust Locally Weighted Regression and Smoothing Scatterplots. *J. of the American Statistical Association*. 74:829-836.

Cleveland WS, Devlin SJ (1988). Locally Weighted Regression: An Approach to Regression Analysis by Local Fitting. *J. of the American Statistical Association.* 83:596-610.

Colorado Bureau of Investigations (2024). Uniform Crime Reporting (UCR) and Colorado Crime Statistics. https://cbi.colorado.gov/sections/crime-information-management-unit/uniform-crime-reporting-ucr-and-colorado-crime. Accessed 1/10/2024.

Colorado Parks and Wildlife (2022). Five Year Big Game Season Structure. Colorado Parks and Wildlife Game Commission. https://cpw.state.co.us/thingstodo/Pages/hunt.aspx

Congram D (2013). Deposition and Dispersal of Human Remains as a Result of Criminal Acts: *Homo sapiens sapiens* as a Taphonomic Agent. In: Pokines JT, Symes SA, eds. Manual of Forensic Taphonomy. Boca Raton, FL: CRC Press; 249-285.

Connor MA, Baigent C, Hansen ES (2018). Testing the use of pigs as human proxies in decomposition studies. *J. Forensic Sci*. 63(5):1350-1355.

Connor MA, Baigent C, Hansen ES (2019). Measuring Desiccation Using Qualitative Changes: A Step Toward Determining Regional Decomposition Sequences. *J. Forensic Sci*. 64(4):1004-1011.

Topping J (2021). 2021 Report of Deaths and Injuries Involving Off-Highway Vehicles with More than Two Wheels. Consumer Product Safety Commission chrome-extension://efaidnbmnnnibpcajpcglclefindmkaj/https://www.cpsc.gov/s3fs-public/2021-Report-of-Deaths-and-Injuries-Invoving-Off-Highway-Vehicles-with-more-than-Two-Wheels.pdf?VersionId=nm0R8oYxTu.mRD7KNRvNp95ogHw2SYOD

Cox M, Flavel A, Hanson I, Laver J, Wessling R (2008). The Scientific Investigation of Mass Graves. New York: Cambridge University Press.

Cromartie J, Bucholtz S (2008). Defining the "Rural" in Rural America. *USDA Feature: Rural Economy & Population.* https://www.ers.usda.*gov*/amber-waves/2008/june/defining-the-rural-in-rural-america. Accessed 01/20/2024.

Crowe S, Cresswell K, Robertson A, Huby G, Avery A, Sheikh A (2011). The case study approach. *BMC Medical Research Methodology.* 11(Article 100):1-9.

Dabbs GR (2010). Caution! All data are not created equal: the hazards of using National Weather Service data for calculating accumulated degree days. *Forensic Sci. Int*. 202(1–3):e49–e52.

Dabbs GR (2015). How should forensic anthropologists correct National Weather Service temperature data for use in estimating the postmortem interval? *J. Forensic Sci.* 60(3):581–587.

Dabbs GR, Connor M, Bytheway JA (2017). Interobserver reliability of the Total Body Score System for quantifying human decomposition. *J. Forensic Sci*. 61(2):445-451.

Dabbs GR, Martin DC (2013) Geographic variation in the taphonomic effect of vulture scavenging: The case for Southern Illinois. *J. Forensic Sci.* 58(S1):S20-S25.

Daubert v. Merrell Dow Pharmaceuticals Inc., 509 U.S. 579 (1993). https://supreme.justia.com/cases/federal/us/509/579/. Accessed 01/20/2024.

Dautartas A, Kenyhercz MW, Vidoli GM, Meadows Jantz L, Mundorff A, Steadman DW (2018). Differential decomposition among pig, rabbit, and human remains. *J. Forensic Sci.* 63(6):1673–1683.

Dawson BM, Wallman JF, Barton PS (2022). How does mass loss compare with total body score when assessing decomposition of human and pig cadavers? *Forensic Sci. Med. Path.* 18: 343–351.

DeJong G, Chadwick JW (1999). Decomposition and arthropod succession on exposed rabbit carrion during summer at high altitudes in Colorado, USA. *J. of Medical Entomology.* 36(6):833-845.

DiMaio VJ, DiMaio D (2001). Time of death. In: Forensic pathology. Boca Raton, FL: CRC Press; 21–42.

DTB Denver Tourism Board (2022). Denver Tourism Surges to 31M+ Visitors in 2021. https://www.denver.org/articles/post/denver-tourism-surges-to-31m-visitors-in-2021/. Accessed 9/29/2023.

Dupras TL, Schultz JJ, Wheeler SM, Williams LJ (2012). Forensic Recovery of Human Remains: Archaeological Approaches. Second Edition. Boca Raton, FL: CRC Press.

Dyson-Hudson R, Smith EA (1978). Human Territoriality: An Ecological Assessment. *American Anthropologist.* 80:21-41.

Efremov IA (1940). Taphonomy a new branch of paleontology. *Pan-American Geologist.* 74: 81-93
Erickson B, Johnson CW, Kivel BD (2009). Rocky Mountain National Park: History and Culture as Factors in African-American Park Visitation. *J. of Leisure Research.* 41(4):529–545.

Forbes SL, Perrault KA, Stefanuto PH, Nizio KD, Focant JF (2014). Comparison of the decomposition VOC profile during winter and summer in a moist, mid-latitude (Cfb) climate. *PLoS One*. 9(11): e113681.
Galloway A, Birkby WH, Jones AM, Henry TE, Parks BO (1989). Decay rates of human remains in an arid environment. *J. Forensic Sci.* 34:607–616.

Galloway A (1997). The process of decomposition: a model from the Arizona-Sonoran desert. In: Haglund H, Sorg M, eds. Forensic taphonomy: the postmortem fate of human remains. Boca Raton, FL: CRC Press. 139–150.

Gamer M, Lemon J, Fellows I (2022). Package 'irr'. R package version 0.84.1. https://CRAN.R-project.org/package=dplyr. Accessed 01/21/2024.

Gastil RG (1976). Cultural Regions of the United States. Seattle, WA: University of Washington Press.

GCT Government of Canada Tourism (2023). Travel and Tourism. https://travel.gc.ca/. Accessed 9/30/2023.

Geertz C (1973). The Interpretation of Cultures. New York, NY: Basic Books.

Georlette D, Blaise V, Collins T, D'Amico S, Gratia E, Hoyoux A, Marx JC, Sonan G, Feller G, Gerday C (2004). Some like it cold: biocatalysis at low temperatures, *FEMS Microbiology Reviews*. 28(1):25–42.

Gibson JJ (1979). The Ecological Approach to Visual Perception. Boulder, Colorado: Taylor & Francis.

Gill-King H (2006). Chemical and Ultrastructural Aspects of Decomposition In: Haglund, WD and Sorg, MH, eds. Forensic Taphonomy: The postmortem Fate of Human Remains. Boca Raton, FL: CRC Press; 93-107.

Girvin L (2023). Fairplay – The Funky, Fun, Charming Next-Door Neighbor of Breckenridge. Mountain Town Magazine, https://mtntownmagazine.com/fairplay-the-funky-fun-charming-next-door-neighbor-of-breckenridge/. Accessed 09/10/2023.

Graber EE (1974). Newcomers and oldtimers: Growth and change in a mountain town. *Rural Sociolog*y. 39(4):504–513.

Grivas CR, Komar D (2008). Kumho, Daubert, and the nature of scientific inquiry: implications for forensic anthropology. *J. Forensic Sci.* 53(4):771–776.

Gwet KL (2014). Handbook of Inter-Rater Reliability: The Definitive Guide to Measuring the Extent of Agreement Among Raters. Fourth ed. Gaithersburg, MD: Advanced Analytics.
Haglund WD, Reay DT, Swindler DR (1988). Canid scavenging/disarticulation sequence of human remains in the Pacific Northwest. *J. Forensic Sci*. 34(3):587–606.

Haglund WD, Reay DT, Swindler DR (1988). Tooth mark artifacts and survival of bones in animal scavenged human skeletons. *J. Forensic Sci*. 33(4):985–97.

Haglund WD, Sorg MH, eds. (1997a). Forensic Taphonomy: The Postmortem Fate of Human Remains, Boca Raton, FL: CRC Press.

Haglund WD, Sorg MH, eds. (1997b). Method and theory of Forensic Taphonomy research. In Forensic Taphonomy: The Postmortem Fate of Human Remains, ed. by WD Haglund and M H Sorg. Boca Raton, FL: CRC Press; 13-26.

Haglund WD, Sorg MH (2001). Advances in Forensic Taphonomy: Method, Theory, and Archaeological Perspectives. Boca Raton, FL: CRC Press.

Haglund WD, Sorg MH (2001). Advancing Forensic Taphonomy: Purpose, Theory, and Process. In: Haglund WD, Sorg MH, eds. Advances in Forensic Taphonomy: Method, Theory, and Archaeological Perspectives. Boca Raton, FL: CRC Press; 1-27.

Halfpenny JC, Tellander T [Illus] (2015). Scats and Tracks of the Rocky Mountains: A Field Guide to the Signs of 70 Wildlife Species (Scats and Tracks Series). Third Edition. Helena, MT: Rowman and Littlefield.

Haynes G (1983). A guide for differentiating mammalian carnivore taxa responsible for gnaw damage to herbivore limb bones. *Paleobiology* 9(2):164–172.

Hillier ML, Bell LS (2007). Differentiating human bone from animal bone: a review of histological methods. *J. Forensic Sci*. 52:249–263.

Hinton AL (2002). The Dark Side of Modernity. In: AL Hinton, ed. Annihilating Difference: The Anthropology of Genocide. Berkley, CA: University of California Press. 1-39.

Holtkamp C, Weaver R, Butler DR (2018). The Rocky Mountains and the Southwest: Using feature names to study two iconic subregions in the American West. *Geographical Review.* 108(3):410–432.

Hornsey MJ, Harris EA, Fielding KS (2018). The psychological roots of anti-vaccination attitudes: A 24-nation investigation. *Health Psychol*. 37(4):307–315.

Imraya C, Wright A, Subudhi A, Roache R (2010). Acute mountain sickness: pathophysiology, prevention, and treatment progress in cardiovascular diseases. *Prog. Cardiovasc. Dis*. 52(6):467–484.

Ingold T (2000). Perception of the Environment. Routledge: New York, NY.

Jacoby W (2000). Loess: a nonparametric, graphical tool for depicting relationships between variables. *Electoral Studies*. 19(4):577-613.

Jones N, Whitworth T, Marshall SA (2019). Blow flies of North America Keys to the subfamilies and genera of Calliphoridae, and to the species of the subfamilies Calliphorinae, Luciliinae and Chrysomyinae. Canadian Journal of Arthropod Identification. doi:10.3752/cjai.2019.39

Kalakonda A, Jenkins BA, John S (2023). Physiology, Bilirubin. In: StatPearls. Treasure Island (FL): StatPearls Publishing; 2023 Jan. https://www.ncbi.nlm.nih.gov/books/NBK470290/. Accessed 01/21/2024.

Keogh N, Myburgh J, Steyn M (2017). Scoring of decomposition: a proposed amendment to the method when using a pig model for human subjects. *J. Forensic Sci*. 62(4):986–993.

Kottek M, Greiser J, Beck C, Rudolf B (2006). World Map of Köppen-Geiger Classification Updated. *Meterol. Z.* 15(3):259-263

Komar DA (1998). Decay rates in a cold climate region: A review of cases involving advanced decomposition from the Medical Examiner's office in Edmonton, Alberta. *J. of Forensic Sci*. 43(1):57-61.

Komar D, Beattie O (1998). Identifying bird scavenging in fleshed and dry remains. *J. Can Soc Forensic Sci.* 31(3):177-188.

Kyunghoon M, Yangsoo S, Chongyoup K, Yejin L, Kyunghi H (2007). Heat and moisture transfer from skin to environment through fabrics: A mathematical model. *Inter. J. of Heat and Mass Transfer.* 50(25–26):5292-5304.

Leyton E (2005). Hunting Humans. McClelland and Stewart, Toronto, Ontario, Canada.

Lindstrom D (2010). Schaum's Easy Outline of Statistics, Second Edition. New York, NY: McGraw-Hill Education.

Liu J, Dalton AN, Lee J (2021). The "Self" under COVID-19: Social role disruptions, self-authenticity and present-focused coping. *PLOS ONE* 16(9): e0256939. https://doi.org/10.1371/journal.pone.0256939. Accessed 01/21/2023.

Listi GA, Manhein MH, Leitner M (2007) Use of the Global Positioning System in the Field Recovery of Scattered Human Remains. *J of Forensic Sci.* 52(1):11-15.

Love J, Marks M (2003). Taphonomy and Time: Estimating the Postmortem Interval.
In: Steadman DW, editor. Hard Evidence: Case Studies in Forensic Anthropology.
Upper Saddle River, NJ: Person Education, Inc. and Prentice Hall; 160-175.

Lu N, Chandar P, Tempesta D, Vincent C, Bajor J, McGuiness H (2014). Characteristic differences in barrier and hygroscopic properties between normal and cosmetic dry skin: Enhanced barrier analysis with sequential tape-stripping. *Int. J. Cosmet. Sci.* 36(2):167-174.

Magni PA, Lawn J, Guareschi EE (2021). A practical review of adipocere: Key findings, case studies and operational considerations from crime scene to autopsy. *Journal of Forensic and Legal Medicine* 78:102109.

Manheim MH, Listi GA, Leitner M (2006). The application of geographic information systems and spatial analysis to assess dumped and subsequently scattered human remains. *J. of Forensic Sci.* 51:469-474.

Marhoff SJ, Fahey P, Forbes SL, Green H (2016). Estimating post-mortem interval using accumulated degree-days and a degree of decomposition index in Australia: a validation study. *Aust. J. Forensic Sci.* 48(1):24-36.

Mazur P (1984). Freezing of living cells: mechanisms and implications. *Am. J. Physiol.* 247(3):C125-42.

McKenna ZJ, Pereira FG, Gillum TL, Amorim FT, Deyhle MR, Mermier CM (2022). High-altitude exposures and intestinal barrier dysfunction. *J. Physiol. Regul. Integr. Comp. Physiol*. 322: R192–R203.

Megyesi M, Nawrocki SP, Haskell NH (2005). Using accumulated degree-days to estimate the postmortem interval from decomposed human remains. *J. Forensic Sci.* 5(3):618- 626.

Meyer B (2021). Colorado Agricultural Statistics. United States Department of Agriculture National Agricultural Statistics Service Mountain Region, Colorado Field Office.

Micozzi MS (1997). Frozen Environments and Soft Tissue Preservation. In: Haglund H, Sorg M editors. Forensic taphonomy: the Postmortem Fate of Human Remains. Boca Raton, FL: CRC Press; 171-80.

Micozzi MS (1986). Experimental study of postmortem changes under field conditions: effects of freezing, thawing, and mechanical injury. J. Forensic Sci. 31(3):953-961.

Moleón M, Sánchez-Zapata JA, Margalida A, Carrete M, Owen-Smith N, Donázar JA (2014). Humans and scavengers: The evolution of interactions and ecosystem services. *BioScience.* 64:394–403.

Moffatt C, Simmons T, Lynch-Aird J (2016). An improved equation for TBS and ADD: Establishing a reliable postmortem interval framework for casework and experimental studies. J. Forensic Sci. 61(Suppl 1):S201-207.

Mountain Migration Report (2021). Are COVID Impacts on Housing & Services Here to Stay? Northwest Colorado Council of Governments, Colorado Association of Ski Towns, U.S. Economic Development Administration, and Colorado Department of Local Affairs. Summit County: CO.

MRLC Multi-Resolution Land Characteristics Consortium (2022). U.S. Geological Survey (USGS) Earth Resources Observation and Science (EROS) Center, Sioux Falls, SD. https://www.mrlc.gov/ Accessed 9/05/2022.

Myburgh J, L'Abbé E, Steyn M, Becker P (2013). Estimating the postmortem interval (PMI) using accumulated degree-days (ADD) in a temperate region of South Africa. Forensic Sci. Int. 229(1-3):165.e1-6.

NAACP (2023). NAACP Issues Travel Advisory in Florida. Press Statement 5/30/2023. https://naacp.org/articles/naacp-issues-travel-advisory-florida. Accessed 9/29/2023.

NIST/SEMATECH e-Handbook of Statistical Methods, http://www.itl.nist.gov/div898/handbook/. Accessed 09/03/2023.

Nawrocki S (2009). Forensic Taphonomy In: Blau, S and Ubelaker, DH, eds. Handbook of Forensic Anthropology and Archaeology. Walnut Creek, CA: Left Coast Press, Inc; 284-294.

Netzer N, Strohl K, Faulhaber M, Gatterer H, Burtscher M (2013). Hypoxia-related altitude illnesses. *J Travel Med*. doi: 10.1111/jtm.12017.

Nigam Y, Bexfield A, Thomas S, Ratcliffe NA (2006). Maggot therapy: The science and implication for CAM Part I-History and bacterial resistance. *Evid. Based Complement. Alternat. Med*. 3(2):223-227.

Öberg S, Andresen K, Rosenberg J (2017). Etiology of Inguinal Hernias: A Comprehensive Review. *Frontiers in Surgery*. 4:52.

Olson ZH, Beasley JC, Rhodes OE Jr. (2016). Carcass Type Affects Local Scavenger Guilds More than Habitat Connectivity. *PLoS ONE*. 11(2):e0147798. doi:10.1371/journal.pone.0147798

Park Conty Government (2022). GIS Mapping. maps.parkco.us. Accessed 10/10/2022.

Park County Government (2023). Park County is Proud to be a Right-to-Farm and Ranch County. https://www.parkco.us/417/Park-County-Ranching. Accessed 02/12/2023.

Park M, Derrien M, Geczi E, Stokowski PA (2019) Grappling with Growth: Perceptions of Development and Preservation in Faster- and Slower-Growing Amenity Communities. *Society & Natural Resources*. 32(1):73-92

Pegg SCH, Brown SD, Ojha S. Seffernick J, Meng EC, Morris JH, Chang PJ, Huang CC, Ferrin TE, Babbitt PC (2006). Leveraging enzyme structure–function relationships for functional inference and experimental design: The structure–function linkage database. *Biochemistry.* 45:2545–2555.

Piazina H (1996). The effect of altitude upon the solar UV-B and UV-A irradiance in the tropical Chilean Andes. *Solar Energy*. 57(2):133-140.

Pilkington E (2023). 'Death Star law' to Abortion: The New Rightwing Laws Taking Effect in Texas. The Guardian, UK. https://www.theguardian.com/us-news/2023/sep/01/texas-new-laws-republican-legislature. Accessed 11/15/2023.

Pilloud MA, Megyesi MA, Truffer M, Congram D (2016). The taphonomy of human remains in a glacial environment. Forensic Sci. Int. 261(1):161.e1-8.

Powell R, Mitchell ME (2012). What is a home range? *J. of Mammalogy*. *93*(4):948–958.

Reed HB (1958). A study of dog carcass communities in Tennessee, with special reference to the insects. *American Midland Naturalist*. 59:213-245.

Reed JK (2021). Impacts of Marijuana Legalization in Colorado. Colorado Department of Public Safety Division of Criminal Justice. A Report Pursuant to C.R.S. 24-33.4-516.

Reeves NM (2009). Taphonomic effects of vulture scavenging. *J. Forensic Sci.* 54(3):523–528.

Reno E, Brown TL, Betz ME, Allen MH, Hoffecker L, Reitinger J (2017). Suicide and high altitude: an integrative review*. High Alt. Med. Biol*. doi:10.1089/ham.2016.0131.

Rhine S, Dawson J (1998). Estimation of Time Since Death in the Southwestern United States. In: Reichs KJ, ed. Forensic Osteology: Advances in the Identification of Human Remains. Second Edition. Springfield, IL: Charles C. Thomas; 145-159.

Rice WJ, Rushing JR, Thomsen J, Whitney PS (2022). Exclusionary effects of campsite allocation through reservations in U.S. National Parks: Evidence from mobile device location data. *J. of Park and Recreation Administration*. *40*(4):45–65.

Rodriguez WC (1982). Insect Activity and Its Relationship to Decay Rates of Human Cadavers in East Tennessee. Master of Arts Thesis, University of Tennessee, Knoxville.

Roberts LG, Dabbs GR (2015). A taphonomic study exploring the differences in decomposition rate and manner between frozen and never frozen domestic pigs (*Sus scrofa*). *J Forensic Sci.* 60(3):588–594.

Rolston III H (2008). Mountain majesties above fruited plains: Culture, nature, and rocky mountain aesthetics. *Environmental Ethics.* 30(1):3-20.

Ropero-Miller JD, McClary CR, Fulginiti LC, Williams CK, Thompson CR, Geradts ZJ (2020). AAFS Statement in Response to Diversity Opinion Article. Forensic: On the Scene and in the Lab. https://www.forensicmag.com/570554-AAFS-Statement-in-Response-to-Diversity-Opinion-Article/. Accessed 01/29/2023.

Ross AH, Williams SE (2021). Ancestry studies in forensic anthropology: Back on the frontier of racism. *Biology.* 10(7):602.

Rupert JL, Hochachka PW (2001). The evidence for hereditary factors contributing to high altitude adaptation in Andean natives: A review. *High Alt. Med. Biol*. 2(2):235-56.

Sah P, Moghadas SM, Vilches TN, Shoukat A, Singer BH, Hotez PJ, Schneider EC, Galvani AP (2021). Implications of suboptimal COVID-19 vaccination coverage in Florida and Texas. *Lancet Infect. Dis.* 21(11):1493-1494.

Saladie P, Huguet R, Diez C, Rodriguez-Hidalgo A, Carbonell E (2013). Taphonomic modifications produced by modern brown bears (*Ursus arctos*). *Int. J. of Osteoarcheology*. 23(1):13-33.

Sanford MR, Byrd JH, Tomberlin JK, Wallace JR (2020). Entomological Evidence Collections Methods: American Board of Forensic Entomology Approved Protocols. In: Byrd JH and Tomberlin JK, eds. Forensic Entomology: The Utility of Arthropods in Legal Investigations, Third Edition. Boca Raton, FL: CRC Press; 64-87.

Scarbrough LA (2001). Geology and Mineral Resources of Park County, Colorado. Colorado Geological Survey Division of Minerals and Geology Department of Natural Resources Denver, Colorado.

Scheinfeldt LB, Tishkof SA (2010). Living the high life: High-altitude adaptation, *Genome Biol*. 11(9):133.

Schwab F, Gastmeier P, Meyer E (2014). The warmer the weather, the more gram-negative bacteria - Impact of temperature on clinical isolates in intensive care units. *PLoS One.* 9(3):e91105.

Sherzer J. (1970). Talking Backwards in Cuna: The Sociological Reality of Phonological Descriptions. Southwestern Journal of Anthropology. 26(4):343–353.

Sincerbox SN, DiGangi EA (2018). Forensic Taphonomy and Ecology of North American Scavengers. San Diego, CA: Academic Press.

Skinner M., Fernández A, Congram D (2009). Material culture analysis in forensic cases: A call for formal recognition by forensic anthropologists. Proceedings of the American Academy of Forensic Sciences 15:336-337.

Smith MD, Krannich RS (2000). "Culture clash" revisited: Newcomer and longer-term residents' attitudes toward land use, development, and environmental issue in rural communities in the Rocky Mountain West. *Rural Sociology.* 63(3):396-421.

Sorg, MH (2013). Developing Regional Taphonomic Standards. U.S. Department of Justice; National Institute of Justice, Federal Grant Number 2008-DN-BX-K177.

Spencer, JR (2013). Defining Postmortem Changes in Western Montana: The Effects of Climate And Environment on The Rate and Sequence of Decomposition Using Pig (*Sus Scrofa*) Cadavers. Master's thesis, University of Montana, Missoula.

Spradley MK, Hamilton MD, Giordano A (2012). Spatial patterning of vulture scavenged human remains. *Forensic Sci. Int*. 219:57-63.

Steadman DW (2008). Hard Evidence: Case Studies in Forensic Anthropology. New York, NY: Routledge Taylor and Francis Group.

Stodolska M, Shinew KJ, Acevedo JC, Izenstark D (2011). Perceptions of urban parks as havens and contested terrains by Mexican-Americans in Chicago neighborhoods. *Leisure Sciences*. 33:103–126.

Stodolska M, Shinew KJ, Camarillo LN (2020). Constraints on recreation among people of color: Toward a new constraints model. *Leisure Sciences*. *42*(5–6):533–551.

Stokowski PA (1996). Riches and Regrets: Betting on Gambling in Two Colorado Mountain Towns. Niwot, CO: University Press of Colorado.

Suckling JK (2011). A Longitudinal Study on the Outdoor Human Decomposition Sequence in Central Texas. Master's Thesis, Texas State University - San Marcos, Department of Anthropology.

Summit County Commuter (2024). Park County Commuter. Summit County Colorado Government https://www.summitcountyco.gov/1300/Park-County-Commuter

Sutherland A, Myburgh J, Steyn M, Becker PJ (2013). The effect of body size on the rate of decomposition in a temperate region of South Africa. *Forensic Sci. Int*. 231:257–262.

Takatori T, Yamaoka A (1977). The mechanism of adipocere formation. II. Separation and identification of oxo fatty acids in adipocere. *Forensic Sci Int*., 10(2):117–125.

Tallman SD (2020). Opinion: The Forensic Sciences Have a Diversity, Inclusion Problem. Forensic: On the Scene and In the Lab. https://www.forensicmag.com/569912-Opinion-The-Forensic-Sciences-Have-a-Diversity-Inclusion-Problem/. Accessed 01/29/2023.

Tallman SD, Bird CE (2022). Diversity and inclusion in forensic anthropology: Where we stand and prospects for the future. *Forensic Anthropology* 5(2):84-101.

Tersigni MA (2007). Frozen human bone: a microscopic investigation. *J. Forensic Sci*. 52(1):16-20.

Theriault D, Mowatt RA (2020). Both sides now: Transgression and oppression in African Americans' historical relationships with nature. *Leisure Sciences*. 42(1):15–31.

Thyssen PJ (2010). Keys for Identification of Immature Insects. In: Amendt J, Goff ML, Campobasso CP, Grassberger M eds. Current Concepts in Forensic Entomology. Boca Raton, FL: CRC Press; 25-42.

Town of Alma (2023). About Alma. https://townofalma.com/content/about_alma.html. Accessed 9/29/2023.

Tuma F, Lopez RA, Varacallo M (2022). Anatomy, Abdomen and Pelvis: Inguinal Region (Inguinal Canal) In: StatPearls. Treasure Island, FL: StatPearls Publishing.

Turner V (1967). The Forest of Symbols. Ithaca, NY: Cornell University Press

Turner V (1969). The Ritual Process. Chicago, IL: Aldine.

Turpin C (2017). The micro-taphonomy of cold: Differential microcracking in response to experimental cold-stresses. *J. Forensic Sci.* 62(5):1134-1139.

Ubelaker DH (2018). A history of forensic anthropology. *Am. J. Phys. Anthropology.* 165:915–923.

United States Census Bureau (2022). Quick Facts, Park County. https://www.census.gov/quickfacts/parkcountycolorado. Accessed 1/29/2023.

USCCA, United States Concealed Carry Association (2023). The Most Armed States. https://www.usconcealedcarry.com/blog/the-most-armed-states/. Accessed 01/29/2023.

Van Gennep (1960). The Rights of Passage. London, UK: Routledge University Press.

Vass AA (2011). The elusive postmortem interval formula. *Forensic Sci. Int.* 204(1–3):34–40.

Vass AA, Bass WM, Wolt JD, Foss JE, Ammons JT (1992). Time since death determinations of human cadavers using soil solution. *J. Forensic Sci.* 37(5):1236–1253.

VRBO (2023). Park County Vacation Rentals. https://www.vrbo.com/vacation-rentals/usa/colorado/park-county. Accessed 1/29/2023.

Weidner LM, Powell GS (2021). Key to the forensically important beetle (Insecta: Coleoptera) families of North America. *J Forensic Sci Educ*. 3(1): 1-13.

Whiteman CD (2000). Mountain Meteorology: Fundamentals and Applications. First Edition. New York, NY: Oxford University Press.

Whitford WG, Steinberger Y (2010). Pack rats (*Neotoma spp*.): Keystone ecological engineers? *J. of Arid Environments*. 74(11):1450-1455.

Willey P, Snyder LM (1989). Canid Modifications of Human Remains: Implications for Time-Since-Death Estimations. *J. Forensic Sci* 34:894–901.

Winburn AP, Jennings AL, Steadman DW, DiGangi EA (2022). Ancestral diversity in skeletal collections: Perspectives on African American body donation. *Forensic Anthropology.* 5(2):141-152.

World Population Review (2024). Colorado Population 2024. https://worldpopulationreview.com/states/colorado-population. Accessed 1/10/2024.

Yudell M (2014). Race Unmasked: Biology and Race in the 20th Century. New York, NY: Columbia Univ. Press.

Zapf A, Castell S, Morawietz L, Karch A (2016). Measuring inter-rater reliability for nominal data - which coefficients and confidence intervals are appropriate? *BMC Med Res Methodol* 16:93. doi: 10.1186/s12874-016-0200-9.

Zhang D, Hui D, Luo Y, Zhou G (2008). Rates of litter decomposition in terrestrial ecosystems: Global patterns and controlling factors. *Journal of Plant Ecology* 1(2): 85–93.

APPENDIX A

LIST OF ACRONYMS

AAFS	America Academy of Forensic Sciences
ADD	Accumulated Degree Days
ADD^C	Accumulated Degree Days Celsius
AMSL	Above Mean Sea Level
APD	Accumulated Pressure Days
APreD	Accumulated Precipitation Days
ARD	Accumulated Rain Days
ARHD	Accumulated Relative Humidity Days
ASRD	Accumulated Solar Radiation Days
ATP	Adenosine Triphosphate
AWSD	Accumulated Wind Speed Days
BMI	Body Mass Index
CDC	Center for Disease Control
CRC	Colorado Forensic Canines
CoRM	Colorado Rocky Mountains
CMU	Colorado Mesa University
DNA	Deoxyribonucleic acid
DOW	Department of Wildlife
HAFE	High-altitude flatus expulsion
GIS	Geographic Information System
GSW	Gunshot Wound
FIRS	Forensic Investigation Research Station
FIRS-TB40	Forensic Investigation Research Station: The Back 40 (FIRS satellite facility/project site)
HACE	High-altitude Cerebral Edema
HAFE	High-altitude Flatus Expulsion
HAPE	High-altitude Pulmonary Edema
IRB	Institutional Review Board
LOESS	Locally Weighted Scatter Plot Smoother
MRLC	Multi-Resolution Land Characteristics Consortium
PCCO	Park County Coroner's Office
PCSAR	Park County Search and Rescue
PCSO	Park County Sheriff's Office
PMI	Postmortem Interval
ROS	Reactive Oxygen Species
SIUC	Southern Illinois University Carbondale
TBS	Total Body Score
TM	Trademark
UCR	Uniform Crime Reporting Program
USDA	United States Department of Agriculture
UV	Ultraviolet
VOCs	Volatile Organic Compounds

APPENDIX B

PERMISSION TO USE CASE DATA – PARK COUNTY CORONER DAVID KINTZ JR.

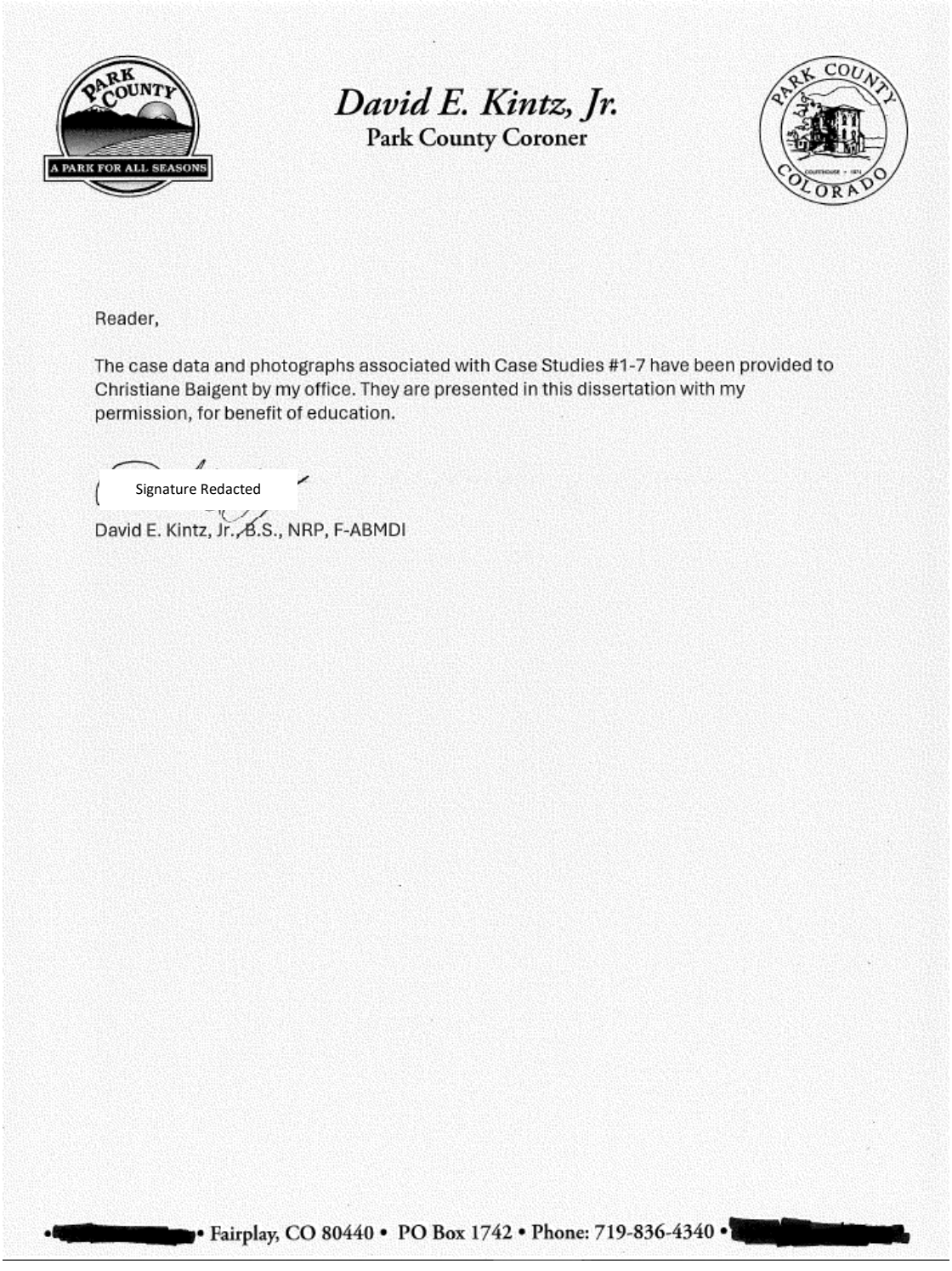

David E. Kintz, Jr.
Park County Coroner

Reader,

The case data and photographs associated with Case Studies #1-7 have been provided to Christiane Baigent by my office. They are presented in this dissertation with my permission, for benefit of education.

Signature Redacted

David E. Kintz, Jr., B.S., NRP, F-ABMDI

[redacted] • Fairplay, CO 80440 • PO Box 1742 • Phone: 719-836-4340 • [redacted]

VITA

Graduate School
Southern Illinois University Carbondale

Christiane Irene Baigent

cbaigent@gmail.com

University College London
Master of Science, Forensic Archaeological Sciences, November 2014

Metropolitan State University of Denver
Bachelor of Arts, Anthropology and IDP Forensic Sciences, May 2012

Special Honors and Awards:

Financial - Research

2018-2022	National Institute of Justice (2018-R2-CX-0014) Graduate Research Fellowship The Effect of Altitude on Decomposition: Toward an Understanding the Postmortem Interval in the Rocky Mountain Region. Research funding and salary stipend.
2017	Southern Illinois University Graduate and Professional Student Research Award
2014	UCL Institute of Archaeology Master's Prize Bursary for outstanding dissertation
2012	Undergraduate Research Grant Metropolitan State University Denver – High-altitude decomposition.

Financial – Scholarship

2023	Colorado Coroners Association Conference Scholarship
2022	International Association of Coroners and Medicolegal death Investigators Conference Attendance Scholarship
2020	Forensic Sciences Foundation Student Travel Grant
2015	American Academy of Forensic Sciences Forensic Sciences Foundation Student

Scholarship Award

2013	Phil Nowick Memorial Scholarship
2013	President's Academic Achievement Award, Metropolitan State University of Denver
2012	President's Academic Achievement Award, Metropolitan State University of Denver
2012	Gardner Scholarship
2012	Women's Club Scholarship
2011	Metro Scholars Award

Dissertation Paper Title:

THE EFFECT OF ALTITUDE ON DECOMPOSITION: TOWARD AN UNDERSTANDING THE POSTMORTEM INTERVAL IN THE ROCKY MOUNTAIN REGION

Major Professor: Gretchen R. Dabbs

PUBLICATIONS

2020 **Baigent, C.I.,** Agan, C., Connor, M.A., Hansen, E.S. Autopsy as a form of evisceration: Implications for decomposition rate, pattern, and estimation of postmortem interval. *Forensic Science International* 306:1-8.

2019 Garcia S.A, Smith A.J., **Baigent C.I.**, Connor M.A. The Scavenging Patterns of Feral Cats on Human Remains in an Outdoor Setting. *Journal of Forensic Sciences* 65(3):948-952.

2019 Connor M.A., **C.I. Baigent**, E.S. Hansen. Measuring Desiccation Using Qualitative Changes: A Step Toward Determining Regional Decomposition Sequences. 64(4):1004-1011

2018 Connor M.A., **C.I. Baigent**, E.S. Hansen. Testing the use of pigs as human proxies in decomposition studies. *Journal of Forensic Sciences* 63(5):1350-1355.

2018 Hansen, E.S., **C.I. Baigent**, S.I. Reck, and M.A. Connor. Bioelectrical Impedance as a Technique for Estimating Postmortem Interval. *Journal of Forensic Sciences* 63(4):1186-1190.

PUBLISHED ABSTRACTS AND PRESENTATIONS

2024 **Baigent, C.I.** Small but mighty: Controlled observation of magpie scavenging among a cohort of human remains in the Rocky Mountain Region of Colorado. Accepted for podium presentation at the 76th Annual Scientific Meeting of the American Academy of Forensic Sciences, Denver, CO., February 19-24, 2024.

2024 **Baigent, C.I.** Longitudinal observation of pattern and trajectory of packrat scavenging among a cohort of human donors. Accepted for poster presentation at the 76th Annual Scientific Meeting of the American Academy of Forensic Sciences, Denver, CO., February 19-24, 2024.

2023 Baigent, C.I. From Analytical to Practical: The Relationship Between Research and Medicolegal Death Investigation. Podium training/lecture, Colorado Coroner's Association Rocky Mountain Death Investigators Conference, Greeley, CO., October 4-7, 2023.

2022 **Baigent, C.I.** Taphonomy in a high-altitude environment. Poster Presentation, International Association of Coroner's and Medical Examiners Annual Training Symposium, Las Vegas, NV., July 16-22, 2022.

2022 **Baigent, C.I.** Toward a model for estimating postmortem interval at high-altitude: Categorical Macromorphoscopic changes observed throughout the trajectory of human decomposition in the Colorado Rocky Mountains. Podium presentation, 73rd Annual Scientific Meeting of the American Academy of Forensic Sciences, Seattle, WA., February 21-25, 2022.

2021 **Baigent, C.I.** Decomposition at High-Altitude, the Rocky Mountain Region of CO.

Podium Presentation, Special Section. Rocky Mountain Division of the International Association for Identification Annual Meeting, Black Hawk, CO., July 7-9, 2021.

2020 Dabbs, G.R., **Baigent, C.I.** A Paired Comparison of the Rate and Pattern of Decomposition in Small- and Large-Bodied Human Cadavers. Poster presentation at the 72nd Annual Scientific Meeting of the American Academy of Forensic Sciences, Anaheim, CA., February 17-22, 2020.

2020 **Baigent, C.I**.*, Kintz, D.J., Connor, M.A., Dabbs, G.R. Coyote Pup Scavenging as Distinct from Adult Behavior: The Potential for Reproductive Patterns to Inform the Estimation of Postmortem Interval. Poster presentation at the 72nd Annual Scientific Meeting of the American Academy of Forensic Sciences, Anaheim, CA., February 17-22, 2020.

2019 **Baigent, C.I**.*, Connor, M.A., Dabbs, G.R. Introducing FIRS-TB40: Scavenger Succession and Progression at a High-Altitude site in Colorado. Podium presentation at the 71st Annual Scientific Meeting of the American Academy of Forensic Sciences, Baltimore, MD., February 18-23, 2019.

2019 a. Connor, MA*, **Baigent, CI**: Session 1 Decomposition on the Western Slope of Colorado

b. **Baigent, CI**, Connor, MA: Session 2 Decomposition at High-Altitude, the Rocky Mountain Region of CO.

Human Decomposition throughout Colorado: Colorado Mesa University Forensic Investigation Research Station's New Altitude. Podium Presentation, Special Section. Rocky Mountain Division of the International Association for Identification Annual Meeting, Denver, CO., May 15-17, 2019.

2019 **Baigent, C.I**.*, Connor, M.A., Dabbs, G.R. Introducing FIRS-TB40: Scavenger Succession and Progression at a High-Altitude site in Colorado. Podium presentation at the 71st Annual Scientific Meeting of the American Academy of Forensic Sciences, Baltimore, MD., February 18-23, 2019.

2019 Garcia, S., A. Smith, **C.I. Baigent**, M.A. Connor. Scavenging Patterns of Feral Cats on Human Remains in an Outdoor Setting. Submitted for podium presentation at the 71st Annual Scientific Meeting of the American Academy of Forensic Sciences, Baltimore, MD., February 18-23, 2019.

2018 Connor, M.A.*, **C.I. Baigent,** and E.S. Hansen. Deconstructing Desiccation and Decomposition. Accepted for podium presentation at the 70th Annual Scientific Meeting of the American Academy of Forensic Sciences, Seattle, WA., February 19-24, 2018.

2018 Hansen, E.S.*, **C.I. Baigent,** and M.A. Connor. A Comparison of Bioelectrical Impedance Analysis Techniques for Estimating Postmortem Interval. Accepted for podium presentation at the 70th Annual Scientific Meeting of the American Academy of Forensic Sciences, Seattle, WA., February 19-24, 2018.

2018 Agan, C*, **C.I. Baigent*,** M.A. Connor, and E.S. Hansen. Decomposition Rates: Autopsied vs. Non-Autopsied Human Remains. Accepted for podium presentation at the 70th Annual Scientific Meeting of the American Academy of Forensic Sciences, Seattle, WA., February 19-24, 2018.

2017 Hansen, E.S.*, M.A. Connor, and **C.I. Baigent**. Bioelectrical Impedance Analysis as a Technique for Estimating the Postmortem Interval in Human Remains. Accepted for podium presentation at the 69th Annual Scientific Meeting of the American Academy of Forensic Sciences, New Orleans, LA., February 13-18, 2017.

2017 Connor, M.A.*, **C.I. Baigent**, and E.S. Hansen. Measuring Desiccation Using Morphological Changes. Accepted for podium presentation at the 69th Annual Scientific Meeting of the American Academy of Forensic Sciences, New Orleans, LA., February 13-18, 2017.

2017 Hansen, E.S., M.A. Connor, and **C.I. Baigent***. Future Techniques for Estimating the Postmortem Interval in Human Remains. Accepted for podium presentation at the 2017 NIJ Forensic Science R&D Symposium, February 14, 2017, during the 69th Annual Scientific Meeting of the American Academy of Forensic Sciences, New Orleans, LA., February 13-18, 2017.

2016 **Christiane Baigent**.* Taphonomy of the Perinate Skeleton: Redefining Structural Norms and Building Analytical Models. Podium presentation at the 68th Annual Scientific Meeting of the American Academy of Forensic Sciences, Las Vegas, NV., February 22-27, 2016.

2016 **Christiane Baigent***, Gary T. Scott**.** The Mummy in the Microwave: The Efficacy of the Microwave Method for the Maceration of Desiccated Tissue. Poster presentation at the 68th Annual Scientific Meeting of the American Academy of Forensic Sciences, Las Vegas, NV., February 22-27, 2016.

2016 **Christiane Baigent***, Catherine M. Gaither. Students in the Forensic Laboratory: Fostering Education While Maintaining Quality. Poster presentation 68th Annual Scientific Meeting of the American Academy of Forensic Sciences, Las Vegas, NV., February 22-27, 2016.

2015 **Christiane Baigent*,** Catherine Gaither. Students in the Forensic Laboratory: Fostering Education While Maintaining Quality. Podium presentation, NIST International Symposium on Forensic Science Error Management in Washington, DC., July 20-24, 2015.

2014 **Christiane Baigent***, Catherine Gaither, Ciara Campbell. The effect of altitude on decomposition: a validation study of the Megyesi method. Podium presentation, 66th Annual Scientific Meeting of the American Academy of Forensic Sciences, Seattle, WA. February 17-22, 2014.

2014 Camp, Jeremiah*; Gaither, Catherine; Herrera, Fernando; **Baigent, Christiane**, Arndt, Emilie; Bish, Jack; Repka, Nicholas; Theige, Brandon; Walther, Lauren. Analysis of human remains from Tupac Amaru B: A working class perspective. Poster presented at the 2014 Institute of Andean Studies 54th Annual Meeting, January 10-11, 2014, Berkeley CA.

PUBLISHED BOOK REVIEWS

2019 **Baigent, C.I.** Review - Massacres: Bioarcheology and Forensic Anthropology Approaches. Andersen CP and Martin DL, eds. Midcontinental Journal of Archaeology, 44(1):1-7. https://www.midwestarchaeology.org/mcja/book-reviews